# Biological selenium removal from wastewaters

Markus Lenz

PROMOTOREN

Prof. Dr. Ir. C. J.N. Buisman
Hoogleraar in de biologische kringlooptechnologie

Prof. Dr. Ir. P.N.L Lens
Hoogleraar in de Milieubiotechnologie, UNESCO-IHE, Delft

SAMENSTELLING PROMOTIECOMMISSIE

| | |
|---|---|
| Prof. Dr. T. G. Chasteen | Sam Houston State University, Huntsville, USA |
| Dr. L. Diels | Vlaamse instituut voor technologisch onderzoek, Mol, B |
| Prof. Dr. J. Llyod | Manchester University, UK |
| Prof. Dr. Ir. A. J. M. Stams | Wageningen Universiteit, NL |

Dit onderzoek is uitgevoerd binnen de onderzoekschool SENSE (Socio-Economic and Natural Sciences of the Environment).

# Biological selenium removal from wastewaters

Markus Lenz

**Proefschrift**
ter verkrijging van de graad van doctor
op gezag van de rector magnificus
van Wageningen Universiteit
Prof. Dr. M. J. Kropff
in het openbaar te verdedigen
op dinsdag 27 Mei 2008
des namiddags te half twee in de Aula

Author: Lenz, Markus
Title: Biological selenium removal from wastewaters
Publication year: 2008
ISBN: 978-90-8504-801-5

Ph.D. Thesis Wageningen University, Wageningen, The Netherlands – with references – with summaries in English and Dutch

# Abstract

Markus Lenz (2008). Biological selenium removal from wastewaters. Doctoral thesis, Wageningen, The Netherlands, 206 pages.

Selenium has been referred to as an “essential toxin” due to the fact that it shows only a marginal line between the nutritious requirement and toxic effects upon exposure. The environmental fate of selenium compounds varies greatly in dependence of its complex speciation. Different current and future aqueous selenium waste streams call for an efficient low-tech cleanup solution.

In this thesis, microbial conversion of water-soluble, highly toxic forms of selenium (selenate, selenite) to less bioavailable elemental selenium was investigated. By the exploitation of different groups of microorganisms (selenium-respiring, nitrate-reducing and sulfate-reducing bacteria, methanogenic archaea) the operational window of conventional and new hybrid anaerobic bioreactors treating selenium containing anthropogenic waste streams has been determined.

A special focus was given to selenium speciation in solid, liquid and gas phase. Selenium speciation in the solid phase was assessed by direct and non-destructive X-ray absorption fine structure spectroscopy. It was demonstrated that selenium solid phase speciation is more complex than initially expected, as different side products such as metal selenides and organic selenium compounds are (trans)formed. Regarding the liquid/gas phase speciation, selenium forms volatile alkylated species under interaction with reduced sulfur compounds depending on operational parameters applied. Selenium oxyanions are not only toxic to animal and human populations, but are here shown to largely influence anaerobic food webs, due to their effect on acetoclastic and hydrogenotrophic methanogens.

# Table of contents

1. Introduction

pp. 1-22

2. Analytical tools for selenium speciation

pp. 23-36

3. Selenium speciation in anaerobic granular sludge studied by XAFS

pp. 37-46

4. Selenate removal in methanogenic and sulfate-reducing upflow anaerobic sludge bed reactors

pp. 47-64

5. Biological alkylation and colloid formation of selenium in methanogenic UASB reactors

pp. 65-84

6. Induced changes in selenium speciation during sequential extraction assessed by XANES spectroscopy

pp. 85-96

7. Inhibition of hydrogenotrophic and acetoclastic methanogenesis by selenium oxyanions

pp. 97-112

8. Bioaugmentation with immobilized *Sulfurospirillum barnesii* for simultaneous selenate and nitrate removal

pp. 113-128

9. Summary and discussion

pp. 129-144

9´. Samenvatting en discussie

pp. 145-162

References

pp. 163-199

Acknowledgements, about the author, list of publications

pp. 200-206

What has been thought once cannot be redeemed.

Johann Wilhelm Möbius in “Die Physiker” (Friedrich Dürrenmatt, 1961)

# Introduction

# 1


This chapter was submitted for publication as: Lenz, M., Lens, P. N. L. (2006). The essential toxin: the changing perception of selenium in environmental sciences.

# 1.1 Preface



During the last decades, the perception of selenium has undergone substantial changes. While its toxic effects were recognized causing hair and hoof loss in animals during the 1930s, its essential role in microbial, animal and human metabolism has been recognized later, i.e. with the discovery of selenium deficiency causing “white muscle disease” in feedstock in the 1950s [60; 78]. Nowadays, the positive effect of systematic selenium supplementation is discussed in manifold topics such as cancer [284] or diabetes [138] prevention and avian influenza susceptibility [20; 63].

Treatment of selenium containing waste streams poses a notable challenge to environmental engineers, and to date no ultimate solution has been found for e.g. the selenium contamination in agricultural areas of the western USA [182]. For the future, selenium contamination carries an imminent danger, if the increasing energy demand is covered by combustion of fossil fuels, leading to major selenium emission [263] and toxicity [59]. Consequently, the search for feasible treatment options targeting a variety of current and future waste streams needs to be pursued with great insistence.

# 1.2. Natural and anthropogenic selenium cycling

## 1.2.1 Occurrence of selenium in the environment

Selenium is a metalloid that was discovered in 1818 by the Swedish Chemist Jons Jakob Berzelius in leaden chamber mud during sulfuric acid production. It was given the name selenium in resemblance after the Greek goddess of the moon “Selene”, in homology to the chemically similar tellurium (after *lat.* tellus = earth) [266].

Selenium belongs to the group of chalcogens (periodic table group 16), thus displays a chemical behavior similar to sulfur. As a result, selenium is found associated with natural sulfides like pyrite ($FeS_2$), chalcopyrite ($CuFeS_2$) and sphalerite [(Zn, Fe)S] [266] mainly in trace concentrations, but there are no economically significant selenium ores or ore deposits [19]. Selenium is present in high-sulfur coals found e.g. in the USA, Russia and China, with a selenium content up to 43 mg Se $kg^{-1}$, although the world average is only 1.6 and 1.0 mg Se $kg^{-1}$ (hard coals and brown coals, respectively) [279]. Furthermore, black slate and

volcanic tuff can contain high selenium concentrations (e.g. 22 and 32 mg $kg^{-1}$ in the Daba region, China [112]).

Selenium is inhomogeneously distributed in the earth's crust resulting in the fact that particular countries, most prominently China and Brazil, suffer from both selenium deficient (< 0.1 mg $kg^{-1}$) and seleniferous (> 0.5 mg Se $kg^{-1}$) soils [34], sometimes separated by a distance of just 20 km [59]. Although generally in the low µg $kg^{-1}$ range, some soils in e.g. Ireland, India and the United States display very high selenium concentrations of up to 100 mg Se $kg^{-1}$ [35; 59]. An overview of the unequal selenium distribution in USA soils is given in Figure 1.1.



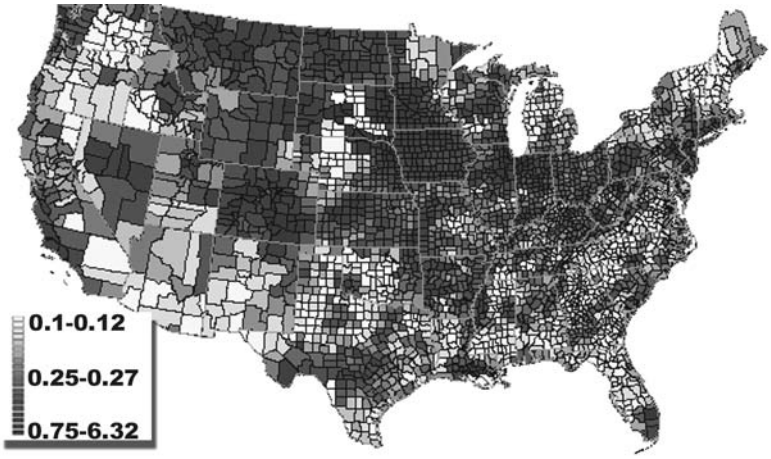


Figure 1.1 Selenium distribution in soil [mg $kg^{-1}$] of the USA [247]; soils with < 0.1 mg Se $kg^{-1}$ are considered selenium deficient, soils with > 0.5 mg Se $kg^{-1}$ as seleniferous [34]

## 1.2.2 Applications / Uses of selenium

Selenium is used in the glass industry for either ruby red coloring (as cadmium sulfo-selenide pigments) or for counteracting green tint caused by iron oxides impurities [244]. The photoelectric and semiconducting properties are widely exploited in electronics [80]. Selenium fertilizers and dietary supplements are used to counteract selenium deficiency [244], selenium sulfide is used in fungicides and in antidandruff shampoos [248]. An emerging application of selenium is the "amorphous selenium detector" in mammographic instruments [100].

Selenium is commercially produced mainly as a by-product during copper electrolytic refining, where it is found in the generated anode slimes [80]. This conjunction with copper production caused strong fluctuation in selenium prices during the last decades, making selenium a valuable product in periods of comparatively low copper production. A shortage in selenium due to increased selenium demand of mainly China has caused the large peak in selenium price during the last few years (Figure 1.2).

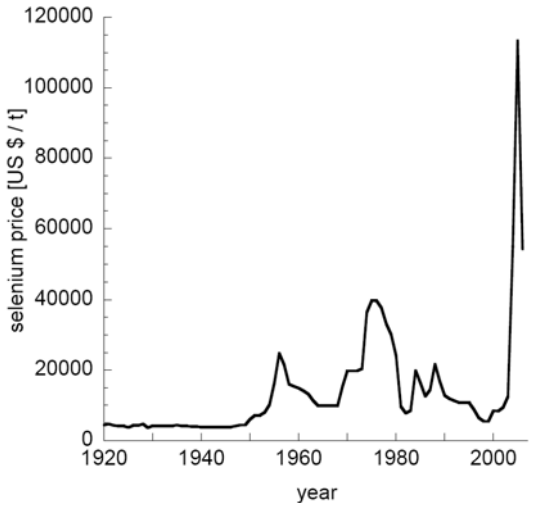


Figure 1.2 Selenium price [US $ / t] during the years 1920 to 2006 [245; 246]

## 1.2.3 Global selenium cycling

Anthropogenic activities interfere with the global selenium cycle on different insertion points and influence it in a crucial way (Figure 1.3). It has been estimated that between 37.5% and 40.6% of the total selenium emissions to the atmosphere are due to anthropogenic activities [263], including foremost the combustion of coal and oil, nonferrous metal melting and utilization of agriculture products. In the atmosphere, selenium is transported associated to particulate matter [16] and subsequently dry and wet deposited. Agricultural drainage waters [8], oil refining waste waters [256] and coal combustion residues [190] contaminate the lotic, lentic and marine environment [57; 83]. Selenium is introduced in the terrestrial compartment mainly as fertilizer or by mining activities. The global selenium cycle is largely influenced by biota changing selenium speciation (section 1.3.2).

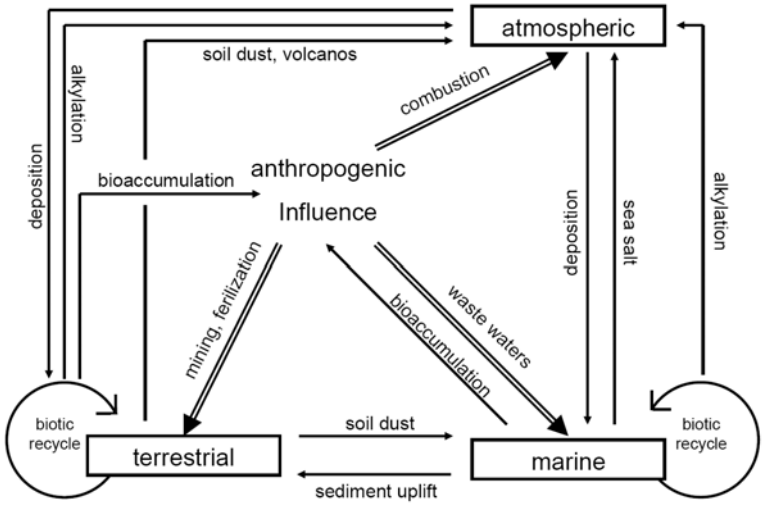


Figure 1.3 Overview on global selenium cycle with the interference of anthropogenic activities; modified after [80]

# 1.3 Selenium speciation in the environment

## 1.3.1 Abiotic selenium transformations

Selenium speciation is complex due to the fact that it exists in the oxidation states -II, -I, 0, +IV and +VI in nature, in both inorganic and organic forms, in solid, liquid and gas phase and in 6 stable isotopes. An exemplary Pourbaix diagram (Figure 1.4) gives a simplified overview over the thermodynamically most stable aqueous / solid selenium species at 25°C.

The most oxidized species, selenate and selenite, are frequently encountered in surface waters [42] from where they are transported mostly in particulate-associated form [80]. Both selenate and selenite display a high bioavailability and bioaccumulation potential (section 1.4.3).

Compared to selenate and selenite, the formation of elemental selenium is expected under more reducing conditions (Figure 1.4). The chemistry of elemental selenium is complex as different allotropic forms can exist. Seven different crystalline forms have been described, including trigonal (grey) (Figure 1.5), different monoclinic (red), different cubic, rhombohedric and ortho-rhombic forms. Red, black and vitreous amorphous forms can

exist as well [148]. Moreover, elemental selenium can be mixed with sulfur in any ratio [222; 266].



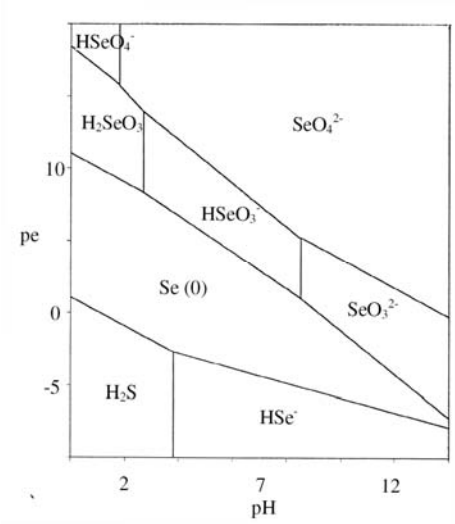


Figure 1.4 Selenium Pourbaix (pe–pH) diagram at 25°C, 1 bar pressure and I=0 for a dissolved selenium activity of $10^{-6}$ mol $L^{-1}$ [207]

Most reduced selenium species include inorganic metal selenides, organic selenium compounds and highly toxic, volatile $H_2Se$, which is formed as an analogue to $H_2S$ under strongly reducing conditions (Figure 1.4).

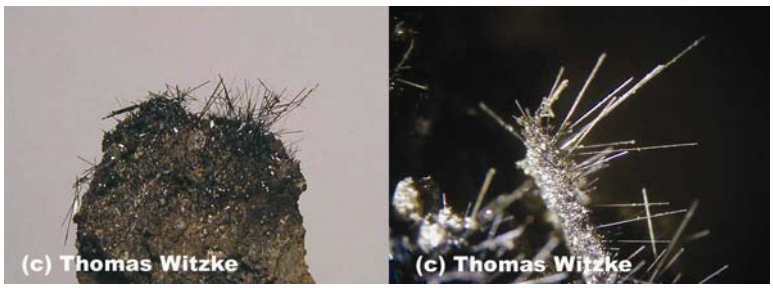


Figure 1.5 Native, trigonal elemental selenium species, found at Ronneburg Uranium deposit, Thuringia, Germany (a) and Anna Mine, Alsdorf-Aachen, North Rhine Westphalia, Germany (b). With courtesy of Thomas Witzke [268]

## 1.3.2 Biological transformation of selenium

Biotic transformations of selenium species are manifold (Figure 1.6) and can be categorized in assimilatory and dissimilatory reduction, alkylation, dealkylation and oxidation.



Water soluble selenite and selenate can be reduced to insoluble elemental selenium ($Se^0$), due to anaerobic microbial selenium respiration (section 1.3.2.1), but also mediated by unspecific reductions via sulfate [234] or nitrate reducers [193] as well as archaea [86]. The formation of elemental selenium is desired in selenium treatment systems (section 1.5), as it is considered to be less soluble and thus less bioavailable [29] compared to the oxyanions, yet biologically formed elemental selenium can be assimilated by e.g. bivalves [131; 202]. Insoluble elemental selenium can be mobilized by microbial re-oxidation to soluble oxyanions (mostly selenite) in oxic conditions [37; 126; 199], but with a 3 to 4 orders of magnitude lower rate constant compared to microbial reduction [37]. Solubilization of elemental selenium can proceed alternatively by reduction to dissolved selenide [82], which readily reacts with metal cations forming strong metal selenide precipitates [207]. Even strong metal selenide complexes are subject to oxidation by microorganisms, as has been demonstrated for the dissolution of copper selenide (CuSe), one of the most insoluble metal selenides ($pK_s$ = 48.1) by *Thiobacillus ferrooxidans* [233]. The chemical precipitation of dissolved selenide metal cations [82; 207] or coprecipitation of dissolved sulfide with selenite [85] can be classified as biologically induced [49; 82], in contrast to biologically controlled precipitation of elemental selenium via microbial respiration.

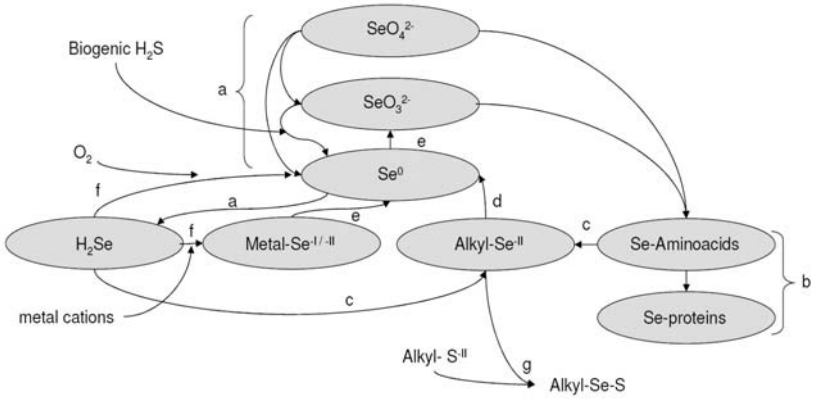


Figure 1.6 Simplified biochemical selenium cycle with a) dissimilatory reduction (biocontrolled precipitation), b) assimilatory reduction, c) alkylation, d) dealkylation, e) oxidation, f) bioinduced precipitation and g) disproportionation

The main contribution to the alkylated selenium pool in the atmosphere, surface waters and marine environments is due to biological mediation by animals, plants and microorganisms [24; 102; 253], although it was demonstrated that alkylated forms can be formed abiotically in photochemical reactions [70]. Alkylated selenium species can interact with their sulfur analogues by disproportionation to mixed selenium-sulfur species [206]. During deprivation of selenium, dimethylselenide can be degraded during methanogenesis [42; 158], yet the degradation does not support growth [264].

It is evident that a "cocktail" of different selenium species can be present in selenium contaminated environments due to the variety of both abiotic and biotic conversions, posing a major challenge to selenium speciation analysis.

### 1.3.2.1 Dissimilatory metal reduction

In anoxic environments, microorganisms have developed strategies to use alternative electron acceptors to oxygen for the production of energy for growth. Prominent examples are iron and manganese reducers, but alternative electron acceptors are manifold, including metalloids like arsenic and selenium, radionuclides like uranium, neptunium, plutonium and technetium, and different transition metals like molybdenum, vanadium and chromium [125; 127]. These anaerobic respiratory processes are summarized typically under the term "dissimilatory metal(loid) reduction", distinguishing these modes of respiration from processes related with metal assimilation. Table 1.1 illustrates that selenate and selenite reduction can yield high energies compared to e.g. sulfate reduction, commonly encountered in anoxic environments.

Efforts were made to apply this mode of microbial respiration in the treatment of selenite and selenate contamination for different reasons: Most importantly, by formation of elemental selenium as an insoluble product, the reduction unifies the removal of selenium oxyanions from the aqueous phase with a detoxification, as elemental selenium is less bioavailable. Dissimilatory selenium reducers possess highly specific enzymes that are independent (i.e. not inhibited by the presence) of e.g. nitrate, nitrite and sulfate [205; 260], thus possess a high selectivity for the targeted selenium oxyanions. Selenium respirers are highly selenium tolerant, thus applicable for concentrated waste streams [64]. Selenium respirers can use a variety of different electron donors, amongst others different simple organic acids [103], alcohols [5], molasses [289] , hydrogen [26] or humic substances [128]. Potentially, elemental selenium can be recovered from the waste streams and thus lower operational costs, as described for the recovery of other by-products during selenium treatment [214].

Table 1.1 Standard free energy change for the respiration of different electron acceptors using hydrogen as electron donor; modified after [129; 156; 228]

| Electron acceptor | | | |
|---|---|---|---|
| Oxygen | $O_2 + 2H_2$ | → | $2\ H_2O$ |
| Iron | $Fe^{3+} + 0.5\ H_2$ | → | $Fe^{2+} + H^+$ |
| Nitrate | $NO_3^- + 2.5\ H_2 + H^+$ | → | $0.5\ N_2\ (g) + 3H_2O$ |
| Manganese | $MnO_2 + HCO_3^- + H_2 + H^+$ | → | $MnCO_3 + 2H_2O$ |
| Selenate | $SeO_4^{2-} + 3H_2 + 2H^+$ | → | $Se^\circ + 4H_2O$ |
| Selenite | $HSeO_3^- + 2H_2 + H^+$ | → | $Se^\circ + 3H_2O$ |
| Arsenate | $H_2AsO_4^- + H_2 + H^+$ | → | $H_3AsO_3 + H_2O$ |
| Sulfate | $SO_4^{2-} + 4H_2 + 2H^+$ | → | $H_2S + 4H_2O$ |
| Chromate | $CrO_4^{2-} + 1.5\ H_2 + 2H^+$ | → | $Cr(OH)_3 + 3\ H_2O$ |

# 1.4 Biochemical functions of selenium

Selenium is an essential element in animals, as seleno-proteins are involved in redox regulation of intracellular signaling, redox homeostasis and thyroid hormone metabolism [248]. Historically, glutathione peroxidase, protecting the cell against oxidative damage, was the first enzyme identified as containing selenium [58; 189]. Later, selenium was identified in a variety of different seleno-proteins, including at least 25 seleno-proteins in human [172], yet the function of many seleno-proteins remained unknown so far.

The selenol group (-SeH) of selenocysteine in thioredoxine reductases plays a fundamental role in protection against free radicals [172; 225]. Selenomethionine is involved in protection against radiation and UV-light–induced damage [204]. Since the late 1960s anticarcinogenic properties of selenium have been discussed, based on an inverse relationship of selenium nutritional status and risk towards various cancer forms [284]. In this context, mandatory selenium fortification of agricultural fertilizers was introduced by Finland in 1984, due to the observed relationship between low selenium intake and lung cancer [76]. However, the mechanism that mediates the anticarcinogenic effect is still not fully understood to date [17; 38; 284]. Recently, the role of selenium in detoxification of arsenic and mercury compounds by complexation has been discussed [183].

In prokaryotes, selenium is present in a variety of seleno-proteins, e.g. in formate dehydrogenases (*Methanococcus jannaschii*) [97], formylmethanofuran dehydrogenase (*Methanopyrus kandleri*) [257], in thiol / disulphide oxidoreductases (*Geobacter sulfurreducens*) and in glycine / proline reductase (*Clostridium difficile*) [110].

## 1.4.1 Deficiency

Selenium deficiency in humans is regarded a major health problem for 0.5 to 1 billion people worldwide [79]. The so called "Keshan disease", a potentially fatal form of cardiomyopathy (disease of the heart muscle), was first observed in the selenium-poor Keshan province in China [229]. The Keshan disease can be efficiently prevented by supplementation with 20 µg Se $day^{-1}$ [229] and the symptoms can be completely reversed by selenium supplementation [172; 229]. Recommended intakes for selenium vary within geographic regions between 30 and 85 µg Se $day^{-1}$ for men and 30 to 70 µg Se $day^{-1}$ for women, respectively [229]. Selenium supplementation can be completed by multivitamin tablets, containing either sodium selenite or selenomethionine from selenium enriched yeast [10; 204]. Selenium supply has to be controlled with great care, as the range between human dietary requirement and chronic toxicity levels (400 µg Se $day^{-1}$) stretches only by one order of magnitude [59].

If selenium supply falls below the optimal level of 50 to 100 µg Se $kg^{-1}$ dry forage feed, livestock can develop so called "white muscle disease" [13; 258], ultimately resulting in sudden heart failure by mineralization of the heart muscle (Figure 1.7). Deficiency can be counteracted by fertilization of selenium depleted soils [196] or by supplementation of livestock with selenium compounds and selenium accumulating plants [132; 171].

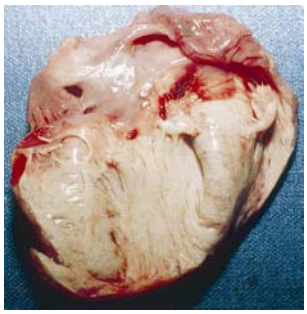

Figure 1.7 Chalky-white necrosis and mineralization of the heart muscles, symptoms of the "white muscle disease" in selenium deficient lambs [13]

## 1.4.2 Toxicity

The effects of selenosis in humans are typically dermal or neurological and comprise defective nails and skin, hair loss, unsteady gait and paralysis. Acute oral exposure to high selenium doses leads to nausea, vomiting and diarrhea and occasionally cardiovascular

symptoms [248]. Inhalation exposure to selenium compounds, esp. the highly toxic hydrogen selenide, results primarily in respiratory effects, including coughing, eyes irritation, headaches, vomiting, nausea bronchial spasms, bronchitis and chemical pneumonia [3; 248], but cardio vascular effects were also reported.

Only a few fatalities by acute selenium poisoning have been reported, mainly by ingestion of inorganic selenium compounds [10; 89; 208]. Consumption of *Lecythis ollaria* nuts led to several cases of acute selenium intoxication in Venezuela, marked by the death of an infant and vomiting and diarrhea followed by hair and nail loss in several adults [59]. In cattle and horses, alkali disease, a dystrophic change in hooves, is caused by high selenium concentrations in forage (5 to 50 mg Se $kg^{-1}$) and is the principal manifestation of chronic selenium toxicity [10; 171]. Especially grazing on selenium (hyper)accumulating plants, such as *Astragalus*, *Stanleya* or *Oonopsis*, that can contain up to 0.6% of their dry weight as selenium [75] can result in severe selenosis.

Little is known concerning the precise mechanism of selenium toxicity [248], but it has been speculated that it is associated with the generation of free radical species inducing DNA damage, and its reactivity with thiols, affecting integrity and/or function of DNA repair proteins [121]. The substitution of cysteine by selenocysteine can alter protein function, as at physiological pH the selenol group is ionized, displaying a higher reactivity in comparison to the protonated thiol [96]. Selenomethionine in contrast, does not significantly alter protein structure when substituting methionine, but may influence the activity of enzymes, if the seleno-aminoacid replaces its sulfur analogue in the vicinity of the active site [204], because the selenoether is more hydrophobic compared to the sulfur moiety.

In areas most affected by human selenosis [112] average soil selenium concentration can be as high as 26 mg Se $kg^{-1}$, although concentrations of only 3 mg Se $kg^{-1}$ in soil resulted in selenosis in some Chinese regions [224]. Thus, total selenium values are not an adequate indicator for selenium hazard, as the toxicity of selenium compounds greatly depends on its speciation [55; 171] and on bioaccumulation (section 1.4.3). For instance, *L*ethal *D*oses 50 ($LD_{50}$) can differ as much as factor 2680 between water soluble selenite ($LD_{50}$ = 2.5 mg Se $kg^{-1}$ body weight, oral administration, rat) compared to insoluble elemental selenium [248].

## 1.4.3 Ecotoxicological impact of selenium

In the aquatic environment, selenium poses its particular threat to wildlife due to its bioaccumulation (increased concentration in an organism compared to the surrounding medium) and biomagnification (increasing concentration by food chain transfer) potential. Accordingly, selenium concentrations in the tissues of lower invertebrates or fish can reach

concentrations up to 2000 times the selenium water concentration [270]. Plant tissue bioconcentration factors of more than 10,000 were observed comparing water to root selenium concentrations of *Typha angustifolia* in wetlands treating flue gas desulfurization waters [219]. It has been shown that adverse effects on fish can arise at a waterborne selenium concentration of 5 µg $L^{-1}$, but do not necessarily occur at higher concentrations [60; 73]. Consequently, the United States Environmental Protection Agency has proposed tissue concentration based chronic criterion values as a more appropriate measure for ecotoxicological risk compared to waterborne concentration based values [72; 243].

The most extensively examined case of selenium contamination on wildlife has been the incident in the National Wildlife Refuge Kesterson Reservoir, California, USA [73; 182]. In this case, weathering marine sedimentary rocks and seleniferous soils provided selenium rich irrigation water. Following concentration by evaporation, subsurface drainage water entered a series of ponds within the wildlife refuge at an average selenium concentration of 300 µg $L^{-1}$, yet in some acid seeps, the concentrations were as high as 4,200 µg Se $L^{-1}$ [106]. By exposure through e.g. water, detritus, plant material or aquatic prey, selenium contamination resulted in grave consequences for fish and water bird populations. A study of nesting birds found developmental abnormalities in 20% of all investigated nests, while more than 40% of the nests contained one or more dead embryos [163]. Furthermore, selenium caused deformities and reduced survival of different fish species, e.g. larval bluegills (*Lepomis macrochiros*).

Although the old drain was closed in 1986 and the former Wildlife Reserve was declared as a toxic waste dump in 1987 [180] selenium is still entering the adjacent San Francisco Bay Delta (Figure 1.8). Current forecasts predict selenium tissue levels to exceed guidelines despite the preventive scenario chosen (low, medium or high input via San Luis Drain) [182]. In the aftermath, the biogeochemical pathway that lead from the origin of selenium (weathering rock and soil) to high selenium tissue concentrations of aquatic birds and disastrous effects on ecosystem level, has since then been called the “Kesterson Effect” or simply “from rock to duck.” [180]. The Kesterson case and a vast list of other dramatic examples [73; 118] underline the need for the development of a feasible selenium removal technique.

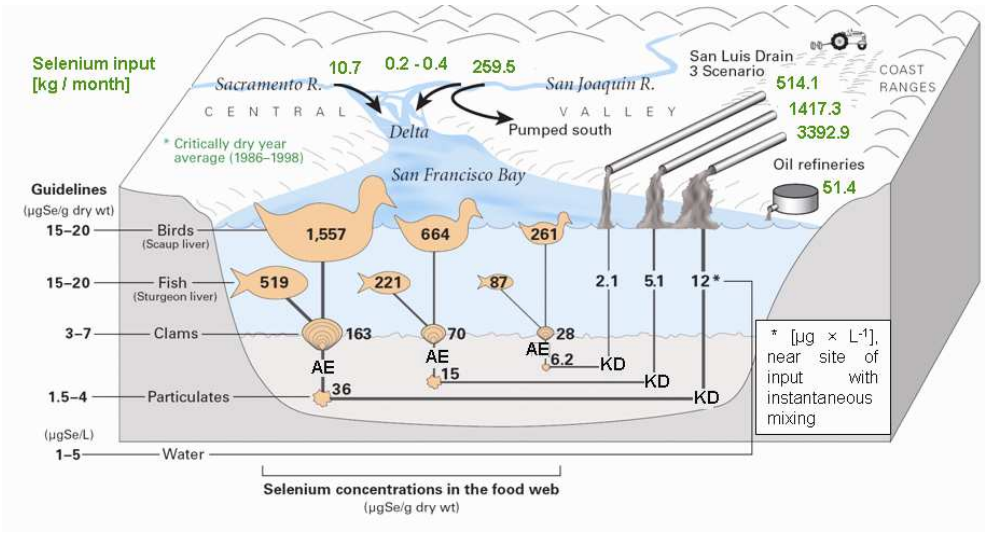


Figure 1.8 Forecast of selenium bioaccumulation in San Francisco Bay-Delta with 3 alternative loading scenarios by conveyance of agricultural drainage through the San Luis Drain, assuming a partitioning coefficient KD = ($\mu g\,Se \cdot kg^{-1}$ particulate) : ($\mu g\,Se \cdot kg^{-1}$ water) of 3,000 and bivalve assimilation efficiency [AE] of 0.55; modified after [182]

# 1.5 Treatment options for selenium removal from anthropogenic waste streams

Selenium containing waste streams are manifold in composition and differ in selenium concentration and speciation. Consequently, a variety of different physico-chemical, biological or combined treatment methods have been elucidated. Table 1.2 gives an overview of most applied treatment options. Regarding the achieved total selenium effluent concentrations, different approaches including filtration, adsorption and / or reductive processes appear promising.

## 1.5.1 Physical-chemical processes

### 1.5.1.1 Nanofiltration / reverse osmosis



Nanofiltration and reverse osmosis rely on separation processes on micropores (< 2nm) by hydrostatic pressure, rejecting particles as small as 1 nm and 0.1 nm, respectively [226], and have been applied in the treatment of selenium contaminated agricultural drainage waters [106; 139; 140]. Kharaka and coworkers estimated, that approximately 90 % of the agricultural drainage waters in the Kesterson Reservoir could be treated by nanofiltration regarding the achieved removal efficiencies [106]. High-rejection reverse osmosis membranes have been tested with multicomponent electrolyte solutions simulating pretreated agricultural drainage return water, achieving more than 99.5 % rejection for selenium oxyanions and 99% for nitrate [140]. These techniques are, however, expensive (Table 1.2) and limited by different constraints, such as gypsum precipitation observed at higher water recoveries [106]. Both filtration techniques generate only small volumes of concentrate, yet the total volume in case of agricultural drainage waters is still immense [182]. In addition, the oxyanions are not detoxified by reduction and the brines need to be disposed safely or further treated. Due to the low residual selenium concentrations, reverse osmosis techniques might be applied e.g. in the purification of drinking water.

### 1.5.1.2 Ion exchange

Different synthetic resins or natural materials (e.g. zeolites [60]) can mediate the electrostatic attachment of selenium oxyanions during ion exchange processes. Polyamine ion exchange resins can adsorb both selenite and selenate in a wide range of pH, but ion exchange of selenate faces a typical limitation of reduced adsorption ability in waste streams containing sulfate [160] (Table 4.1, Chapter 4). Although cheap, ion exchange is not applicable for most anthropogenic selenium containing wastewaters due to the insufficient selenium removal, but might be applied as pre-treatment to alternative removal techniques.

### 1.5.1.3 Ferrihydrite adsorption / precipitation

Adsorption and concurrent precipitation of selenate on ferrihydrite (Figure 1.9) has been tested in large scale for the treatment of groundwaters highly contaminated by mining activities (up to 10,000 µg Se $L^{-1}$ ) [240].

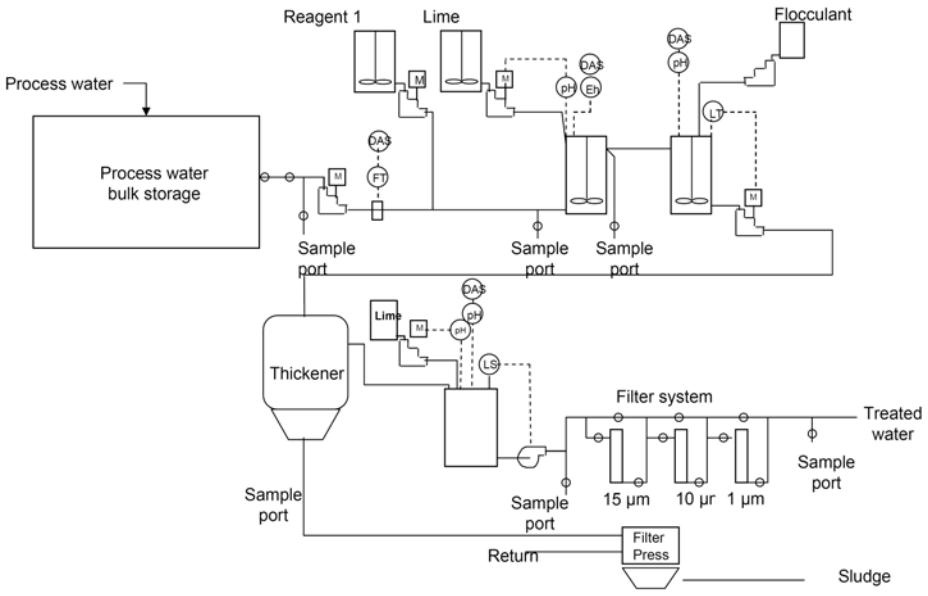


Figure 1.9 Ferrihydrite precipitation process flow scheme; modified after [240]

Yet, ferrihydrite precipitation achieved the set target values of <50 µg Se $L^{-1}$, substantial iron addition was required and technical prerequisites were high, resulting in high estimated annual operating and maintenance costs [240] (Table 1.2).

## 1.5.1.4 Chemical reduction by zero valent iron

Zero valent iron (ZVI) is a relatively inexpensive and moderately strong reducing agent [294] that has been applied recently in the treatment of different inorganic and organic contaminants [81; 151; 286; 290]. In lab-batch experiments ZVI removed selenate and selenite from different salt containing solutions [290], yet sulfate, phosphate and carbonate anions significantly reduced removal efficiencies [290], thus limiting the application to anthropogenic waste waters. Furthermore, a quick cementation of the catalyst with precipitates was observed [60], resulting in questionable long term performance [81]. The application of ZVI subsequent to a biological reduction step, however, showed promising results, both residual oxyanion and organic selenium compounds concentrations were reduced [294]. The removal of organic selenium compounds is of particular importance, as these can display a higher bioavailability [4].

Table 1.2. Summary of possible physical-chemical and biological treatment options to selenium contamination [20; 60; 64; 106; 139; 140; 161; 286; 290]

| | option | removal mechanism | $Se_{effluent}$ | costs [US $ × $m^{-3}$] | constraints | reference |
|---|---|---|---|---|---|---|
| **physico / chemical** | Nanofiltration | Filtration | ≥ 1 ppb | 0.71[1)] | TDS, operational costs, disposal of brines, fouling | Kharaka et al. (1996), Frankenberger et al. (2004). |
| | Reverse Osmosis | Filtration | ≥ 2 ppb | 0.79[1)] | TDS, operational costs, disposal of brines, fouling | Marinas et a. (1992), Frankenberger et al. (2004).; NSMP (2007) |
| | Ion exchange | Adsorption | ≥ 50 ppb | 0.06[1)] | Insufficient selenium removal, disturbed by sulfate, fouling | NSMP (2007) |
| | Ferrihydrite | Adsorption/ precipitation | ≥ 35 ppb | 3.96[1)]; 3.67[2)] | Costs, high iron addition | NSMP (2007), USEPA (2001) |
| | Zero Valent Iron | Reduction/ adsorption | < 4 ppb | n.a. | Disturbed by sulfate, phosphate, carbonate; long term efficiency ? | Zhang et al. (2005) |
| **biological** | Constructed wetlands | Reduction/ adsorption/ volatilization | ≥ 5 ppb | 0.26[1)] | Space and time requirement, exposure to wildlife | NSMP (2007) |
| | Anaerobic bacterial removal | Reduction | < 2 ppb | 0.40[1)]; 0.35[2)] | Cost electron donor | NSMP (2007), USEPA (2001) |
| | Algal-bacterial removal | Reduction | ≥ 32 ppb | 0.21[1)] | Increasing bioavailability, space requirement | NSMP (2007), Quinn et al. (2000) |
| | *Bacillus sp. SF-1* (Chemostat) | Reduction | < 50 ppb | n.a. | Tested under sterile conditions; selenite accumulation | Fujita et al. (2002) |
| | *T. selenatis* (Packed bed) | Reduction | ≥ 5 ppb | 0.2-0.62[3)] | Competitive bacterial growth, post treatment (coagulation) | Cantafio et al. (1996) |

[1)] costs for selenate and nitrate removal from agricultural drainage waters [161]

[2)] costs for treatment of mine waters (1.1 $m^3$ $min^{-1}$) [60; 240]

[3)] costs for treatment of agricultural drainage waters (0.51 $m^3$ $min^{-1}$) according to [20]

## 1.5.2 Biological Treatment

Biological conversions, i.e. uptake, reduction and volatilization processes have gained importance in the treatment of agricultural drainage waters and mine waters [161; 240], as they can reduce selenium to low target levels treating high waste water volumes. However, biological treatment utilizing "unspecific" enzymatic reductions, i.e. the reduction of selenate via sulfate [235] or nitrate reducers [193], faces a similar limitation of competitive inhibition by alternative anions [60] compared to adsorptive techniques.

### 1.5.2.1 Wetlands

Flow through or subsurface wetlands offer a relatively cheap, low tech option for selenium treatment of large volume wastewaters, thus have been applied to treat e.g. agricultural drainage waters [67] or flue gas desulfurization wastewaters [219]. Water soluble selenium is removed by different processes, such as uptake by plants (phytoextraction), volatilization by plants, fungi and bacteria and geochemical / microbial reduction [66; 143]. However, concerns of bioaccumulation and exposure to wildlife arise (section 1.4.3) and consequently selenium treatment in wetlands should be evaluated critically.

### 1.5.2.2 Algal-bacterial removal

The Algal-Bacterial Selenium Removal (ABSeR) system has been applied to avoid the commonly encountered competitive inhibition of nitrate on selenate reduction. In the ABSeR system, microalgae are grown in a first step to reduce nitrate concentrations, and subsequently the settled algal biomass is used as a carbon source for selenium reducing bacteria in a spatially separated treatment step (Figure 1.10) [4; 60; 69].

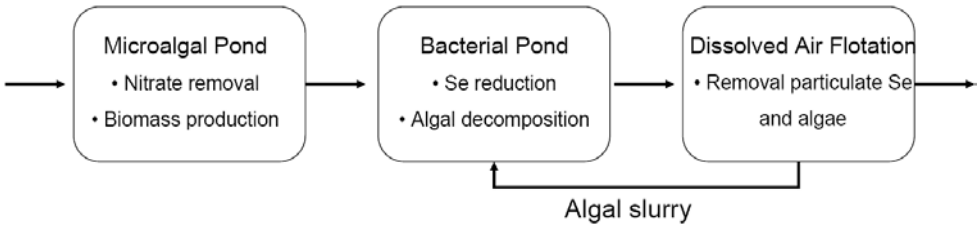


Figure 1.10 Flow scheme of algal-bacterial selenium removal (ABSR) technology operated in low cost modification; modified after [185]

The need for spatial separation of the two processes increases the capital and operational costs. High removal efficiencies are achieved only, when an external organic electron donor is added to the bacterial pond and dissolved air flotation combined with slow sand filtration is applied as a post treatment. A major problem arising is that the effluent displays increased bioavailability of selenium towards aquatic invertebrates [4]. As a result, the ABSeR treatment system is considered promising, yet leaving many possibilities for optimization.

### 1.5.2.3 Biological selenium removal using dissimilatory metal reducers

Selenium waters containing very high levels of selenium, e.g. such of selenium processing industries (620 mg Se $L^{-1}$) [64] might only be treatable by highly selenium-tolerant specialists [134], due to toxicity effects on other bacterial groups [84; 283]. Selenate concentrations of 41.8 mg Se $L^{-1}$ in a synthetic wastewater have been treated by a pure culture of *Bacillus* sp. SF-1 in a laboratory scale, completely mixed chemostat under excess of lactate. At elongated cell retention times (95.2 h) more than 99% of the selenate was reduced to elemental selenium under these idealized conditions, while lower retention times (48 h) resulted in selenite accumulation.

Agricultural drainage waters were treated in a pilot-scale reactor inoculated with *Thauera selenatis* using acetate as electron donor [20]. The reactor consisted of 4 packed bed tanks, filled with carrier hollow plastic spheres and silica sand (Figure 1.11A). Dissolved selenium was reduced efficiently to elemental selenium, suspended in the effluent with a concentration of 237 µg Se $L^{-1}$. Post treatment by coagulation reduced the effluent concentration further to an average of 12 µg Se $L^{-1}$. Difficulties regarding incomplete nitrate reduction and selenium removal (≤20%) were reported for the first 136 days of operation, due to the growth of flock forming bacteria other than *T. selenatis*.

Moving sand bed filters (Figure 1.11B) have been applied in the treatment of metal rich waste waters. They rely on the principle of microbially induced precipitation (i.e. sulfidic precipitation of heavy metals) within the sand coating biofilm and precipitate separation by subsequent turbulent mixing. In a pilot study, a sand filter inoculated (amongst others) with *Ralstonia metallidurans* (a selenite but not selenate dissimilatory reducing bacterium), removed selenium to ≥ 80% from non-ferrous industrial waste water [36]. When treated in fixed sand bed column with *Pseudomonas fluorescens* as inoculum, selenate concentration in such wastewaters was reduced from 2.6 to 0.5 mg $L^{-1}$ within 6 days of operation [230]. However, selenate reduction was hampered by the presence of 10 to 50 mg $L^{-1}$ nitrate.

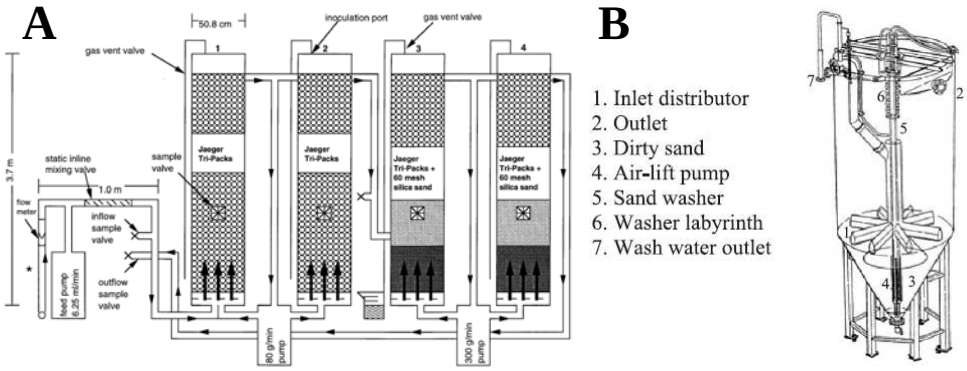


Figure 1.11A (A) Process flow scheme of the pilot scale bioreactor for treatment of selenium containing agricultural drainage water inoculated with *Thauera selenatis* [20] and (B) schematic overview of moving sand bed filter concept [36]

# 1.6 Outline of the thesis



Chemical speciation determines the environmental fate and toxicity of selenium. Therefore, selenium speciation has to be assessed by chemical analytical methods that are species specific and preserve the sample selenium speciation. Such methods for gas, liquid and solid phases are developed in chapter II and subsequently applied in the remaining chapters in order to close the selenium balances.

Chapter III establishes the basis for direct solid phase selenium speciation analysis by investigation of the X-ray Absorption Near Edge Structure (XANES). A large set of selenium model compounds, including models of all naturally occurring oxidation states is investigated. XANES spectroscopy is then applied to anaerobic biofilms after long term operation (115 days) under methanogenic and sulfate-reducing conditions.

Many waste streams contain sulfate and selenate concomitantly, thus sulfate reducers have been used in batch assays to remove selenate [84]. The observed removal success, however, might not be durable when selenate is fed continuously, due to the toxicity of selenate to sulfate-reducing bacteria [84; 283]. Furthermore the unspecific removal of selenate via sulfate-reducing enzymatic systems might be inhibited by the higher selectivity towards sulfate. Chapter IV presents experiments supplying an *U*pflow *A*naerobic *S*ludge *B*lanket (UASB) bioreactor with sulfate in excess to selenate and varying sulfate to selenate ratios. The selenate removal efficiency is compared to a control reactor operated under methanogenic conditions without sulfate in the feed.

For a sustainable process aiming at the recovery and reuse, it is desirable to form elemental selenium as the only product of reduction in large selenium particles that can be easily separated from the aqueous phase. Furthermore, the yield of elemental selenium during microbial treatment can be decreased by alkylation to volatile selenium compounds. Consequently, the particle size distribution of the formed precipitates and the loss by alkylated selenium species is investigated during long term (175 days) reactor operation in chapter V. Furthermore, the influence of disturbances in operational conditions, commonly occurring in full-scale applications (T, upflow velocity, and pH) on the latter processes is determined.

Sequential extraction methods are applied on a routine basis to assess selenium fractionation [32; 93; 269]. However, the susceptibility of both the matrix and the selenium speciation to ambient air oxidation induced during field sampling or subsequent extraction has so far been neglected. In chapter VI, a sequential extraction protocol was validated by

spiking experiments, and selenium speciation changes are investigated by XANES spectroscopy.

Although the treatment of selenium containing waters in anaerobic systems has been studied, the inhibitory influence of low (10 µM) and high (10 mM) selenium oxyanion concentrations on methanogenesis, the key process for feasible anaerobic digestion reactor operation [226], has so far not been addressed. Inhibition of selenate and selenite to acetotrophic and hydrogenotrophic methanogenesis is investigated in chapter VII, distinguishing permanent from transient effects.

Bioaugmentation – the addition of specialized microorganisms - has been tested in many different cases of environmental pollution [46; 149], but has so far not had a breakthrough due to the usually encountered wash out or out-competition of the added organisms by endogenous populations during continuous operation. In chapter VIII, a novel approach for bioaugmentation by immobilizing selenium-respiring bacteria (*Sulfurospirillum barnesii*) in non-degradable gels is tested in the treatment of agricultural drainage waters. The bioaugmentation success is evaluated by comparing selenate, nitrate and sulfate removal efficiencies to conventional UASB reactors. Furthermore, the performance of a hybrid sludge bed bioreactor, consisting of anaerobic granular sludge and gel immobilized specialists, is evaluated.

Chapter IX concludes this thesis with a critical evaluation on the applicability of biological reduction processes in the treatment of selenium contaminated anthropogenic waste streams.

# 2

# Analytical tools for selenium speciation

This chapter was published as: Lenz, M., Gmerek, A., Lens, P. N. L. (2006). Selenium speciation in anaerobic granular sludge. International Journal of Environmental Analytical Chemistry, 86 (9/10), 615-627.

# Abstract



Chromatographic (IC-CD, GC-FID) and spectroscopic (XRD) techniques that allow the specific determination of several selenium species present or formed during bioremediation processes of selenate contaminated drinking, ground or wastewaters have been established. The developed techniques are shown to be applicable in determining selenium species in the range of target concentrations for emissions and are thus appropriate to characterize bioremediation processes. The applied techniques offer advantages regarding short analytical times without loss of satisfactory accurateness towards more sophisticated methods. By means of IC-CD, selenate and selenite can be detected specifically to concentrations far below allowance levels for metal finishing industries (20 µg $L^{-1}$ selenate, 40 µg $L^{-1}$ selenite) within 16.0 minutes. Thus, the reduction of selenate by anaerobic granular sludge was quantified by IC-CD and the concomitantly formed, red colored precipitate was analyzed by XRD and ICP-OES. Hexagonal elemental selenium was indicated within the precipitate by the XRD analysis, but no metal selenides were detected, even if the precipitate contained iron and zinc as shown by ICP-OES. GC-FID method developed determines two major volatile selenium species - dimethylselenide and dimethyldiselenide - formed during bioremediation of selenium contaminated waters at a detection limit of 1 ng and 2 ng, respectively, without further chemical derivatization within 7.4 minutes, offering adequate detection by simple technical means.

# 2.1 Introduction



The toxicity of selenium compounds greatly depends on its speciation. For instance, *L*ethal *D*oses 50 ($LD_{50}$) for oral administration in rats are much lower for selenate (2.5 mg Se $kg^{-1}$ body weight) than for selenite (4.8-7.0 mg Se $kg^{-1}$ body weight) or for elemental selenium (6,700 mg Se $kg^{-1}$ body weight) according to the U.S. National Institute of Occupational Safety and Health [159]. Therefore, it is necessary to investigate the speciation of selenium during removal processes treating drinking, irrigation or wastewaters. However, the great variety of environmentally occurring selenium compounds poses a special challenge to speciation analysis, as selenium occurs in different oxidation states and both in organic and inorganic forms [141; 288].

As there is a legal need to reduce selenium emissions [14; 45; 248], different selenium removal processes have been developed [237] to remove selenium compounds from ground, irrigation and wastewaters. In general, anaerobic treatment processes offer advantages compared to aerobic treatment. Those advantages are lower sludge production, energy savings because of dispensable aeration, cost savings in nutrient supply, smaller reactor volumes and the possibility of energy recovery by methane production [226]. One well established reactor type in anaerobic treatment is the *U*pflow *A*naerobic *S*ludge *B*lanket (UASB) reactor (Figure 2.1). It shows potential for the treatment of selenium-contaminated wastewaters, as special bioconversions can occur [122] in the bacterial granules formed in these reactors [88].

In contrast to adsorptive or chemical precipitation methods for selenium removal [237], application of a UASB reactor also allows for the treatment of the organic fraction of contaminated waters. Therefore, granular sludge originating from a full scale UASB reactor was tested towards its remediation capacity for selenate under anaerobic conditions. The optimization of the selenate removal process should not only consider to form high amounts of pure elemental selenium, which forms a solid phase and thus can be removed from contaminated waters, but also aims to prevent the formation of other toxic selenium species (i.e. selenite, hydrogen selenide or seleno-aminoacids). Consequently, selenium should not be determined as total selenium, but species specific where possible. As selenium can be present in the liquid, solid and gas phase, analytical methods for each of these phases were developed in this chapter. It has to be stated that this chapter is not focused on lowering detection limits by applying hyphenated methods [238], but on the species-specific methods, that have a relatively simple instrumental requirement, yet are still appropriate to characterize selenium bioremediation processes.

# 2.2. Experimental

## 2.2.1. Instrumentation



The Ion-Chromatographic system consisted of a Dionex DX 600 (Bavel, The Netherlands), equipped with an IonPac AS19 column (4 mm x 250 mm), an EG40 online eluent generator (potassium hydroxide), an ASRS Ultra II suppressor and a conductivity detector (IC-CD). Alternatively, an IonPac AS17 column (2 mm x 250 mm) was used in the same system as well. The applied flows were 1.1 mL $min^{-1}$ (AS19) and 0.25 mL $min^{-1}$ (AS17). Sample loops of respectively 25 µL and 5 µL were used.

Gas-chromatographic analyses were performed on a Hewlett-Packard 5890 II series *G*as *C*hromatograph with a *F*lame *I*onization *D*etection (GC-FID) system. The column used for separation was a Chrompack CP-PoraBOND Q with an internal diameter of 0.53 mm, a length of 25 m and a film thickness of 10 µm (Varian, Middleburg, The Netherlands). Liquid samples of 1µL were injected using splitless injection mode (purge on at 1.5 min). Helium was used as carrier gas at an inlet head pressure of 80 kPa. The FID detector was operated at 235°C at a hydrogen flow of 42 mL $min^{-1}$ and airflow of 276 mL $min^{-1}$.

A Varian Vista-MPX Simultaneous *I*nductively *C*oupled *P*lasma *O*ptical *E*mission *S*pectroscopy (ICP-OES) system with CCD detector was used with a plasma flow of 15 L $min^{-1}$, auxiliary flow of 1.5 L $min^{-1}$ and a nebulizer flow of 0.9 L $min^{-1}$. The generator power was 1 300 W.

X-ray Diffraction Spectroscopy (XRD) was conducted with a PANalytical Expert Pro System (Almelo, Netherlands) by using nickel-filtered CuKα radiation (tube operating at 40 kV and 40 mA). The data were collected by using an automated divergence slit (5 mm irradiated length) and a 0.2 mm receiving slit.

## 2.2.2. Chemicals

Sodium selenate (SigmaUltra® grade), sodium selenite (99 %) and elemental selenium (99.999 %) were purchased from Sigma Aldrich (Steinheim, Germany). The anion standard for the IC measurement was provided by Dionex (Bavel, The Netherlands). A 1000 mg $L^{-1}$ selenate and selenite stock solution was prepared by dissolving the respective sodium salts in Millipore Milli-Q water. This stock solution was diluted and mixed with the anion standard. Subsequently, the accuracy of the mixed standards was verified via ICP-OES.

For the ICP-OES measurements, calibration standards were prepared by stepwise dilution of multielement ICP standard solutions under addition of appropriate amounts of selenium and sulfur ICP standards (Merck, Darmstadt, Germany).

Dimethylselenide (DMSe) and dimethyldiselenide (DMDSe) were purchased from Sigma-Aldrich as well. Standard solutions of the latter compounds were prepared by diluting standard-solutions in HPLC-grade methanol (LabScale, Dublin, Ireland). All other chemicals used were of analytical grade.



## 2.2.3 Source of biomass and experimental set up

Anaerobic granular sludge originating from a full-scale UASB reactor treating paper mill wastewater (Industriewater Eerbeek B.V., Eerbeek, The Netherlands) was tested towards its selenate removal capacity in both batch and continuous experiments. Both the physico-chemical [120] and microbiological [187] characteristics of this sludge have been well studied.

In batch tests, 0.5 g of wet sludge and 50 mL of mineral medium were put in a 125 mL glass serum bottle, sealed with a butyl rubber stopper and flushed with nitrogen. The bottles were placed onto a horizontal shaker (75 rotations $min^{-1}$) at 30 °C. The mineral medium was prepared in Millipore Milli-Q water after Stams et al. [215], but omitting sulfide, selenite and using a 40 mM $L^{-1}$ (mM) $PO_4^{3-}$ buffer at pH 7.0 ± 0.1 instead of the carbonate buffer. Lactate (20 mM) was used as electron donor. To monitor the bioconversions during incubation, liquid and gas phase samples were taken anaerobically ($N_2$ atmosphere) at regular time intervals. The solid phase was sampled upon termination of the experiments. All batch experiments were done in triplicate.

The UASB reactor (0.46 L working volume) was inoculated with the same anaerobic granular sludge, operated at pH 7.0, a superficial upflow velocity of 1 m $h^{-1}$ and a hydraulic retention time of 6 h. The design and operation of the UASB reactor (Figure 2.1) are described in detail by Omil et al. [165]. Lactate was used as electron donor at an organic loading rate of 5 g COD $L^{-1}$ $d^{-1}$. The selenate influent concentration was 10 µM. In order to trap volatile organic selenium compounds, the biogas was bubbled through ethylene glycol [124].

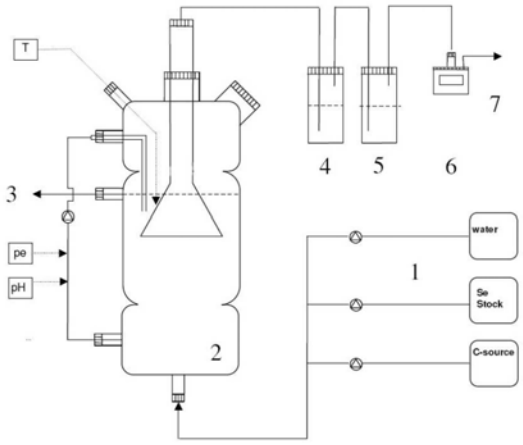


Figure 2.1 Schematic overview of an UASB reactor used for the simultaneous treatment of sulfate and selenate. (1) feed solutions, (2) UASB reactor, (3) effluent, (4) ethylene glycol trap, (5) NaOH trap, (6) gas meter, (7) gas outlet.

# 2.3. Results

## 2.3.1 Specific determination of selenate and selenite by IC-CD

Under the pre-requisite of achieving separation of a high number of major anions in short analytical times, a method has been developed, separating eight anions (fluoride, chloride, nitrite, bromide, nitrate, carbonate, sulfate and phosphate) from selenite and selenate in less than 22 minutes using an IonPac AS19 anion exchange column. The chromatogram for separation of the anion standard can be seen in Figure 2.2, the applied gradients in Table 2.1.

Table 2.1 IC-Gradient applied for columns AS19 and AS17

| Time [min] | Concentration Eluent AS19 [mM KOH] | Time [min] | Concentration Eluent AS17 [mM KOH] |
|---|---|---|---|
| 0 | 15 | 0 | 10 |
| 16.0 | 15 | 5.5 | 10 |
| 16.0 | 50 | 10 | 50 |
| 19.5 | 50 | 14 | 50 |
| 19.5 | 15 | 14 | 10 |
| 21.5 | end | 16 | end |

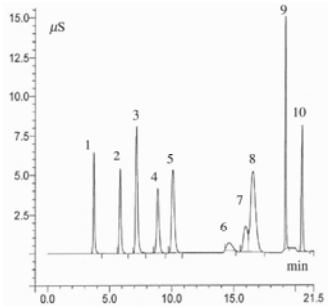


Figure 2.2 IC-Chromatogram showing separation of an anion standard by means of an IonPac AS19 column at [mg $L^{-1}$]: (1) $F^-$ 1.62, (2) $Cl^-$ 2.4, (3) $NO_2^-$ 7.9, (4) $Br^-$ 8.04, (5) $NO_3^-$ 8.10, (6) $CO_3^{2-}$ not quantified, (7) $SeO_3^{2-}$ 11.52, (8) $SO_4^{2-}$ 11.99, (9) $SeO_4^{2-}$ 9.79, (10) $PO_4^{3-}$ 12.33



The method quantification limits are 0.05 mg $L^{-1}$ for selenate (0.028 mg Se $L^{-1}$) and 0.25 mg $L^{-1}$ for selenite (0.138 mg Se $L^{-1}$). The method was used to show that anaerobic granular sludge is able to remove selenate from the liquid phase in the presence of nitrate / nitrite (initial nitrate concentration 5 mM, Figure 2.3).

In order to improve the separation of sulfate and selenite, an IonPac AS17 column was applied (Table 2.1), resulting in baseline separation of the two anions (compare peaks 6 & 8 in Figure 2.4 versus peaks 7 & 8 in Figure 2.2). The resulting method quantification limits were 0.04 mg $L^{-1}$ for selenite (0.025 mg Se $L^{-1}$) and 0.02 mg $L^{-1}$ (0.011 mg Se $L^{-1}$) for selenate. The reproducibility for 3 subsequent injections of selenate and selenite standards is given in Table 2.2.

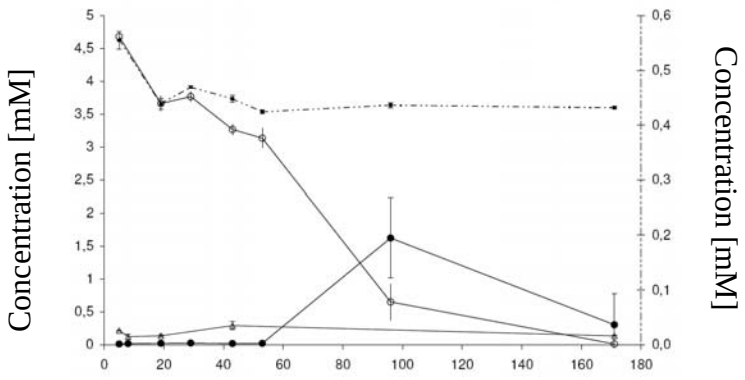


Figure 2.3 Bioconversion of 0.5 mM selenate and 5 mM nitrate by anaerobic granular sludge in batch incubation; nitrite (●), nitrate (○) and sulfate (Δ) in [mM] (primary y-axis), selenate (---) in [mM] (secondary y-axis). Concentrations were determined via IC-CD with column IonPac AS19

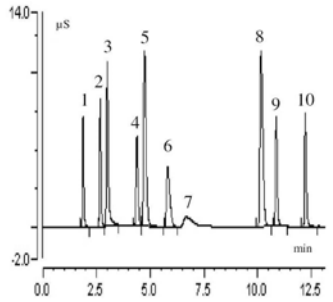


Figure 2.4 IC-Chromatogram showing separation of an anion standard (IonPac AS17 column) at [mg $L^{-1}$]: (1) $F^-$ 1.00, (2) $Cl^-$ 1.51, (3) $NO_2^-$ 5, (4) $Br^-$ 4.99, (5) $NO_3^-$ 5.00, (6) $SeO_3^{2-}$ 10.00, (7) $CO_3^{2-}$ not quantified, (8) $SO_4^{2-}$ 7.45, (9) $SeO_4^{2-}$ 5.00, (10) $PO_4^{3-}$ 7.45

Table 2.2 Reproducibility of the IC method (AS17 column) for 3 subsequent injections of the selenate and selenite standard

| compound | Reproducibility (R.S.D., %, n=3) | | | | Calibration (y= mx + b)* | | |
|---|---|---|---|---|---|---|---|
| | 0.05 ppm | 0.25 ppm | 2.5 ppm | 25 ppm | m | b | $r^2$ |
| Selenite | 7.1 | 1.4 | 0.9 | 0.4 | 0.0745 | -0.01 | 0.9997 |
| Selenate | 5.8 | 3.2 | 0.4 | 0.1 | 0.1406 | -0.003 | 0.9999 |

The applicability of the method under high sulfate conditions was shown by an exemplary determination of anions in the influent (A) and the effluent (B) of a continuous UASB reactor treating sulfate and selenate simultaneously (Figure 2.5).

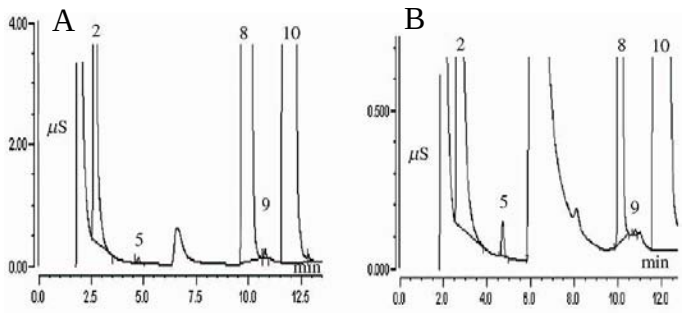


Figure 2.5 (A) Separation of anions (IonPac AS17 column) present in the influent of a in continuous reactor system treating selenate and sulfate at [mg $L^{-1}$]: (2) $Cl^-$ 336.15, (5) $NO_3^-$ 0.41, (8) $SO_4^{2-}$ 383.64, (9) $SeO_4^{2-}$ 1.03, (19) $PO_4^{3-}$ 3011; and (B) anions in the effluent at [mg $L^{-1}$]: (2) $Cl^-$ 330.19, (5) $NO_3^-$ 0.56, (8) $SO_4^{2-}$ 52.45, (9) $SeO_4^{2-}$ 0.15, (10) $PO_4^{3-}$ 2883

## 2.3.2 XRD and ICP-OES investigation of the bioprecipitate

Batch incubations of granular sludge were able to convert selenate at high concentrations (1.6 g $L^{-1}$ $Se_{total}$) removing significant amounts of selenate (262 mg $L^{-1}$) during 10 days of incubation under formation of a red precipitate (Figure 2.6 A, B). Subsequent to separation by centrifugation, the precipitate was washed two times with oxygen-free Millipore water under $N_2$ atmosphere. The formation of crystalline selenium phases within this precipitate was investigated using XRD (Figure 2.7 and Table 2.3).



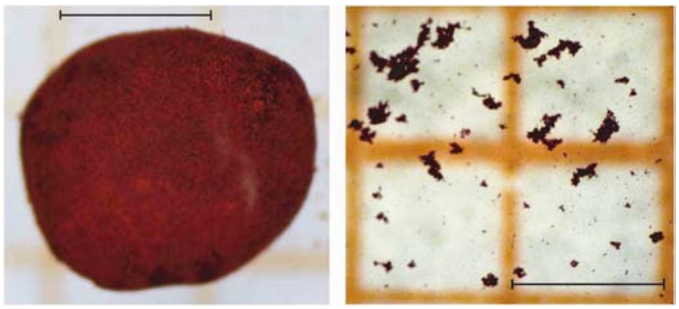

Figure 2.6 Reflected-light microscopic picture of an anaerobic sludge granule originating from batch culture treating selenate solutions (1.6 g $L^{-1}$ selenium) covered with red precipitate (A) and precipitate floating in mineral medium (B); bars correspond to 1 mm

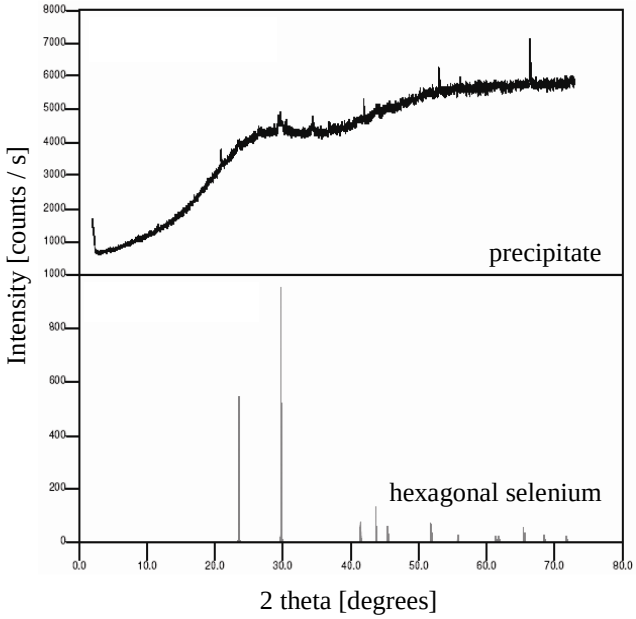


Figure 2.7 XRD diffractogram of the biologically formed precipitate (top) and the selenium standard of the hexagonal crystalline form (bottom)

Table 2.3 Peaks identified in XRD diffractogram (Figure 2.7 top), sorted by relative intensity; peaks indicating hexagonal elemental selenium (Figure 2.7 bottom) in bold

| Peak No. | d-spacing (Å) | Intensity (%) | Peak Height (counts/s) | Angle (°2Theta) | Background (counts/s) | d-spacing in hexagonal selenium | Relative Intensity in hexagonal selenium |
|---|---|---|---|---|---|---|---|
| 1 | 1.40755 | 100 | 544.89 | 66.357 | 2291.53 | | |
| 2 | 1.72646 | 53.9 | 293.67 | 52.996 | 2204.07 | | |
| 3 | 1.40405 | 48.4 | 263.54 | 66.544 | 2291.15 | | |
| 4 | 4.23787 | 41.5 | 226 | 20.945 | 1282.12 | | |
| **5** | **3.01206** | **32.5** | **176.8** | **29.634** | **1723.96** | **3.00** | **100** |
| 6 | 2.60293 | 29.2 | 159.04 | 34.426 | 1707.53 | | |
| 7 | 1.72238 | 29.0 | 157.84 | 53.131 | 2206.15 | | |
| 8 | 2.14948 | 25.8 | 140.34 | 41.999 | 1873.51 | | |
| 9 | 2.43621 | 16.0 | 87.3 | 36.864 | 1733.13 | | |
| **10** | **3.78129** | **15.6** | **84.75** | **23.508** | **1494.41** | **3.78** | **55** |
| 11 | 2.9256 | 15.5 | 84.28 | 30.531 | 1723.07 | | |
| **12** | **2.06361** | **10.3** | **55.99** | **43.835** | **1942.68** | **2.07** | **35** |
| 13 | 7.57447 | 8.1 | 44.03 | 11.673 | 544.3 | | |

Peaks number 5, 10 and 12 match with the 100, 101 and 102 plane of elemental selenium with a hexagonal crystalline structure in d-spacing, with minor differences on the second decimal place. Furthermore, the peak at an angle of 2θ =23.50° yields the highest relative intensity, 2θ= 29.63° shows the second highest and 2θ = 43.83° the lowest relative intensity. This is in accordance with the standard for elemental selenium. Further selenium planes could not be identified, as the baseline noise was too high.

In order to limit the number of minerals to be compared in detail with standard diffractograms, the precipitate was further studied. Elemental analysis by ICP-OES was conducted after microwave-assisted aqua regia destruction of the precipitate. Dry weights [%] of the investigated elements of the precipitate are shown in Table 2.4.

Table 2.4 Elemental composition of precipitate formed by anaerobic granular sludge (pH 7.0, 20 mM $SeO_4^{2-}$, 20 mM Lactate)

| Element | Dry-weight [%] |
|---|---|
| Se | 49.85 |
| Ca | 3.38 |
| Na | 1.94 |
| Mg | 0.88 |
| Fe | 0.27 |
| K | 0.13 |
| Zn | 0.02 |
| Ag, Cd, Co, Cu, Mn, Ni, S | < 0.007 |

Table 2.4 shows that iron and zinc are the only potential elements present in the precipitate in significant amounts that could form selenium minerals[11]. A comparison with the highest

intensity peaks of the standard diffractograms of dzharkenite ($FeSe_2$), achavalite (FeSe), mandarinoite ($Fe_2^{3+}Se_3O_9$ X $6H_2O$), stilleite (ZnSe) and sophiite ($Zn_2(SeO_3)Cl_2$) did not result in any matches with the sample investigated (maximum difference of 0.01 Å). Only peak number 6 is in accordance with the highest intensity peak of ferroselite ($FeSe_2$). As the second highest peak belonging to a d-spacing of 2.49 Å of ferroselite (85 % relative intensity) is completely missing in the sample, also ferroselite could not be shown to be present in the sample.



## 2.3.3 Optimization of a GC-FID method for DMSe, DMDSe determination

A Chrompack CP-PoraBOND Q column was used for separation of DMSe and DMDSe. No interference with the methanol peak was observed until a temperature of 140 °C, resulting in a retention time of 3.54 min for DMSe. For the resolution and detection of DMDSe, the temperature was subsequently increased at a maximal rate of 70°C $min^{-1}$ to 240 °C. To obtain a stable baseline, this temperature was not elevated further. The result was a short analytical time of 7.4 minutes (Figure 2.8), with detection limits (3 σ of blanc) of 1 ng total amount injected for DMSe and 2 ng for DMDSe, respectively.

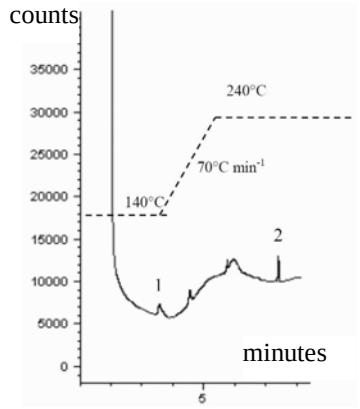


Figure 2.8 Separation of (1) DMSe (3.54 minutes) and (2) DMDSe (7.37 minutes) by GC-FID, injected amount 10 ng each. The dashed line represents the temperature program applied

Gas phase aliquots (50 mL) of the batch cultures were collected via syringe and carefully bubbled through 2 mL of methanol using a glass frit in order to pre-concentrate organic selenium compounds. The methanol extract was injected into the GC, but neither DMSe nor DMDSe could be detected. The ethylene glycol trap of the continuous bioreactor (Figure 2.1) was sampled after 30 days of biological selenate treatment by diluting different

amounts of ethylene glycol in methanol under addition of an internal standard; but neither DMSe nor DMDSe were detected using the developed method.

# 2.4. Discussion



## 2.4.1 Liquid phase analysis

Among the currently applied techniques for the determination of selenate and selenite, *H*ydride-*G*eneration coupled to *A*tomic *A*bsorption *S*pectroscopy (HG-AAS) [203] or ICP (HG-ICP) is commonly used (e.g. [188]). As the hydride formation is selective for the selenite, a quantitative reduction of selenate to selenite is required. This is disadvantageous, because of possible losses or incomplete chemical conversion between the selenium species. In contrast to this, ion-chromatography does not require species interconversion and has little sample preparation. Using the IonPac AS17 column as described in this work (Table 2.1), the analysis is completed in 16.0 minutes (Figure 2.4). Additionally, Ion Chromatography offers the possibility to determine a variety of other anions simultaneously, which is important to monitor remediation processes in bioreactors. Achieved method quantification levels were lower when applying the AS17 column due to the lower diameter compared to the IonPac AS19. Hence, the achieved method quantification limits allow monitoring of selenate and selenite as low as the µg $L^{-1}$ range, much lower (90 times for selenate and 40 times for selenite respectively) than the allowance levels for liquid effluents in metal finishing industries of 1 mg $L^{-1}$ $Se_{total}$ applied in some European countries (e.g. Germany) [14]. Hence, the developed IC methods have shown to be sufficient in determining selenium species in concentrations related to bioremediation processes. One future application for this IC method might be its adoption to other water-soluble oxyanions that can pose an environmental hazard, e.g. molybdate, chromate or uranates.

## 2.4.2 Solid phase analysis

Anaerobic granular sludge exposed to high concentrations of selenate (1.6 g $L^{-1}$ $Se_{total}$) formed a red precipitate during the removal of water-soluble selenate (Figure 2.6). This can be due to amorphous selenium (red in powder form) or crystalline monoclinic selenium (deep red) [148]. Trigonal selenium has a metallic grey color; amorphous selenium is black in vitreous form [148]. The total metal analysis via ICP-OES showed that 49.8 % (dry weight) of the formed precipitate is selenium, only minor fractions consist of iron and zinc (Table 2.4). Thus, the formation of stable metal selenides with silver, cadmium, cobalt and

copper in significant amounts is not indicated by ICP-OES, limiting the number of possible compounds formed.

In the subsequent XRD analysis, it was indicated that a minor part of the precipitate is elemental selenium with a hexagonal crystalline structure. The obtained diffractogram (Figure 2.7 & Table 2.3) showed a high baseline noise and small signal for crystalline selenium. This can be due to the small amount of precipitate investigated or the low content of crystalline selenium in the sample. However, the d-spacing characteristic for hexagonal selenium could be identified in the diffractogram with differences of 0.01 Å to the selenium standard. Monoclinic red elemental selenium was not indicated to be present. As insoluble metal selenides can be formed under reducing conditions [248], standard diffractograms of 6 minerals containing iron and zinc were compared to the sample (see section 2.3.2). The standard peaks could not be matched to the peaks obtained in the precipitate. However, the high baseline noise hinders to safely exclude their formation. Both the formation of these metal selenides and the crystalline forms of selenium need further investigation. Higher amounts of precipitate (some mg) would be appropriate to further confirm the formation of hexagonal selenium. Such higher amounts of precipitate could be produced by a continuous bioreactor equipped with a settler.

As XRD analysis is not suitable for the confirmation of elemental selenium at a high number of samples, it is a future goal to find applicable methods that give an indication of selenium binding forms in the solid phase. Combining fractionation methods like sequential extraction schemes with the determination of ‘acid volatile selenium’ could be well suited. Unlike ‘acid volatile sulfur’ fractionation, which is commonly used to characterize sulfur-binding forms [186], its analogue ‘acid volatile selenium’ still needs to be developed and validated using reference materials.

### 2.4.3 Gas phase analysis

Dimethylselenide and dimethyldiselenide represent two major volatile organic selenium species in the environment [101]. The formation of methylated compounds by plants and associated bacteria is used in large-scale bioremediation projects [253]. In the methods developed by Hunter et al. [90], interferences of dimethylselenide and dimethyldiselenide with the methanol injection peak were encountered, resulting in limitations for the detection limit. The authors used two single injections in order to analyze the latter compounds. In the present work, these problems have been overcome by the substitution of the used Porous Layer Open Tubular (PLOT) column by a recently developed Chrompak Capillary CP-Pora Q column and applying an appropriate temperature program (Figure 2.8). Thus,

the application range for the determination of DMSe and DMDSe was enlarged by the resulting lower detection limits (5 and 2.5 times, respectively). The method was applied both to batch cultures treating high selenate loads and in the continuous bioreactor system, but neither DMSe nor DMDSe could be detected. The method represents, nevertheless, a simple technique to analyze two main products of selenium biomethylation. In order to rule out the formation of these compounds, the detection limit can be lowered from the nano-gram range to pico-gram range by using a photo-ionization detector [90]. The adaptation of the GC-FID method to other organic selenium compounds, e.g. diethyldiselenide or mixed selenium sulfur compounds [21; 146], enlarging the spectrum of possibly formed volatile organic selenium species, is promising.

# 3

# Selenium speciation in anaerobic granular sludge studied by XAFS

This chapter was published in shortened form as: Van Hullebusch, E., Farges, F., Lenz, M., Lens, P., G. E. Brown, Jr. (2007). Selenium Speciation in Biofilms from Granular Sludge Bed Reactors Used for Wastewater Treatment. AIP Conference Proceedings 882, 229 – 231.

# Abstract

X-ray absorption fine structure (XAFS) spectroscopy offers the possibility of assessing selenium solid phase speciation in a direct, non-destructive way. XAFS is particularly suited for the investigation of selenium bioprecipitates, as it does not require crystallinity of the analyte, in contrast to classical techniques such as XRD. In this chapter, the basis for speciation analysis was established by investigating XANES (X-ray Absorption Near-Edge Structure) spectra in a large set of model compounds with natural and synthetic origin, including previously neglected Se (-I) selenides. It was demonstrated that no simple relation between the selenium oxidation state and the selenium K-edge position or the first inflection point is found. However, using both features in combination allows identification of the selenium oxidation state and coordination environment. XANES spectroscopy applied biofilm samples from methanogenic and sulfate-reducing upflow anaerobic sludge blanket (UASB) bioreactors indicated the presence of trigonal elemental selenium. However, EXAFS (Extended X-ray Absorption Fine-Structure) analysis elucidated that selenium is present in a yet unknown modification due to the different short-range structure.

# 3.1. Introduction



Due to the disastrous effects on wildlife [73; 270], different approaches have tried to convert water soluble selenium forms into elemental, bio-unavailable form. However, the end products of these biological reductions may be not restricted to elemental selenium, solely, and include highly toxic aqueous selenide [82; 84], bioavailable organo-selenium compounds (i.e. seleno-amino acids)[216] or volatile alkylated compounds [24; 62] (Chapter 5). Furthermore, UASB reactors represent strongly reducing, metal rich environments, thus thermodynamically stable and insoluble metal selenides [i.e. Se (-I) and Se(-II)] can form [207]. As a result, significantly different environmental fate for these compounds in comparison to elemental selenium has to be expected; thus a precise determination of selenium solid phase speciation is necessary.

X-ray absorption fine structure (XAFS) spectroscopy can be used to elucidate the oxidation state and coordination environment in a non-destructive and direct way. Yet, the precise determination of the speciation requires the careful analysis of a sufficiently large set of model compounds, especially when applied to such complex samples as selenate reducing anaerobic granular sludges. In this chapter, members of all environmentally occurring formal oxidation states of selenium have been investigated regarding their X-ray Absorption Near-Edge Structure (XANES) spectra at the selenium K-edge. The compounds investigated include less studied Se(-I) selenides, organic selenium compounds and metal selenides of natural and synthetic origin. Using this large database of model compounds, the speciation of selenium accumulated in anaerobic granular sludge operated in lab-scale UASB reactors under stable, long-term methanogenic and sulfate-reducing conditions was determined.

# 3.2. Materials and methods

## 3.2.1 Source of biofilms

Two lab-scale (0.46 L operating volume) UASB were operated as described in Chapter 4 under mesophilic (30 ± 1°C) conditions with a superficial liquid upflow velocity of 1 m $h^{-1}$. One reactor (SR-R) was operated under sulfate-reducing conditions, while another reactor (MG-R) was methanogenic (without sulfate in the feed). Sludge samples were harvested after 115 days of operation at a selenate loading rate of 3.16 mg Se $L^{-1}$ $d^{-1}$. Selenium had accumulated to 81 and 189 µg Se $g^{-1}$ (wet weight) in SR-R and MG-R, respectively.

### 3.2.2 XANES spectroscopy

XAFS experiments were performed *in-situ* (i.e. in anoxic conditions) at the beamline 11-2 (SSRL, Stanford, USA), at the Dubble beamline (ID 26, ESRF, Grenoble, France) and at the MicroXAS beamline (X05, SLS, Villingen, Switzerland). At SSRL and ESRF, focused beams (~0.2 x 0.5 mm and ~ 0.2 x 3 mm, respectively) were used to obtain systematic "bulk" XANES information, while at the SLS, a microfocused beam (~ 3 x 3 $\mu m^2$) was used to collect µ-XANES spectra on selected areas of the samples. No photoreduction due to the X-ray beam was observed during the measurements.



A series of selenium model compounds (natural and synthetic, all in solid state and powdered) with variable oxidation states were studied. Table 3.1 lists their origin, their formal oxidation state and the main features (main edge crest or "white line" and first inflection point) of the XANES spectra recorded. Model mineral compounds were verified using a Gandolfi-type micro X-ray diffraction (µ-XRD) built at the Museum National d'Histoire Naturelle (MNHN), Paris, France [173].

## 3.3. Results

### 3.3.1 XANES calibration for the oxidation state in selenium compounds

Sodium selenate (+VI) and sodium selenite (+IV) showed the highest energies regarding the position of the first inflection point and main edge crest (Figure 3.1A, Table 3.1).

The α-red polymorph of elemental selenium is distinguished by a difference of +0.4 eV form both the vitreous black and trigonal polymorph, while all polymorphs displayed clearly different first inflection points (Table 3.1). Isometric-diploidal Se(-I) compounds (penroseite, krutaite) displayed nearly identical main edge crests and first inflection point positions in their XANES spectra and were thus clearly different from orthorhombic-dipyramidal Se (-I) ferroselite (shift of +0.7eV in main edge crest and ~ + 1.0 eV in the position of the first inflection point ) (Table 3.1, Figure 3.1A). Cubic Se(-II) compounds were shifted up to + 4.6 eV in the main edge crest and up to +3.1 eV in the first inflection point compared to dihexagonal-dipyramidal forms (berzelianite versus achavalite and klockmannite) (Table 3.1, Figure 3.1B).

Table 3.1 Selenium model compounds studied with main edge crest and first inflection points of the XANES spectra spectraspectra.

| specimen | chemical formula | origin | formal oxidation state | crystal system | space group | main edge crest [ eV ] | first inflection point [ eV ] |
|---|---|---|---|---|---|---|---|
| Achavalite | FeSe | synthetic | -II | Dihexagonal Dipyramidal | P 6/mmc | 12662.3 | 12659.9 |
| Klockmannite | CuSe | synthetic | -II | Dihexagonal Dipyramidal | P 6/mmc | 12662.3 | 12660.0 |
| Selenocysteine | $C_3H_7NO_2Se$ | synthetic | -II | - | - | 12663.4 | 12660.7 |
| Sodium selenide | $Na_2Se$ | synthetic | -II | Cubic | F m3m | 12665.8 | 12661.1 |
| Stilleite | ZnSe | synthetic | -II | Cubic | F 43m | 12665.7 | 12662.9 |
| Berzelianite | $Cu_2Se$ | Czech Republic | -II | Cubic | F 43m | 12666.6 | 12663.0 |
| Berzelianite | $Cu_2Se$ | Sweden | -II | Cubic | F 43m | 12666.9 | 12662.9 |
| Penroseite | $(Ni,Co,Cu)Se_2$ | Bolivia | -I | Isometric – Diploidal | P a3 | 12662.1 | 12659.9 |
| Krutaite | $CuSe_2$ | Bolivia | -I | Isometric – Diploidal | P a3 | 12662.1 | 12659.8 |
| Ferroselite | $FeSe_2$ | Utah (USA) | -I | Orthorhombic – Dipyramidal | P nnm | 12662.8 | 12660.9 |
| Red α-monoclinic $Se^0$ | Se | synthetic | 0 | Monoclinic | P 2/n | 12662.1 | 12659.5 |
| Black, vitreous $Se^0$ | Se | synthetic | 0 | Amorphous | - | 12662.5 | 12660.0 |
| Grey $Se^0$ | Se | New Mexico (USA) | 0 | Trigonal | P 321 | 12662.5 | 12661.1 |
| Sodium Selenite | $Na_2SeO_3$ | synthetic | +IV | Monoclinic | P 2/c | 12667.3 | 12664.1 |
| Sodium Selenate | $Na_2SeO_4$ | synthetic | +VI | Orthorhombic | F ddd | 12670.8 | 12667.9 |
| Sample SR-R | | sulfate reducing reactor | | | | 12662.5 | 12660.6 |
| Sample MG-R | | methanogenic reactor | | | | 12662.5 | 12660.5 |

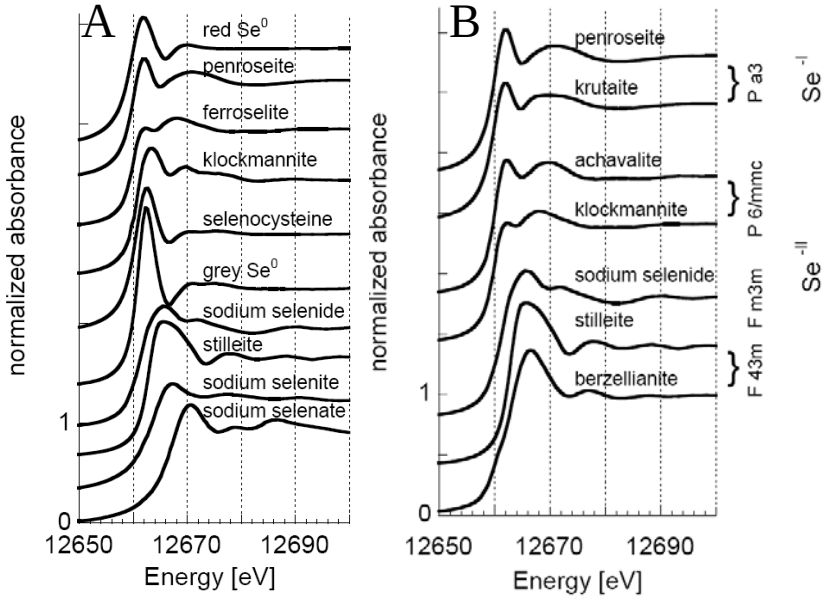


Figure 3.1 Normalized selenium K-Edge XANES of selected model compounds (A) with (B) highlighting differences in XANES between different formal oxidation states and crystal space groups

Within the cubic Se(-II) compounds, a shift was observed in the first inflection point of the XANES spectra considering different mineral space groups, i.e. F 43m and F m3m. Minerals with F 43m were clearly shifted in comparison to sodium selenide with F m3m space group (+1.8 eV) (Figure 3.1B). Selenocysteine was clearly different from all other Se (-II) compounds regarding both features.

## 3.3.2 Selenium speciation in anaerobic granular sludge

The biofilm samples showed the same main edge crest and virtually identical first inflection point positions (± 0.1 eV), yet a higher relative intensity of the white line in SR-R compared to MG-R was observed (Figure 3.2A). The first inflection points of the biofilm samples were comparable to trigonal elemental selenium, ferroselite and selenocysteine (Figure 3.2A), while the main edge crest position was identical to trigonal or vitreous elemental selenium (Table 3.1, Figure 3.2B). A shift of -0.2 and 0.3 eV in the latter feature was found in comparison to achavalite and ferroselite (Table 3.1, Figure 3.2A).

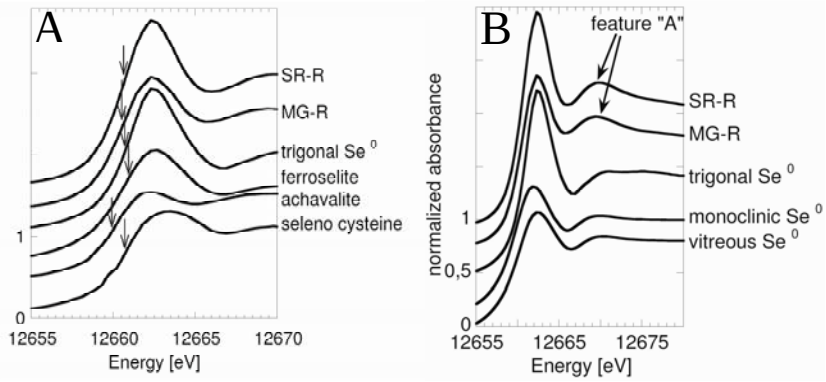




Figure 3.2 Selenium K-edge XANES of sulfate-reducing (SR-R) and methanogenic UASB reactor (MG-R) sludge samples treating selenate. Comparison to selected selenium model compounds (first inflection point marked by arrows) (A) and different elemental selenium polymorphs (B) (feature "A" exclusively present in the bioreactor samples)

Linear combination using the least square approach yielded best fits for SR-R by the exclusive contribution of trigonal elemental selenium. MG-R selenium speciation was mainly described by trigonal elemental selenium with a minor contribution of selenocysteine (14 atom %), whereas selenides contributed less (<10 atom %) to the modeled XANES spectrum. The combined modeled signals were well representing the course of the absorption edge, yet the first oscillation (feature "A") was poorly fitted (Figure 3.3A) and not present in the elemental model compounds (Figure 3.2B).

The Fourier Transform (FT) of the EXAFS spectra (Figure 3.3B) showed Se-Se pairs near 2.05 Å for both elemental selenium model compounds and biofilm samples (uncorrected for backscattering phase-shifts), whereas the second neighbor Se-Se pairs located at 3.05 and 3.35 Å were exclusively found for the trigonal and monoclinic polymorphs of elemental selenium, respectively.

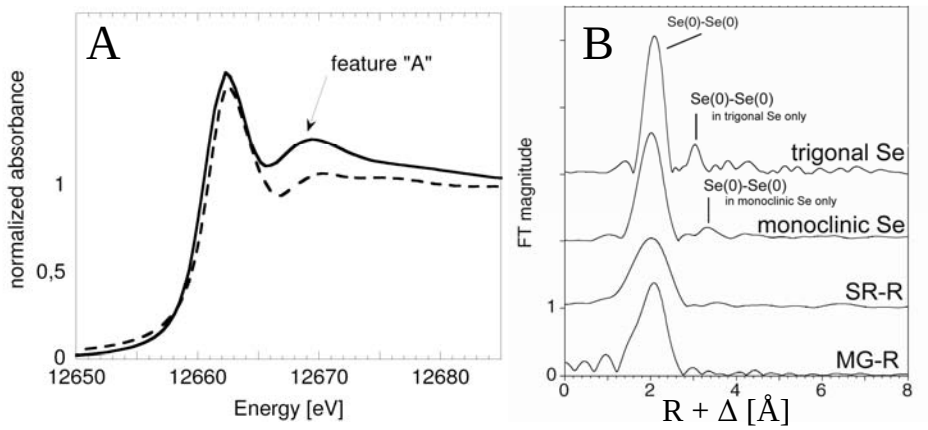


Figure 3.3 Normalized Se K-edge XANES spectrum for the methanogenic UASB sludge sample (MG-R) and best fit by linear combination to model compounds (dashed line) (A); Fourier Transforms of the EXAFS spectra (SR-R = sulfate-reducing UASB sludge sample) (B)

# 3.4 Discussion

This chapter shows that the main edge crest ("white line") position and the first inflection point should be used in combination to assure a safer determination of the selenium oxidation state by XANES, as different valences can show an identical main edge crest or first inflection point (Table 3.1, Figure 3.1A and B), due to interferences from the signals arising from the local geometry interactions. In contrast to sulfur K-edge XANES [92], a shift of these features to lower energies does not imply a further reduced oxidation state [e.g. red α-monoclinic Se (0) showed the lowest main edge crest and inflection point, Table 3.1]. Nevertheless, selenate (+VI) and selenite (+IV), members of the highest oxidation states, showed these features at higher energies, in agreement with a number of previous studies [175; 191; 200].

In the past, numerous studies have based the determination of the selenium oxidation state exclusively on either the "white line" position [18; 104; 137; 154; 162; 200] or the first inflection point [162; 191; 192; 209]. However, the present set of model shows that this protocol requires major adjustments, especially if the sample is complex, i.e. rich in metals (such as anaerobic granular sludge). In such cases, the determination of selenium speciation should be based on using both features and supported by applying linear combination speciation modeling with a sufficiently large set of selenium model compounds [especially often neglected Se(-I) selenides]. Using both features allows differentiating between crystal space groups of same oxidation state, e.g. between sodium selenide versus stilleite / berzelianite

and versus achavalite / klockmannite (Table 3.1, Figure 3.1B). This confirms that the selenium K-edge XANES positions (inflexion point and edge crest maximum) can be used to derive valence information for selenium, yet these features are also influenced by the selenium local-geometry. The use of the main edge crest relative intensity to determine oxidation states of selenium at the K-edge [201] works well on iron selenides, but is here demonstrated not to work on copper selenides (Figure 3.1A, B). Therefore, this method must be discarded.



Regarding the main edge crests and the first inflection point positions solely, the selenium speciation in the bioreactor samples can be assigned to trigonal grey selenium, although contribution of Se(-I) (ferroselite related compounds) cannot be excluded (both features shifted by only 0.3 eV). Both selenate and selenite have significantly different XANES (Table 3.1, Figure 3.1A) and do thus not contribute to the speciation in the sludges.

For the SR-R sample, the linearly combined modeled speciation indeed showed exclusively the contribution of trigonal grey selenium, whereas the speciation in MG-R includes a contribution of Se(-II) selenides. This apparent difference can be explained by the high dissolved sulfide concentration in SR-R (127 mg $S^{2-}$ $L^{-1}$ on day 115 of operation, Figure 4.2A, Chapter 4), resulting in sulfidic metal precipitation [49; 195], depleting the aqueous phase from metal cations. MG-R in contrast did not receive sulfate in the feed, consequently metal cations can be provided via the influent (amongst others 7.5 µM iron; 0.5 µM zinc; 0.1 µM copper), resulting in minor amounts of selenium precipitating as insoluble metal selenides.

Although main edge crests / inflection point and linear combination indicated trigonal elemental selenium, the EXAFS FT did not show the second selenium neighbors in the bioreactor samples observed in this model compound (Figure 3.3B). Furthermore none of the investigated elemental selenium standards corresponded with the first oscillation (Feature A, Figure 3.2B) that was observed in both bioreactor samples. Based on the XANES, EXAFS FT and linear combination information, it is suggested that selenium is present in the samples SR-R and MG-R dominantly as some aperiodic form of elemental Se (0) not included in the model compound database. Such a aperiodic form might be red amorphous selenium[148], due to the optically observed color and the lack of a XRD signal for crystalline selenium.

It can be concluded that sludges from both sulfate-reducing and methanogenic UASB reactors represent an efficient sink for water soluble selenium species (selenate, selenite) by forming either elemental selenium or metal selenides. In the future, especially spatially resolved studies using nano-focused beams should be applied, as precise determination of selenium speciation can be hampered by contribution of several species to the XAFS

signals. Scanning transmission x-ray microscopy (at the selenium L-edge) offers a great potential as a spatial resolution better than 50 nm can be achieved [276] and samples are prepared as thin sections, avoiding the contribution of several layers with different selenium speciation.

# 4

# Selenate removal in methanogenic and sulfate-reducing upflow anaerobic sludge bed reactors

This chapter was published as: Lenz, M., Van Hullebusch, E., Hommes, G., Corvini, P. F. X., Lens, P. N. L. (2008). Selenate removal in methanogenic and sulfate-reducing upflow anaerobic sludge bed reactors. Water research 42 (8/9), 2184-2194.

# Abstract

This chapter evaluates the use of Upflow Anaerobic Sludge Bed (UASB) bioreactors (30°C, pH= 7.0) to remove selenium oxyanions from contaminated waters (790 µg Se $L^{-1}$) under methanogenic and sulfate-reducing conditions using lactate as electron donor. One UASB reactor received sulfate at different sulfate to selenate ratios, while another UASB was operated under methanogenic conditions for 132 days without sulfate in the influent. The selenate effluent concentrations in the sulfate-reducing and methanogenic reactor were 24 µg Se $L^{-1}$ and 8 µg Se $L^{-1}$, corresponding to removal efficiencies of 97% and 99%, respectively. XRD analysis and sequential extractions showed that selenium was mainly retained as elemental selenium in the biomass. However, the total dissolved selenium effluent concentrations amounted to 73 and 80 µg Se $L^{-1}$, respectively, suggesting that selenate was partly converted to another selenium compound, most likely colloidally dispersed $Se^0$ nanoparticles. Possible intermediates of selenium reduction (selenite, dimethylselenide, dimethyldiselenide, $H_2Se$) could not be detected. Sulfate reducers removed selenate at molar excess of sulfate to selenate (up to a factor of 2600) and elevated dissolved sulfide concentrations (up to 168 mg $L^{-1}$), but selenium removal efficiencies were limited by the applied sulfate loading rate. In the methanogenic bioreactor, selenate and dissolved selenium removal were independent of the sulfate load, but inhibited by sulfide (101 mg $L^{-1}$). The selenium removal efficiency of the methanogenic UASB abruptly improved after 58 days of operation, suggesting that a specialized selenium converting population developed in the reactor. This chapter demonstrates that both sulfate-reducing and methanogenic UASB reactors can be applied to remove selenate from contaminated natural waters and anthropogenic waste streams, e.g. agricultural drainage waters, acid mine drainage and flue gas desulfurization bleeds.

# 4.1. Introduction

During the last decades, the hazards associated with selenium contaminated aqueous streams became a matter of public and scientific attention [73; 270]. Selenium substitutes for sulfur due to chemical similarities [28] and is thus present in sulfide ores of e.g. copper and lead/zinc mines [19]. Smelting of these ores in refining factories constitutes an important anthropogenic source of selenium in the environment [40]. During the combustion of selenium-bearing coal [27] in power plants, selenium contaminates either the flue gas or fly ash [272], thus leading to selenium pollution by direct emission or uncontrolled leaching [169]. The selenium concentrations in flue gas desulfurization (FGD) scrubber liquids vary between 0.5 and 2 mg $L^{-1}$, with high amounts of sulfate (815 to 4,730 mg $L^{-1}$) simultaneously present [22]. In nature, the oxidation of selenium-containing pyrite leads to high selenate and sulfate concentrations in ground waters [39] and acid mine drainage (AMD). Acid seeps in the Moreno Shale (United States) contained up to 420 µg $L^{-1}$ selenium and 12,500 mg $L^{-1}$ sulfate [181]. While AMD waters are generally well characterized concerning heavy metal concentrations, their selenium contamination is only rarely reported (Table 4.1).



Table 4.1 Overview of sulfate and selenate concentrations in selenium contaminated waste streams [22; 48; 144; 181; 210; 212]

| Waste stream | $SO_4^{2-}$ [mM ] | $SeO_4^{2-}$ [mM ] | Ratio $SeO_4^{2-}$ / $SO_4^{2-}$ [mM/mM] |
|---|---|---|---|
| Acid mine drainage | 19.6 | $2.0 \times 10^{-4}$ a) | $1.0 \times 10^{-5}$ |
| | 78.4 | $7.2 \times 10^{-4}$ a) | $9.2 \times 10^{-6}$ |
| | 28.4 | $2.5 \times 10^{-4}$ a) | $8.9 \times 10^{-7}$ |
| | 11.9 | $6.2 \times 10^{-3}$ a) | $5.2 \times 10^{-4}$ |
| | - | $2.8 \times 10^{-4}$ a) | - |
| Acid seeps (Moreno shale, USA) | 130.2 | $5.3 \times 10^{-3}$ | $4.1 \times 10^{-5}$ |
| | 359.4 | $2.5 \times 10^{-3}$ | $6.9 \times 10^{-6}$ |
| FGD purge waters | 8.5 | $6.8 \times 10^{-3}$ | $8.0 \times 10^{-4}$ |
| | 49.2 | $2.6 \times 10^{-3}$ | $5.3 \times 10^{-5}$ |
| | - | $3.8 \times 10^{-3}$ to $5.1 \times 10^{-2}$ | - |

a) given in reference as total selenium

Water-soluble forms of selenium can be microbiologically converted to elemental selenium, providing energy for the growth of specialized bacteria [205]. Elemental selenium is less bioavailable and generally less toxic than other selenium species, although e.g. bivalves can

assimilate elemental selenium produced in sediments [131]. Furthermore, elemental selenium is a solid that can potentially be separated from the aqueous waste stream. This separation is particularly important, as re-oxidation of elemental selenium can occur under oxidizing environments [291] when leaving the treatment system. The low levels of selenium negatively affecting the environment [270], the often high ratios of sulfur to selenium oxyanions (Table 4.1) and the poor adsorptive / precipitative properties of selenate [237] offer a promising niche for the simultaneous treatment of selenate and sulfate in bioreactors. Bioreactors have so far been mainly evaluated to treat nitrate rich agricultural drainage waters [170]. In previous studies, anaerobic granular sludge was shown to be a potent inoculum for selenium bioreduction (Chapter 2) [5] converting high selenate concentrations (up to 20 mM) with different electron donors to elemental selenium precipitates. In order to validate these results obtained by batch experiments and to assess the potential of further technical applications, continuous upflow anaerobic sludge bed (UASB) bioreactor systems were investigated in this chapter. The bioreactor operation was evaluated by determining commonly occurring selenium species in the gas, liquid and solid phase. Also the sulfate-reducing and methanogenic performance of the reactors was assessed. The metabolic, microbial and mineralogical properties of the sludges that developed in both UASB reactors were characterized as well.



# 4.2. Materials and Methods

## 4.2.1 Source of biomass

The inoculum of the UASB reactors, anaerobic granular sludge (100 g wet weight), originated from a full scale UASB reactor treating wastewater of four paper mills (Industriewater Eerbeek B.V., Eerbeek, Netherlands). This inoculum has been described in detail by Roest et al. [187].

## 4.2.2 Synthetic wastewater

The UASB reactors were fed with a synthetic wastewater containing trace metals, prepared according to Stams et al. [215], but omitting selenite, sodium sulfide and yeast extract. Instead of carbonate, a phosphate buffer (40 mM) was used to maintain the pH of the reactor mixed liquor at 7.0 (± 0.2). Lactate was used as sole electron donor at a concentration of 1,172 mg $L^{-1}$, corresponding to an organic loading rate of 5 g Chemical Oxygen Demand (COD) $(L\ d)^{-1}$.

## 4.2.3 UASB operation

The mesophilic (30 ± 2°C) reactors were operated at a hydraulic retention time (HRT) of 6 h and a superficial liquid upflow velocity of 1 m $h^{-1}$. To stimulate co-reduction of selenate during sulfate reduction [84], one UASB reactor (R1) was operated under sulfate-reducing conditions. Sulfate and selenate were fed to R1 at varying concentrations (Table 4.2). The performance of R1 was compared to that of a second UASB reactor (R2) to which no sulfate was supplied in the first 132 days of operation, and thus was operating under methanogenic conditions. The effect of sulfate on the performance of R2 was investigated at the end of the experiment (days 132-143). No selenate was added during the start-up of both bioreactors (Period I and $I_2$, days 0 to 23).



Table 4.2 Sulfate and selenate content of the reactor feeding of both R1 and R2

| Reactor | Period | Day of operation | $SeO_4^{2-}$ Influent R1 and R2 [mM] | $SO_4^{2-}$ [mM] | $SeO_4^{2-}$ / $SO_4^{2-}$ ratio [mM/mM] | COD / $SO_4^{2-}$ ratio [mg/L]/ [mg/L] |
|---|---|---|---|---|---|---|
| R1 | I | 0-23 | n.a. | 26 | - | 0.5 |
| | II | 24-35 | $10^{-2}$ | 26 | $3.85 \times 10^{-4}$ | 0.5 |
| | III | 36-107 | $10^{-2}$ | 1.3 | $1.92\times 10^{-3}$ | 10 |
| | IV | 108-150 | $10^{-2}$ | 26 | $3.85 \times 10^{-4}$ | 0.5 |
| R2 | $I_2$ | 0-23 | n.a. | n.a. | - | - |
| | $II_2$ | 24-131 | $10^{-2}$ | n.a. | - | - |
| | $III_2$ | 132-143 | $10^{-2}$ | 26 | $3.85 \times 10^{-4}$ | 0.5 |
| | $IV_2$ | 144-150 | $10^{-2}$ | n.a. | - | - |

n.a. = not applicable

## 4.2.4 Batch experiments

Adaptation of the bioreactor sludges to selenate was determined using inoculum sludge and reactor sludges sampled after 23, 107 and 150 days of operation in batch activity tests as described in Chapter 2. Wet sludge (0.5 g) was incubated with 50 mL of synthetic wastewater containing lactate (20 mM) as electron donor in the presence of 5 mM $SO_4^{2-}$ and 0, 50 or 100 µM $SeO_4^{2-}$. Sulfate and selenate reduction efficiencies and specific reduction rates were determined after 72 h.

## 4.2.5 Analytical techniques

Selenate, selenite, dimethylselenide and dimethyldiselenide were determined by ion chromatography and gas chromatography as described in Chapter 2. Total dissolved selenium (Sedis) was determined by Inductively Coupled Plasma-Optical Emission Spectroscopy (ICP-OES). Effluent samples were filtered using a 0.45 µm filter. Sludge samples were destructed by aqua regia assisted microwave digestion [5]. The gas phase of the UASB reactors was passed through a NaOH solution to trap H2Se [82] and the solution was analyzed via ICP-OES (Chapter 2) in regular intervals. To characterize crystalline precipitates in the solid phase, the reactor sludges sampled after 150 days of operation were investigated using X-Ray diffraction (XRD) (Chapter 2). Sequential extractions for selenium fractionation [269] were carried out under a N2 atmosphere.



Volatile Fatty Acids (VFAs) and biogas composition were determined by Gas Chromatography [262]. Methane yield was calculated as [(gCODmethane L-1 d-1) / (gCODinfluent L-1 d-1)-1] × 100. The dissolved sulfide concentration of the effluent was determined colorimetrically (Dr. Lange, LYW653, Germany). Volatile Suspended Solids (VSS) were determined following standard procedures [44].

Environmental Scanning Electron Microscopy with energy dispersive x-ray analysis (ESEM-EDX) was performed on an Electroscan (Wilmington, USA) Type II LaB6gun microscope [87]. Energy dispersive X-ray analysis for qualitative element analysis was conducted in selected areas of 24 $\mu m^2$.

Changes of the bacterial community structures in time were analyzed using Denaturing Gradient Gel Electrophoresis (DGGE) with subsequent sequencing of the bands of interest. DNA was extracted using a DNeasy Plant Mini Kit (Qiagen, Germany). The 16S rDNA genes were amplified [213] using Red'y'Starmix (Eurogentech, Belgium) DNA amplification kit and the universal primer U968 (MWG biotech, Germany) [187]. DGGE was performed using gels containing a 47-70% denaturing gradient (100% defined as 7M urea and 42% formamide). For sequencing, DNA bands of interest were excised using a sterile scalpel, immersed in RNase-free water (Qiagen, Germany) and frozen for 12 h. After thawing, a TOPO TA Cloning® Kit (Invitrogen, Germany) was used to clone the DNA fragments contained in the supernatant for further amplification and sequencing.

# 4.3. Results

## 4.3.1. Sulfate-reducing UASB reactor

After a start-up period without selenate (Period I), the simultaneous feeding of both selenate and sulfate in Period II (Table 4.2) to the sulfate-reducing reactor (R1) resulted in a poor selenate removal efficiency stabilizing at 25% at day 34 (Figure 4.1A). Surprisingly, the $Se_{dis}$ removal efficiency was lower than the selenate removal efficiency, with a gap ranging between 12% and 59%. In Period III, a high selenate removal efficiency was observed immediately upon raising the selenate to sulfate ratio from 3.85 $10^{-4}$ to 1.92 $10^{-3}$. From day 41 onwards, the selenate removal efficiency exceeded 80% with a maximum of 97 % at day 69. It should be noted that the $Se_{dis}$ was removed to only 89% at best in R1 (Figure 4.1A), with 73 µg Se $L^{-1}$ as the lowest selenium effluent concentration on that day.



The highest dissolved sulfide concentration in Period III (110 mg $L^{-1}$) was reached at day 102 (Figure 4.2A), on which a selenate removal efficiency of >93% was obtained. The $Se_{dis}$ removal efficiency was lower than the selenate removal efficiency over the entire Period III, the gap ranged between 0.8 % on day 83 up to 43% on days 65 and 102.

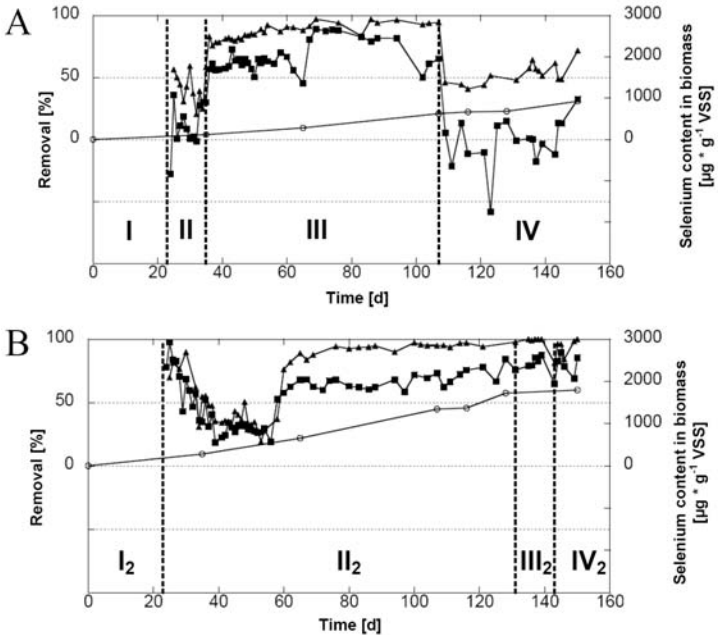


Figure 4.1 Reactor performance of R1 (A) and R2 (B): (▲) selenate and (■) dissolved selenium removed [%] from liquid phase, (○) selenium content in biomass [µg $gVSS^{-1}$]

When lowering the selenate to sulfate ratio back to 3.85 $10^{-4}$ in Period IV (Table 4.2), both the selenate and $Se_{dis}$ removal efficiency dropped immediately (Figure 4.1A). While selenate removal stabilized above 40% (at sulfide concentrations up to 168 mg $L^{-1}$ on day 145, Figure 4.2A), $Se_{dis}$ was removed to a lesser extent or even washed out from the reactor (Figure 4.1A). A massive wash out of dissolved selenium was observed at day 123. While the effluent $Se_{dis}$ concentration was 58% higher than in the influent, selenate was still removed by 50%.

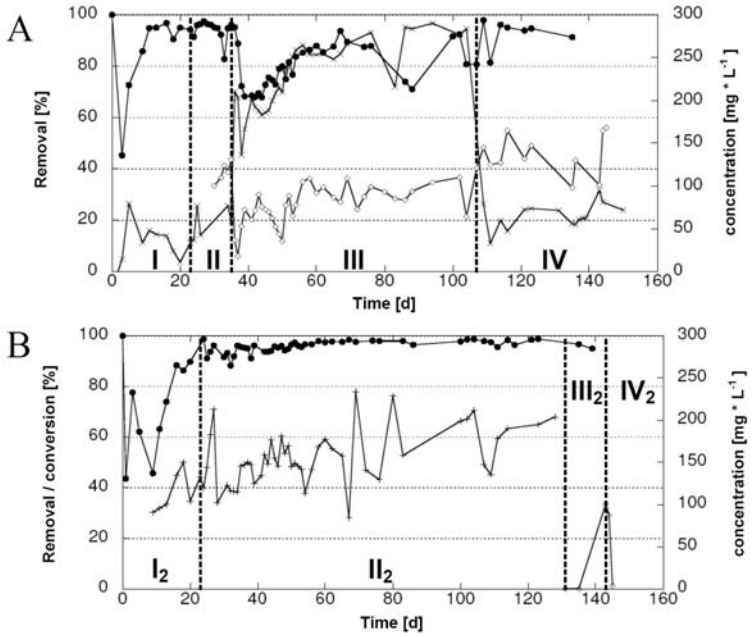


Figure 4.2 Reactor performance of R1 (A) and R2 (B): (●) COD removal efficiency [%], (×) sulfate removal efficiency [%], (+) methane conversion efficiency [methane recovered × theoretical methane$^{-1}$] × 100; secondary y-axis (◊) dissolved sulfide [mg $L^{-1}$]

A nearly complete COD removal efficiency was achieved in the sulfate-reducing reactor after the start-up period of 11 days (Figure 4.2A). The non-converted COD consisted mainly of propionate (data not shown). The sulfate-reducing efficiency (Figure 4.2A) reached 26% (day 34) and 27% (day 144) at a high sulfate loading rate (Period II + IV), while it was much higher (95% at day 104) at the low sulfate loading rate (Period III).

## 4.3.2 Methanogenic reactor

Subsequently to the start-up period without selenate in the influent (Period $I_2$, Table 4.2), the selenate and $Se_{dis}$ removal efficiency of the methanogenic reactor stabilized at approximately 30% until day 58 (Figure 4.1B). After 58 days of operation, both the selenate and $Se_{dis}$ removal efficiency steeply increased and further rose in Period $II_2$. While the selenate removal was almost complete from day 76 onwards, the $Se_{dis}$ removal efficiency was still incomplete with a maximum gap of 33% at day 86. Nevertheless, the gap became smaller upon prolonged reactor operation (up to day 135).



When sulfate was fed to the methanogenic reactor at a selenate to sulfate ratio of 3.85 $10^{-4}$ (Period $III_2$), the selenate removal efficiency remained nearly complete for 8 days (32 hydraulic retention times). The maximal $Se_{dis}$ removal efficiency (89%) was reached on day 145, corresponding to the lowest effluent concentration (80 µg Se $L^{-1}$). However, the formation of 101 mg $L^{-1}$ dissolved sulfide in the liquid phase (day 143, Figure 4.2B) lead to a decrease in selenate and $Se_{dis}$ removal efficiency from 100% to 81.2% and 87.5 to 64.8%, respectively.

The COD removal was complete after a 16 days start-up period for the whole experiment and methane was produced up to a yield of 78 % at day 69 (Figure 4.2B). The remaining COD was either converted to $CO_2$ dissolved in the effluent or to biomass growth, as VFAs did not accumulate in the effluent (Figure 4.2B)

## 4.3.3 Metabolic properties of the sulfate-reducing sludge (R1)

The inoculum sludge showed low sulfate reduction rates (initial concentration 5 mM sulfate) with lactate as the substrate, independent of the selenate concentration (Figure 4.3A). The sludge sampled from R1 after 23 days of operation had a maximal specific sulfate reduction rate of 1,204 µg S g $VSS^{-1}$ $h^{-1}$ in the absence of selenate (Figure 4.3A). At day 107, the sulfate reduction rate was not significantly different compared to day 23, while the specific activity of the R1 sludge sampled at day 150 amounted only 994 µg S g $VSS^{-1}$ $h^{-1}$ in the absence of selenate.

The presence of 10 µM $SeO_4^{2-}$ (corresponding to a selenate / sulfate molar ratio of 2.0 × $10^{-3}$) inhibited sulfate reduction with lactate as electron donor in the R1 sludge sampled after 23 and 107 days of operation by 12 % and 11 %, respectively, in comparison to selenate free batches (Figure 4.3A). At day 150, the latter selenate concentration did not significantly inhibit sulfate reduction anymore, while 100 µM $SeO_4^{2-}$ addition (ratio selenate to sulfate = 2.0 $10^{-2}$) inhibited sulfate reduction the most (81 %). The highest

specific selenate reduction rate for R1 sludge [28 µg Se $gVSS^{-1}$ $h)^{-1}$] was observed with sludge sampled on day 107 upon the addition of 100 µM $SeO_4^{2-}$ (Figure 4.3B).

## 4.3.4 Metabolic properties of the methanogenic sludge (R2)

In the presence of 5 mM sulfate, the R2 sludge sampled after 150 days of operation showed the highest specific selenate reduction rates at all selenate concentrations tested: 3.1 µg Se g $VSS^{-1}$ $h^{-1}$ at 10 µM $SeO_4^{2-}$, 21.0 µg Se g $VSS^{-1}$ $h^{-1}$ at 50 µM and 36.2 µg Se g $VSS^{-1}$ $h^{-1}$ at 100 µM $SeO_4^{2-}$ (Figure 4.3C). The reduction rate of this R2 sludge at 100 µM $SeO_4^{2-}$ was the highest observed in all batch experiments performed with both R1 and R2 sludges with lactate as electron donor.



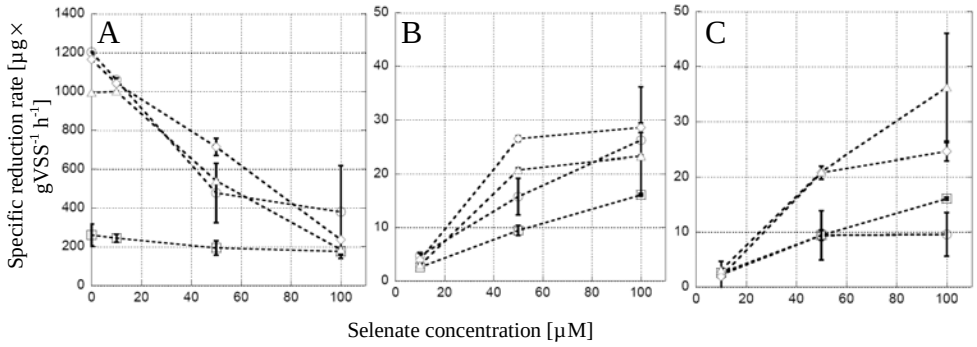


Figure 4.3 Effect of selenate on the specific sulfate [µg S g $VSS^{-1}$ $h^{-1}$] (A) and selenate [µg Se g $VSS^{-1}$ $h^{-1}$] (B,C) reduction rates with lactate as electron donor (pH = 7; 30°C) determined after 72h incubation in batch experiments by R1 reactor sludge (A,B) and R2 sludge (C). Inoculum (□) and after 23 (○), 107 (◊), and 150 (△) days of operation

## 4.3.5 Microbial community analysis

The DNA-band pattern observed using DGGE technique displayed additional DNA bands in extracts from R2 sludge sampled at 150 days of operation (lane G, bands 1-3, Figure 4.4). This was indicative for the development of additional microorganisms in R2 sludges since corresponding bands were not observed for 16S rDNA extracts of R1 sludges. These bands were further excised and prepared for DNA sequencing. One of the determined sequences (band 1, Figure 4.4) presented 79 % of similarity (276 of 348 nucleotides matched) to that of *Dendrosporobacter quercicolus* (formerly *Clostridium*

*quercicolum*, Accession Number AJ010962 NCBI CoreNucleotide Database). The DNA sequences of the bands 2 and band 3 were similar to sequences obtained for uncultured bacterial clones B2 (Accession Number AY426442, 81 % homology, 329 of 406 nucleotides matched) and BA149 (Accession Number AF323777 89 % homology, 341 of 384 nucleotides matched), respectively.

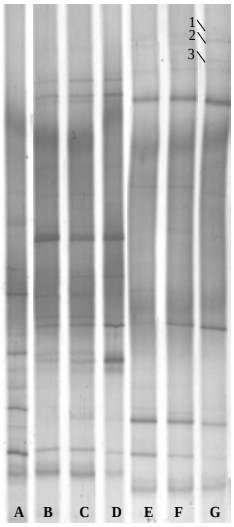


Figure 4.4 DGGE profile (47% denaturing agent on top, 70% denaturing agent on bottom) of 16S rDNA PCR fragments (U968 bacterial primer) of inoculum (A) and sludges after 65, 95 and 150 days of operation (R1: lanes B-D; R2: lanes E-G). DNA fragments resembled to sequences of (1) Dendrosporobacter quercicolus and bacterial clones (2) B2 and (3) BA149



## 4.3.6 Solid phase analysis

The selenium content in the biomass (normalized to VSS) increased during reactor operation (Figure 4.1A and 1B), resulting in a 1.9 times higher selenium content in the methanogenic compared to the sulfate-reducing UASB reactor sludge (1,785 vs. 918 µg Se g $VSS^{-1}$). Within the 150 days of operation, this accumulation was not yet saturated. A slight red color developed on the methanogenic granules and in the biofilm formed in the tubes of this reactor (Figure 4.5 B, C). In contrast, no red color developed in the sulfate-reducing reactor (Figure 4.5A).


Figure 4.5 Reflected-light microscopic pictures of anaerobic sludge granules originating from R1 (A) and R2 (B) at 150 days of operation and biofilm originating from tubing of R2 (C). Bars correspond to 2 mm, arrow marks red spots of elemental selenium



Sequential extraction of both R1 and R2 sludge on days 129 and day 150 showed that most selenium was extracted in the elemental fraction (Figure 4.6). Only negligible amounts (between 0.1 and 1.6%) of selenium were present in the soluble/ exchangeable and adsorbed fraction. R1 sludge showed a smaller fraction of elemental selenium (57.0 ± 8.5%) at day 150 compared to day 129 (67.6 ± 0.8%) and a larger fraction of residual selenium from 7.6 (± 1.4) % at 129 days compared to 26.1 (± 7.4) % at day 150. In contrast, R2 showed a larger fraction of elemental selenium at day 150 (72.2 ± 2.0%) in comparison to day 129 (59.2 ± 9.1%), but the total recovery for these samples was higher than 100% (Figure 4.6).

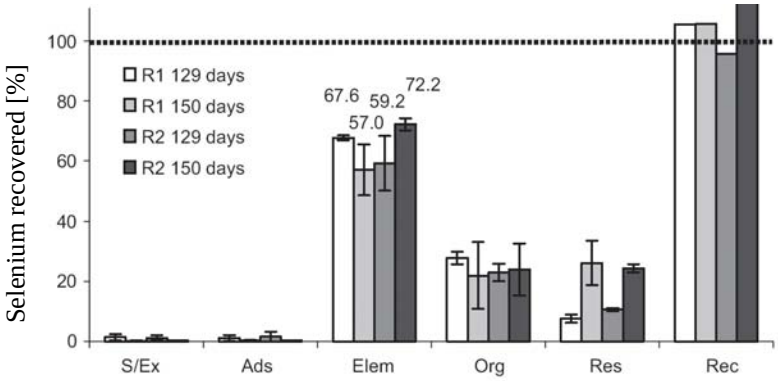


Figure 4.6 Selenium fractionation determined by sequential extraction. Soluble/exchangeable (S/Ex), adsorbed (Ads), elemental (Elem), organically associated (Org), residual (Res) fraction and recovery (Rec)

XRD spectra of both reactor sludges after 150 days of reactor operation did not reveal the presence of crystalline selenium or metal selenides. The spectra matched with two different crystalline compounds: brushite [$CaHPO_4$ * 2($H_2O$)] and calcite [$Ca(CO_3)$] (Figure 4.7). Brushite was present with a probability of 60% in R1 sludge, while brushite (59% probability) and/or calcite (56% probability) were present in R2 sludge.

Selenium precipitates could also not be observed by ESEM analysis of the R1 and R2 reactor sludge granules, nor was selenium detectable in the EDX surface scan analysis (Figure 4.8A, B). When exposing the inoculum sludge to bioreactor operation conditions, but with a higher selenate concentration (10 mM $SeO_4^{2-}$) for 10 days, globules in the 100 - 500 nm size range developed on the granule surface (Figure 4.8 C). The EDX analysis confirmed these globules consisted of selenium, with phosphorus, potassium, chlorine and zinc as further constituents.



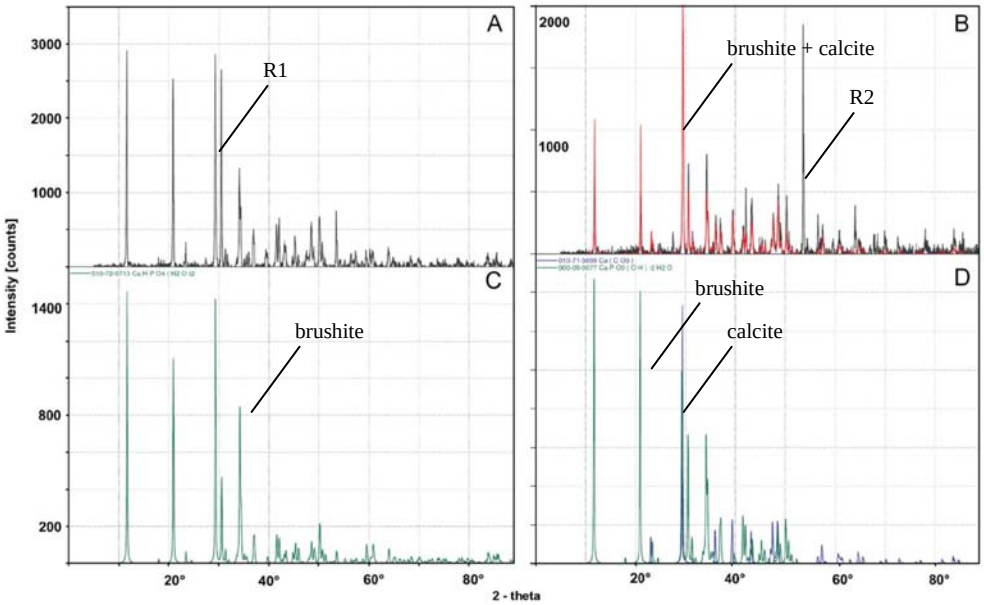


Figure 4.7 XRD Diffractograms of R1 (A) and R2 (B) reactor sludges and matched standards (C, D) with diffractograms corrected for background

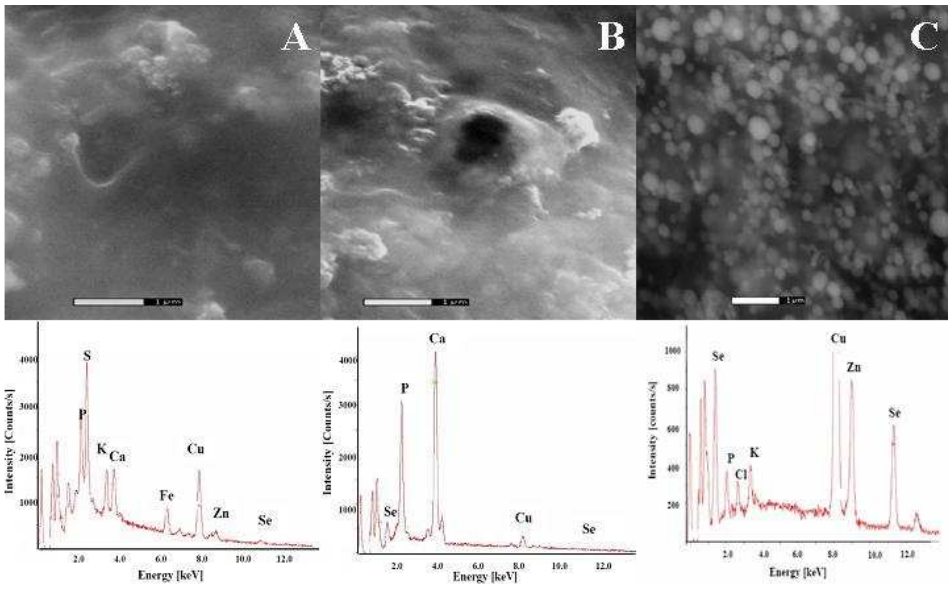


Figure 4.8 ESEM pictures of sludge from R1 (A) and R2 (B) after 150 days of operation and inoculum sludge treating 10 mM $SeO_4^{2-}$ in a 10 days batch experiment (C). EDX spectra are surface scans (area 24 $\mu m^2$) from R1 and R2 (A, B) and beam focused on a selenium nanosphere solely (C). White bars represent 1 µm. Note that the presence of copper is due to the sample holder

# 4. Discussion

## 4.4.1 Selenate removal by the sulfate-reducing bioreactor (R1)

In R1, selenate and $Se_{dis}$ removal occurred under molar excess of sulfate (selenate to sulfate ratio: 1.92 $10^{-3}$), while a higher excess of sulfate (ratio: 3.85 $10^{-4}$) reduced the selenate removal efficiency (Figure 4.1A). The competitive effect between selenate and sulfate, especially during the transition between Period II/III and III/IV (Figure 4.1A), suggests that selenate was removed by sulfate-reducing bacteria (SRB) in R1. The achieved effluent concentration of 73 µg Se $L^{-1}$ was well below the USEPA Universal Treatment Standards [242] for wastewater of 820 µg Se $L^{-1}$.

The bacteria responsible for selenate reduction in R1 were sulfide tolerant, as selenium removal proceeded at dissolved sulfide concentrations of up to 110 mg $L^{-1}$ in Period III and 168 mg $L^{-1}$ in Period IV (Figure 4.1A, 2A). This is highly desired for treatment of acid mine drainage or other strongly metal contaminated streams, as the application of these

sludges offers the possibility to combine sulfidic heavy metal precipitation [195] with the removal of selenium oxyanions. Although sulfate removal efficiencies increased during Period III, efficiencies in Period IV were comparative low than in Period II (Figure 4.2A). This might be explained by a lack of COD necessary for sulfate reduction (COD removal already ~ 80% during transition from period III to IV, Figure 4.2A).

The inhibition of sulfate reduction by selenate depends on the ratio between the two anions [26] up to a threshold concentration of ≤ 1mM selenate [283]. Above this concentration selenate becomes completely inhibiting, independent of the sulfate concentration present. Addition of 10 µM selenate to R1 sludges in batch toxicity assays after 23 and 107 days of operation (ratio $SeO_4^{2-}$ : $SO_4^{2-}$ = 2.0 $10^{-3}$) resulted in a 12% decrease of the sulfate reduction rate (Figure 4.3A). This is in agreement with previous reports [84], that found 25% inhibition of the sulfate-reducing activity of lactate grown *Desulfomicrobium sp.* (pH = 7; 30°C) by 25 µM $SeO_4^{2-}$ in 5 mM $SO_4^{2-}$ medium (ratio $SeO_4^{2-}$ : $SO_4^{2-}$ = 5.0 $10^{-3}$). The selenate to sulfate ratio applied to R1 in Period II was lower (ratio $SeO_4^{2-}$ : $SO_4^{2-}$ = 3.85 $10^{-4}$) and was thus not inhibiting sulfate reduction (Figure 4.2A). The incomplete sulfate reduction during Period III (Figure 4.2A) is most probably due to inhibition of SRB by selenate, as the ratio $SeO_4^{2-}$ : $SO_4^{2-}$ (1.9210$^{-3}$) inhibited sulfate reduction in batch cultures by 12%. Nevertheless, it has to be noted that selenate removal efficiencies stabilized at >93% for 114 HRTs (days 85-104).



This chapter thus showed that, despite the inhibitory effect of selenate to SRB, bioreactors based on these microorganisms can be applied for continuous selenium removal, if the selenate to sulfate ratio is controlled carefully: the ratio of selenate to sulfate should be higher than 1.92 $10^{-3}$, but the selenate threshold concentration of < 1 mM should not be exceeded. All waste streams summarized in Table 4.1, however, display ratios of selenate to sulfate < 8.0 $10^{-4}$, thus an incomplete selenate and $Se_{dis}$ removal efficiency has to be expected, if these are treated under sulfate-reducing conditions.

## 4.4.2 Selenate removal by the methanogenic reactor (R2)

The stable high selenium removal efficiencies over a time period of almost 100 days (Figure 4.1B) showed that a selenium removing population established in R2. Sludge sampled after 150 days of operation showed the highest selenate reduction rates with all selenate concentrations tested (Figure 4.3C). The fact that the highest specific $SeO_4^{2-}$ reduction rate was observed at the highest selenate concentration (100 µM) after 145 days of operation indicates an adaptation of the sludge towards selenate during the reactor operation. The complete selenate removal (days 131-139) under the continuous presence of

high sulfate concentrations in R2 for 48 HRTs (Period $III_2$, Figure 4.1B) suggests that selenium-respiring specialists developed, which are unaffected by sulfate as their selenate reductases function independent of sulfate [205]. Note that the selenate reducing microorganisms in R2 were sensitive to sulfide (101 mg $L^{-1}$) (Period $III_2$), in contrast to the selenate reducing SRB in R1. In Period $IV_2$, selenate removal efficiencies recovered instantaneously when sulfide was absent again.

DGGE analyses confirmed the different populations in R1 and R2, i.e. bacterial bands developing in R2 (Figure 4.4). This was consistent with the rapid increase in selenium removal efficiency after day 58 (Figure 4.1B). Further DNA sequencing indicated that *Dendrosporobacter quercicolus* was present in R2. This anaerobic selenate reducing bacterium growing at 25-30°C has been previously isolated from a two chamber subsurface passive bioreactor/wetland system treating mining seeps contaminated with 250 – 1,000 µg $L^{-1}$ selenium as selenate [108]. Selenate reduction observed in R2 might be assigned to these bacteria. Two further microorganisms growing in R2 were closely related to uncultured bacterial clones, which have been described to proliferate in methanogenic reactors. Furthermore, the presence of clone B2 was reported in the same inoculum as used in this chapter [187].



The treatment of sulfate rich waters in a previously selenate adapted reactor under methanogenic conditions should be explored further, as high sulfate loading rates did not interfere with the selenate removal efficiency for the time period investigated, once the presumed population of specialists had developed. Additionally, the $Se_{dis}$ effluent concentration of 80 µg Se $L^{-1}$ fell well below the US EPA Universal Treatment Standards [242] for wastewater (820 µg Se $L^{-1}$). Note that inhibiting effects of sulfide have to be avoided, which can be achieved by different process technological measures, e.g. sulfide stripping [119].In the methanogenic reactor, lactate was converted to methane with a yield of < 80% (Figure 4.2B). Further research is required to determine, if 10 µM selenate was inhibiting methanogenic activity.

## 4.4.3 Selenium speciation

Elemental selenium was the main fraction in the solid phase of both sludges (Figure 4.6). The red color observed in the R2 sludge and tubings was probably due to amorphous red elemental selenium, as this is the main constituent of the precipitate obtained in batch experiments using the same inoculum and electron donor (Chapter 2). In the sulfate-reducing reactor, red elemental selenium might also have been formed, whereas the red color remained covered by dark metal sulfides, i.e. iron sulfides.

In previous batch experiments, a minor part within the non-diffracting red selenium precipitate was hexagonal black selenium (Chapter 2). The precipitates within the R1 and R2 sludges did, however, not match with this standard (Figure 4.7). The highest intensity peak for brushite on 2-theta = 29.290° corresponds to a d-spacing of 3.047 Å, thus showing the same d-spacing as the highest peak for black hexagonal elemental selenium (101 plane, d-spacing = 3.0 Å). Also the second highest peak of the sample (d-spacing = 3.798 Å) overlaps with the corresponding peak in hexagonal elemental selenium (100 plane, d-spacing = 3.78 Å). Similarly, the main peak for selenium (101 plane) overlaps with calcite (d-spacing = 3.03 Å) in the diffractogram of the R2 sludge. The second highest intensity peak of hexagonal selenium (d-spacing = 3.78 Å) is present in the R2 sludge (d-spacing = 3.77 Å), but with a very low intensity. Therefore, the presence of hexagonal black elemental selenium within the biomass of both reactors cannot be excluded. X-ray absorption fine structure (XAFS) spectroscopy showed that most selenium is present in an aperiodic form of elemental selenium in both sludges (Chapter 3).



Selenium washed out from the sulfate-reducing reactor over almost the complete Period IV (Figure 4.1A), but not in the methanogenic reactor operating under identical conditions in Period $III_2$ (Figure 4.1B). This is not due to a chemical exchange of ionic selenium species with sulfate, as only negligible proportions of selenium were found in the soluble / exchangeable and adsorbed fractions (Figure 4.6). The fact that the $Se_{dis}$ concentration exceeded the selenium concentration determined as selenate in the effluent liquid phase might be due to either the presence of an undetermined dissolved selenium species or by wash out of colloidally dispersed elemental selenium.

The first hypothesis is supported by the fact that organically associated and residual fractions were found in the sequential extractions of the sludge samples (Figure 4.6). These possibly consist of seleno-aminoacids and / or seleno-proteins [236] and could be released upon lysis of SRB. Other dissolved selenium species are potentially formed upon the reaction of aqueous selenide and elemental sulfur to sulfur-selenium-heterocycles [155]. None of the selenium species described to be formed by SRBs, namely $H_2Se$ [155], selenite [26], dimethylselenide and dimethyldiselenide [147], could be detected at any time in R1 or R2 . This is a very important fact as, for example, selenite is more toxic to aquatic invertebrates and fish compared to selenate [73].

The second hypothesis is that the $Se_{dis}$ fraction is overestimated due to the wash out of colloidal selenium with a size smaller than the applied filters (0.45 µm). This is supported by the particle size of the selenium nanospheres (200 - 400 nm) formed by selenium-respiring microorganisms [167]. Even if not observed in the ESEM pictures of the R1 and R2 sludges (Figure 4.8 A,B), probably due to the low selenium content (EDX surface scan in Figure 4.8A, B), similar particles (100-500 nm) were formed by exposing the inoculum

sludge to higher (10 mM) selenate concentrations (Figure 4.8C). Moreover, the sequential extractions (Figure 4.6) showed a lower mean proportion of elemental selenium in R1 sludge (150 days of operation) after the extensive period of $Se_{dis}$ wash out (Period IV). If the SRB population in R1 produces such selenium nanospheres, the sudden wash out during the transition of Periods III to IV could be due to a detachment of the extracellular nanospheres [84] to the medium or due to a release of intracellular nanospheres [232] after lysis of SRB cells.

Particularly under unstable operational conditions, selenium speciation should be monitored carefully (including bioavailable organic selenium forms), as formerly bioaccumulated selenium can abruptly washout. The gap between selenate and $Se_{dis}$ would not have been revealed by common analytical procedures for selenium determination [e.g. Standard methods examination water wastewater Nr. 3114 [44]], as selenate is determined indirectly in these procedures. This underlines the importance of species-specific analysis for the evaluation of selenium biotreatment systems, as other selenium species can be misinterpreted as selenate or selenite.

# 5

# Biological alkylation and colloid formation of selenium in methanogenic UASB reactors

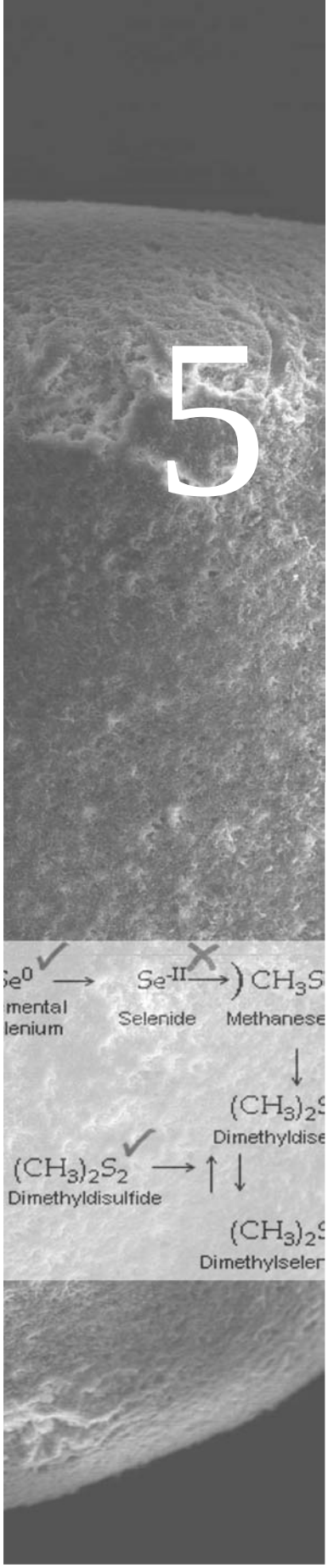


This chapter has been accepted for publication by Journal of Environmental Quality as: Lenz, M., Smit, M., Binder, P., van Aelst, A.C., Lens, P. N. L. (2008). Biological alkylation and colloid formation of selenium in methanogenic UASB reactors.

# Abstract

Bioalkylation and colloid formation of selenium during selenate removal in Upflow Anaerobic Sludge Bed (UASB) bioreactors was investigated. The mesophilic (30°C) UASB reactor (pH = 7.0) was operated for 175 days with lactate as electron donor at an organic loading rate of 2 g COD $L^{-1}$ $d^{-1}$ and a selenium loading rate of 3.16 mg Se $L^{-1}$ $d^{-1}$. Combining sequential filtration with ion chromatographic analysis for selenium oxyanions and Solid Phase Micro Extraction Gas Chromatography Mass Spectrometry (SPME-GC-MS) for alkylated selenium compounds allowed the closure of the selenium mass balance in the liquid phase for most of the UASB operational runtime. Although more than 98.6% selenate was removed from the liquid phase, a less efficient removal of dissolved selenium was observed due to the presence of dissolved alkylated selenium species (dimethylselenide and dimethyldiselenide) and colloidal selenium particles in the effluent. The alkylated and the colloidal fractions contributed up to 15% and 31%, respectively, to the dissolved selenium concentration. The size fractions of the colloidal dispersion were: 4 to 0.45 µm: up to 21%, 0.45 to 0.2 µm: up to 11%, and particles smaller than 0.2 µm: up to 8%. Particles of 4 to 0.45 µm were formed in the external settler, but did not settle. SEM-EDX analysis showed that microorganisms form these selenium containing colloidal particles extracellularly on their surface. Lowering the temperature by 10°C for 6h resulted in drastically reduced selenate removal efficiencies (after a delay of 1.5 days), accompanied by the temporary formation of an unknown, soluble, organic selenium species. This chapter shows that a careful process control is a prerequisite for selenium treatment in UASB bioreactors, as disturbances in the operational conditions induce elevated selenium effluent concentrations by alkylation and colloid formation.

# 5.1 Introduction

Selenium is a metalloid with a narrow threshold between being either beneficial as an essential trace element or harmful as a potent toxin to biota [73]. The latter was illustrated by ecotoxicological effects to birds and aquatic organisms in the Kesterson Reservoir (California, USA) [270]. Both characteristics strongly depend on the bioavailability of selenium, determined by its chemical speciation [278].

To deal with selenium contamination of water and soil, several treatment options have been developed [237]. A treatment option used for soils contaminated with geogenic and agricultural selenium sources relies on "biovolatilization" [9], i.e. the methylation of selenium to dimethylselenide (DMSe) and dimethyldiselenide (DMDSe) by plants and associated microorganisms. As DMSe and DMDSe show low acute toxicity [2], soil detoxification is achieved by dilution of the volatile selenium compounds into the atmosphere. However, industrial applications demand different approaches due to the high dissolved selenium concentrations (Chapter 4 and 7) and low total maximum daily loads (TMDL) [117] that can be discharged without exceeding the tissue concentration based chronic freshwater aquatic life criterion [243], thus protecting aquatic life against adverse effects from long-term (continuous) exposure to selenium [198].



Especially the microbial conversion of water-soluble, highly toxic forms of selenium (selenate, selenite) to elemental selenium, which is generally considered less bioavailable [291], is a preferred option for industrial and agricultural wastewaters. This reduction can be mediated by specific enzymes of selenium-respiring microorganisms that conserve energy for growth from selenium reduction, forming intra- or extracellular elemental selenium nanospheres of ~ 300 nm diameter [167]. In contrast, unspecific enzymatic selenium reduction by sulfate or nitrate-reducing bacteria can yield not only elemental selenium, but also different side products - e.g. acutely toxic $H_2Se$ [155].

Methanogenic UASB bioreactors can efficiently reduce selenate contaminations, even in the presence of its structural analogue sulfate, while fixing selenium in elemental form in the biomass, presented in Chapter 4. In Chapter 4, however, high removal efficiencies were obtained under constant operational conditions. Microbial selenium conversions, however, are strongly dependent on e.g. temperature and pH [43; 65; 295], which can vary strongly in full scale applications [170]. Moreover, the upflow velocity applied determines the hydraulic shearing force, thus influencing the particle size of washed out precipitates [135]. This chapter, therefore, evaluates the influence of operational disturbances (temperature, pH, upflow velocity) on the treatment efficiency of UASB bioreactors treating synthetic selenium contaminated wastewater. Special attention was given to the size fractionation of

colloidally dispersed selenium and formation of dissolved, alkylated selenium compounds. Furthermore, the potential of an external settler to recover bio-precipitated selenium from the aqueous phase is explored.

# 5.2. Materials and Methods

## 5.2.1. Source of biomass



The UASB reactor was inoculated with anaerobic granular sludge (100 g wet weight) originating from a full scale UASB reactor treating wastewater of four paper mills (Industriewater Eerbeek B.V., Eerbeek, The Netherlands). This inoculum has been microbially characterized by Roest et al. [187] and has been previously described to be effective for selenate removal from wastewaters (Chapter 4) [5].

## 5.2.2. Synthetic wastewater

The UASB reactors were fed with an oxygen-free synthetic wastewater containing trace metals, prepared according to Stams et al. [215], but omitting selenite, sodium sulfide and yeast extract. Instead of carbonate, a phosphate buffer (40 mM) was used to maintain the pH of the reactor mixed liquor at 7.0 (± 0.1). Lactate was used as sole electron donor at an organic loading rate of 2 g Chemical Oxygen Demand (COD) $L^{-1}$ $d^{-1}$, corresponding to a specific organic loading rate of 53.5 mg COD g Volatile Suspended Solids (VSS) $^{-1}$ $d^{-1}$, based on the initial VSS concentration of 37.4 $gVSS^{-1}$ $L^{-1}$ used to inoculate the UASB reactor. The selenate influent concentration was 790 µg $L^{-1}$, resulting in a selenium loading rate of 3.16 mg Se $L^{-1}$ $d^{-1}$ (84.5 µg Se $gVSS^{-1}$ $d^{-1}$). To prevent selenate bioconversion in the storage vessels, the selenate solution was prepared separately and mixed with the buffered synthetic wastewater prior to entering the bioreactor.

## 5.2.3 Reactor operation

Experiments were done in a glass UASB reactor (0.46 L working volume) as described in Chapters 2 and 4. It was operated under mesophilic conditions (30 ± 1°C) at a hydraulic retention time (HRT) of 6 h. The effluent was recycled via a Watson Marlow 503U peristaltic pump (Rotterdam, The Netherlands) to obtain a superficial liquid upflow velocity

($v_{up}$) of 1 m $h^{-1}$. All reactor tubing was made of polytetrafluoroethylene (PTFE) (Polyfluor BV, Oosterhout, The Netherlands).

During the reactor operation, the effect of disturbances in operational T, pH, and $v_{up}$ was investigated, as detailed in Table 5.1. The reactor was subjected to a modest decrease in temperature (3°C, $D_1$) and two major temperature decreases (10°C, $D_3$ and $D_5$) of different duration (Table 5.1). The temperature decrease with longer duration resulted in acidification of the reactor ($D_4$) yielding a pH of 6.1. Failure of the recycle pump decreased the upflow velocity temporarily ($D_2$) from 1 m $h^{-1}$ to 0.08 m $h^{-1}$.

Table 5.1 Operational phases and disturbances applied to the UASB reactor

| Phase / disturbance | Time of operation [days] | Disturbance | Effect |
|---|---|---|---|
| Phase I | 0 - 23 | No disturbance [a] | n.a. |
| Phase II | 23 - 51 | No disturbance [a] | n.a. |
| $D_1$ | 51 -53 | T = 27 ± 1 °C | $Se_{dis}$ removal decreased<br>Formation of DMDSe<br>Propionate accumulation |
| Phase III | 53 -62 | No disturbance [a] | n.a. |
| $D_2$ | 62 -65 | Failure recycle pump → $v_{up}$ = 0.08 m $h^{-1}$ | Selenate and $Se_{dis}$ removal decreased |
| Phase IV | 65 - 93 | No disturbance [a] | Colloidal Se washing out |
| $D_3$ | 93 – 93.75 | T = 20 ± 1 °C | Acidification ($D_4$)<br>DMSe production |
| $D_4$ | 93.75 - 103 | Acidification of reactor to pH = 6.1 | Selenate and $Se_{dis}$ removal decreased<br>DM(D)Se production |
| Phase V | 103 - 122 | OLR = 0.5 g COD $L^{-1}$ $d^{-1}$ | Colloidal selenium washing out |
| Phase VI | 122 - 156 | No disturbance [a] | n.a. |
| $D_5$ [c] | 156 – 156.25 | T = 20 ± 1 °C | Selenate and $Se_{dis}$ removal decreased<br>Formation of DMSeS [b] |
| Phase VIII [c] | 156.25 - 176 | No disturbance [a] | n.a. |

[a] OLR = 2 g COD $L^{-1}$ $d^{-1}$; T = 30°C; $v_{up}$ = 1 m $h^{-1}$; [b] indicated by SPME-GC-MS; [c] Results presented separately in Figure 5.6; n.a. … not applicable

## 5.2.4. Batch experiments

Selenium alkylation from endogenous selenium sources was studied in batch experiments with reactor sludge (0.5 g wet weight corresponding to 86 µg VSS) sampled after 60 days of reactor operation. The tests were performed in 125 mL serum bottles with 50 mL selenate free synthetic wastewater under anaerobic conditions as described in Chapter 2. Batches "A" and "C" received lactate as electron donor (2 gCOD $L^{-1}$), while no lactate was added to batch "B". Batch "A" and "B" were incubated at 30 (± 1)°C whereas batch "C" at 20 (± 1)°C. Controls included batch tests with autoclaved biomass, with sulfide addition (20 mM), and with a medium of pH = 2 ± 0.1 (40 mM phosphate buffer, adjusted to final pH with phosphoric acid). DMSe and DMDSe concentrations in the liquid phase of the batch bottles were determined after 1 week of incubation.



## 5.2.5. Analytical techniques

Selenate [Method Quantification Limit (MQL) 11 µg Se $L^{-1}$] and selenite (MQL: 24 µg Se $L^{-1}$) were determined by ion chromatography as described in Chapter 2. Total dissolved selenium ($Se_{dis}$) was determined by Inductively Coupled Plasma-Optical Emission Spectroscopy (ICP-OES) (detection limit 10 µg Se $L^{-1}$). Effluent samples were treated by a sequential filtration (see Figure 5.1) using filters of 4, 0.45, and 0.2 µm pore size. Subsequently, the samples were centrifuged for 20 min at 10,000 g in a table centrifuge (Microlite IEC, Thermo Fisher, Breda, The Netherlands). Removal efficiencies, the proportion of alkylated selenium species and the proportion of colloidal selenium in effluent were related to measured $Se_{in}$, not calculated $Se_{in}$.

Dimethylselenide (DMSe) and dimethyldiselenide (DMDSe) were determined by Solid Phase Micro Extraction Gas Chromatography Mass Spectrometry (SPME-GC-MS) (fraction C, Figure 5.1). Aqueous effluent samples were filled into GC crimp cap vials, capped under exclusion of the gas phase, and exposed for 5 min at 20 (±0.1)°C to the SPME-fiber consisting of carboxen / polydimethylsiloxane (CAR/PDMS, 75 µm film thickness) (Supelco, Zwijndrecht, The Netherlands). For separation, a WCOT fused silica CP-SIL 8 CB low bleed / MS column (0.25 mm × 50 m × 0.25 µm ) was used in a Thermo Finnigan Trace GC with a Polaris Q MS detector (Thermo Fisher, Breda, The Netherlands), operated in a mode to scan m/z = 60 to 192. The liner temperature was set to 250°C, the oven was heated by applying a temperature program (0 to 4 min at 40°C, 25°C $min^{-1}$ to 250 °C, 2 min hold). Fragmentation patterns were obtained using the Mass Frontier software (HighChem, Slovakia). The MQL was 1.5 and 2.5 µg Se $L^{-1}$ for DMSe and DMDSe, respectively.

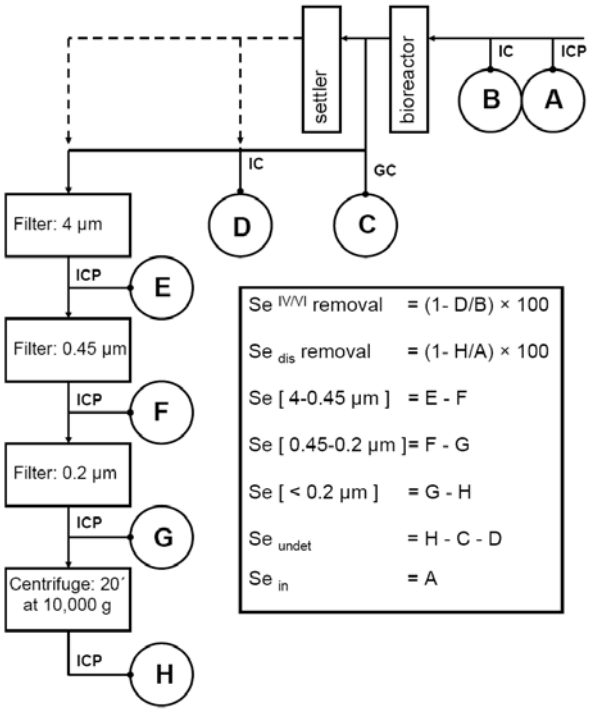


Figure 5.1 Sampling scheme and calculations to fractionate selenium colloids in the effluent based on their particle size



Volatile Fatty Acids (VFAs) and biogas composition were determined by Gas Chromatography [262]. For Scanning Electron Microscopy with Energy Dispersive X-ray analysis (SEM-EDX), samples were fixed for 1 h in aqueous glutaraldehyde solution (2.5%), rinsed with water and subjected to a series of ethanol rinses (10, 30, 50, 70, 90, 100%; 20 min per step) before critical-point drying with carbon dioxide (CPD 020, Balzers, Liechtenstein). Samples were then fit on a brass sample holder with carbon adhesive tabs (Electron Microscopy Sciences, Hatfield PA, USA) and coated with carbon. An additional 5 nm platinum coating was applied by magnetron sputtering. Specimens were analyzed with a field emission scanning electron microscope (JEOL 6300 F, Tokyo, Japan) at room temperature at a working distance between 8 and 15 mm, with selenium detection at 3.5 kV. All images were recorded digitally (Orion 6, E.L.I. sprl., Belgium) at a scan rate of 100 seconds (full frame) at a size of 2528 x 2030, 8 bit. The images were optimized and resized with Adobe Photoshop CS (San Jose CA, USA). EDX analyses (INCA energy,

Oxford Instruments Analytical, High Wycombe, England) were performed with a voltage of 15 kV and a working distance of 15 mm.

# 5.3. Results

## 5.3.1. Selenate and selenium removal by the UASB reactor under stable reactor operation



Subsequently to the start up of 23 days (phase I), the selenate and selenium removal efficiency of the UASB reactor steeply increased in phase II (Table 5.1). The selenate removal efficiency stabilized at values exceeding 91.9% (phase II, III, IV, V), with complete selenate removal (> 98.6%; MQL) on days 97, 116 and 118 (Figure 5.2A). Complete selenate removal was achieved on 5 additional days when the settler was considered as well. Dissolved selenium ($Se_{dis}$) removal developed in a similar manner (Figure 5.2B), but generally with lower removal efficiencies. Towards the end of the reactor run (phase VI and VII), $Se_{dis}$ removal efficiencies stabilized around 90% (phase V).

DMDSe and DMSe were initially detected in the reactor effluent after 13 and 17 days of operation, respectively (phase I, Figure 5.3). Until the end of phase II (operation day 47), the concentration of alkylated selenium compounds remained below 2.2% of the total selenium concentration present in the influent ($Se_{in}$). Different disturbances caused an increased concentration of methylated selenium species. Towards the end of the reactor operation (phase VI), however, DMDSe and DMSe concentrations decreased, accounting for a maximum of 7 µg Se $L^{-1}$ as DMDSe (1.1% of $Se_{in}$) and 26 µg Se $L^{-1}$ as DMSe (4.1 % of $Se_{in}$). Dimethysulfide and dimethyldisulfide were formed during the reactor operation, with concentrations of up to 6.6 µg S $L^{-1}$ and 15.8 µg S $L^{-1}$, respectively (data not shown).

During the start up of the reactor (phase I), colloidally dispersed selenium accounted for less than 5% of the $Se_{in}$ (Figure 5.4A). Subsequently, more selenium was converted to colloidal particles (31% of $Se_{in}$, phase II), with the main contribution by larger selenium particles (4 to 0.45 µm). While the total amount of colloidal selenium was comparable, the latter particle sizes were found in higher amounts in the settler effluent compared to the reactor effluent between days 51 and 100 (period III and IV). For most sample times, smaller size fractions (0.2 to 0.45 µm and <0.2 µm) contributed to less than 6% and 5% of $Se_{in}$, respectively.

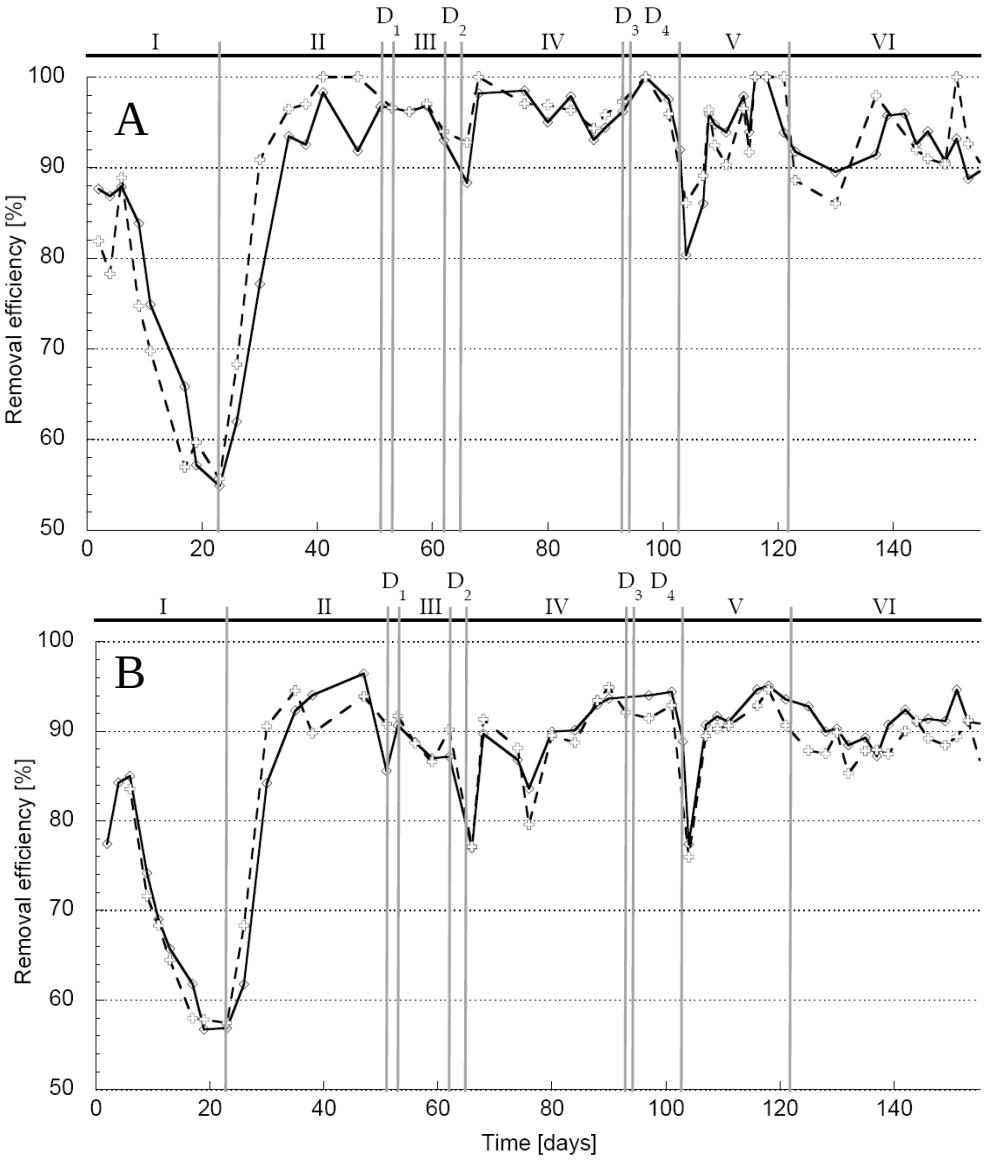


Figure 5.2 Selenate removal (A) and dissolved selenium ($Se_{dis}$) removal (B) in reactor (—◇—) and settler (–✣–)

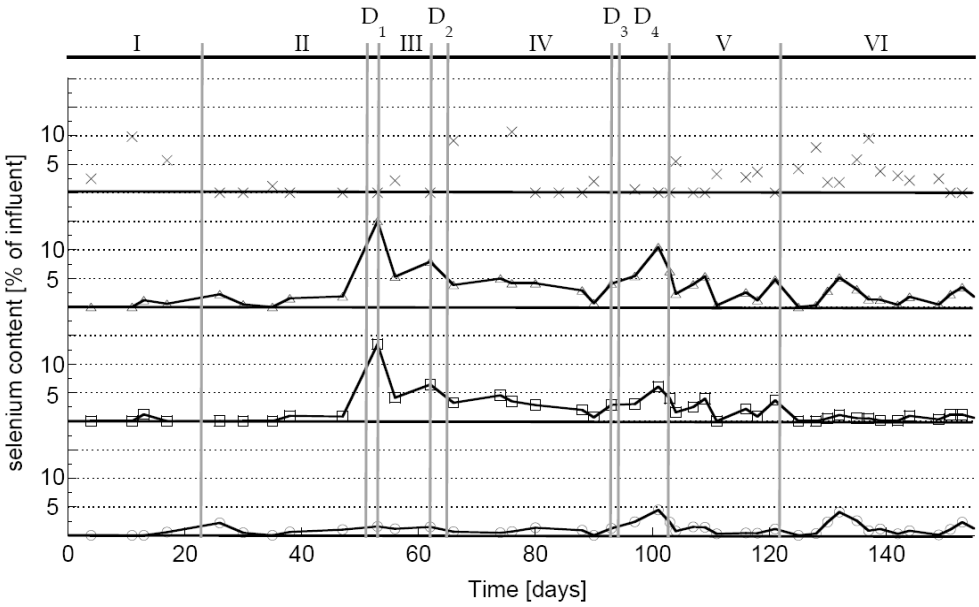


Figure 5.3 Selenium liquid phase speciation in relation to selenium in the influent [%]: (—○—) dimethylselenide, (—□—) dimethyldiselenide, (—△—) sum of dimethylselenide and dimethyldiselenide, (×) selenium undetermined



No selenium containing precipitates could be found on the microbial surfaces of the anaerobic granules from the UASB sludge bed sampled after 60 days of operation, even after extensive search. The SEM pictures of the biofilm growing in the PTFE tubes of the bioreactor, however, showed microorganisms of approximately 1.2 to 1.6 µm length and 0.5 µm in diameter, covered with a crust of particles with a size between 50 and 100 nm (Figure 5.4B). Furthermore, amorphous precipitates of approximately 150 nm diameter were observed (area “c”, Figure 5.4B). The EDX surface scan analysis of the selected area “a” including several microorganisms (Figure 5.4B) showed the presence of carbon, oxygen, copper, selenium, platinum, and iron. The same elements were detected in a surface scan of an area containing only the larger diameter precipitates (area “c”, Figure 5.4B). When focusing on a single microorganism (signal “b”, Figure 5.4B), however, the EDX analysis showed the presence of all the latter elements, except for iron.

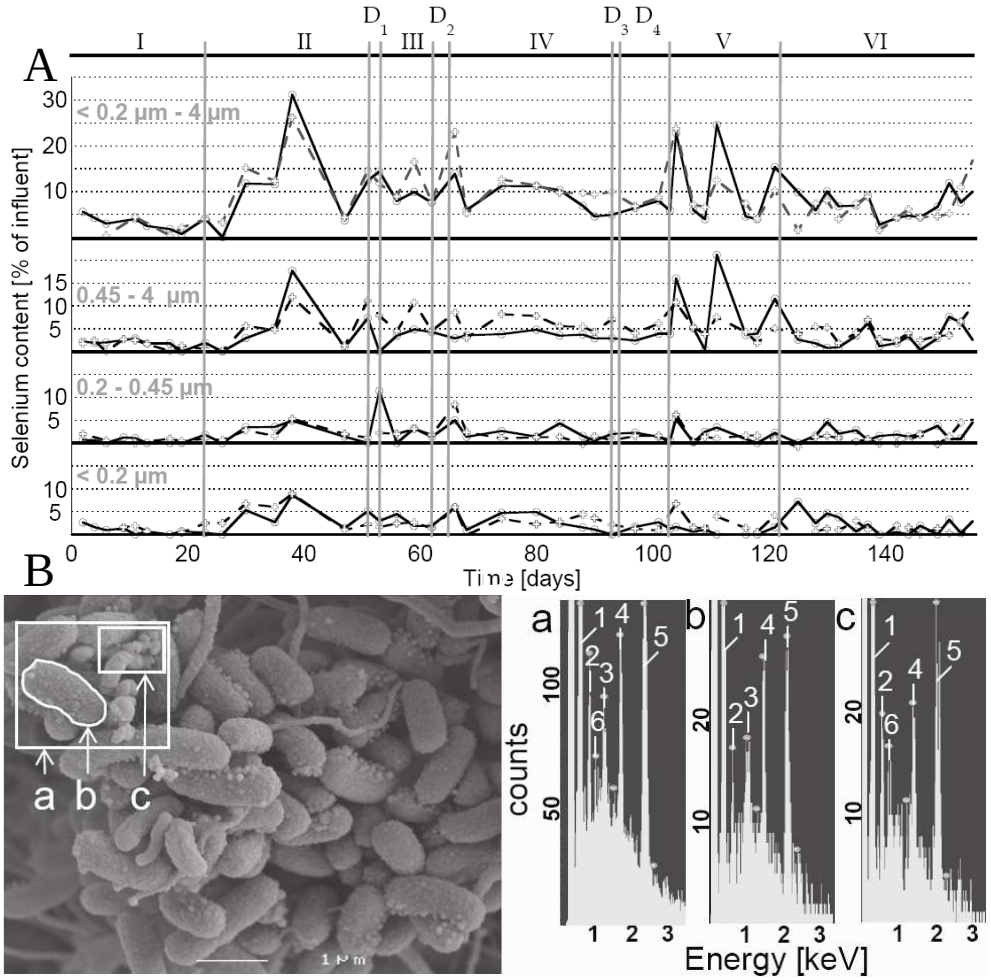


Figure 5.4 Particle size distribution of colloidally dispersed selenium (A) in (—o—) reactor effluent [%] and (–□–) settler effluent [%] and SEM pictures of biofilm proliferating in tubings (B) with EDX scans of selected areas (a-c), operational phases (roman numbers) and disturbances ($D_x$) are described in Table 5.1. Elements detected were carbon (1), oxygen (2), copper (3), selenium (4), platinum (5) and iron (6). Note that the presence of copper is due to the sample holder, the presence of carbon and platinum due to the coating.

Settling colloidally dispersed selenium by centrifugation together with specific determination of selenate, DMSe and DMDSe allowed to close the selenium liquid phase balance almost completely during the first 155 days of reactor operation (phases I to VI, Figure 5.3). Undetermined selenium species ($Se_{undet}$) in the liquid phase accounted for less than 5% for most sample times, with a few exceptions showing higher $Se_{undet}$ values.

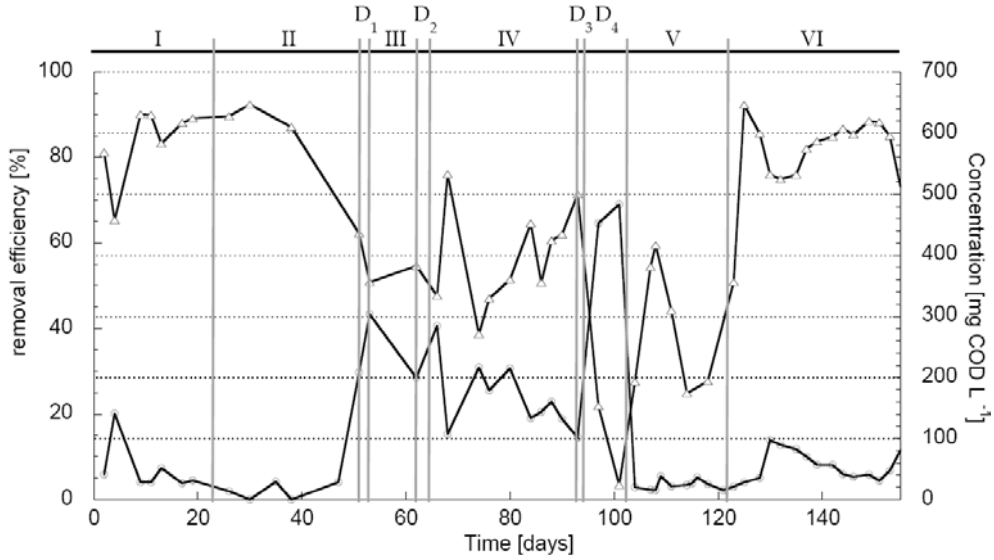


Figure 5.5 Reactor performance: (—△—) COD removal efficiency [%]; secondary y-axis (—○—) propionate concentration in the effluent [mgCOD $L^{-1}$]

In the beginning of the reactor operation (phases I and II), the COD removal efficiency stabilized around 85%, with non-converted COD mainly consisting of propionate (Figure 5.5) and minor amounts of acetate (data not shown). The COD removal efficiency was subsequently influenced by the reactor disturbances, reaching again 85% in phase VI of the reactor operation. The residual COD was removed in the settler, resulting in COD removal efficiencies exceeding 93% after phase V (data not shown).

## 5.3.2 Effect of disturbances in operational temperature

Disturbance $D_1$ did not influence the selenate removal efficiency (Figure 5.2A), but the $Se_{dis}$ removal decreased (Figure 5.2B), caused by the formation of methylated selenium compounds of up to 15.1% of $Se_{in}$ (Figure 5.3). DMDSe showed a maximum

of 91 µg Se $L^{-1}$, while the contribution of DMSe was of minor importance (maximum 11 µg Se $L^{-1}$). The DMDSe concentration decreased quickly to 31 µg Se $L^{-1}$ 3 days after cooling (day 56 of operation). Propionate accumulated to 303 mg COD $L^{-1}$ in the effluent (Figure 5.5), resulting in a reduced COD removal efficiency (53%), but not in acidification of the reactor (pH = 6.9).

Disturbance $D_5$, in contrast, caused a decrease in selenate and $Se_{dis}$ removal efficiency 9 HRTs after cooling of the reactor to 20°C (Figure 5.6). The selenate removal efficiency recovered after 16 HRTs, but $Se_{dis}$ continued to decrease until day 163 (HRT 28). This reduced removal efficiency originated from the formation of an unknown selenium species (up to 22% of $Se_{in}$), as both DMSe and DMDSe did not significantly contribute to $Se_{undet}$. SPME-GC-MS revealed two major mass fragments at m/z= 142 and m/z=127 (retention time 9.82 min, Figure 5.7). These might indicate either dimethyl selenenyl sulfide (DMSeS) or dimethylselenone ($DMSeO_2$), with fragments m/z= 142 and m/z=127 originating from $^{80}Se$ and the surrounding isotopic pattern around these m/z values from other stable Se isotopes ($^{78}Se$, $^{76}Se$, $^{82}Se$, $^{77}Se$). Note that these compounds could not be detected during the first 155 days of operation (GC-MS signals examined at times with $Se_{undet}$ > 5%, Figure 5.3). The distinction between DMSeS and $DMSeO_2$ was not directly possible due to the unavailability of standards and the fact that a disturbing signal was underlying the peak of interest (retention time 9.4 to 10.6 min, Figure 5.7), causing abundant mass fragments of m/z= 96, 133, 161, 163, 177, 179, and 191.



During the disturbance $D_5$, the COD removal efficiency was lowered (68%) only immediately after cooling, but recovered within 1 day (4 HRTs) and remained higher than 83% afterwards (data not shown) without acidification.

Decreasing the temperature to 20°C for 3 HRTs (disturbance $D_3$) resulted in acidification ($D_4$) of the reactor effluent yielding a pH of 6.1 due to the accumulation of VFAs, in contrast to the disturbances $D_1$ and $D_5$ (VFA accumulation not accompanied by a pH drop). Propionate accumulated up to 482 mg COD $L^{-1}$, resulting in no net-COD removal and a pH drop from 6.9 (day 93) to 6.1 (day 103) ($D_4$). Selenate and $Se_{dis}$ removal efficiencies remained high before a strong decrease was observed on day 103. Part of the residual selenate in the reactor effluent was removed in the settler, resulting in a 5.8% smaller drop in removal efficiency on day 104. An increase in alkylated selenium species was observed (up to 10.3% of $Se_{in}$), with DMSe contributing to higher amounts compared to the previous reactor operation (Figure 5.3). Selenium was partly re-oxidized to selenate in the settler during later sampling times (days 109 to 115, days 123 to 130) (Figure 5.2A).

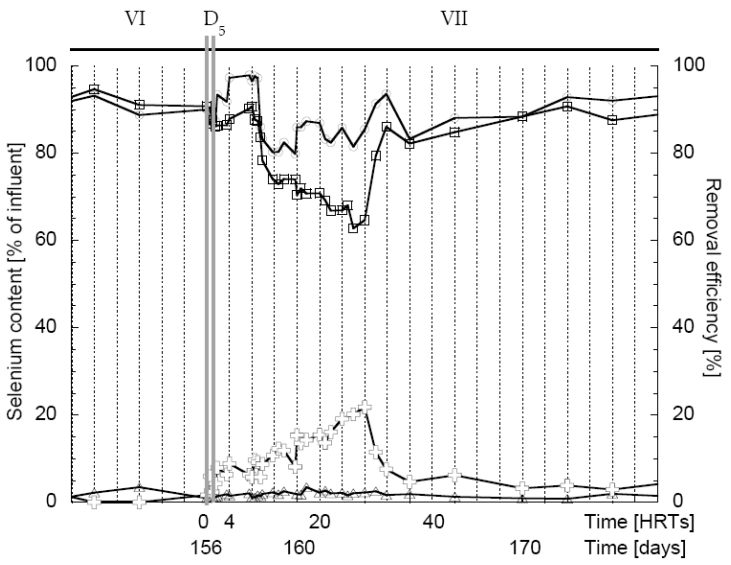


Figure 5.6 Effects of reactor cooling on the formation of (—△—) alkylated selenium species [%] and (—□—) selenium undetermined [%]; secondary y-axis removal efficiency [%] of (—○—) selenate and (—■—) selenium dissolved [%]

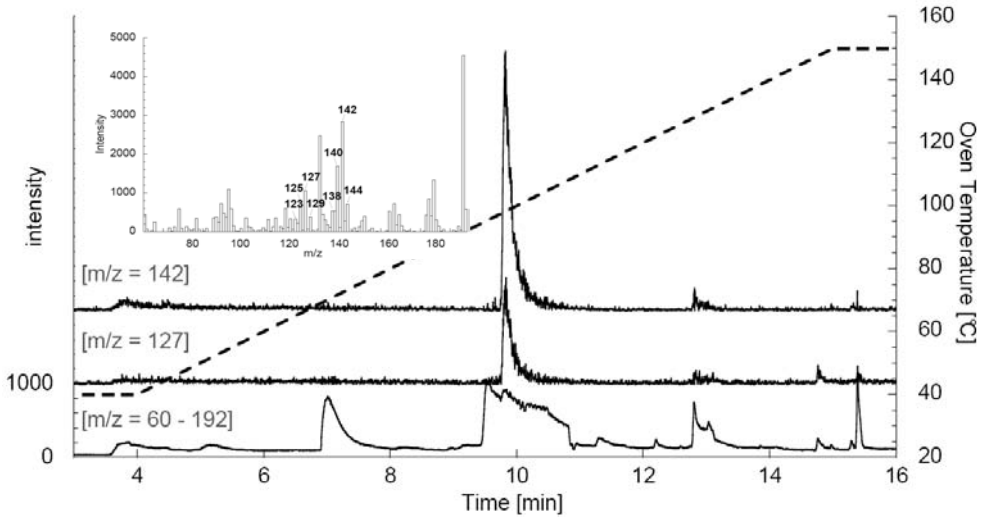


Figure 5.7 Chromatogram of liquid phase sample (28 HRTs after disturbance $D_5$) with mass spectra of unidentified selenium species at retention time 9.82 min. Intensity of the full spectrum (m/z = 60-192) is lowered by the factor ×100 for better display

By lowering the OLR (phase V), the pH increased within one day to pH 6.6 and lower amounts of VFAs accumulated (< 37 mg $COD_{propionate}$ $L^{-1}$). During this recovery of the reactor, only DMDSe was formed in significant amounts (Figure 5.3). Colloidal selenium was increasingly washing out from the reactor, mainly dispersed in the effluent as particles of 0.45 to 4 µm (Figure 5.4A).

## 5.3.3 Effect of disturbance in operational upflow velocity

During disturbance $D_2$ both the selenate and $Se_{dis}$ removal efficiency decreased, with a higher decrease in the $Se_{dis}$ (10.0%) than in the selenate (4.4%) removal efficiency. This was due to an increase in the $Se_{undet}$ concentration (10.6%, 79.7 µg Se $L^{-1}$), as the DMSe and DMDSe concentration decreased (Figure 5.3). Selenate washing out from the reactor was converted in the settler liquid, but the $Se_{dis}$ concentrations were comparable to the reactor liquid concentrations (Figure 5.2A and B). After the reconstitution of the recycle flow on day 66 ($v_{up}$ = 1 m $h^{-1}$, phase IV), 23.6% of $Se_{in}$ was washing out in colloidal form from the settler, mainly by larger particle sizes (0.45 to 4 µm and 0.2 to 0.45 µm) (Figure 5.4A).



## 5.3.4 Endogenous selenium alkylation by reactor sludge

Most selenium was methylated (DMSe + DMDSe) in batch "C" at 20°C, whereas DMDSe was exclusively formed at 30°C (Table 5.2). When adding lactate as electron donor (batch "A"), 49% more DMSe was formed in comparison to the batch without lactate addition (batch "B"). No methylated selenium compounds were formed in the autoclaved controls nor batches with inhibited metabolic activity (lactate degradation) by a low pH or high $S^{2-}$ concentration.

Table 5.2 Selenium alkylation from endogenous selenium sources (in the absence of selenate) by reactor sludge sampled after 60 days of operation.

| batch | e-donor [g-$COD_{Lactate}$ x $L^{-1}$ ] | T [°C] | DMSe [µg Se x $L^{-1}$] | DMDSe [µg Se x $L^{-1}$] | Sum [µg Se x $L^{-1}$] |
|---|---|---|---|---|---|
| A | 2 | 30 | 14.9 ± 1.6 | n.d. | 14.9 |
| B | 0 | 30 | 10.0 ± 0.7 | n.d. | 10 |
| C | 2 | 20 | 12.4 ± 4 | 9.6 ± 0.1 | 22 |
| autoclaved | 2 | 30 | n.d. | n.d. | 0 |
| pH = 2 | 2 | 30 | n.d. | n.d. | 0 |
| 20 mM $S^{2-}$ | 2 | 30 | n.d. | n.d. | 0 |

n.d. = not detected (MQL = 1.5 and 2.5 µg Se $L^{-1}$ for DMSe and DMDSe, respectively)

# 5.4 Discussion

## 5.4.1 Biological selenate removal in methanogenic UASB reactors

This chapter shows that methanogenic UASB reactors nearly completely remove selenate (<98.6%) from the liquid phase (Figure 5.2A and B) and reduce the $Se_{dis}$ concentration to a minimal value of 28 µg Se $L^{-1}$. These effluent concentrations meet the current water quality criterion for salt waters (71 µg Se $L^{-1}$) set by the United States Environmental Protection Agency [241]. UASB reactors have been evaluated previously for the treatment of real [170] or synthetic (Chapter 4) selenate contaminated wastewaters. Minimal effluent concentrations reported here are in accordance to previously reported values e.g. 20 µg Se $L^{-1}$ at pH 6.9 [170]. However, here these effluent concentrations were achieved feeding more selenate (≈ 2 times) using a 3 times shorter HRT in comparison to Owens (1997). The improvement in removal efficiency is probably due to the more constant temperature applied in this chapter, as selenate and $Se_{dis}$ removal were shown to be strongly temperature dependent (Figure 5.2A and B, Table 5.1).



## 5.4.2 Alkylation products

Here it was demonstrated that substantial quantities of the selenium (up to 118 µg Se $L^{-1}$) were alkylated, mainly following temperature decreases ($D_1$ and $D_3$, Figure 5.3). Batch incubations showed that previously accumulated selenium was alkylated in a biological reaction (Table 5.2). DMDSe was the main alkylated compound for most of the runtime (Figure 5.3) and DMSe was only during a few sampling times the major product. This contrasts e.g. Dungan and Frankenberger [41], who reported DMSe to be the major volatile gas produced by most selenium alkylating bacteria and fungi. DMDSe sorbs to aerobic soils, where it is subsequently converted to Se(+IV), Se (0), and Se (-II) [142]. In methanogenic UASB reactors, however, this mechanism most probably plays a minor role due to the strongly reduced environment ($p_e$ < -300 mV). The lower concentrations of DMSe in the liquid phase during stable operation (phases I to IV) can also be explained by its degradation to methane and carbon dioxide by methylotropic methanogens [158; 168], which have been shown to be present in the inoculum [33].

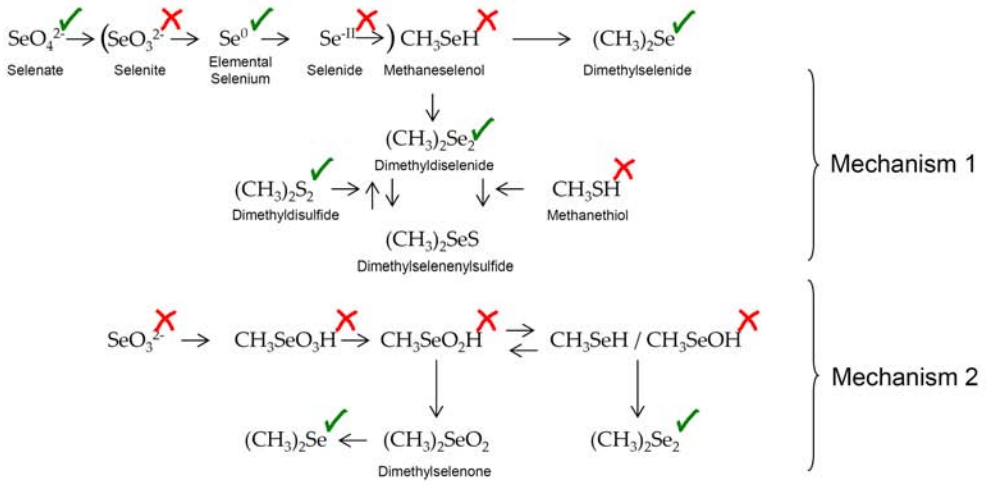




Figure 5.8 Mechanisms of selenium alkylation modified after Chasteen (1993), Chasteen and Bentley (2003)[23; 24]. Compounds detected in this chapter are marked by a hook (✓), undetected compounds by a cross (✗)

The major mass fragments m/z = 142 and m/z = 127, observed after disturbance $D_5$, can be assigned to either DMSeS or $DMSeO_2$, which have both been proposed as possible alkylation intermediates (Figure 5.8). Although the boiling point of $DMSeO_2$ has not been determined so far, the boiling point of its sulfur analogue (Dimethyl sulfone) is considerably higher than the applied oven temperature (238°C), thus elution of $DMSeO_2$ between DMSe and DMDSe (boiling points of 58 and 154°C, respectively) is unlikely [23]. Furthermore, the fact that selenate, elemental selenium, DMSe, DMDSe, and DMDS were detected here indicates that disproportionation of DMDSe and DMDS leads to the formation to DMSeS, according to mechanism 1 (Figure 5.8).

The alternative mechanism 2 via dimethylselenone is still discussed in the literature [41; 292] as $DMSeO_2$ can be used for the methylation to DMSe. It is not likely to occur in the sludge studied, as none of the intermediates, especially selenite, was detected. DMSeS has so far been found in cultures isolated from selenium contaminated environments [23] and in genetically modified *Escherischia coli*, carrying a gene of the metal resistant *Geobacillus stearothermophilus* [221]. It can thus be assumed that DMSeS is present in the liquid phase, contributing to the $Se_{undet}$ here. If a purely chemical disproportionation of DMDSe and DMDS to DMSeS takes place [23; 24], DMSeS should be detectable during stable reactor operation, as both DMDSe and DMDS were simultaneously present in the reactor liquid. It

is possible that DMSeS is indeed formed by chemical disproportionation, but not detected (closed selenium liquid phase mass balance, Figure 5.3) as it is microbially degraded during stable operation. Operational disturbances alter the microbial degradation rates, which would then allow the temporary detection of DMSeS.

## 5.4.3 Formation of colloidally dispersed selenium

The complete surface of the microorganism found in the reactor tubes was crusted with nano-sized (50 to 100 nm), amorphous particles (Figure 5.4B). In contrast, when incubating pure cultures of selenate respirers [167] or anaerobic granular sludge under higher selenate conditions (Chapter 4) in batch tests, globular particles of ~300 nm were observed. In the latter cases, the globular particles were loosely attached on the bacterial surfaces in pearl necklet form. The difference in shape and size of the selenium particles in this chapter might be due to the higher sheer forces induced by the high upflow velocity (38 m $h^{-1}$) in the recycle tube, possibly resulting in wash out of larger particles (4 to 0.45 µm) (Figure 5.4A). Indeed, after reconstitution of the recycle flow (transition between $D_2$ and phase IV), a wash out of 0.45 to 4 µm selenium particles was observed (Figure 5.4A). Interestingly, *E. coli S17-1* cells expressing the *E. cloacae fnr* gene (genetic regulator that controls selenate reductases activity) precipitate slightly smaller selenium particles (with diameters of 100 to 150 nm) than those of the original *E. cloacae* strain [275]. Consequently, other factors (e.g. different growth conditions or growth phase) also influence the particle size distribution and shape of the selenium precipitates, and thus need to be considered, if one aims at production of larger selenium particles.



The EDX analysis of the smaller particles observed here (Area B, Figure 5.4B) indicated that selenium is rather present in its elemental state than as metal selenides, as no further elements than those introduced by the sample preparation were observed. However, this hypothesis has to be considered with caution, as EDX analysis gives no information on selenium speciation. Yet, an elemental character would confirm the results of chapters 3 and 6. EDX signals of the complete scan area (area A, Figure 5.4B) also showed the presence of iron, but this is most probably due to iron sulfides formed under reducing conditions [251].

## 5.4.4 Implications for selenate removal in practice

This chapter demonstrates that high selenate conversion efficiencies can be achieved in methanogenic UASB reactors, but that careful process control is a prerequisite for

successful removal in full scale applications. This is due to the fact that both the formation of selenium nanospheres and alkylated selenium species significantly contribute to selenium effluent concentrations in disturbed bioremediation processes. The selenium nanospheres are not separable by simple technical means, but the recovery of biologically formed elemental selenium before discharge of the effluent is of particular importance for practical applications, as re-oxidation of selenium can occur in oxidizing environments [291] and biologically formed, nano-sized particles are potentially bioavailable [131; 285].

The formation of alkylated selenium compounds in sealed bioreactors is not advantageous, because selenium concentrations can be up to 620 mg $L^{-1}$ in industrial waste streams [64], thus posing a potential health risk to workers. Simple dilution of DMSe and DMDSe to the atmosphere is not an option, due to the fact that alkylated selenium compounds are malodorous in trace concentrations [206]. Furthermore, the long term toxicological effect of the latter compounds on living organisms has not yet been investigated. They also show a strong synergistic toxicity with other toxins such as arsenic [99]. The fact that selenium containing UASB reactor biomass formed alkylated selenium compounds endogenously (Table 5.2) should be considered, especially when biomass from full scale reactors is harvested and stored.



Particularly under unstable operational conditions, selenium speciation (including bioavailable organic selenium forms) should be monitored carefully, as high amounts of alkylated selenium or seleno-sulfur species can be formed. This chapter showed that the formation of alkylated species occurred with a delay to the temperature decrease (disturbance $D_5$, Figure 5.6). For selenium treatment plant operators, this offers the possibility to prevent $Se_{dis}$ wash out by carefully controlling temperature and e.g. applying additional buffer tanks after disturbances.

A start-up of the reactor during 23 days of operation (phase I) was necessary before a steep increase in the $Se_{dis}$ and selenate removal efficiency by the reactor was observed (phase II), probably due to the proliferation of a selenium-respiring specialist (Chapter 4). The increase in selenate reduction rate (due to growth or induction of higher selenate reducing activity) by the biomass retained in the reactor can be fitted linearly ($r^2$=0.995; days 23-35) with 1.32 µM selenate $L_{reactor}^{-1}$ $d^{-2}$. Such a linear increase in selenate reduction rate has been observed before under similar conditions (HRT = 6h, pH = 7.0; T= 30°C) in Chapter 4. However, the increase observed here was 1.85 times lower due to the 2.5 times lower OLR applied in this chapter. The linearity suggests a capability of the retained biomass to treat even higher selenate influent concentrations. However, this might induce toxic effects on the anaerobic food web (Chapter 7) or increased formation of alkylated selenium species. Note that in case of high (10 mM) selenate concentrations, the granules become encrusted by a layer of red elemental selenium, which can reduce mass transfer (Chapter 7).

As elemental selenium is a valuable product [245], selenium recovery could improve the cost-benefit ratio of reactor operation, similar to the recovery of other by-products during selenium removal processes [214]. Despite the fact that the external settler retained fractions with a larger particle size (0.45 to 4 µm) during normal reactor operation (Figure 5.4A), the formed particles were not large enough to settle and remained dispersed in solution. In order to meet total maximum daily loads for selenium, dissolved gas flotation could be applied [271], as it can remove the colloidal selenium particles [185] and will also strip the alkylated selenium compounds. The fact that no selenite was detected (MQL: 24 µg Se $L^{-1}$; 3% of $Se_{in}$) in the effluents of neither the reactor nor the settler at any time is of particular importance, as selenite is considered to be more toxic to aquatic invertebrates and fish compared to selenate [73].



A minor part of the selenate that washed out of the reactor was reduced by suspended biomass using residual COD (mainly propionate) as electron donor in the settler liquid, especially after the disturbance in $v_{up}$ ($D_2$) and the acidification ($D_4$) (Figure 5.2A). Consequently, one could argue that the present reactor was not merely a UASB reactor system, but a chemostat from which the selenium reducing biomass washed out and consequently that the settler was actually a second bioreactor. Accordingly, systems with suspended biomass retention (e.g. a membrane bioreactor) should be rather used in practice. However, the utilization of an UASB reactor system should not be abolished for selenate biotreatment for different reasons. First of all, sludges operated under similar conditions display improved selenate removal efficiency upon prolonged reactor operation (Chapter 4). Secondly, the biodiversity of sludge granules is high [33; 187], making the reactor less vulnerable to disturbances than systems that rely on a single or a few specialized microorganisms. Thirdly, the organization in a dense biofilm can result in concentration gradients from the bulk liquid to the inside of the granule [68; 197], possibly protecting inner microorganisms from toxins. Finally, the sludge bed can convert high loads of COD, preventing the wash out of VFAs by converting them into methane and thus offering energy recovery via biogas production. When using an UASB system, a high HRT (>> 6h) or buffer tanks should be considered to guarantee a complete removal of the selenate load.

# 6

# Induced changes in selenium speciation during sequential extraction assessed by XANES spectroscopy

This chapter was submitted for publication as: Lenz, M., van Hullebusch, E. D., Farges, F., Nikitenko, S., Borca, C.N., Grolimund, D., Lens, P.N.L. Selenium speciation in anaerobic biofilms assessed by X-ray absorption spectroscopy and sequential extraction procedures.

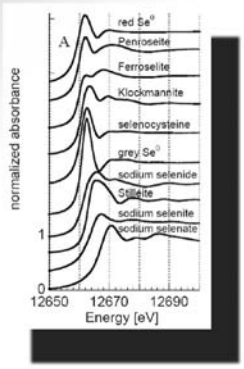

# Abstract

Wet chemical methods such as sequential extraction procedures are commonly used to assess selenium fractionation in anaerobic environments, allowing an estimation of the mobility and bioavailability of selenium. However, the interpretation can be biased by unselective extraction of targeted species and artifacts introduced during the extraction. Here, the selectivity of the single extraction steps are scrutinized for the first time by direct, non destructive X-ray absorption near edge structure (XANES) spectroscopy. The sequential extraction procedures seriously overestimated the elemental selenium fraction, as major parts (58%) of the total selenium were present as metal selenides and organic selenium compounds, although extracted in the elemental fraction.

Decomposition of the XANES spectra by the least square linear combination method utilizing a large set of model compounds, including previously neglected Se(-I) selenides, showed a novel degree of complexity in the speciation of selenium treating biofilms, with up to 4 pseudo-compounds, i.e. different elemental, organic and metal bound selenium species, present in the biofilms. Furthermore, it was shown that a short exposure (10 min) to ambient air during the SEP induced oxidation of organic selenium compounds, revealing the fragility of selenium speciation in anaerobic biofilms.

# 6.1. Introduction

Selenium is characterized by its ambivalent character of being both essential and toxic to living organisms. It is present in the environment in at least five oxidation states (-II, -I, 0, IV, VI) [154] in a variety of organic and inorganic compounds. The environmental fate and the toxicity of selenium strongly depends on its chemical speciation [278], thus a determination of the total selenium content is insufficient to assess the impact of selenium contamination.

To estimate risks posed by selenium contamination, sequential extraction procedures (SEPs) operationally define fractions of selenium by applying different extractants and extraction conditions [141; 184; 231; 269]. As SEPs do not require sophisticated analytical equipment, they can be used on a routine basis. Although applied to anaerobic environments like sediments [141; 269] or deep soil layers [111; 259], the alteration of selenium speciation by oxidation through ambient air during extraction has thus far not been given attention [164; 239]. In this context, the fractionation can be biased by both oxidation of the matrix (e.g. oxidation of sulfides [113]) or by changes in selenium speciation [111]. If the speciation is not preserved or the SEPs are not selective for the targeted species, bioavailable fractions can be seriously underestimated.



This chapter investigates the speciation changes during short exposure to ambient air, e.g. during field sampling or sample preparation. The applicability of SEPs is tested on anaerobic granular sludge, originating from an upflow anaerobic sludge bed (UASB) reactor treating selenate contaminated synthetic wastewater under disturbed operational conditions (Chapter 5).

Solid phase speciation and changes induced by ambient air were assessed by X-ray absorption near edge structure (XANES) spectroscopy. Linear combinations with a variety of natural and synthetic reference model compounds were used to assess the local structural environment. Special care was given to assess the presence of Se(-I), an oxidation state that has often been neglected in past XANES studies. Furthermore, selenium model compounds that have previously not been included in SEP studies (aqueous selenide and selenocysteine) were spiked to the anaerobic biofilm and the possible influence of oxidation by ambient air on selenium fractionation was investigated.

# 6.2. Material and methods

## 6.2.1 Source of Biomass

Anaerobic granular sludge from a full scale UASB reactor treating paper mill wastewater (Industriewater Eerbeek B.V., Eerbeek, Netherlands) was utilized for the selenium spiking experiments and as inoculum for a lab-scale bioreactor, operated under methanogenic conditions treating 40 µM $L_{reactor}^{-1}$ $d^{-1}$ selenate (Chapter 5). Biomass of the lab-scale reactor was harvested after 60 days of operation and SEPs were applied to the sludges.

## 6.2.2 Spiking experiments



Granular sludge was autoclaved for 20 min at 121°C, either in glass serum bottles sealed with a butyl rubber stopper and flushed with $N_2$, or in cotton plugged aerobic glass serum bottles. Selenocysteine (ultra-pure quality; Sigma-Aldrich, Zwijndrecht, Netherlands) was spiked in solid form (ultra-fine balance AT21, Mettler Toledo, Tiel, Netherlands) to the autoclaved sludge (0.15 g wet weight), while sodium selenide (ultra-pure quality; Alfa Aesar, Karlsruhe, Germany) was dissolved in an anaerobic stock solution (phosphate buffer, 40 mM, pH = 7.0 ± 0.1).

## 6.2.3 Sequential Extractions

SEPs for selenium fractionation were done as described by Wright et al. (2003) [269], but using a 10 times higher extractant : solid ratio, due to incomplete selenium recoveries observed in pre-experiments. Prior to the extraction, the samples were homogenized using a glass stick. Briefly, fraction I targeted soluble/exchangeable selenium (extraction with 0.25 M KCl), fraction II the adsorbed selenium (extraction with 0.1 M $K_2HPO_4$), fraction III elemental selenium (extraction with 0.25 M $Na_2SO_3$, sonication at 20 kHz for 2 min, then ultrasonic bath for 4h) and fraction IV organically associated selenium (extraction with 5% NaOCl).

The SEPs were carried out either under a $N_2$ atmosphere in an anaerobic glove box or aerobically on the lab bench, exposing the samples 10 min to ambient air prior to continuation with each extraction step. In case of the anaerobic extraction, centrifugation was conducted in airtight high purity polypropylene copolymer (PPCO) vials (Nalgene,

Neerijse, Belgium). Selenium was determined by Inductively Coupled Plasma-Optical Emission Spectroscopy (ICP-OES) (Chapter 2).

Subsequent to each extraction step, one batch of the respective samples was placed in a custom made sample holder of polytetrafluoroethylene using the anaerobic glove box. Samples were sealed from ambient air by kapton tape. The sample holders were stored (4°C) under $N_2$ in a wide mouth bottle until the XANES measurements. The residues of the first, second and third extraction step are referred to as R1, R2 and R3, while residues of extraction conducted under ambient air are referred to as "$O_2$" and anaerobic extractions as "$N_2$".

## 6.2.4 Selenium solid phase speciation



Selenium K-edge (12.66 keV) X-ray absorption fine structure (XAFS) experiments were performed at the Dubble beamline (ID 26, ESRF, Grenoble, France) and at the MicroXAS beamline (X05, SLS, Villingen, Switzerland). The first beamline was used to obtain systematic "bulk" XANES information, whereas the second beamline was used to collect µ-XANES spectra on selected areas of the samples. At the ESRF, a focused beam (~ 0.2 x 3 mm) with a 9-elements solid-state Ge detector was used. At the SLS, a microfocused beam (~ 3 x 3 $\mu m^2$) with a 32-elements solid-state Ge detector was utilized. At both beamlines, Si(111) double-crystal monochromators were applied, ensuring a comparable energy resolution of about 2.5 eV at 13 KeV. The energy calibration for both monochromators was achieved using grey, trigonal selenium placed in the second ionization chamber (transmission mode), using the main crest edge at 12662.5 eV. All biofilm samples were recorded in fluorescence mode, placed at an angle of 45° relative to the incoming X-ray beam, while model compounds were measured in transmission and fluorescence modes (positioned normal to the incoming beam to minimize self-absorption effects). No photoreduction due to the X-ray beam was observed during the measurements.

## 6.2.5 XAFS data reduction and calculations

XANES spectra were normalized using the XAFS software package [267] using standard procedures [51]. Least square linear combination XANES fittings were done using MS Excel SOLVER, using the recorded spectra at energies between 12,635 to 12,700 eV of a variety of model compounds, including natural and synthetic samples of all environmentally occurring formal oxidation states (Table 3.1).

# 6.3. Results

## 6.3.1 Effect of ambient air on fractionation by sequential extraction

The spiking experiments demonstrated that selenocysteine was yielded mainly in the soluble / exchangeable fraction, while minor parts adsorbed to the sludge, independent from the presence or absence of oxygen (Table 6.1). Selenide was found to higher amounts in the elemental fraction during the aerobic extraction (88.6% versus 72.1%) and more selenium was yielded in the organically associated and residual fraction when treated anaerobically (Table 6.1). Only minor differences were noted in the soluble/exchangeable and adsorbed fractions. Red precipitates (probably red elemental selenium) were noted upon spiking of the selenide solution in both extractions, although the anaerobic aqueous spiking solution was stable.



Table 6.1 Selenium fractionation by sequential extraction: bioreactor samples and spiking experiments

| sample | extraction condition | soluble / exchangeable (Fraction I) | adsorbed (Fraction II) | elemental (Fraction III) | organically associated (Fraction IV) | residual | Σ |
|---|---|---|---|---|---|---|---|
| bioreactor sludge | $O_2$ | 2.0 ± 0.3 | 2.5 ± 0.1 | 109.2 ± 1.9 | 0.2 ± 0.0 | 0.5 ± 0.3 | 114.4 |
| | $N_2$ | 0.8 ± 0.1 | 1.5 ± 0.1 | 86.8 ± 4.8 | 0.4 ± 0.1 | 0.7 ± 0.3 | 90.2 |
| selenocysteine | $O_2$ | 88.1 ± 2.7 | 8.5 ± 1.9 | 1.0 ± 0.2 | 0.1 ± 0.0 | 0.1 ± 0.0 | 97.9 |
| | $N_2$ | 87.8 ± 1.6 | 7.8 ± 0.1 | 2.3 ± 0.3 | 0.3 ± 0.0 | 0.1 ± 0.0 | 98.2 |
| $HSe^-$ | $O_2$ | 2.7 ± 0.2 | 0.5 ± 0.1 | 88.6 ± 2.1 | 7.3 ± 0.2 | 1.4 ± 0.6 | 100.5 |
| | $N_2$ | 2.2 ± 0.3 | 0.2 ± 0.0 | 72.1 ± 2.6 | 19.9 ± 1.3 | 7.0 ± 1.1 | 101.4 |

The SEPs conducted with selenium containing bioreactor sludges yielded most selenium in the elemental fraction (fraction III), while minor amounts (≤ 1.5% in the presence of $N_2$; ≤ 2.5% in the presence of air) were found in the other fractions (Table 6.1). Extraction in the presence of air resulted in a larger elemental fraction, but total selenium recoveries were higher compared to the anaerobic extraction.

The XANES spectra of the residues obtained after the first (R1) and second (R2) sequential extraction step displayed a shifted main crest edge (≤ +0.7eV) and inflection point (≤ +0.9eV) when the SEP was conducted anaerobically ($RxN_2$) in comparison to extraction under ambient air ($RxO_2$) (Figure 6.1A, Table 6.2). A shift (-0.9eV) in the first inflection point position was determined in the third residue ($R3O_2$ versus $R3N_2$).

Table 6.2 Main XANES features for SEP residues

| specimen | extraction condition | residue | main edge crest [ eV ] | first inflection point [ eV ] |
|---|---|---|---|---|
| $R1N_2$ | $N_2$ | 1st | 12662.8 | 12660.6 |
| $R2N_2$ | $N_2$ | 2nd | 12662.9 | 12660.8 |
| $R3N_2$ | $N_2$ | 3rd | 12662.6 | 12660.0 |
| $R1O_2$ | $O_2$ | 1st | 12662.3 | 12660.1 |
| $R2O_2$ | $O_2$ | 2nd | 12662.2 | 12659.9 |
| $R3O_3$ | $O_2$ | 3rd | 12662.8 | 12660.9 |

Linear combinations suggested that the first two residuals extracted anaerobically ($R1N_2$ and $R2N_2$) were mainly composed of compounds related to trigonal Se (0) and cubic Se(-II) selenides (stilleite and berzelianite related) (Figure 6.1B). Minor contributions were due to organic selenium (related to selenocysteine) in R1 and to selenate in R2, respectively. Trigonal Se (0) and cubic Se(-II) (sodium selenide) like compounds were mainly contributing to the modeled $R3N_2$ spectrum. In contrast, a dihexagonal-dipyramidal (achavalite) type (Figure 6.1C) mineral contributed to the selenium speciation in $R1O_2$ and $R2O_2$. A marginal contribution (3%) of selenate to $R3O_2$ is reported but not considered further. The selenium content in the samples after the fourth extraction step was low (Table 6.1), thus XANES spectra for R4 could not be recorded during the beam time available.



# 6.4. Discussion

## 6.4.1 Selenium speciation in methanogenic granular sludge

An accurate description of selenium speciation in anaerobic biological samples, e.g. methanogenic granules, can be achieved by the investigated set of model compounds (Table 3.1) using linear combinations, demonstrated by the accurate best fits shown in Figure 6.1B and 6.1C. Although the number of reference compounds used to model the experimental XANES spectra was limited as much as possible, considerably better fits were achieved using 4 model compounds, demonstrating the complexity of selenium speciation in selenate treating UASB granules. Two components are, however, dominant in all models: trigonal Se (0) is dominant in all residues, stilleite or sodium selenide are relevant in the anaerobic extractions, while stilleite or achavalite are determining speciation in the aerobic extraction (Figure 6.1B and C). Thus, it is postulated that the two components are significantly determining the selenium speciation in the investigated samples, leaving uncertainties on the two others.

Figure 6.1 Normalized Se K-edge XANES spectra: residues of the sequential extractions (A) conducted anaerobically (grey line) and in the presence of ambient air (black line); residues R1 to R3 (solid lines) and best fit by linear combination to model compounds (×) after extraction performed anaerobically (B) and under ambient air (C). Contributions of model compounds to the best fit results are given in atom %

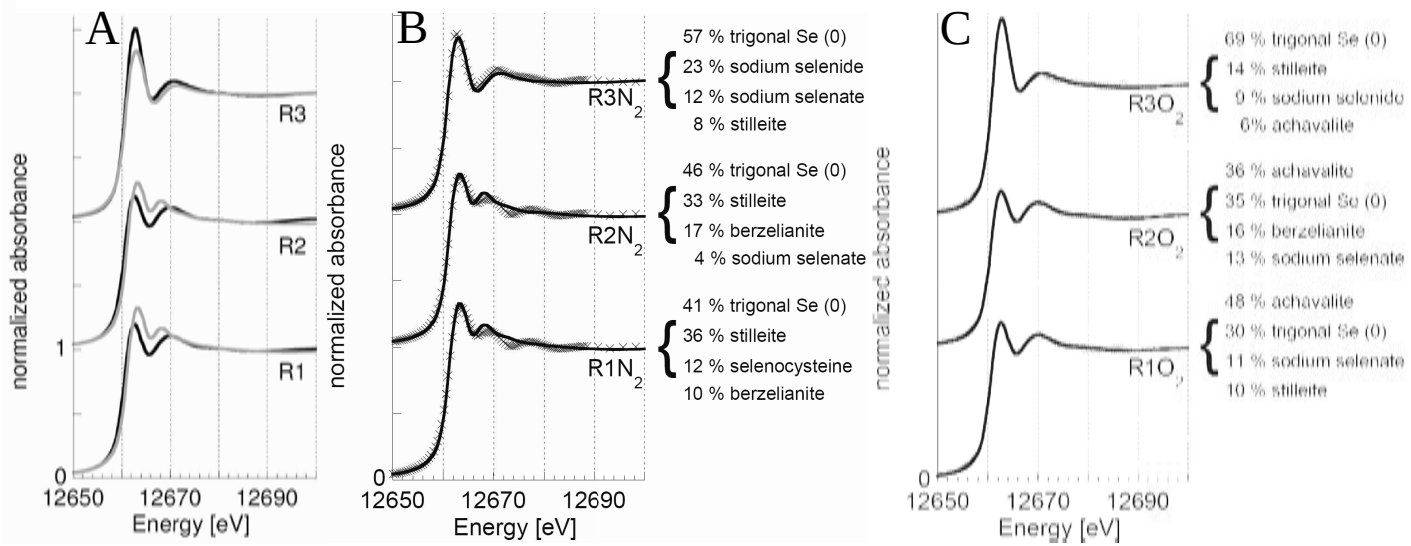

It can be assumed that the speciation of the bioreactor sludge during treatment of selenium containing wastewater is close to the modeled speciation in $R1N_2$ due to the fact that only minor amounts (0.8%) of soluble / exchangeable selenium were extracted (Table 6.1) and that the extractant (0.25 M KCl) is a constituent of the bioreactor feed, although in a lower concentration (5.6 mM). The XANES model demonstrated that most selenium (88%) was present in Se (0) and Se(-II) cubic form, thus confirming the ability of methanogenic UASB reactors to immobilize bioavailable (water soluble) selenium oxyanions to insoluble mineral phases. The fact that no metal selenide was so far detected by XRD methods in these sludges (Chapter 2 and 4) [5] can be explained by nanocrystallized (<100 nm) forms [7]. Indeed, when operated continuously in UASB reactors under methanogenic conditions, anaerobic granular sludge converts selenate to selenium containing particles of < 200 nm particle size, colloidally dispersed in the effluent (Chapter 5). The contribution of selenocysteine observed here (and in Chapter 3) can represent a precursor to selenium alkylation [24], as the sludges form dimethylselenide and dimethyldiselenide from endogenous selenium sources (Chapter 5). The higher contribution of elemental selenium to the modeled selenium speciation in the methanogenic anaerobic granular sludge investigated in Chapter 3 (67 atom %) can be explained by the longer reactor operation upon sludge sampling, if more selenium is fixed in the biomass as elemental selenium in comparison to metal selenides upon prolonged reactor operation. However, the modeling also implies that the total amount of selenium potentially being alkylated from endogenous sources increases as well, as contribution of selenocysteine is constant (12% here versus 14% after 115 days of operation), but the selenium sludge content higher.



In general, experimental XANES spectra obtained in methanogenic granules were well represented by the combination of model compounds used here (Figure 6.1B and C). Under high sulfur conditions, e.g. in sulfate-reducing biofilms, however, the interpretation of the XANES spectra might be complicated by the fact that selenium can be replaced by sulfur and precipitated selenides might comprise mixtures in different selenium:sulfur ratio, e.g. as mixed FeS/Se [84].

### 6.4.2 Influence of ambient air on selenium speciation / fractionation

This chapter shows that a short exposure (10 minutes) to ambient air, likely to occur during field sampling of e.g. contaminated sediments or anaerobic bioremediation systems, can induce a change in selenium speciation (Table 6.2, Figure 6.1A) and consequently fractionation (Table 6.1) in anaerobic biofilms.

The decomposition of the XANES spectra showed the presence of a highly oxidized (selenate-like) species in $R1O_2$ and $R2O_2$, which can be explained by the complete oxidation of organic (selenocysteine like) species [31; 74] to selenate ($R1N_2$ versus $R1O_2$). However, this oxidation is not reflected in different selenium yields in the first fractions of the SEP investigated, as both selenate [269] and selenocysteine are co-extracted in this fraction (Table 6.1). For the disposal of bioreactor excess sludge under aerobic conditions selenate formation is particularly problematic, as it adsorbs only badly to the sludge matrix [5] and might thus leach out.

In $R1O_2$ and $R2O_2$, a dihexagonal-dipyramidal Se(-II) selenide of achavalite type (space group: P 6/mmc, Table 3.1) was found in the best fitted linear combinations, in contrast to a F 43m cubic Se(-II) selenide (here: stilleite) in $R1N_2$ and $R2N_2$ (Figure 6.1B versus C). Due to the presence of cobalt and nickel in both the bioreactor feed (0.5 and 0.1 µM, respectively) and in the inoculum sludge, however, alternative selenides with the same space group (P 6/mmc) should also be considered, e.g. freboldite (CoSe, pKs= 31.2) or sederholmite (NiSe, pKs= 32.7) [207]. Due to the contribution of several species to the reconstructed XANES spectra and to the possible nanocrystallized character hindering exact identification by XRD, a precise mechanism for the mineral transition observed here cannot be assigned. Hypothetically, parallels to sulfur mineral chemistry might be drawn, where a transformation of chalcocite ($Cu_2S$) to covellite (CuS) by oxygen in sulfate solutions has been demonstrated [56]. To the best of our knowledge, the direct evidence of the berzelianite ($Cu_2Se$, F 43m) oxidation to klockmannite (CuSe, P 6/mmc) by ambient air has not been described in literature. A time resolved µ-XRF study could shed light on this oxidation mechanism.



The reconstructed XANES spectra suggest that the change in speciation of $R3O_2$ in comparison to $R3N_2$ (Figure 6.1A) was attributed to the oxidation of a cubic (sodium selenide) Se(-II) type to elemental selenium (Figure 6.1B versus C). However, the presence of sodium selenide as such is unlikely, as it is water soluble. It was furthermore demonstrated that aqueous selenide is highly labile even under strict anaerobic conditions and instantly oxidized to elemental selenium, as a red colored precipitate formed upon spiking to the sludge and the SEP yielded most selenium in the elemental fraction (Table 6.1), although insoluble selenides might also form, suggested by the organically associated fraction. Persistence of aqueous selenide formed by microbial processes [82; 84; 283] is thus unlikely in metal rich environments, e.g. anaerobic granular sludge or contaminated sediments represents, providing a sink for highly toxic aqueous selenide. Alternatively, an insoluble cubic Se(-II) type with a F m3m space group, e.g. clausthalite (PbSe, pKs = 42.10 [207]) might rather explain the modeled selenium speciation in $R3N_2$, as the inoculum is metal rich [281] and originates from a full scale wastewater treatment bioreactor.

## 6.4.3 Extraction selectivity of the SEP

This chapter demonstrates that the SEP achieves selectivity for selenocysteine, as mainly found in the soluble / exchangeable fraction (Table 6.1) in the spiking experiments and furthermore only contributing to the modeled speciation of $R1N_2$, but not $R2N_2$. Selenate, however, targeted in fraction 1 [269] contributed to the speciation of $R1O_2$ (Figure 6.1C) and is thus insufficiently extracted. The selectivity for elemental selenium targeted in fraction 3 is poor, as the decomposition of the XANES spectra suggested a high contribution of Se (0) like species to $R3O_2$ and $R3N_2$. Furthermore, the contribution of stilleite / berzelianite (Figure 6.1B) and achavalite species (Figure 6.1C) decreased between R2 and R3, demonstrating that the dissolution of these minerals leads to an overestimation of the elemental fraction, as observed by the high amounts of selenium yielded in the elemental fraction (Table 6.1). This implies a serious misinterpretation when evaluating detoxification from selenate by formation of elemental selenium in bioremediation applications.



## 6.4.4 Conclusion

In summary, this chapter shows that the applied SEP, although validated for several selenium species [269], gives an inaccurate description of the actual selenium speciation in complex matrixes including anaerobic granular sludge. Such a selectivity lack using sequential extraction procedures has previously been demonstrated by a XAS study for reduced sulfur species [174]. While sulfur fractionation determined by sequential extraction procedures can be verified in conjunction with alternative wet chemical methods, i.e. acid volatile sulfur [186], such routine methods have not been developed for selenium fractionation. Thus, the precise description of the selenium solid phase speciation relies on non-destructive, direct, species specific analytical methods, such as XAFS using careful speciation modeling with a sufficiently large number of selenium model compounds.

# 7

# Inhibition of hydrogenotrophic and acetoclastic methanogenesis by selenium oxyanions

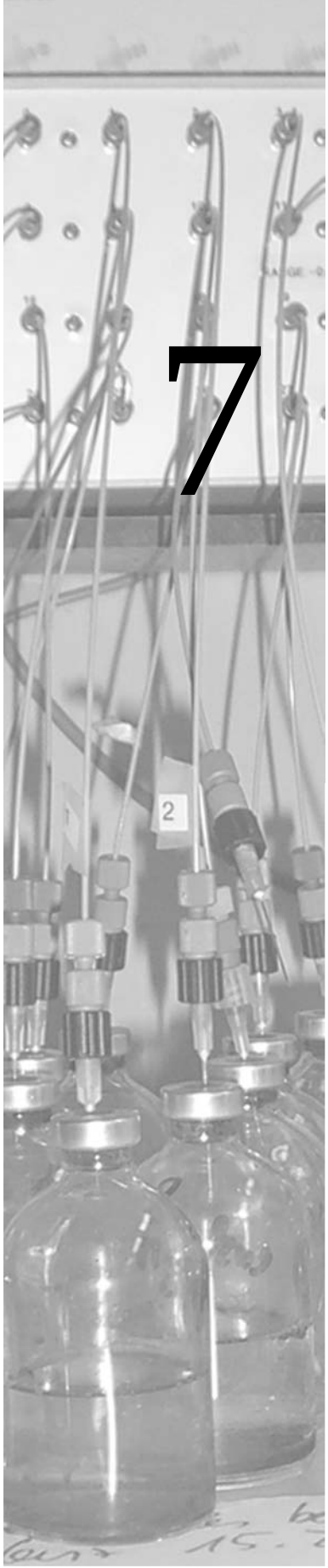


This chapter was submitted for publication as: Lenz, M., Janzen, N., Lens, P. N. L. (2007). Inhibition of hydrogenotrophic and acetoclastic methanogenesis by selenium oxyanions.

# Abstract

Inhibitory effects of selenite and selenate towards hydrogenotrophic and acetoclastic methanogenesis were evaluated in anaerobic toxicity assays. The 50% inhibitory concentrations ($IC_{50}$) for both selenium oxyanions were below 61 µM in hydrogenotrophic assays. Inhibition to acetoclastic methanogens was lower, as indicated by the higher $IC_{50}$ values, 83 µM and 552 µM for selenite and selenate, respectively. Selenite completely inhibits methanogenesis from both substrates tested at concentrations ≥ 1 mM selenite, while only marginal methanogenic activities occur at equimolar concentrations of selenate. Selenite becomes already inhibitory upon a single exposure, selenate inhibits methanogens upon repeated exposure. The inhibition had a permanent character, as it persisted in the absence of selenium oxyanions. Consequently, methane can not be recovered during biotreatment of highly selenium contaminated waste streams in methanogenic bioreactors.

# 7.1. Introduction

Selenium displays an ambivalent character of being both essential as nutrient, but becoming toxic to biota at elevated concentrations [270]. The border between its nutritional and toxic limit in animals and humans is narrow [265] and depends on the chemical speciation of selenium [278]. Consequently, both the selenium concentration and speciation need to be controlled carefully during water and wastewater treatment. Several physico-chemical [237] and biological selenium removal techniques have been developed [6; 9; 61], with microbial remediation techniques being promising due to their high selectivity for the prevalently targeted selenium oxyanions selenate and selenite (Chapter 4) [205].

Anaerobic treatment of selenium containing (waste)water streams under methanogenic conditions offers the possibility to convert soluble selenium oxyanions to insoluble, less toxic elemental selenium, and simultaneously conserve energy as methane from the organic matter present (Chapters 4 and 5). Methanogenic anaerobic granular sludge is a potent inoculum to remove both low ($10^{-5}$ M) (Chapters 4 and 5) and high ($10^{-2}$ M) [5] concentrations of selenium oxyanions, immobilizing selenium mainly as elemental selenium in the biomass (Chapter 3 and 6). Not only drainage and mine waters (Table 7.1), but also highly concentrated selenium containing waste streams, e.g. wastewater from selenium processing industries with a total soluble selenium concentration of up to 620 mg $L^{-1}$ ($7.8 \times 10^{-3}$ M) could potentially be treated in methanogenic upflow anaerobic sludge bed (UASB) bioreactors [64].



Table 7.1 Overview of highly selenium contaminated aqueous waste streams [20; 22; 64; 114; 144; 181; 194]

| Waste stream | Selenium content [$10^{-3}$ M] | Selenium speciation | pH | COD [mg/L] |
|---|---|---|---|---|
| Agricultural drainage waters (San Luis drain, California USA) | 0.004 | $SeO_4^{2-}$ $SeO_3^{2-}$ < 5 ppb | 6.8 -7.0 | 32 |
| Acid mine drainage (T&T coal Mine, West Virginia, USA) | 0.006 | n.a. | 2.71 | n.a. |
| Selenium compounds industries (Japan) | 7.848 | n.a. | n.a. | n.a. |
| Municipal solid waste incineration ash leachate (Tokio, Japan) | 0.016 | $SeO_4^{2-}$ | 10.1 | n.a. |
| Oil refinery effluents (Shell oil refinery, California, USA) | 0.004 | $SeO_3^{2-}$ | n.a. | n.a. |
| Oil refinery effluents (pre-concentrated, Houston, Texas, USA) | 0.052 | 87 % $SeO_3^{2-}$ 13% $SeO_4^{2-}$ | 11 | n.a. |
| Flue Gas Desulphurization scrubber waters | 0.007 | n.a. | 6.3 | 1,34 |

The influence of elevated concentrations of selenium oxyanions on anaerobic bioconversions in methanogenic systems has, however, received little attention so far. It is, nevertheless, crucial to bioreactor design, as a decrease in methanogenic activity will reduce the potential of the UASB reactor to remove COD and recover energy via methane [226]. Selenium oxyanions can either influence directly fermentation and methanogenesis via inhibition and toxicity of the microorganisms involved, or indirectly by altering the electron flow in the food web, as selenium respirers use hydrogen [26] and acetate [134] as substrates (Figure 7.1). While competition for the electron donor can be overcome by higher organic loading rates, toxicity might irreversibly affect the reactor operation.



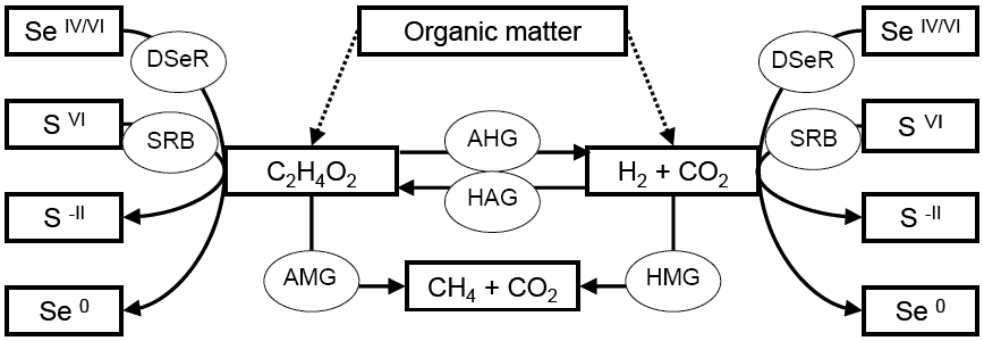


Figure 7.1 Simplified scheme of anaerobic food web with interaction of sulfate and selenate reducing microorganisms. (DSeR = Dissimilatory Selenium Reducers; SRB = Sulfate Reducing Bacteria; AHG = Acetoclastic Hydrogenogens; HAG = Hydrogenotrophic Acetogens; AMG = Acetoclastic Methanogens; HMG = Hydrogenotrophic Methanogens)

This chapter investigates the inhibition of selenite and selenate on methanogenesis with acetate and hydrogen / carbon dioxide as the electron donor in anaerobic granular sludge. Inhibitory concentrations ($IC_{50}$) were determined, representing the concentration causing a 50% decrease of the maximum specific methanogenic activity with acetate as the substrate, and total methane production with hydrogen / carbon dioxide as the substrate compared to an uninhibited control. Inhibition upon repeated exposure to selenium oxyanions was studied by weekly / biweekly replacing the batch liquid phase by fresh selenium containing medium. Transient inhibition was distinguished from permanent effects by replacing the batch liquid phase with selenium-free medium.

# 7.2. Materials and methods

## 7.2.1 Source of biomass

Anaerobic granular sludge from a full scale UASB reactor treating wastewater of four paper mills (Industriewater Eerbeek B.V., Eerbeek, Netherlands) was utilized as inoculum. Its bacterial and archaeal sludge community has been described in detail by Roest et al. [187].

## 7.2.2 Anaerobic toxicity tests

Toxicity of selenite and selenate to methanogenesis was investigated in batch activity tests using 0.5 g (wet weight) anaerobic granular sludge in 50 mL methanogenic medium as described in Chapter 2. The specific maximal methanogenic activity with acetate as the substrate (SMA-Ac) was derived by measuring the pressure increase (corrected for methane partial pressure) in half-hour intervals using an online pressure measurement system [282]. The total methane production with hydrogen / carbon dioxide as the substrate (TMP-$H_2$) was determined in weekly intervals. Acetate was added by diluting a neutralized concentrated stock solution to a final concentration of 1.88 g $L^{-1}$, corresponding to 2 g Chemical Oxygen Demand (COD) $L^{-1}$. In the batch tests with hydrogen, the serum bottles were flushed with a $H_2$:$CO_2$ mixture (80:20, v/v) instead of $N_2$, and the final headspace pressure adjusted to 1.7 bar (corresponding to 1,160 mgCOD $L^{-1}$). Note that both substrates were provided in excess for selenium oxyanion reduction. Selenium oxyanions were added from concentrated stock solutions to final concentrations of $10^{-5}$ to $10^{-2}$ mM selenite and selenate. Selenium-free bottles were used as control.



The sludges were incubated for 4 weeks in the presence of selenium, whereas the medium was renewed weekly using $H_2$/$CO_2$ as the substrate, and biweekly using acetate as the substrate, respectively. Subsequently, the medium was replaced twice against selenium-free medium. $IC_{50}$ values were calculated, plotting either percentage of SMA-Ac or TMP-$H_2$ compared to the uninhibited control against the logarithmic inhibitor concentration, by linear regression as no hormosis effect was observed. In case of persistent inhibition in the absence of selenium oxyanions, $IC_{50}$ values are related to initial selenium concentrations given to the assays during the first weeks of incubation.

### 7.2.3 Analytical techniques

Selenite and selenate were determined by ion chromatography as described in Chapter 2. Volatile Fatty Acids (VFAs), methane and hydrogen were determined as described by Weijma et al. [262]. Volatile Suspended Solids (VSS) were determined following standard procedures [44].

## 7.3. Results

### 7.3.1 Inhibition of hydrogenotrophic methanogenesis by selenium oxyanions

Addition of low selenite concentrations ($10^{-4}$ M) significantly reduced the TMP-$H_2$ by 26% during the first week of incubation compared to the control, while the acetate concentration simultaneously increased (Figure 7.2A).



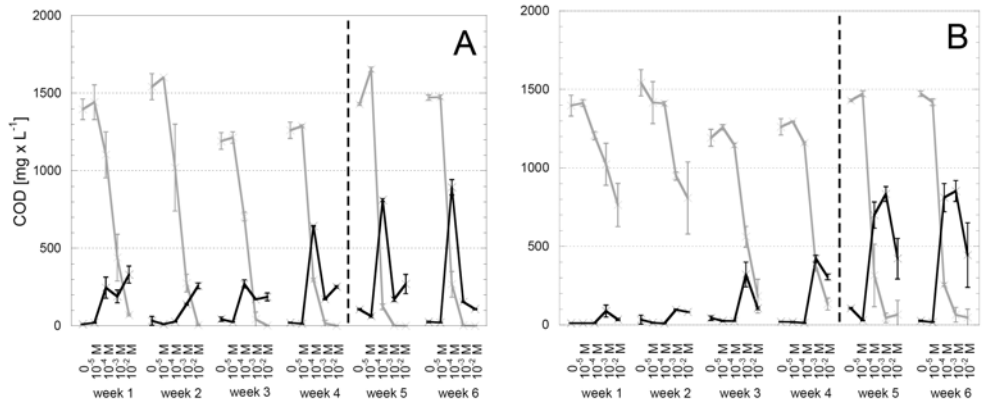


Figure 7.2 Influence of selenite (A) and selenate (B) concentration [0 to $10^{-2}$M] on hydrogenotrophic methane production (grey line) and acetogenesis (black line) in batch experiments in the presence (week 1 to 4) and absence (week 5 to 6) of selenium oxyanions

This trend became more apparent in weeks 2 to 4, reverting the amount of COD converted to methane and acetate in week 4, and persisted in the absence of selenite (weeks 5 to 6). At higher selenite concentrations, a virtually complete inhibition of TMP-$H_2$ (<96%) was observed after renewal of the selenium containing medium in $10^{-3}$ M batches. The complete

inhibition of methane production persisted and acetate production was low upon omitting selenite from the feed, in contrast to the batch that received $10^{-4}$ M selenite.

The TMP-$H_2$ was inhibited by equimolar concentrations of selenate ($10^{-4}$ M), albeit to a lesser extent compared to selenite (Figure 7.2B). In contrast to the assays with selenite, acetate concentrations remained at a low level in the $10^{-4}$ M batch in the presence of selenite, whereas high acetate accumulation and a strong decrease in TMP-$H_2$ occurred the absence of selenate (weeks 5 to 6). The addition of higher selenate concentrations (>$10^{-3}$ M) resulted in further decreased, but not completely inhibited, methane production and elevated acetate concentrations, which contrasts the equimolar selenite toxicity assays (Figure 7.2A). The methane production remained low in the absence of selenate.

$IC_{50}$ values for inhibition of the TMP-$H_2$ decreased from initially 0.437 × $10^{-3}$ M to 0.070 × $10^{-3}$ M upon repeated selenite exposure (Table 7.2). After changing to selenite free medium, the $IC_{50}$ values remained comparatively low. Although single addition of $10^{-2}$ M selenate did not inhibit the TMP-$H_2$ by 50 % in the first week compared to the control (Figure 7.2B), the $IC_{50}$ values strongly (~factor 15) decreased between weeks 2 and 3, resulting in a minimum $IC_{50}$ value of 0.058 × $10^{-3}$ M in the absence of selenate (Table 7.2).



Selenite was nearly completely removed in the $H_2$/CO2 fed batches with an initial selenite concentration of ≤ $10^{-3}$ M, whereas the addition of $10^{-2}$ M selenite resulted in strongly decreased removal efficiencies during repeated incubation with selenite (Figure 7.3A). However, the total amounts of selenite removed from the liquid phase were the highest in the latter $H_2/CO_2$ fed batches in the first 3 weeks, with a maximum of 5.6 (± 0.3) × $10^{-3}$ M removed (week 1). In contrast, selenate was removed incompletely in all batches, except for the $10^{-5}$ M selenate initial concentration. Decreasing removal efficiencies during prolonged selenate exposure were observed (Figure 7.3B). The highest total amount of selenate reduced (0.54 × $10^{-3}$ M) was approximately ten-fold lower than under equimolar selenite concentrations.

Table 7.2 Concentrations of selenium inhibiting total methane production in hydrogenotrophic batch assays and specific methanogenic activities in acetoclastic batch assays by 50 % ($IC_{50}$). Note that weeks 1 to 4 were under presence, weeks 5 to 8 under selenium oxyanions absence

| | $IC_{50}$ [$10^{-3}$ M $Se^{IV}$] | $r^2$ | $H_2$ / $CO_2$ regression model | $IC_{50}$ [$10^{-3}$ M $Se^{VI}$] | $r^2$ | regression model |
|---|---|---|---|---|---|---|
| Week 1 | 0.437 | 0.98 | | 24586 | 0.99 | |
| Week 2 | 0.262 | 0.97 | | 13853 | 0.88 | |
| Week 3 | 0.126 | 0.99 | 1 | 0.929 | 0.95 | 1 |
| Week 4 | 0.070 | 0.90 | | 0.574 | 0.93 | |
| Week 5 | 0.071 | 0.81 | | 0.071 | 0.89 | |
| Week 6 | 0.061 | 0.88 | | 0.058 | 0.85 | |
| | $IC_{50}$ [$10^{-3}$ M $Se^{IV}$] | $r^2$ | Acetate regression model | $IC_{50}$ [$10^{-3}$ M $Se^{VI}$] | $r^2$ | regression model |
| Week 1-2 | 0.575 | 0.94 | | 8973 | 0.99 | 2 |
| Week 3-4 | 0.141 | 0.93 | 1 | 0.808 | 0.99 | |
| Week 5-6 | 0.083 | 0.99 | | 0.552 | 0.99 | 1 |
| Week 7-8 | 0.103 | 0.98 | | 0.579 | 0.96 | |

1) linear-logarithmic regression model, 2) linear-exponential regression model



## 7.3.2 Inhibition of acetoclastic methanogenesis by selenium oxyanions

The lowest concentration of selenite causing inhibition (25.1 %) to acetoclastic methanogens was $10^{-4}$ M (Figure 7.4), with persistence in the absence of selenite (weeks 5 to 8). Higher concentrations of selenite caused a marginal activity (<0.02 $gCOD\text{-}CH_4$ $gVSS^{-1}$ $d^{-1}$) at $10^{-3}$M and complete inhibition at $10^{-2}$ M. No hydrogen accumulation was detected in the headspace at any time (data not shown). The lowest concentration of selenate resulting in a significantly decreased SMA-Ac was 10 fold lower ($10^{-5}$ M) and observed under repeated selenate exposure (Figure 7.4). The SMA-Ac was fully restored after the second transfer to selenate free medium. The addition of $10^{-4}$ M selenate resulted in an irreversibly lower SMA-Ac. In contrast to selenite, addition of

$10^{-2}$ M selenate did not completely inhibit the SMA-Ac [0.04 (± 0.00) g COD-$CH_4$ $gVSS^{-1}$ $d^{-1}$ in week 3 to 4].

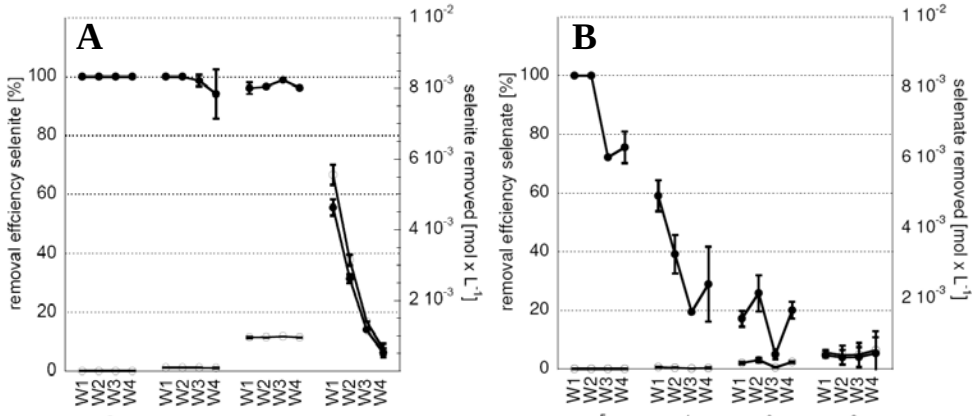


Figure 7.3 Selenite (A) and selenate removal (B) removal in hydrogenotrophic toxicity assays during 4 weeks (W1 to W4) expressed as removal efficiency [%] in filled symbols and as [mol $L^{-1}$] in open symbols (secondary y-axis)



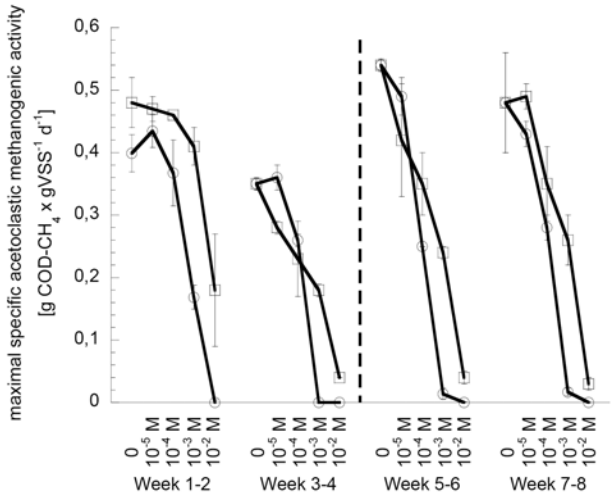


Figure 7.4 Influence of selenium oxyanions in acetoclastic toxicity assays: (A) influence of selenite (○) and selenate (□) on maximal specific acetoclastic methanogenic activity in the presence (weeks 1 to 4) and absence (weeks 5 to 8) of selenium oxyanions

Selenite showed a progressively stronger inhibiting effect on the SMA-Ac, reflected by the decreased $IC_{50}$ values during selenite exposure. The inhibition was persistent as the lowest $IC_{50}$ value was $0.083 \times 10^{-3}$ M in the absence of selenite (Table 7.2). However, the higher $IC_{50}$ values after repeated transfers to selenite free medium indicate that the SMA-Ac recovered slightly. The inhibition of selenate towards SMA-Ac was initially lower compared to the selenite assays, but the $IC_{50}$ value decreased by a factor >10 during selenate exposure. Inhibition by selenate was persistent, but the $IC_{50}$ values were by a factor >5 higher compared to the selenite assays (Table 7.2).

In selenite containing batches, the highest activity for the $10^{-3}$ M incubations was observed upon selenite removal to levels below $0.2 \times 10^{-3}$ M after a lag phase of ~60 h (Figure 7.5A). Selenate containing SMA-Ac batches did not display such a lag phase (Figure 7.5B) and the highest activities were observed at the same time than in uninhibited controls.

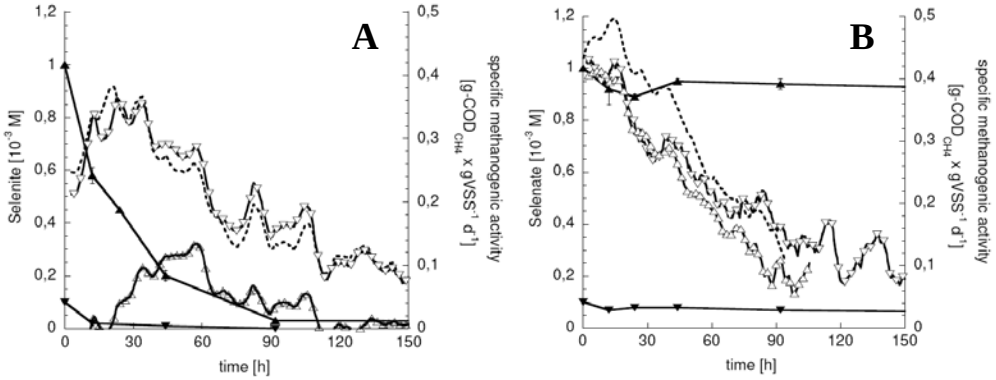


Figure 7.5 Selenite (A) and selenate (B) removal in $10^{-4}$M (▼) and $10^{-3}$M (▲) acetoclastic assays and influence on specific acetoclastic methanogenic activity in 0 (---), $10^{-4}$M (▽) and $10^{-3}$M (△) batches (secondary y-axis)

Selenite removal was almost complete in all batches receiving ≤ $10^{-3}$ M [< 96.9 (± 0.2) %] (Figure 7.6A), resulting in granule cross sections displaying red elemental selenium in the core and outer layers (Figure 7.7A). The highest concentration of selenite reduced [2.81 (± 0.1) × $10^{-3}$ M] was observed in the $10^{-2}$ M batch, although a repeated exposure to selenite resulted in a decreased selenite reduction efficiency. Selenate removal was only complete during the first two weeks of the $10^{-5}$ M batch (Figure 7.6B) and renewal of the medium resulted in incomplete selenium removal in all batches. The lower total amounts of

selenate reduced are reflected in granule cross sections colored by red elemental selenium, solely in the outer layer (Figure 7.7B). The highest concentration of selenate reduced was 0.96 (± 0.3) × $10^{-3}$ M.

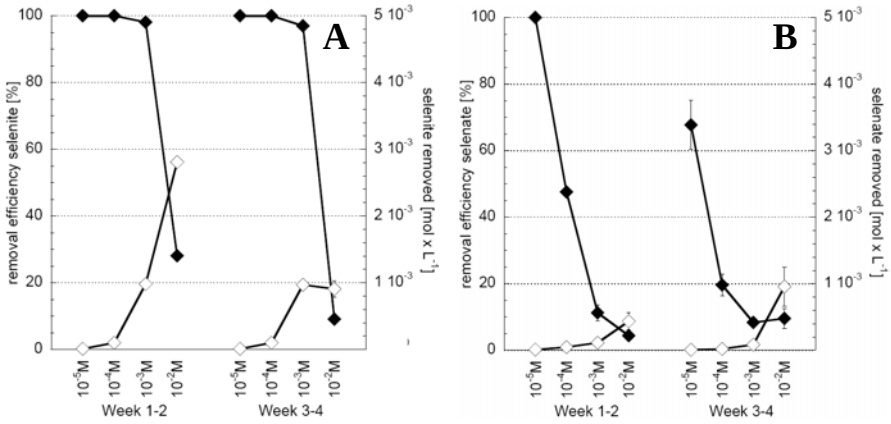




Figure 7.6 Selenite (A) and selenate (B) removal in acetoclastic toxicity assays expressed as removal efficiency [%] in filled symbols and as [mol $L^{-1}$] in open symbols (secondary y-axis)

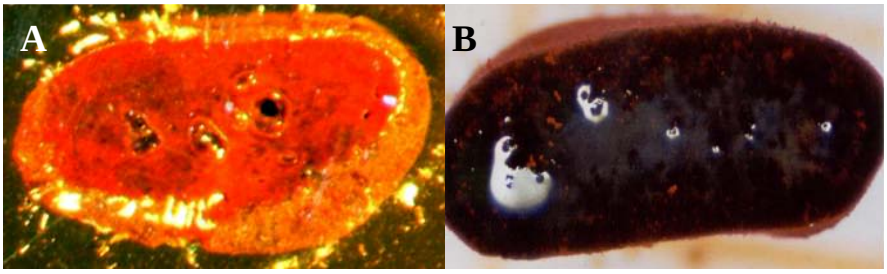


Figure 7.7 Reflected-light microscopic photographs of cross sections of anaerobic sludge granules treating $10^{-2}$ M selenite (A) and $10^{-2}$ M selenate (B). Note that bright spots within the granules were caused by light reflection

# 7.4 Discussion

## 7.4.1 Influence of selenium oxyanions to methanogens

This chapter showed for the first time that selenite and selenate strongly influence anaerobic food webs, and ultimately methane production during anaerobic digestion. Moreover, inhibition occurs already at low [<100 µM $SeO_3^{2-}$; <10 µM $SeO_4^{2-}$] concentrations and within a short time span ($SeO_3^{2-}$: 1 week, $SeO_4^{2-}$: 2 weeks). $IC_{50}$ values in hydrogenotrophic assays were less than 61 µM for both selenium oxyanions, while inhibition was lower in acetoclastic assays (Table 7.2). The inhibition of methanogenesis is permanent, as the lowest $IC_{50}$ values (aceto- and hydrogenotrophic assays) were observed upon feeding the sludges selenium oxyanion free medium, repeatedly (Table 7.2). However, the SMA-Ac of the $10^{-5}$ M selenate assay recovered fully in the absence of selenium (Figure 7.4). The $IC_{50}$ values for the first week(s) of incubation (Table 7.2) show that selenite inhibits methanogens already during a single exposure, while selenate unfolds its inhibitory effect during repeated exposure.



Interestingly, inhibition of acetoclastic and hydrogenotrophic methanogenesis by selenium oxyanions was best described by a linear relation (inhibition vs. logarithmic selenium oxyanion concentration) (Table 7.2), whereas selenate inhibition on SMA-Ac was better fitted nonlinearly (exponential) (Table 7.2). An exponential relation is expected when additional toxic compounds (e.g. $H_2Se$ or seleno-aminoacids) are formed during the conversion of the original toxin (here selenate), resulting in synergistic toxicity. Possibly $H_2Se$, as formed by different microbial groups [82; 84], could interfere here with the sulfur metabolism by formation of selenocysteine and selenomethionine instead of their sulfur analogues [236]. These seleno-aminoacids are subsequently incorporated unspecifically into enzymes [152], changing enzyme functionality. Several enzymes involved in methane production from $H_2/CO_2$ or acetate contain cysteine (e.g. Coenzyme M [53]), that could potentially be altered in this way and contribute to the inhibitory effect of selenium oxyanions on methanogenesis. Selenate and selenite toxicity has also been associated with increased production of reactive oxygen species (ROS), as e.g. $O_2^-$ and $H_2O_2$ [105], possible explaining inhibition, as methanogenic archaea are strict anaerobes and thus sensitive to ROS [30].

Selenite treating granules contained elemental selenium deposits over the whole cross section (Figure 7.7A), whereas selenate treating granules showed elemental selenium deposits only on the outer layer (<< 200 µm, Figure 7.7B). The selenium deposits at the periphery of the granule might have retarded selenate oxyanions transport similar to cementation by calcium carbonate precipitation in anaerobic granular sludge [254], possibly

resulting in lower toxin concentrations of the inner layers of the granules as compared to the bulk liquid. Consequently, mass transfer limitation of selenate could explain the incomplete inhibition of hydrogenotrophic and acetoclastic methanogens observed in the presence of $10^{-2}$ M selenate (Figure 7.2B and 7.4) in comparison to selenite (Figures 7.2A and 7.4). In this way, archaea protected in the core of the sludge granules, e.g. *Methanosaeta* species [197], could explain the marginal methanogenic activities that were observed in the presence of selenate ($0.04 \pm 0.00$ gCOD-$CH_4$ $gVSS^{-1}$ $d^{-1}$).

## 7.4.2 Influence of selenium oxyanions on anaerobic food webs

Selenite and selenate inhibition of acetoclastic methanogens (AMG) yielded a reduced SMA-Ac (Figure 7.4). This is in agreement with the hydrogenotrophic assays, where acetate also accumulated (Figure 7.2A and B). No hydrogen accumulation was detected in the presence or absence of the oxyanions, suggesting that hydrogenotrophic methanogens (HMG) are either not involved or not inhibited in the batches using acetate as the substrate.



Interestingly, $10^{-4}$ M selenate resulted in acetate accumulation in $H_2/CO_2$ fed batches only after the change to selenate free medium (transition between weeks 4 and 5, Figure 7.2B), while it already occurred in the presence of selenite (Figure 7.2A). Figure 7.2B suggests a non-persistent inhibition of hydrogenotrophic acetogens (HAG) and a persistent inhibition of AMG by selenate. Accordingly, methanogenesis could proceed mainly over HMG in the presence of selenate, as HAG and AMG are inhibited. In the absence of selenate, however, this inhibition of HAG is reversed and acetate is formed (Figure 7.2B). Acetate accumulated as inhibition of AMG persists. The assumed inhibition of AMG by selenate was confirmed in acetoclastic incubations (Figure 7.4). The inhibition of HAG, however, has to be partial, as higher selenate concentrations resulted in acetate accumulation in the presence of the oxyanion (Figure 7.2B). In contrast to selenate, acetate accumulated in the presence of selenite (Figure 7.2A), possibly due to the stronger inhibition of AMG by selenite compared to selenate (Table 7.2). Under even higher selenite concentrations ($10^{-3}$ M), the AMG are completely inhibited (Figure 7.4).

Repeated selenite bioconversion to elemental red selenium (Figure 7.7A) during total inhibition of methanogenesis (Figure 7.2A versus 7.3A and Figure 7.4 versus 7.6A) showed that selenite reduction is not mediated by methanogens, but by other microorganisms e.g. selenium-respiring bacteria or archaea (Chapter 4)[5] using either hydrogen or acetate as electron donor.

Methanogenesis is the result of the activity of different microbial groups, hence it cannot be excluded that certain genera of bacteria and methanogens are more sensitive to selenium

oxyanions than others, causing changes in the predominant metabolic pathways and the microbial composition. Molecular biology imaging methods (fluorescent in situ hybridization – microautoradiography, FISH-MAR) [157] or Denaturing Gradient Gel Electrophoresis (DGGE) and sequencing [187] might help to identify less selenium sensitive microorganisms that are present in the inoculum used in this chapter and could be applied in anaerobic treatment of highly concentrated waste streams.

In the past, selenate (next to molybdate) has been applied as so called "specific inhibitor" for sulfate-reducing bacteria [47; 54]. The strong inhibitory effect on sulfate-reducing bacteria is due to the fact that selenate can be transported into the cells via sulfate permeases [12], but is not cycled via the respiratory chain conserving energy in sulfate-reducing bacteria [283]. This chapter shows that such a use of selenate has to be seen very critically. Some authors used selenate in high concentrations in order to inhibit sulfate reduction (e.g. $5 \times 10^{-3}$ M in [54]; $2 \times 10^{-2}$ M in [47]), although Table 7.2 shows that these concentrations are highly inhibiting methanogens as well. Consequently, errorous conclusions from the use of selenate as specific inhibitor can be drawn and careful analysis of the food web is required.



### 7.4.3 Implications for selenium bioremediation under methanogenic conditions

In anaerobic digestion, selenite is added as a micronutrient to wastewaters, as it strongly stimulates methanogenesis in different archaea [280]. A hormosis effect could be expected, but was not observed during exposure to low selenium concentrations (Figure 7.2A, 7.2B and 7.4). Interestingly, the nutrient requirement for selenium for UASB reactors in medium strength wastewater (2-10 gCOD $L^{-1}$ ) is reported to be $2.5 \times 10^{-7}$ mol up to $6.3 \times 10^{-6}$ mol $gCOD^{-1}$ [211]. In the experiments presented here, already a concentration of $0.5 \times 10^{-4}$ mol $gCOD^{-1}$ selenite decreased the TMP-$H_2$ (Figure 7.2A) and SMA-Ac (Figure 7.4). Consequently, the range between selenium requirement and toxicity in methanogenic anaerobic granular sludge is indeed narrow and amounts to a factor of 8 to 200.

This chapter demonstrates that the selenium concentration will determine the applicability of an anaerobic treatment system. Agricultural drainage waters usually have a low COD content, so that the cost for the electron donor is the key parameter for a cost-effective treatment [287]. If waste products from other industries are available, e.g. molasses [289], methanol [170] or rice straw [293], methane production and recovery would be an approach to retrieve some of the operational costs. However, already low selenate concentrations ($10^{-5}$ M), occurring in a variety of different waste streams (Table 7.1), will reduce the COD

removal efficiency and the potential for energy recuperation via methane from waste streams. Selenium compound processing industries (Table 7.1) might not at all be treatable under methanogenic conditions.

The fact that irreversible inhibition occurs upon single exposure might deteriorate methanogenic treatment capacity of waste streams containing high selenite concentrations, e.g. pre-concentrated oil refinery effluents (Table 7.1). Even if the selenite levels are reduced to below inhibitory concentrations by selenium-respiring specialists that develop during UASB operation (Chapter 4), selenite concentrations might be temporarily and spatially higher due to inhomogeneous mixing at the influent inlet point, thus irreversibly inhibiting methanogens. Consequently, efficient influent distribution systems (e.g. perforated distribution plates) or mixing with the effluent recycle prior to entering the reactor are necessary for selenite treating UASB reactors.

# 8

# Bioaugmentation with immobilized *Sulfurospirillum barnesii* for simultaneous selenate and nitrate removal

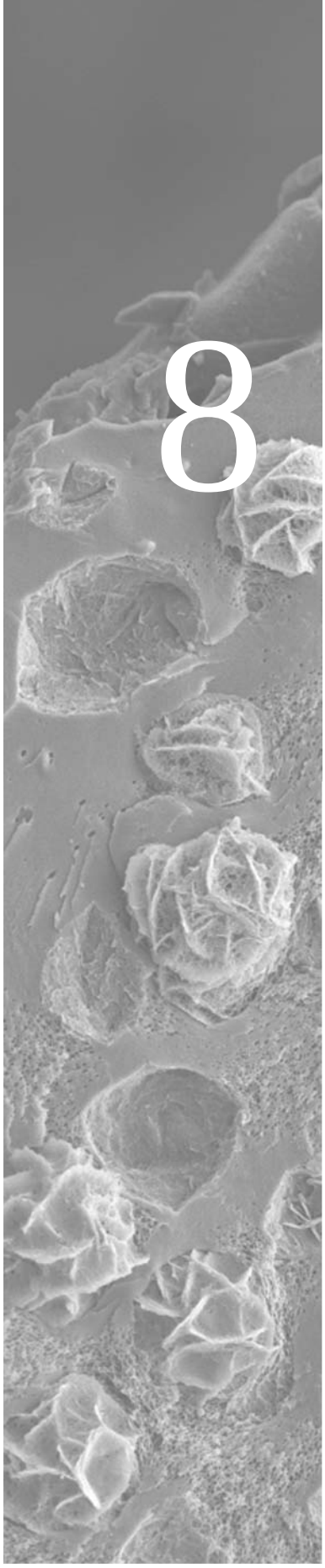

This chapter is in preparation for submission.

# Abstract

Whole cell immobilization of selenate respiring *Sulfurospirillum barnesii* in polyacrylamide gels was investigated to optimize the treatment of selenate contaminated waters (790 µg Se $L^{-1}$), under high molar excess of nitrate (1500 times) and sulfate (200 times). Gel immobilized cells were used to inoculate a mesophilic (30°C) bioreactor fed with lactate as electron donor at an organic loading rate of 5 g COD × $L^{-1}d^{-1}$. Selenate was reduced efficiently (>97 %) and minimal effluent concentrations of 39 µg Se × $L^{-1}$ were achieved. SEM-EDX analysis revealed spherical bioprecipitates of ≤2 µm diameter mostly on the gel surface, consisting of selenium with a minor contribution of sulfur. To validate the bioaugmentation success under microbial competition, immobilized cells were added to an UASB reactor, resulting in earlier selenate (24 HRTs) and sulfate (44 HRTs) removal and higher nitrate / nitrite removal compared to a not-bioaugmented control reactor. *S. barnesii* was efficiently immobilized inside the reactors as the selenate reducing activity was maintained during long term operation (60 days). Thus, this chapter demonstrates that utilizing gel immobilization of specialized bacterial strains can supersede wash out and out-competition of added microorganisms in continuous bioaugmented systems.

# 8.1. Introduction

Selenium contamination of soil and water is a problem of global importance. Ecotoxicological effects of selenium poisoning were documented in the western US already 30 years ago, however a cost-effective solution to the problem has not yet been found and the thread to wildlife persists [73; 182; 270]. Biological processes to decontaminate large quantities of water polluted with low concentrations (< 1 mg $L^{-1}$) soluble selenium oxyanions (selenite and selenate) are considered promising due to their high selectivity towards targeted anions.

Denitrifying microorganisms have been proposed as key biocatalysts for the treatment of selenium contaminated agricultural drainage and oil refinery waters due to the selenium oxyanion reducing ability of both membrane bound and periplasmatic nitrate reductases [193]. The specific activities for selenate reduction, however, are 15 to 518 times lower compared to the nitrate reduction [261] and the affinity constants ($K_M$) 2.3 times higher for selenate [193]. Thus, selenate is reduced under low nitrate levels only [60]. One approach to reach low nitrate levels allowing selenate reduction is via a two compartment reactor system, implemented in e.g. the algal-bacterial selenium reduction (ABSR) system [4]. Firstly, nitrate levels are reduced in a high rate pond by microalgal assimilation and secondly, selenate is biologically reduced to levels of <100 µg $L^{-1}$ by bacteria in anaerobic ponds [69]. However, the space prerequisite for these reduction steps is high and further treatment steps (dissolved air floatation and slow sand filtration) need to be applied to reduce selenium concentrations prior to the discharge of the effluent to the environment.



Selenate respiring organisms contain specific selenate reductases not competitively inhibited by nitrate [205] and might offer an alternative to the two-step process currently applied. However, bioaugmentation by simple addition is typically limited by wash-out and out-competition of the added microorganisms [46]. Immobilization in gels might counteract these limitations, although so far not tested in continuous experiments [150; 234].

In this chapter, inoculation of bioreactors with immobilized selenium-respiring microorganisms was investigated to supersede the problem of anion inhibition in waters contaminated with a molar excess of nitrate (1500 times) and sulfate (200 times) (Chapter 4) compared to selenate. *Sulfurospirillum barnesii* [166; 217] was chosen, as it can respire a variety of substrates (including both selenium oxyanions, nitrate and nitrite), produces elemental selenium as end-product of selenium respiration and is non-pathogenic.

To validate the applicability of gel immobilization under microbial competition conditions, the UASB reactor was inoculated with both immobilized bacteria and anaerobic granular sludge and the selenate removal success was evaluated in comparison to a non

bioaugmented reactor. Anaerobic granular sludge was chosen as inoculum, as it could simultaneously reduce nitrate/nitrite and selenate in batch assays (Chapter 2) and can contain selenium-respiring organisms (Chapter 4).

The chemical composition of the formed selenium bioprecipitates was investigated by scanning electron microscopy with energy dispersive X-ray analysis (SEM-EDX). Denaturing gradient gel electrophoresis (DGGE) and sequencing were used to evaluate changes in the bacterial community structure of the bioreactors.

# 8.2. Materials and Methods

## 8.2.1 Source of biomass

*Sulfurospirillum barnesii* (strain 10660) was obtained from the German Collection of Microorganisms and Cell Cultures (DSMZ, Braunschweig, Germany). Anaerobic granular sludge originated from a full scale UASB reactor treating wastewater of four paper mills (Industriewater Eerbeek B.V., Eerbeek, The Netherlands).



## 8.2.2 Biomass immobilization

For *S. barnesii* cell immobilization, bacterial cells were pre-grown in medium prepared according to DSMZ. Cells were harvested in the exponential growth phase by centrifugation of 20 mL cell suspension at 11,000 g for 20 min (IEC CL31R Multispeed Centrifuge, Thermo Scientific, Breda, The Netherland). The pellet was re-suspended in 500 µl of *S. barnesii* medium and 125 µL of this suspension was added to 50 mL of polymerizing gel and stirred gently. Gelling conditions were used according to Tucker et al. (1998) [234], but using 1:10, 1:20 and 1:30 ratios of N,N'-methylenebisacrylamide (MBAA) : acrylamide (AA). The gel was poured into sterile plastic containers of 8cm × 8cm × 4mm. After the gel had set, it was cut into cubes of 64 $mm^3$. All immobilization steps were conducted under $N_2$ atmosphere using a glove-box.

## 8.2.3 Characterization of the *S. barnesii* cubes

To investigate the effect of the gelling conditions on the fracture stress, the gel was cut into cubes of 1 $cm^3$ and the strength needed to burst the gel at the brittle point was measured by

a penetrometer (Overload Dynamics S900, Overload Dynamics, Schiedam, The Netherlands).

The influence of the gel composition on the selenate reduction efficiency was studied in 125 mL batch bottles containing 10 cubes (total of 16.1 µg biomass dry weight) of gel immobilized *S. barnesii* submerged in 50 mL of synthetic wastewater as described in Chapter 2. Selenate was added from a concentrated stock solution to a final concentration of 100 µM. The batch bottles were subsequently flushed with a sterile steam of $N_2$ and incubated at 30°C on a horizontal shaker at 120 rpm. Liquid phase samples were withdrawn via syringe and selenate concentrations monitored in regular intervals.

## 8.2.4 Continuous UASB reactor set-up

Experiments were done in UASB reactors (0.46 L working volume) as described in Chapter 2 and 4. The UASB reactors were operated under mesophilic conditions (30 ± 1°C) and a hydraulic retention time (HRT) of 6 h. The effluent was recycled via a Watson Marlow 503U peristaltic pump (Rotterdam, The Netherlands) to obtain a superficial liquid upflow velocity ($v_{up}$) of 1 m $h^{-1}$. During operation, R1 was continuously flushed with a stream of $N_2$ to prevent intrusion of ambient air. To avoid nitrate, selenate or sulfate bioconversion in the storage vessels, influents were composed of three different streams, fed in the same ratios to the reactor: (1) selenate, sulfate, nitrate, macro- / micronutrients and vitamins; (2) lactate and phosphate buffer; and (3) dilution water.



## 8.2.5 Bioreactor operation

Three UASB reactors were inoculated as follows: Reactor 1 (R1) received 25 gel cubes (1:30, MBAA : AA). Reactor 2 (R2) was inoculated with 100 g wet weight [37.4 g volatile suspended solids $(VSS)^{-1}$ $L^{-1}$] of anaerobic granular sludge. Reactor 3 (R3) received both cubes and sludge in the same quantities used to inoculate R1 and R2, respectively.

The UASB reactors were fed with oxygen-free synthetic wastewater, containing macronutrients, micronutrients (Chapter 2) and vitamin solution (DMSZ *S. barnesii* medium). The medium was buffered at pH = 7.0 (± 0.1) using a 40 mM phosphate buffer. Lactate was used as sole electron donor at an influent concentration of 13 mM, resulting in an organic loading rate of 5 g Chemical Oxygen Demand (COD) $L^{-1}$ $d^{-1}$ corresponding to a specific organic loading rate of 134 mgCOD $gVSS^{-1}$ $d^{-1}$. Nitrate was fed to the reactors at an influent concentration of 15 mM in period I (days 0 to 24) and period III (days 43 to 58),

whereas no nitrate was fed in period II (days 25 to 42). Sulfate and selenate were fed at influent concentrations of 2 mM and 10 µM, respectively, during the whole reactor operation.

## 8.2.6 Microscopy

For Scanning Electron Microscopy with Energy Dispersive X-ray analysis (SEM-EDX), samples were fixed for 1 h in aqueous glutaraldehyde solution (2.5%), rinsed with water and dried either in a stream of $N_2$ or in a series of ethanol solutions (Chapter 5). Samples were then fit on a brass sample holder with carbon adhesive tabs (Electron Microscopy Sciences, Hatfield, USA) and coated with 5 nm platinum by magnetron sputtering. Specimens were analyzed with a field emission scanning electron microscope (JEOL 6300 F, Tokyo, Japan) and EDX analyses (INCA energy, Oxford Instruments Analytical, High Wycombe, England) were performed at a voltage of 15 kV and a working distance of 15 mm.



## 8.2.7 Microbial community structure analysis

### 8.2.7.1 DNA extraction and PCR-amplification of 16S rRNA genes

Total genomic DNA was extracted from a R2 sludge sample (60 days of operation) using a DNeasy® Plant Mini Kit (Qiagen, Germany) as per manufacturer's instructions.

Bacterial 16S rRNA genes were amplified with the forward primer 341F and reverse primer 517R under addition of a 40-base pair GC-clamp to the 5' terminus of the forward primer [153]. PCR was performed in 50 µl reactions containing: 200 ng of template DNA, 12.5 pmol of each primer, 0.125 mM $MgCl_2$, 5 µl 1X$NH_4$ reaction buffer ($(NH_4)_2SO_4$, 16 mM; Tris-HCL [pH 8.8 at 25°C], 67 mM; 0.01% Tween-20), 10 nM dNTP [dATP, dCTP, dGTP, and dTTP] and 0.5 U *Taq* DNA polymerase. The bacterial PCR cycles used were: denaturing at 94°C for 2min, followed by 14 cycles of denaturing at 94°C for 45 s, annealing of primer at 55°C for 30 s and extension at 72°C for 45 s; followed by 19 cycles of denaturing at 94°C for 45 s, annealing of primer at 53°C for 30 s and extension at 72°C for 45 s; a final 5-min elongation incubation was performed at 72°C. Negative controls containing no DNA were used to screen for contaminated amplification, while DNA from pure cultures of *Escherichia coli* was used to positively control PCRs.

### 8.2.7.2 Analysis of PCR products by DGGE

Aliquots of 20 µl of respective GC-clamped PCR products were used for DGGE [153], which was performed according to the D-Code system (BioRad, USA). Polyacrylamide gels were prepared with denaturing gradients ranging from 30% to 70% denaturant (100% denaturant = 7 M urea + 40% formamide) and were run at 65°C and 75 V for 16 h. Following this, gels were stained for 10 minutes in 1XTAE buffer with ethidum bromide (15 µl $mL^{-1}$), de-stained for 3 minutes in 1XTAE buffer and photographed on a UV transillumination table. Bands selected for analysis were aseptically excised from the DGGE gels, using a sterile scalpel blade, suspended in 50 µl of sterile water and stored at room temperature for 6 h to facilitate the elution of DNA. This process (both the PCR and PCR product analysis) was repeated up to five times to achieve a single band with new DNA eluted from the most recent DGGE gel as template in PCR reactions.

### 8.2.7.3 Sequencing of 16S rRNA gene fragments



PCR was performed under the same conditions as described above, but without GC-clamps attached to the forward primers. Sequences were determined using a capillary sequencer (MWG Biotech, Germany) and aligned with 16S rRNA gene sequences retrieved from the Ribosomal Database Project (RDP) [136].

## 8.2.8 Analytical techniques

Selenate, selenite, nitrate, nitrite and sulfate were determined by ion chromatography as described in Chapter 2. The dissolved sulfide concentration of the effluent was determined colorimetrically (Dr. Lange, LYW653, Germany). Total dissolved selenium ($Se_{dis}$) was determined by Inductively Coupled Plasma-Optical Emission Spectroscopy (ICP-OES) (method detection limit 10 µg Se $\times L^{-1}$) after filtration using a 0.45 µm pore size syringe filter (Whatman, Hertogenbosch, The Netherlands). Volatile Fatty Acids (VFAs) and biogas composition were determined by Gas Chromatography [262].

# 8.3. Results

## 8.3.1. Selenate removal in batch assays

Gels containing MBAA:AA in a ratio 1:30 had the highest fracture stress (Table 8.1). Higher AA concentrations resulted in hard, shattering gels, whereas lower concentrations caused incomplete gelling. Furthermore, the selenate removal rates in the 1:30 MBAA:AA gels were 14% and 41% higher compared to gels with a ratio of 1:20 and 1:40, respectively. Consequently the 1:30 gel cubes were used to inoculate R1 and R3.

Table 8.1 Influence of different N,N'-methylenebisacrylamide : acrylamide compositions on gel strength and selenate reduction rates by immobilized *S. barnesii* cells

| ratio N,N'-methylenebisacrylamide : acrylamide | fracture stress [N/cm²] | selenate removal [µg Se ×g $dw^{-1}$ $h^{-1}$] |
|---|---|---|
| 1 : 5 [a)] | - | - |
| 1 : 10 [b)] | 6.0 ± 2.3 | - |
| 1 : 20 | 23.5 ± 4.4 | 60.5 ± 0.4 |
| 1 : 30 | 39.3 ± 10.9 | 69.1 ± 3.9 |
| 1 : 40 | 9.3 ± 3.0 | 49.0 ± 7.1 |

[a)] gel did not harden; [b)] gel hardened in 15 minutes



## 8.3.2 Start-up of the reactors

During the start-up period I, low selenate and $Se_{dis}$ removal efficiencies were observed in all three reactors (Figure 8.1, A1-3). R3 showed highest selenate reduction of the three reactors on the end of period I (20.2 % on day 22), however selenium was washing out with the effluent (3.8% of influent selenium).

Nitrate was removed completely from R1 and R2 within 8 and 6 days of operation, whereas R3 showed already complete removal 20 and 12 HRTs earlier, respectively (Figure 8.1, B1-3). In R2, complete nitrate removal was not sustained and nitrate followed nitrite accumulation in the effluent after 13 days of operation (Figure 8.1B2). Sulfate was not removed in any of the reactors in period I (Figure 8.2, C1-3).

The COD removal efficiency was higher than 82% and 87% throughout period I in R1 and R3, respectively, after a start-up period of approximately 6 days (Figure 8.1D1 and D3). When nitrate was accumulating to high amounts in R2 (9.2 mM nitrate + 0.7 mM nitrite)

(Figure 8.1B2), a slight accumulation of acetate (2.7 mM) was observed, resulting in reduced COD removal efficiency of 54 %.

## 8.3.3 Effect of bioaugmentation on reactor performance in the absence of nitrate

When omitting nitrate from the feed in period II, R1 and R3 reacted with an immediate increase in both selenate and $Se_{dis}$ removal efficiencies (Figure 8.1A1 and A3). R2 showed a delay of 5 days (20 HRT) (Figure 8.1A2) until it achieved comparative removal efficiencies.

Generally, the $Se_{dis}$ removal efficiency was lower than the selenate removal efficiency in all three reactors, resulting in maximal differences of 36.9%, 33.6% and 42.5% (R1 to R3, respectively). Towards the end of period II, the difference became smaller in all three reactors. The lowest $Se_{dis}$ concentration was 39 µg Se × $L^{-1}$ in R1, while R2 and R3 reduced $Se_{dis}$ less efficiently (120 and 174 µg Se × $L^{-1}$, respectively).

Immediately upon the transition from period I to II, the sulfate removal efficiency increased in the bioaugmented reactors (R1 and R3, Figure 8.1C1 and C3), while this occurred in R2 with a delay of more than 8 days of operation (32 HRT) (Figure 8.1C2). The highest amounts of dissolved sulfide accumulated in R3 (1.2 mM, Figure 8.1C3), while 41% less dissolved sulfide was formed in R1. COD removal efficiencies were generally low in period II compared to period I and III (Figure 8.1D1 to D3). Propionate was the main VFA accumulating in R2 and R3, while propionate and acetate accumulated in R1 (Figure 8.1D1).



## 8.3.4 Effect of bioaugmentation on reactor performance in the presence of nitrate

When resuming the nitrate feed in period III, an immediate decrease in selenate and $Se_{dis}$ was observed in R2 and R3 (Figure 8.1A2 and A3), while in R1 this decrease occurred with a delay of 2 days of operation (8 HRT). However, upon termination of the reactor operation, an almost complete selenate removal was achieved in R2 (<97%), while R3 removed only 56%. Due to a blockage of the nutrient line, only lactate and dilution water was fed to R1 subsequent to day 51 of operation, thus selenate and $Se_{dis}$ removal efficiencies could not be determined upon the end of period III .

Figure 6.1. Reactor performance of R1 to R3. Primary axis: removal efficiency (-●-) selenate, (-▼-) dissolved selenium (A); removal efficiencies (- - -) for nitrate/nitrite (B), sulfate (C) and COD (D); (-✚-) nitrite, (-△-) nitrate, (-▭-) dissolved sulphide, (-▽-) acetate and (-○-) propionate effluent concentration [mM] (secondary y-axis).

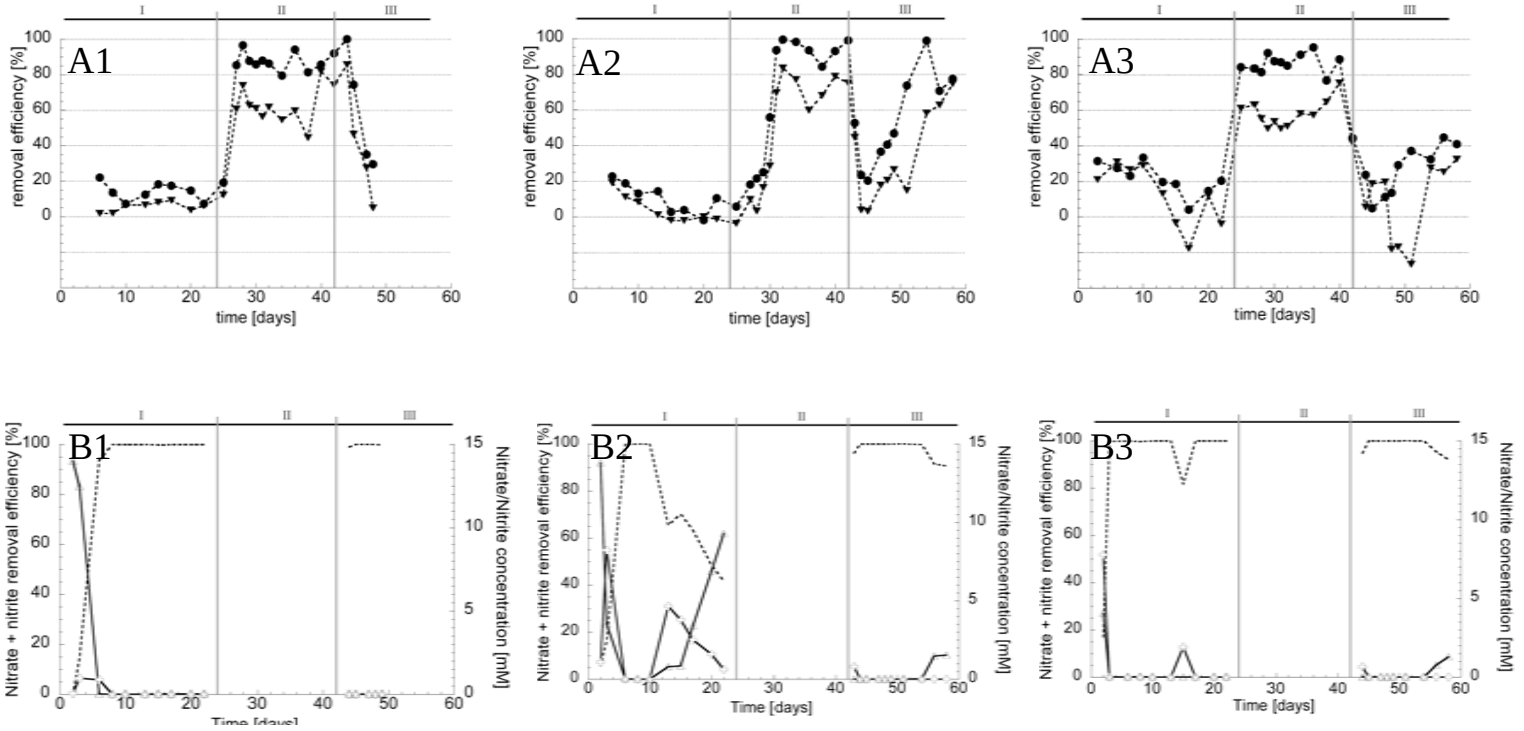

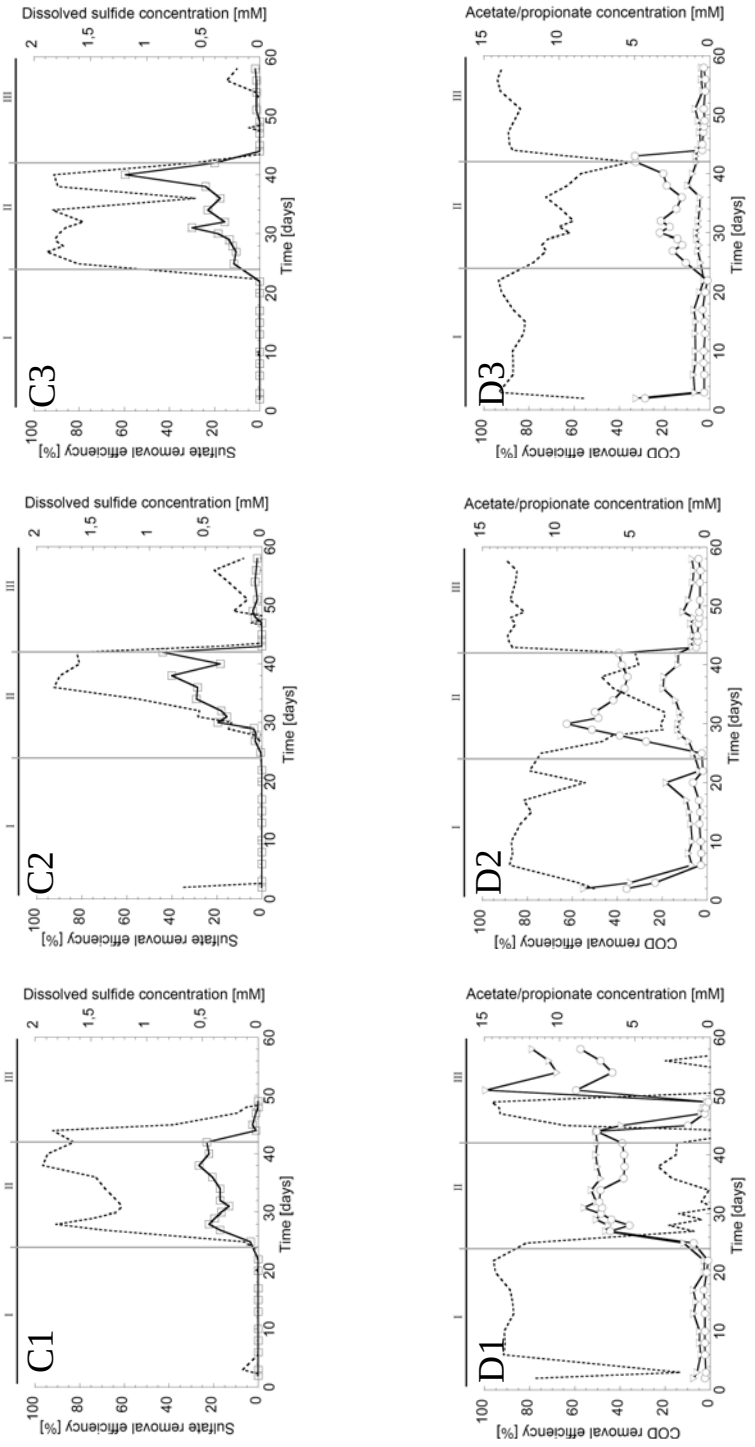
Dissolved sulfide concentration [mM]
Acetate/propionate concentration [mM]
Sulfate removal efficiency [%]
COD removal efficiency [%]
Time [days]
I
II
III
C3
D3
C2
D2
C1
D1

Again, $Se_{dis}$ was removed less efficiently than selenate, with a difference of up to 59% (R2) and 64% (R3), and $Se_{dis}$ was washing out in R3 in period III (Figure 8.1A3). Filtration of the R2 effluent liquid with a 0.1 µm subsequent to the 0.45 µm filter resulted in reduction of $Se_{dis}$ by 11% to 48% (period III, data not shown).

Immediately upon resuming the nitrate feed, high nitrate / nitrite removal efficiencies were achieved that exceeded more than 91% in R2 and R3 during period III (Figure 8.1B2 and B3), while sulfate removal efficiencies dropped upon transition to period III (Figure 8.1C1 to C3). The COD removal efficiency was high (> 82%) throughout the whole period III in both R2 and R3 (Figure 8.1D2 and D3). R1 accumulated both acetate and propionate in the effluent, resulting in no net-COD removal upon the end of the reactor operation (Figure 8.1D1).

### 8.3.5 Biomass characterization and microbial community structure



During the reactor operation the sludge volume of R2 and R3 more than doubled (~220 mL final volume) and a color change from dark black to light grey with slime embedding the granules was observed, yet the granular character of the sludge remained. Selenium accumulated in the sludge granules (and the embedding slime) of R2 and R3 up to 1067 (R2) and 1194 µg Se × $gVSS^{-1}$, respectively. In R1, only low amounts of white flocks formed, that were loosely deposited on top of the cube-bed.

Analysis of the additional DNA bands in R2 sludge samples compared to R1 samples were not indicative for a microorganism described as selenium respirer in literature. Best matches to the determined sequences are presented in Table 8.2.

Table 8.2 Identities of bacterial 16S rRNA genes retrieved from Reactor 2 sludge and percent similarities to the closest related sequence in the RDP database

| Sample ID | closest related sequenced in database (RPD) | % similarity |
|---|---|---|
| 1 | *Chryseobacterium sp.* PC IW 30 / TS IW 15 | 83.9 |
| | *Chryseobacterium hispanicum* | 67.2 |
| 2 | *Bacteroides sp. 253c* | 92.8 |
| | Bacteroides stercoris | 71.0 |
| 3 | uncultured bacterium MBR283-61 (Familiy: *Comamonadac* | 87.4 |
| | *Diaphorobacter nitroreducens* | 76.8 |
| 4 | uncultured bacterium *TP35* | 80.4 |
| | Deinococcus pimensis | 76.1 |

## 8.3.6 Characterization of the selenium precipitate

During batch incubation of immobilized *S. barnesii* with selenate, a red colored precipitate was first observed within the cubes and subsequently in the whole batch medium (Figure 8.2A). SEM analysis of the gel cubes following the batch experiments showed that the gel cube surface was entirely covered with selenium precipitates (Figure 8.2B), whereas the inside of the cube contained fewer, but larger selenium precipitates (Figure 8.2C). The EDX maps showed these consisted mainly of selenium, with smaller contributions of sulfur (Scan S1, Figure 8.2C and D).

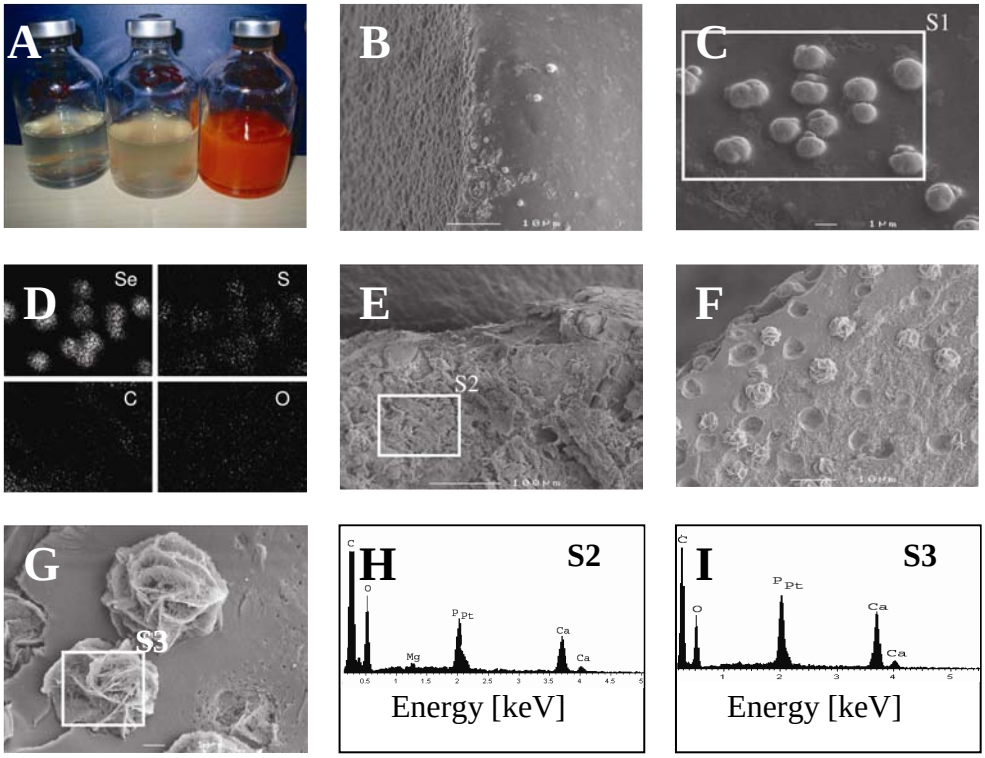


Figure 8.2 Photograph (A) of immobilized *S. barnesii* cells during production of elemental red selenium (0, 48 and 168 h) and SEM pictures of batch cubes (B,C) with EDX mapping (D) of selected area (S1) containing precipitates. Surface (E) and cross section (F,G) of a cube sampled after 58 days of reactor operation with (H) EDX surface and (I) precipitate scan within the cube

The gel cubes obtained from R1 upon termination of the reactor operation were entirely crusted by calcium and phosphorous containing precipitates, as demonstrated by the EDX surface scan (spectrum S2, Figure 8.2E and H). Inside the cubes, flower like structures were observed 70 µm from the edge of the cube (Figures 8.2F and G), mainly consisting of calcium and phosphorous (spectrum S3, Figure 8.2I).

# 8.4. Discussion

## 8.4.1 Whole cell immobilization of *S. barnesii*

This chapter shows that gel immobilization can be used to immobilize both microorganisms and their precipitation products (Figures 8.2B and C), i.e. elemental selenium, and sustain microbial reductive activity under long term (58 days) reactor operation (Figure 8.1A1 and 8.1A3). Immobilization was achieved in non-biodegradable polyacrylamide gels [116], which is important when considering application in environmental conditions.



Although nitrate / nitrite concentrations were reduced to < 1 µM, selenate was not reduced at the start-up of the reactor. When incubating *S. barnesii* under high excess of nitrate (5 mM) and selenate (50 µM) with lactate as electron donor, Oremland [166] observed selenate reduction with a strongly decreased rate (factor > 48) compared to incubation without nitrate. Consequently, the incomplete removal efficiencies observed in period I of R1 and R3 can be explained by a kinetic limitation, as the reactor medium is continuously replaced. The increase in selenate reduction rate during transition to period II (due to induction of higher selenate reducing activity) can be fitted linearly (days 25-28, R1; days 22 -25, R3) with 0.097 (R1) and 0.099 µM selenate µg $S.barnesii_{initial}^{-1}$ $d^{-2}$ (R2).

## 8.4.2 Bioaugmentation of UASB reactors by gel immobilized *S. barnesii* cells

This chapter shows the earlier selenate and sulfate reduction in the bioaugmented UASB is due to the addition of immobilized *S. barnesii* cells, as increased removal efficiencies for the latter anions occurred concurrently in R1 and R3, but delayed (24 and 44 HRTs, respectively) in R2 (Figure 8.1A and C). Furthermore, nitrate/nitrite reduction was complete during the start-up (period I, Figure 8.1B) of the bioaugmented reactors in comparison to the control reactor. The fact that $Se_{dis}$ and selenate removal efficiencies in R3 were lower compared to R2 in period III, might be explained by sulfide toxicity

(Chapter 4), as dissolved sulfide concentrations build up to higher levels (1.2 mM) and selenium conversion was already affected negatively before resuming nitrate feeding (day 42).

## 8.4.3 Selenate removal in denitrifying UASB reactors

Here it was shown that UASB reactors can reduce selenate under completely denitrifying conditions (period III, Figure 8.1A2) and might thus be applied as an alternative to a two step denitrifying-selenate reducing process or to the bioaugmentation with selenium-respiring organisms.

The simultaneous reduction of both electron acceptors can be due to the proliferation of a selenium-respiring specialist, previously described for the same inoculum operated in methanogenic conditions (Chapters 4 and 5) in period II. However, this hypothesis could not be further underlined by the DGGE analysis of the sludge. This is probably due to the low population size of the selenium respirer compared to nitrate-reducing bacteria, as nitrate (and lactate) were feed at high molar excess compared to selenate.



## 8.4.4 Implications for practical applications

This chapter demonstrates that the need for a two step process separating nitrate from selenate reduction spatially can be superseded by applying either denitrifying UASB reactors or bioaugmented systems immobilizing selenium-respiring organisms. Furthermore, hydraulic retention times applied here are much shorter (6 hours versus 10-16 days in the algal-bacterial system [69]). In acute contamination situations, e.g. in case of spillages of ore processing waste [223], the application of bioaugmented systems might be advantageous, due to the high time requirement for start-up in regular UASB reactors. It is suggested from batch incubations (Figure 8.2A) that the specialist colonizes the bulk liquid from the gel cubes. Thus, this technique is transferable to other applications, where a continuous release of biomass is required [15].

The effluent $Se_{dis}$ concentrations achieved <were the lowest in R1 (39 µg Se $L^{-1}$) and meet the current acute water quality criterion for salt waters (71 µg Se $L^{-1}$) set by the United States Environmental Protection Agency [241]. As 0.1 µm filtration could reduce $Se_{dis}$ concentrations by up to 48% (R2, period III), $Se_{dis}$ is mainly due to colloidal selenium passing the previously applied 0.45 µm filters. Thus slow sand filtration might be dispensable and dissolved gas flotation should be used as sole post-treatment of the effluent

prior to emission (instead of the combination of both currently applied [69]). It is important to note that no selenite was detected in any sample of R1, R2 or R3 (method detection limit 24 µg Se $L^{-1}$), as selenite is more toxic to aquatic invertebrates and fish than selenate [73]. This is probably due to the expression of nitrite reductases further reducing selenite to elemental selenium [166].

This chapter shows that the particle size of the bioprecipitates is more than a factor 5 bigger (≤ 2 µm, Figure 8.2C) compared to previous studies (Chapter 5) [167] using suspended cultures. Immobilized in gel, selenium precipitates formed by a membrane bound enzyme [166] are not subject to sheer forces and thus not sloughed from the cell, resulting in larger particle sizes. Precipitation within the gel separates part of the selenium from the water phase and prevents potential re-oxidation, when leaving the treatment system [291]. As the gel cubes did not float under the applied superficial upflow velocity, they can be easily recovered by settling for potential selenium re-use. In contrast to previous studies [167], however, here the precipitates consisted of selenium-sulfur mixtures (Figure 8.2D), which will lower the purity when considering selenium re-use. Cementation by inorganic precipitates [254] from the feed medium (here calcium-phosphorous precipitates, Figure 8.2F and G) might limit substrate transport to the organisms in longer (> 58 days) reactor operations.



If a classical UASB or hybrid system (UASB + immobilized cultures) is applied, an additional requirement of electron donor compared to nitrate, sulfate and selenate has to be taken into account to sustain the granular structure of the methanogenic biomass. Here, a factor 2 excess to nitrate (12 moles of electrons donated per mole lactate with 13 mM lactate in influent; 5 moles of electrons reduce 1 mole of nitrate with 15 mM nitrate in influent) was sufficient to maintain the granular structure. As most selenium containing steams are depleted in electron donor and its addition is the primary factor in operating costs [289], this excess should be minimized. As a result, immobilization of a non-nitrate-reducing, dissimilatory selenium respirer alone might be more feasible, as less electron donor is consumed by non selenium converting organisms (i.e. the sludge bed).

# Summary and discussion

# 9

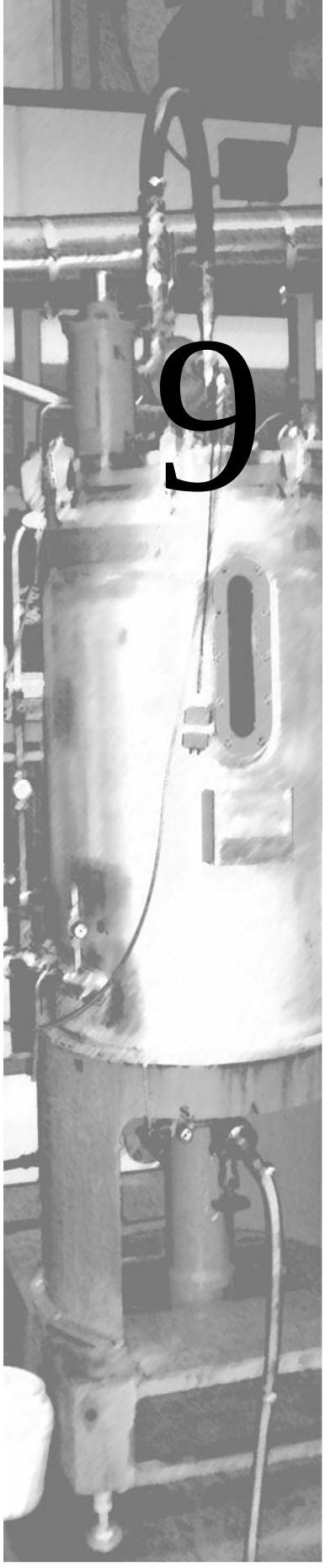

# 9.1. Introduction

Selenium contamination poses current and emerging threats to wildlife and human beings. The steep dose response curve due to bioaccumulation effects have lead to the characterization of selenium as a “time bomb” that can be fused by exceeding a narrow threshold concentration in ecosystems through anthropogenic activities. Ironically, an estimated 0.5 to 1 billion people suffer from selenium deficiency[79]. Consequently, remediative systems aiming at minimizing ecotoxicological risks on the one hand and selenium recovery on the other hand, need to be implemented. While the treatment of selenium contaminated agricultural drainage waters has been given great attention in the past [60], the treatment of industrial waste streams as the cause of manifold problems [73; 219; 220] has been given little attention so far. This thesis aimed at exploring new bioremediative systems for both agricultural (**Chapter 8**) and industrial (**Chapters 4 and 7**) waste streams. The treatment success, however, can only be evaluated, if precise information on selenium speciation in the solid, liquid and gas phase is available. Therefore, methods to determine the speciation by direct methods were developed in **Chapters 2, 3, 5** and **6**.



# 9.2. Selenium speciation

## 9.2. 1. Liquid / gas phase speciation

Selenium speciation in the aqueous phase is commonly assessed using indirect methods, such as hydride generative approaches coupled to different spectroscopic detection systems (e.g. AAS, ICP-OES/MS, AFS) [145; 176; 273]. However, this approach is limited by the complicated conversion of selenate to selenite [77], as selenate is quantified by the difference between total hydrated selenium and selenite, and furthermore by the fact that other dissolved selenium species are neglected. In **Chapter 2**, an Ion Chromatographic (IC) method is developed that separates selenate and selenite from e.g. nitrate, nitrite (**Chapter 8**) and sulfate (**Chapter 4**) present in high molar excess. Sample preparation requires dilution only, thus preserves sample selenium speciation, and limits of quantification were low (11 µg Se $L^{-1}$ as selenate; 28 µg Se $L^{-1}$ as selenite).

The IC method revealed that not all dissolved selenium ($Se_{dis}$) in the mixed liquor of the selenium treating bioreactors was due to selenate or selenite **(Chapters 4, 5** and **8)**. Solid Phase Micro Extraction Gas Chromatography Mass Spectrometry (SPME-GC-MS) revealed that selenate was partially converted to alkylated selenium compounds

(**Chapter 5**). An alternative, direct GC method could separate both dimethylselenide and dimethyldiselenide (**Chapter 2)**, but flame ionization detection proved not sensitive enough to detect these species stripped from the liquid phase of two UASB bioreactors with the biogas produced (**Chapter 4**). Nevertheless, this GC method might be applied either with a more sensitive alternative detection system (e.g. Photoionization Detection, PID) or in waste waters containing higher concentrations of alkylated selenium compounds. SPME-GC-MS closed the selenium liquid phase mass balance during undisturbed bioreactor operation (**Chapter 5**). A mixed selenium-sulfur species (dimethyl selenenyl sulfide) was formed as a result of disturbances during reactor operation (**Chapter 5**), possibly also explaining the large gap in the liquid phase balance of a sulfate-reducing UASB reactor operated in **Chapter 4**.

## 9.2.2 Characterization of the solid phase

### 9.2.2.1 Particle size of the precipitates

Pure cultures of *Sulfurospirillum barnesii* and other selenium respirers incubated in batch assays form globular elemental selenium particles (~ 300 nm diameter), loosely attached on the bacterial surfaces [167]. When incubating non-adapted anaerobic granular sludge with a high selenium concentration (10 mM) in batch, similar sized spherical particles are formed (**Figure 4.8c**), demonstrating that selenium nano-sphere formation is not limited to selenium-respiring organisms solely.



In contrast, *Sulfurospirillum barnesii* immobilized in polyacrylamide gels, formed precipitates within the gel matrix that were a factor 5 larger (~ 1.5 µm, **Figure 8.5C**). Microorganisms proliferating in the recycle lines of a methanogenic UASB reactor showed selenium particles of only 50-100 nm (**Figure 5.4**). These results suggest that larger precipitate particle sizes can be formed when precipitates are not sloughed from the microbial cell. The combination of both harsh and low sheer forces in the recycle lines and the sludge bed, respectively, might thus explain the broad particle size distribution of the selenium precipitates between << 200 nm and 4 µm observed during long term UASB operation (**Chapter 5**).

### 9.2.2.2 Solid phase speciation

**Chapter 2** demonstrates that a part of the precipitates formed in batch (20 mM selenate) was hexagonal black selenium, but the low signal to noise ratio suggested a mainly

amorphous character of the remaining precipitate. The presence of black hexagonal selenium might thus be an artifact of sample drying and storage, as amorphous selenium can transform to thermodynamically more stable polymorphs at room temperature [148]. XRD investigation of the sludges obtained after stable long term operation under sulfate or methanogenic conditions (**Chapter 4**) did neither confirm nor exclude a hexagonal black selenium phase due to overlaying signals.

An identification of crystalline phases by XRD is generally hampered by particle sizes smaller than 1000 Å [7]. Consequently, X-ray Absorption Fine Structure (XAFS) experiments were performed, as these techniques yield the speciation information of both amorphous and crystalline phases in a non destructive way. The oxidation state of elements can be determined by the analysis of the main crest edge or the first inflection point position of their X-ray Absorption Near Edge Structure (XANES). Numerous studies have exclusively utilized only one the latter features to determine selenium oxidation states [18; 104; 137; 154; 162; 191; 192; 200; 209]. **Chapter 3** demonstrates that no simple relation is found between these two XANES features and the selenium valence at the selenium K-edge, thus both features should be considered at the same time. Oversimplified conclusions might be obtained, when considering only one of the two features using a small set of selenium model compounds in metal rich environments.



Short exposure (10 min) to atmospheric oxygen induced changes in selenium speciation (**Chapter 6**) by the oxidation of organic selenium species and transformation of metal selenides, underlining the importance of careful sample handling preserving selenium speciation. It was demonstrated that, although validated with different selenium model compounds previously [269], sequential extraction procedures can lead to an underestimation of the selenide fraction and an overestimation of the elemental selenium fraction (**Chapter 6**).

### 9.2.2.3 Solid phase speciation in methanogenic granules

XANES analysis of selenium speciation in intact biofilms has so far been studied only using cultures of *Burkholderia cepacia* grown on $\alpha$-$Al_2O_3$ surfaces [227], demonstrating selenium oxyanion reduction to red elemental selenium on the bacterial-mineral interface. Yet, this system represents a rather simplified laboratory system, as it is poor in metals that can potentially precipitate to metal selenides. Furthermore, the biofilms were cultivated aerobically, so that interaction with reduced species (e.g. sulfides) taking place in contaminated sediments or anaerobic bioreactors are not considered. These results have thus limited transferability to anaerobic environments.

**Chapters 3** and **6** demonstrated that selenium solid phase speciation in methanogenic granules is characterized by a complex mixture of selenium species, including elemental selenium, organic selenium compounds and metal selenides (**Figure 6.1B**), but no oxidized species (selenite or selenate).

Upon longer reactor operation, elemental selenium contributed to a larger extent to the modeled selenium speciation in the methanogenic granules (41 atom % and 67 atom % on days 60 and 115 of operation, respectively), whereas the total amount of selenium accumulated in the sludge increased as well (**Figure 4.1B**, **Chapter 4**). This demonstrates that anaerobic sludge granules can indeed immobilize selenium in elemental form under long term methanogenic operational conditions. Yet, a minor part of the selenium (12 atom % and 14 atom % on days 60 and 115 of operation, respectively) was present in selenocysteine (or selenocysteine containing proteinous) form. Selenocysteine is a precursor to selenium alkylation [24]. Such alkylation was observed in methanogenic conditions from endogenous selenium sources (**Table 5.2, Chapter 5**). Consequently, the total amount of selenium that can be alkylated with selenocysteine as precursor increases during prolonged reactor operation. This might represent a problem in full scale applications, when the selenium rich excess sludge is disposed after reactor operation.

The formation of metal selenides is probably caused by reduction of selenium oxyanions to dissolved selenide [82] and subsequent precipitation with metals present in the sludge and feed medium. Therefore, metals present in the anaerobic granular sludge represent an important sink for highly toxic, dissolved selenide, preventing a wash out that might occur in metal poor environments. The fact that no metal selenides were so far detected by XRD in the sludges (**Chapters 4** and **5**) might be due to either their low concentration, overlaying signals (**Figure 4.7**) or nano-crystallization [7].



### 9.2.2.4 Biofilm selenium speciation in sulfate-reducing granules

Selenium speciation in sulfate-reducing sludge was fundamentally different compared to the speciation in methanogenic sludge. Although the main XANES features were comparable (**Table 3.1**), linear combination modeling demonstrated the exclusive contribution of trigonal elemental selenium to the speciation in sulfate-reducing sludge (**Chapter 3**). The formation of metal selenides, as observed in methanogenic sludge, is improbable due to prevailing sulfidic metal precipitation, as several millimoles of dissolved sulfide were present in the reactor liquor (**Figure 4.2A**), depleting the bulk liquor from metals. Consequently, aqueous selenide might wash out from sulfate-reducing bioreactors.

In both sludge types (methanogenic and sulfate-reducing) the elemental selenium contribution to the modeled XANES spectra resembled to the trigonal elemental polymorph. Yet, Extended X-ray Absorption Fine Structure (EXAFS) analysis revealed that selenium was present in an aperiodic, elemental form, different from trigonal (and monoclinic red) elemental selenium (**Figure 3.3B**). Possibly, a low symmetry polymorph, such as red amorphous selenium [148], could explain the discrepancy between the modeled XANES speciation and the experimental EXAFS results.

# 9.3. Biotechnological selenium removal

## 9.3.1 Selenium removal by sulfate-reducing bacteria

Some studies have used sulfate-reducing bacteria (SRB) to remove selenate from aqueous phase in batch assays [84; 234], relying on the fact that selenate is reduced as a structural analogue to sulfate. Due to the high toxicity of selenate to SRB [26; 177; 283] batch experiments can only give little information regarding selenate removal in continuous systems. **Chapter 4** demonstrates that the SRB present in UASB granules can be used in continuous selenium biotreatment. Due to the competitive effect between sulfate and selenate, the ratio of selenate to sulfate should be greater than $1.92 \times 10^{-3}$. Consequently, an incomplete selenium removal efficiency has to be expected for most selenate and sulfate containing waste streams (**Table 4.1**) as they display ratios of selenate to sulfate lower than $8.0 \times 10^{-4}$. High concentrations of dissolved sulfide (several millimoles) were not interfering with selenate removal, which offers the possibility to combine (partial) selenium removal with sulfidic heavy metal precipitation [195; 255] in acid mine drainage or other strongly metal contaminated streams, where selenium discharge values are less stringent.



## 9.3.2 Selenium removal in methanogenic UASB reactors

Mesophilic methanogenic UASB reactors removed both selenate and dissolved selenium ($Se_{dis}$) with high efficiencies (**Chapters 4 and 5**) at short hydraulic retention times (6 hours). In comparison to a sulfate-reducing reactor (**Chapter 4**), the methanogenic reactor sludge contained 1.9 times more selenium (1785 µg Se $gVSS^{-1}$) after 150 days of operation, and no saturation of selenium accumulation within the sludge was noted (**Figure 4.1B**).

The fact that selenate removal was nearly complete under 2600 times molar excess of sulfate to selenate (this excess competitively inhibited selenate reduction by SRB, **Chapter 4**, demonstrates the selectivity of the reduction and was explained by the proliferation of a selenium-respiring microorganism (**Chapter 4**). Sequencing of DGGE bands newly developing during the reactor operation, matched, although poorly (79%), with *Dendrosporobacter quercicolus*, a mesophilic, anaerobic selenate reducing bacterium. Selenium-respiring microorganisms were developing in the sludge bed, demonstrated by the higher selenium removal efficiency in the presence of sulfate after prolonged reactor operation (**Figure 4.3**). In addition, microorganisms covered with selenium particles proliferated in the recycle lines (**Chapter 5**). Although most selenate was reduced in the bioreactor (> 90%), residual selenate reducing activity was also found in the supernatant of the external settler (**Chapter 5**), indicating that a part of the selenium reducing microorganisms grew as suspended biomass in the UASB reactor.

Both alkylated selenium species (up to 15%) and colloidally dispersed selenium particles (up to 31%) contributed to the selenium present in the effluent, calling for a post treatment step before discharge. The minimal effluent concentrations achieved in this thesis under methanogenic conditions (**Chapters 4** and **5**) were comparable to previously reported values by Owens [170], who applied methanogenic UASB reactors in the full-scale treatment of agricultural wastewaters. In contrast to this previous study, influent selenate concentrations here were higher (≈ 2 times) and hydraulic retention times shorter (3 times). It was demonstrated that slight disturbances in operational temperature can induce alkylated selenium or mixed selenium / sulfur species production (**Chapter 5**). Thus, the constant removal performance achieved in **Chapter 4** in comparison to **Chapter 5** was due to the constant temperature applied.



## 9.3.3 Selenium removal in denitrifying UASB reactors

The competitive inhibition between nitrate and selenate reduction observed in many treatment applications [60] can be avoided in two stage systems reducing nitrate concentrations prior to selenate reduction [4]. As an alternative, **Chapter 8** shows that UASB reactors can reduce selenate under completely denitrifying conditions in one stage. This is possibly due to the proliferation of a selenium-respiring specialist, as already observed when applying methanogenic conditions to the same inoculum (**Chapter 4**), although its identification by DGGE and sequencing was hampered by the presence of a diverse population of microorganisms, feeding on the supplied lactate and nitrate. A reduction of selenate by nitrate reductases, previously described as a general characteristic

of nitrate reducers [193], was not indicated, as the denitrifying sludge was not able to convert selenate upon omitting nitrate from the feeding (**Figure 8.1A2**).

### 9.3.4 Selenium removal using selenium respirers

Bioaugmentation, the purposeful addition of microorganisms capable of treating a certain pollution, is often limited by wash out and by out-competition of the added microorganisms by endogenous microorganisms [46]. **Chapter 8** delivers evidence that whole cell immobilization of selenium respirers can overcome these constraints in long term continuous bioreactor operation (> 60 days of operation). A reactor inoculated with immobilized bacteria solely removed selenate under completely denitrifying conditions (**Figure 8.1A1**). In a parallel hybrid bioreactor, anaerobic granular sludge was bioaugmented with immobilized bacteria, resulting in earlier selenate, nitrate and nitrite removal and higher COD removal efficiency compared to a non-bioaugmented control reactor (**Figure 8.1**).

The faster start up of the bioaugmented bioreactors (**Figures 8.1A, 8.1C**) might be important in case of urgent incidents, e.g. spillage ore processing waste [223]. The immobilization was achieved in non-biodegradable polyacrylamide gels, offering potential application under environmental conditions. Long term bioremediation might be limited by activity losses due to mass transfer limitation by cementation, as the gel surfaces and the immobilized bacteria were entirely crusted by calcium and phosphorous containing precipitates after 60 days of operation (**Figure 8.2E-G**).



## 9.4. Recommendations for selenium biotreatment

Considerations for best available techniques to mitigate selenium contamination are always related to a case-specific scenario. Thus, the choice for an appropriate selenium treatment system includes technical and economical considerations, but also matters of social acceptance and political prerequisites. **Table 9.1** summarizes major results of this thesis using different microbial groups that should be considered when designing a biological treatment system.

## 9.4.1 Selenium concentration to be treated

The first consideration that needs to be taken into account is the selenium concentration of the waste stream. Treatment of highly concentrated waste streams (up to 620 mg $L^{-1}$ in selenium processing industries [64]) might be treated feasibly by physical-chemical methods such as adsorption, precipitation or filtration (**Table 1.2**). However, especially physical-chemical processes that are not based on reduction of the selenium oxyanions result in highly concentrated brines that need to be disposed safely, reflected by the high operational costs of these systems (**Table 1.2**) [106; 140]. Biological treatment of highly contaminated waste streams could be achieved using selenium-respiring organisms, as these can tolerate and reduce high selenium concentrations. Although tolerant to selenium oxyanions, selenium-respiring organisms might be sensitive to other toxins present in the waste stream, e.g. sulfide toxicity (**Chapter 4**), that can be prevented by appropriate sulfide removal methods [119]. Toxicity of selenium oxyanions towards different microbial groups, amongst others methanogens (**Chapter 7**) and sulfate-reducing bacteria (**Chapter 4**) will limit the application of mixed cultures. Even if the selenium oxyanion concentrations in the bioreactors are reduced to below inhibitory concentrations, homogeneous mixing has to be ensured by efficient influent distribution systems (e.g. perforated distribution plates or membranes) or mixing with the effluent recycle prior to entering the reactor in order to prevent irreversible toxicity (**Chapter 7**).



Treatment of high volume, low selenium concentration waste streams calls for cheap, selective processes, as offered by e.g. biological reduction. While dilution to the atmosphere by biological volatilization, e.g. in low concentrated agricultural drainage waters, might be acceptable in remote areas, the malodorous character [206] and the potential chronic toxicity of alkylated selenium species interfere with an uncontrolled emission to the atmosphere in populated areas. Furthermore, an expositional risk by acute toxicity [25] for workers has to be considered when treating selenium in sealed bioreactors.

## 9.4.2 Desired target values

It has been shown in this thesis that selenate is efficiently reduced in short hydraulic retention times (6 hours) by bioconversion. However, substantial amounts of selenium can be converted to alkylated species or colloidal selenium (**Chapter 5**). If no post-treatment is applied, both fractions will contribute to a higher selenium effluent concentration, as alkylated selenium species are water soluble and colloidal selenium does not settle by simple technical means, e.g. an external settler (**Chapter 5**).

Table 9.1 Evaluation of the major results of this thesis using different microbial groups for biological selenium treatment (numbers in brackets indicate related chapters of this thesis)

| | Methanogenic UASB | | Sulfate reducing UASB | | Nitrate reducing UASB | | Immobilized specialists | |
|---|---|---|---|---|---|---|---|---|
| | + | - | + | - | + | - | + | - |
| Liquid / gas phase speciation | Low $Se_{dis}$ (undisturbed) (4) | High $Se_{dis}$ (disturbed): DM(D)Se DMSeS (5) | | High $Se_{dis}$; unknown Se species (4) | | | Low $Se_{dis}$ (8) | |
| Biomass solid phase speciation | High Se in sludge (4), elem. Se in long term (6) | Se (-II) and organic Se (3,6) | Pure elemental Se in long term (3) | Low Se in sludge (4) | | | | |
| Precipitates | | nm sized (5) | | nm sized (4) | | nm sized (8) | µm sized (8) | Se + S particles (8) |
| Selectivity | High (4) | | | Low (4) | | | | |
| Limitation | | $S^{2-}$ (4), $SeO_3^{2-}$, $SeO_4^{2-}$ inhibition (7) | $S^{2-}$resistance (4) | Ratio $SO_4^{2-}$: $SeO_4^{2-}$ (4); $SeO_4^{2-}$ inhibition | | | | Possible Cementation (8) |
| Costs / Benefits | Energy recovery via $CH_4$ (4,5) | | Sulfidic metal precipitation | | $NO_3^-$ removal (8) | No $SO_4^{2-}$ removal (8) | Versatile applicable (arsenate,…), fast start-up | |

A precise process control can avoid selenium alkylation (**Chapter 5**). The delay between disturbance and alkylation in case of a process control failure (**Figure 5.7**) might offer the possibility to counteract higher selenium effluent concentrations by e.g. applying additional buffer tanks or increased hydraulic retention times. Zero valent iron addition can reduce both selenium oxyanions and organic selenium compounds [294], but is hardly applicable for direct treatment of large volumes of selenium containing waters (**Chapter 1, section 1.5.1.4**). It might, however, represent an alternative post treatment, when discharge values are stringent or organic selenium effluent concentrations are high.

The influent concentration of 790 µg Se $L^{-1}$ was reduced to a minimal value of 73 µg Se $L^{-1}$ applying simple filtration (0.45 µm) in methanogenic UASBs (**Chapter 4**) and 39 µg Se $L^{-1}$ using a selenium-respiring specialist (**Chapter 8**). Filtration (0.2 µm) and subsequent centrifugation further decreased the effluent $Se_{dis}$ concentrations in methanogenic systems to 28 µg Se $L^{-1}$ (**Chapter 5**), thus effluent concentrations were well below the USEPA Universal Treatment Standards [242] for wastewater of 820 µg Se $L^{-1}$. However, the chronic tissue-based freshwater aquatic life criterion, protecting against unacceptable adverse effects resulting from long-term (continuous) exposure might be exceeded due to bioaccumulation, even though effluent concentrations are low (**Figure 1.8**).

The emission of nano-sized selenium particles produced during the biological treatment should be avoided as these can become bioavailable by direct assimilation [131; 202; 285] or re-oxidation [291]. In the past, dissolved air floatation has been applied to remove colloidal selenium particles [69; 185], but re-oxidation of reduced selenium compounds to selenate might occur when using compressed air. Dissolved gas floatation [271], using e.g. biogas, should be investigated as a promising post treatment, as it can simultaneously remove colloidal selenium particles and strip alkylated selenium species. If very low selenium target values are set, a post treatment with reverse osmosis is advisable [160].



## 9.4.3 Economic considerations

In general, the economic feasibility of selenium treatment can be assessed from different motivations: firstly, selenium treatment can be applied to remove selenium from the effluent in order to avoid discharge fines, thus determining the choice towards a “minimal compliance” remediative system [71]. Depending on the set target values, less efficient but cheap systems such as ion exchange (**Table 1.2**) will be applied by companies. More stringent target values can be achieved by biological treatment (**Chapters 4, 5** and **8**).

A part of the investment and operational costs can be recovered when selenium removal is combined with resource recovery in a “process oriented” scheme [71]. In this regards, a

system consisting of a sludge bed reactor, a fluidized bed reactor, flocculation and microfiltration treating selenium and sulfate rich agricultural drainage waters was able to recover more than 90% of its operational cost through byproduct (sodium sulfate) production [214]. Recovery of pure elemental selenium might further reduce costs. In contrast to several other studies [104; 115; 133; 167], it was demonstrated in this thesis that elemental selenium is not the only product of biological selenate reduction (**Chapters 3** and **6**) and can thus not be recovered in pure form. Yet, the precipitate could be upgraded, e.g. in a pyrometallurgical process. Depending on market demands for selenium products, these precipitates can be sold in low quality or upgraded form to external customers in a "market oriented" approach [71]. However, both markets for biologically recovered selenium products and quality control mechanisms for the reclaimed selenium product still need to be developed.

The requirement of an electron donor is often the primary factor in operating costs for biological systems [289] as most selenium contaminated streams are depleted in electron donor (**Table 7.1**). Combination of COD rich waste streams containing e.g. molasses [289] or methanol [170] with selenium contaminated wastewaters might allow energy recovery via methane (**Chapters 4** and **5**). One should consider that during selenium removal, methane yields can be seriously decreased due to selenate and selenite toxicity towards both acetotrophic and hydrogenotrophic methanogens (**Chapter 7**). In this thesis, the lowest organic loading rate (OLR) that could still maintain selenate reduction under methanogenic conditions was 0.5 g COD $L^{-1}$ $day^{-1}$ (**Chapter 5**, 103-122 days of operation), yet lower OLRs might be obtained in the future (compare section 9.5.2.3).



# 9.5. Recommendations for future research

## 9.5.1 Selenium speciation and selenium-sulfur interactions

The interaction of alkylated selenium and sulfur, forming mixed selenium-sulfur compounds (e.g. dimethyl selenenyl sulfide, **Chapter 5**) substantially interferes with the selenium removal efficiency of bioreactors (**Figure 5.6**). This demands an elucidation of both the chemical and microbial basis of formation and degradation of such compounds. The application of mass spectrometric based detection techniques to identify and quantify these species seems to be appropriate. Stable isotope analysis might assist in determining the extent of biological processes involved, in analogy to environmental sulfur isotope analysis [e.g. [107]].

Although the efficiency of biological processes in reducing dissolved selenium concentrations was proven in several Chapters (**Chapters 4, 5** and **8**), a comparison regarding the efficiency in detoxification should be included in future studies, as ecotoxicological effects are not related to the total selenium concentrations [60], but a function of concentration and bioavailability. However, long term experiments using e.g. mesocosms are costly and labor intensive. Solid phase microextraction has recently been applied to estimate the bioavailability of hydrophobic contaminants [e.g. [98; 274; 277]]. This application could be expanded to alkylated selenium species.

Secondary Ion Mass Spectrometry (SIMS) has recently been hyphenated with Fluorescence In Situ Hybridization (FISH) methods, revealing the phylogenetic microbial identity together with isotopic patterns at single cell level [123]. This approach could be used to label selenate reducing microorganisms and follow selenium precipitation in situ.

Selenide oxidation observed during ambient air exposure of selenium accumulating sludge (**Chapter 6**) opens a wide field of research elucidating environmental selenium cycles on aerobic/anaerobic interfaces (e.g. sediment/water or mine tailing/air). Now that a large set of natural and synthetic compounds, including less studied Se (-I) selenides, is available **(Chapter 3),** the application of XAFS based techniques should be enlarged for the determination of mixed selenium-sulfur precipitates (**Chapter 8**). Especially the complementary use of sulfur [178; 179] and selenium XAFS techniques is promising. Due to the fact that macro beams were used, the contribution of several selenium mineral species to the XANES spectra interfered with the elucidation of the precise mechanism of mineral transition. Spatial variation in selenium speciation might, however, be high and increased spatial resolution would therefore give better understanding of the oxidation processes, but also in biofilm functioning regarding selenium deposition (**Figure 7.7A** and **B**). Consequently, µ- or nano XAFS studies [162; 218] should be applied to resolve selenium speciation in different locations of the biofilms. Scanning transmission X-ray microscopy (STXM) (Figure 9.1) could prevent overlaying of different selenium species as the sample is prepared in thin sections. Regrettably, STXM is currently available only at the selenium L-edge and the sensitivity of the method might represent a problem in biological samples treating low selenium concentrations [1]. Time resolved µ-XAFS experiments [200] could quantify oxidation rates of mineral transition. Selenium intermediates accumulating in the sludge as organic selenium compounds (**Chapter 3** and **6**) could potentially be deduced using $^{77}$Se labeled compounds by Nuclear Magnetic Resonance (NMR) spectroscopy [96].

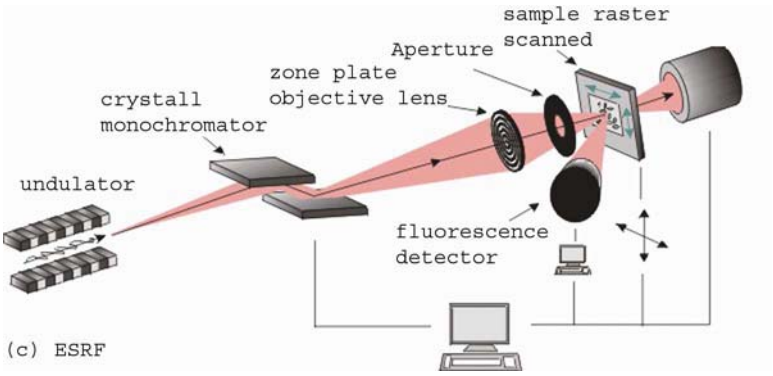


Figure 9.1 Scanning X-ray transmission microscopy set up at beamline "ID21" (European Synchrotron Radiation Facility, Grenoble, France)[50].

## 9.5.2 Process technology

### 9.5.2.1 Inoculum



Anaerobic granular sludge is a versatile source of different groups of microorganisms, including e.g. sulfate-, nitrate reducers and methanogens (**Chapters 4, 5** and **8**), but also specialized selenium-respiring organisms (**Chapters 4, 5** and **8**). In the future, its application might be enlarged for the treatment of other oxyanions, such as chromate, arsenate, molybdate, uranate.

**Chapter 8** demonstrated that selenium-respiring organisms can be immobilized in non-degradable gels, maintaining their selenium reducing activities over a time period of at least 60 days. The organism that was bioaugmented (*Sulfurospirillum barnesii*) is versatile in using electron acceptors (selenate, arsenate, tellurate, etc.) [8; 130], which opens a wide field of bioremediation applications.

### 9.5.2.2 Reactor design and operation

Immobilized bacteria in small sized polyacryamide gel beads, offering an ideal volume to surface ratio, can be applied in packed bed reactors, and prevent out-competition observed in a previous study [20] (**Figure 1.11A**). If immobilization procedures cannot maintain long term selenate reducing activity, selenium respirers might be applied in membrane bioreactors offering biomass retention [250], although application membranes might be

limited by cake formation [94] through colloidal elemental selenium or metal selenide formation.

### 9.5.2.3 Electron donor

As the electron donor usually represents the major costs in bioremediation systems, competition by methanogenesis, nitrate and sulfate reduction conflicts the feasible reactor operation. Co-immobilization of selenium-respiring organisms with hydrogen releasing compounds [109] as electron donor in slow release capsules [91] might be an approach to overcome competition due to the spatial proximity of electron donor and selenium respirer.

The rate of electron donor released should be adjusted to the minimal electron donor necessary for the complete reduction of the selenium oxyanions to elemental selenium. For instance, selenate was fed at a rate of 40 µM $L_{reactor}^{-1}$ $d^{-1}$ in **Chapters 4, 5** and **8**, thus 40 × 6 µmol electrons $L_{reactor}^{-1}$ $d^{-1}$ are required for the reduction of selenate (+VI) to elemental selenium (0), corresponding to e.g. 20 µM lactate $L_{reactor}^{-1}$ $d^{-1}$. However, such low organic loading rates are only sufficient for selenate reduction to elemental selenium under ideal (non competition) conditions, thus further lab / pilot / full scale experiments need to be undertaken to determine the minimal OLR that still results in complete selenium removal.



In highly concentrated streams, $H_2$ might be dosed as an efficient electron donor[26] (**Chapter 7**). $H_2$ can best be distributed by membrane sparkling [26] or by bubbleless supply [52]. Alternatively, $H_2$ could be supplied with synthesis gas in a gas lift reactor (applied in full scale for microbial sulfate reduction [252]), yet operational costs will increase e.g. due to costs for $H_2$ supply and safety provisions.

## 9.5.4 Solid separation

In order to separate selenium particles from the aqueous stream by simple means, i.e. gravitational settling, large, dense and uncharged particles are desired. Yet, **Chapters 2, 3, 4** and **5** evidence that the formed particles are amorphous, small (<0.5 µm) and do not settle easily. Figure 9.2 shows SEM pictures of selenium precipitates formed by anaerobic granular sludge (10 mM selenate). Drying at elevated temperature (105°C, Figure 9.2B) in comparison to drying at room temperature (Figure 9.2A) results in transformation of amorphous bioprecipitates to crystals of larger particle size. This is probably due to the transition of the red amorphous selenium to trigonal or hexagonal elemental selenium [148]. Especially the formation of the trigonal polymorph is

advantegeous, as it is 13% denser compared to amorphous selenium[148] and can form large crystals (**Figure 1.5**). Consequently, thermophilic conditions (or post-treatment) should be explored to improve settleability of selenium precipitates, as these selenium polymorph transformations can be observed at 70°C or less [148], a temperature applicable for e.g. extreme thermophilic sulfate reduction [249]. Furthermore, reactor concepts with low sheer forces should be investigated in future studies in order to gain bigger particle sizes (section 9.2.2.1). Future research should also focus on the questions, if surface charge of the particles can be influenced by the applied operational conditions. This could enhance the bioprecipitate recovery and thus optimize the currently applied coagulation post-treatment [20].

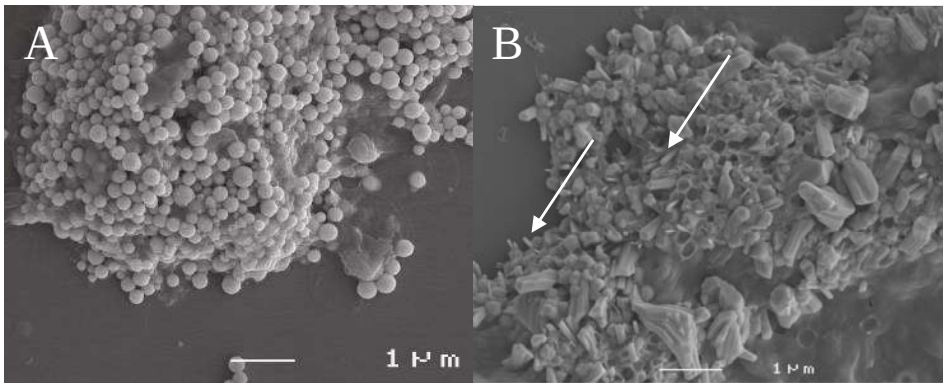




Figure 9.2 Scanning electron microscope pictures of selenium precipitates formed in batch assays of anaerobic granular sludge treating 10 mM selenate. Precipitates dried at 20°C (A) and 105°C (B). Arrows marks mineral structure resembling to trigonal selenium rods (compare [95])

# 9′ Samenvatting en discussie

# 9.1 Introductie

Selenium verontreiniging vormt een bedreiging voor fauna en mensen, zowel nu als in de toekomst. De dosisresponse curve is, als gevolg van bio-accumulatie, steil, waardoor selenium in ecosystemen kan worden gekarakteriseerd als een "tijdbom" die antropogene activiteiten kan worden ontstoken wanneer een drempelwaarde wordt overschreden. Deze drempelwaarde is voor selenium zeer laag. Ironisch genoeg wordt er geschat dat 0,5 tot 1 miljard mensen aan een tekort aan selenium lijden [79]. Derhalve zouden reinigingsystemen enerzijds ecotoxicologische risico's moeten minimaliseren en anderzijds seleniumterugwinning mogelijk moeten maken. De behandeling van met selenium vervuild landbouw drainagewater heeft in het verleden veel aandacht gekregen [60], de behandeling van industriële afvalstromen heeft echter tot nu toe weinig aandacht gekregen, terwijl deze afvalstromen bijdragen aan diverse problemen [73; 219; 220]. Dit proefschrift beoogt nieuwe behandelingssystemen te onderzoeken voor zowel landbouw drainagewater (**Hoofdstuk 8**) als industriële afvalstromen (**Hoofdstukken 4** en **7**). Het succes van een behandelingsmethode kan slechts worden geëvalueerd als speciatie van selenium in vaste, vloeibare en gasvormige fase bekend is. In **Hoofdstukken 2, 3, 5 en 6** zijn daarom directe methodes ontwikkeld om de speciatie te bepalen.



# 9.2. Speciatie van selenium

## 9.2.1. De speciatie in vloeistof/gas fase

De speciatie van selenium in de waterfase wordt in het algemeen bepaald m.b.v. indirecte methodes, zoals het genereren van hydrides in combinatie met verschillende spectroscopische detectiemethodes (bv. AAS, ICP-OES/MS, AFS) [145; 176; 273]. Deze benadering wordt echter beperkt door de moeilijke omzetting van selenaat naar seleniet [77], aangezien selenaat wordt gekwantificeerd door het verschil tussen totaal gehydrateerd selenium en seleniet, en overige opgeloste selenium verbindingen worden verwaarloosd. In **Hoofdstuk 2** wordt een Ion Chromatografie (IC) methode ontwikkeld waarin die selenaat en seleniet kan worden onderscheiden van b.v. nitraat, nitriet (**Hoofdstuk 8**) en sulfaat (**Hoofdstuk 4**) aanwezig in hoge concentraties. De voorbereiding van een monster behelst slechts een verdunningsstap, de selenium speciatie wordt daarom behouden, en de detectielimiet was laag (11 µg Se $L^{-1}$ selenaat; 28 µg Se $L^{-1}$ seleniet).

Op basis van de IC methode werd vastgesteld dat niet al het opgelost selenium ($Se_{dis}$) in bioreactoren, die seleniumhoudend water behandelden, aanwezig was als selenaat of

seleniet (**Hoofdstukken 4,5** en **8**). “Solid Phase Micro Extraction Gas Chromatography Mass Spectrometry” (SPME-GC-MS) maakte duidelijk dat selenaat gedeeltelijk werd omgezet in gealkaliseerde seleniumverbindingen (**Hoofdstuk 5**). Een alternatieve, directe gas chromatografisch (GC) methode kon zowel dimethylselenide als dimethyldiselenide detecteren (**Hoofdstuk 2**), maar deze vlamionisatie methode bleek niet gevoelig genoeg voor de detectie van deze verbindingen in de wasvloeistof van het biogas van twee UASB bioreactoren (**Hoofdstuk 4**). Desalniettemin, zou deze GC methode kunnen worden toegepast met een gevoeliger detectiemethode (bv. detectie m.b.v. foto-ionisering, PID), daarnaast is de GC methode wel geschikt voor afvalwater met hogere concentraties gealkaliseerde seleniumverbindingen. SPME-GC-MS maakte het mogelijk de selenium massabalans in de vloeistoffase tijdens een stabiele reactorrun te sluiten (**Hoofdstuk 5**). Als gevolg van verstoringen tijdens een reactorrun werden verschillende selenium-zwavel verbindingen (dimethyl selenenyl sulfide) gevormd (**Hoofdstuk 5**), deze verklaren het grote gat in de massabalans voor de vloeistoffase in de sulfatenreducerende UASB reactor beschreven in **Hoofdstuk 4**, waar enkel de IC gebruikt was..

## 9.2.2 De karakterisering van de vaste fase

### 9.2.2.1 Deeltjesgrootte van de precipitaten



Rein culturen van *Sulfurospirillum barnesii* en andere in batch gekweekte selenium respireerders vormen bolvormige deeltjes van elementair selenium (~ 300 nm diameter) aan de bacteriële oppervlakte [167]. Wanneer niet-aangepast anaëroob granulair slib wordt geïncubeerd in batch met een hoge seleniumconcentratie (10 mM) worden deeltjes gevormd met vergelijkbare vorm en grootte (**Figuur 4.8c**), dit toont aan dat de vorming van de seleniumdeeltjes niet alleen beperkt is tot selenium respirerende organismen.

*Sulfurospirillum barnesii*, geïmmobiliseerd in polyacrylamidegel, vormt daarentegen precipitaten binnen de gel matrix die een factor 5 groter waren (~ 1,5 µm, **Figuur 8.5C**). Micro-organismen die in de recirculatie lijnen van een methanogene UASB reactor groeide vormden elementair seleniumdeeltjes van slechts 50-100 nm (**Figuur 5.4**). Deze resultaten impliceren dat grotere deeltjes kunnen worden gevormd wanneer precipitaten niet van de microbiële cel worden geschaafd. De afwisseling van stabiele en turbulente condities, in de recirculatielijnen en het slibbed respectievelijk, zou de brede range in de grootte van de seleniumprecipitaten kunnen verklaren in langlopende reactor experimenten, de deeltjesgrootte varieerde van << 200 µm tot 4 µm (**Hoofdstuk 5**).

## 9.2.2.2 De speciatie in de vaste fase

In **Hoofdstuk 2** wordt aangetoond dat een deel van de precipitaten, gevormd tijdens batch experimenten met 20 mM selenate, bestond uit hexagonaal zwart selenium, maar de lage verhouding tussen het signaal en de ruis impliceerde dat het resterende precipitaat vooral een amorf karakter had. De aanwezigheid van zwart hexagonaal selenium zou een artefact kunnen zijn, veroorzaakt door het drogen en opslaan van het monster, aangezien het amorfe selenium bij kamertemperatuur naar het thermodynamisch meer stabiele polymorphs kan worden omgezet [148]. Onderzoek m.b.v. XRD, aan slib verkregen na stabiele langdurige reactorruns bij sulfaatreducerende of methanogene condities (**Hoofdstuk 4**), kon een hexagonale zwarte selenium fase niet bevestigen noch uitsluiten door het overlappen van signalen.

Een identificatie van kristallijne fasen door XRD wordt over het algemeen belemmerd door de aanwezigheid van deeltjes kleiner dan 1000 Å [7]. Derhalve zijn "X-ray Absorption Fine Structure" (XAFS) experimenten uitgevoerd, aangezien m.b.v. deze technieken informatie over de speciatie van zowel amorfe als kristallijne fasen wordt verkregen op een niet destructieve manier. De oxydatie staat van elementen kan worden bepaald door de analyse van de piekpositie of het eerste buigpunt van hun "X-ray Absorption Near Edge Structure" (XANES). Tal van studies hebben uitsluitend slechts één van de laatstgenoemde methodes gebruikt om de oxidatiestaten van selenium te bepalen [18; 104; 137; 154; 162; 191; 192; 200; 209].. **Hoofdstuk 3** toont aan dat er geen eenvoudige relatie is tussen deze twee XANES karakteristieken en de seleniumvalentie van de selenium K-rand, dus zouden de methodes tegelijkertijd moeten worden toegepast. De conclusies kunnen te eenvoudig zijn wanneer slechts één van de twee methodes gebruikt wordt in combinatie met een kleine reeks model verbindingen.



De korte blootstelling (10 min) aan atmosferische zuurstof veroorzaakte veranderingen in de selenium speciatie (**Hoofdstuk 6**) door de oxydatie van organische seleniumverbindingen en transformatie van metaal selenides, wat het belang van zorgvuldige bemonstering en monsterverwerking onderstreept waarbij de selenium speciatie wordt behouden. Men toonde aan dat, hoewel eerder gevalideerd met verschillende selenium modelverbindingen [269], sequentiële extractieprocedures kunnen leiden tot een onderschatting van de selenidefractie en een overschatting van de elementaire selenium fractie (**Hoofdstuk 6**).

### 9.2.2.3 Vaste fase speciatie in methanogene korrels

De selenium speciatie in intacte biofilms is tot dusver alleen m.b.v. XANES bestudeerd in *Burkholderia cepacia* culturen die op α-$Al_2O_3$ oppervlakten zijn gekweekt [227], waarbij selenium oxyanion reductie naar rood elementair selenium op het bacteriële minerale grensvlak werd aangetoond. Dit systeem is echter een nogal vereenvoudigd laboratoriumsysteem, aangezien het metalen arm is, die potentieel als metaalselenides kunnen precipiteren. Voorts waren de biofilms aeroob gecultiveerd, zodat de interacties met gereduceerde verbindingen (bv. sulfiden), die plaatsvinden in vervuilde sedimenten of anaërobe bioreactoren, niet worden beschouwd. Deze resultaten kunnen daarom maar beperkt worden gebruikt voor studies in anaërobe milieus.

**Hoofdstukken 3** en **6** toonde aan dat de selenium speciatie in de vaste fase in methanogene korrels wordt gekarakteriseerd door een complex mengsel van seleniumsoorten, met inbegrip van elementair selenium, organische seleniumverbindingen en metaal selenides (Figuur 6.1B), maar zonder geoxideerde verbindingen (seleniet of selenaat).Tijdens langere reactorruns droeg elementair selenium voor een groter deel bij aan de gemodelleerde selenium speciatie in methanogene korrels (41 atom% versus 67 atom% op dag 60 en 115 respectievelijk), terwijl de totale hoeveelheid selenium die in het slib wordt geaccumuleerd eveneens steeg (**Figuur 4.1B, Hoofdstuk 4**). Dit toont aan dat het anaërobe granulair slib inderdaad selenium kan immobiliseren in elementaire vorm tijdens langdurige methanogene condities. Toch was een klein deel van het selenium (12 atom% en 14 atom% op dagen 60 en 115 respectievelijk) aanwezig als selenocysteine (of selenocysteine bevattende eiwitten). Selenocysteine induceert selenium alkylatie [24]. Dergelijke alkylatie werd waargenomen bij endogene seleniumbronnen tijdens methanogene condities (**Tabel 5.2, Hoofdstuk 5**). Derhalve stijgt de totale hoeveelheid selenium die kan worden gealkyleerd door selenocysteine tijdens langdurende reactor runs. Dit zou een probleem kunnen betekenen voor “full-scale” toepassingen bij het afvoeren van het overtollige selenium rijke slib.



De vorming van metaal selenides wordt waarschijnlijk veroorzaakt door de reductie van selenium oxyanions naar opgelost selenide [82], dat vervolgens precipiteert met metalen aanwezig in het slib of in het medium. De metalen aanwezig in anaërobe granulair slib vangen daarom een belangrijk deel van het zeer giftig opgelost selenide weg, dit voorkomt mogelijke uitspoeling uit metaalarme milieus. Het feit dat er geen metaal selenides tot dusver door XRD in het slib werden gevonden (**Hoofdstukken 4** en **5**) zou kunnen worden toegeschreven aan lage concentraties, overlappende signalen (**Figuur 4.7**) of nano-kristallisatie [7].

### 9.2.2.4 Selenium speciatie in de biofilm van sulfaat reducerende korrels

Selenium speciatie in sulfaat reducerend slib was fundamenteel anders dan in methanogeen slib. Hoewel de belangrijkste XANES resultaten vergelijkbaar waren (**Tabel 3.1**), toonde lineaire combinatie modellering aan dat alleen trigonaal elementair selenium bijdroeg aan de speciatie in sulfaat reducerend slib (**Hoofdstuk 3**). De vorming van metaal selenides, zoals in methanogeen slib wordt waargenomen, is waarschijnlijk niet toe te schrijven aan dominerende sulfide metaal precipitatie, aangezien verscheidene millimol opgelost sulfide in de reactorvloeistof aanwezig waren (**Figuur 4.2A**), zodat geen vrije metalen aanwezig waren in de bulkvloeistof. Derhalve zou selenide in de waterfase van sulfaat reducerende bioreactoren kunnen uitspoelen.

In beide slib types (methanogeen en sulfaat reducerend) leek het aandeel van het elementaire selenium aan de gemodelleerde XANES spectra op trigonaal elementaire polymorf selenium. Maar toch toonde de “Extended X-ray Absorption Fine Structure” (EXAFS) analyzes aan dat het selenium in een onregelmatige, elementaire vorm aanwezig was, anders dan trigonaal (en monoclien rood) elementair selenium (**Figuur 3.3B**). Wellicht kan een polymorf met lage symmetrie, zoals rood amorf selenium [148], de discrepantie tussen gemodelleerde XANES speciatie en de experimentele EXAFS resultaten verklaren.



# 9.3. Biotechnologische seleniumverwijdering

## 9.3.1 Seleniumverwijdering door sulfaat reducerende bacteriën

In sommige studies zijn sulfaat reducerende bacteriën (SRB) gebruikt om selenaat in batch uit de waterfase te verwijderen [84; 234]. De reden hiervoor is dat selenaat wordt gereduceerd i.p.v. sulfaat vanwege de analoge structuur. Vanwege de hoge toxiciteit van selenaat voor SRB [26; 177; 283] kunnen batchexperimenten maar weinig informatie verschaffen over selenaat verwijdering in continue systemen. **Hoofdstuk 4** toont aan dat de SRB aanwezig in granulair UASB slib kunnen worden gebruikt voor selenaat verwijdering in continue systemen. Door de competitie tussen sulfaat en selenaat zou de verhouding tussen selenaat en sulfaat groter moeten zijn dan $1{,}92 \times 10^{-3}$. Hierdoor moet een onvolledige seleniumverwijdering worden verwacht voor de meeste selenaat en sulfaat bevattende afvalstromen (**Table 4.1**) aangezien de verhouding selenaat tot sulfaat in deze afvalstromen lager is dan $8{,}0 \times 10^{-4}$. Hoge concentraties van opgelost sulfide (enkele milimoles)

beïnvloedde de selenaat verwijdering niet, wat het mogelijk maakt om (gedeeltelijke) seleniumverwijdering te combineren met de precipitatie van zware metalen m.b.v. sulfide [195; 255] voor de behandeling het zure mijndrainage water of ander stromen met hoge metaal concentraties waar de lozingseisen voor selenium minder stringent zijn.

## 9.3.2 Selenium verwijdering in methanogene UASB reactoren

Mesofiele methanogene UASB reactoren met korte hydraulische verblijftijden (6 uren) verwijderde zowel selenaat als opgeloste selenium ($Se_{opg}$) (**Hoofdstukken 4** en **5**). Het slib uit een methanogene reactor bevatte na 150 dagen 1,9 keer zoveel selenium (1785 µg Se $gVSS^{-1}$) dan het slib uit een sulfaat reduceerde reactor (**Hoofdstuk 4**), ook was in de methanogene reactor geen verzadiging van selenium accumulatie zichtbaar (**Figuur 4.1B**).

Het feit dat selenaat bijna volledig werd verwijderd wanneer de sulfaat concentratie meer dan 2600 keer hoger was dan de selenaat concentratie (deze overmaat remt selenaat reductie door SRB) (**Hoofdstuk 4)** toont de selectiviteit van de reductie aan. Deze selectiviteit werd verklaard door de proliferatie van een selenium respirerend micro-organisme. De "sequences" van DGGE bandjes die opkwamen tijdens de reactorrun kwamen overeen, maar niet heel goed (79%), met de "sequences" van *Dendrosporobacter quercicolus*, een mesofiele anaërobe selenaat reduceerde bacterie. Selenium respirerende micro-organismen ontwikkelden zich in het slibbed, wat werd gedemonstreerd door de toegenomen seleniumverwijdering in een bioreactor in de aanwezigheid van sulfaat na verloop van tijd (**Figuur 4.3**). Bovendien zaten er met selenium deeltjes bedekte micro-organismen in de recirculatielijnen (**Hoofdstuk 5**). Hoewel het meeste selenaat in de bioreactor (90%) werd gereduceerd, was er nog wat selenaat reduceerde activiteit in het supernatant van de externe bezinker (**Hoofdstuk 5**), wat erop wijst dat een deel van de selenium reduceerde micro-organismen als gesuspendeerde biomassa in de UASB reactor groeide.

Zowel gealkyliseerde seleniumverbindingen (tot 15%) en colloïdaal verspreide seleniumdeeltjes (tot 31%) droegen bij aan het selenium in het effluent, wat een nabehandeling nodig maakt. De minimale effluentconcentraties die bereikt zijn in dit proefschrift onder methanogene condities (**Hoofdstukken 4** en **5**) zijn vergelijkbaar met eerder door Owens [170] gemelde waarden, Owens gebruikte methanogene "full-scale'" UASB reactoren die landbouw afvalwater behandelde. In tegenstelling tot deze vorige studie, waren in deze studie de influent selenaat concentraties hoger (2 keer) en de hydraulische verblijftijden korter (3 keer). Het is aangetoond dat een lichte storingen in reactortemperatuur de productie van gealkyleerde selenium of een mix van selenium- en

zwavelverbindingen kan veroorzaken (**Hoofdstuk 5**). De constante verwijdering in **Hoofdstuk 4** ten opzichte van **Hoofdstuk 5** is daarom toe te schrijven aan de constante temperatuur.

### 9.3.3 Selenium verwijdering in denitrificerende UASB reactoren

De remming door competitie tussen nitraat en selenaat reductie, geobserveerd in vele afvalwaterzuiveringtoepassingen [60], kan worden vermeden in twee-traps systemen waarin eerst nitraat word gereduceerd en vervolgens selenaat [4]. In **Hoofdstuk 8** wordt een alternatief gedemonstreerd waarin selenaat wordt gereduceerd bij volledig denitrificerende condities in een enkele stap. Dit is misschien toe te schrijven aan de proliferatie van een selenium respirerende specialist, zoals reeds waargenomen bij methanogene condities met hetzelfde entmateriaal (**Hoofdstuk 4**), hoewel identificatie m.b.v. DGGE en "sequencing" werd belemmerd door de aanwezigheid van een diverse microbiële populatie, groeiend op het toegevoegde lactaat en nitraat. Er was geen indicatie van selenaat reductie door nitraat reductases, eerder beschreven als algemeen kenmerk van nitraat reduceerders [193], aangezien het denitrificeerende slib geen selenaat kon omzetten na het weglaten van nitraat uit het influent (**Figuur 8.1A2**).



### 9.3.4 Selenium verwijdering met selenium respiratie

Het effect van bioaugmentatie, het toevoegen van micro-organismen die geschikt zijn voor de behandeling van een bepaalde verontreiniging, is vaak gelimiteerd door uitspoeling van de toegevoegde micro-organismen en door verdringing door endogene micro-organismen [46]. **Hoofdstuk 8** laat met langdurige bioreactor experimenten (>60 dagen looptijd) zien, dat deze beperkingen kunnen worden overwonnen door immobilisatie van intacte cellen van seleniumrespireerders. Een reactor die werd aangeënt met geïmmobiliseerde bacteriën, verwijderde alleen selenaat onder volledig denitrificerende condities (**Figuur 8.1A1**). In een parallelle hybride bioreactor werd anaëroob korrelslib ge-bioaugmenteerd met geïmmobiliseerde bacteriën. Dit resulteerde in snellere verwijdering van selenaat, nitraat en nitriet en tevens een hogere COD verwijderings-efficiëntie in vergelijking tot een niet ge-bioaugmenteerde controle reactor (**Figuur 8.1**).

De snellere opstart van ge-bioaugmenteerde bioreactoren (**Figuren 8.1A, 8.1C**), zou van belang kunnen zijn bij acute incidenten, zoals het lekken van afval van ertsverwerking [223]. Immobilisatie werd toegepast met behulp van niet bio-afbreekbare polyacrylamide gels, wat een mogelijke toepassing biedt onder natuurlijke omstandigheden. Omdat na 60 dagen

looptijd de geloppervlakken en geïmmobiliseerde bacteriën volledig waren ingekapseld door calcium- en fosfor precipitaten, kan bioremediatie op de lange termijn worden gelimiteerd door activiteitsverlies vanwege massa-overdrachtslimitatie door cementatie (**Figuur 8.2E-G**).

# 9.4 Aanbevelingen voor de biologische behandeling van selenium houdende waters

De beslissing welke van de beschikbare technieken het meest geschikt is voor de aanpak van seleniumvervuiling, is altijd gerelateerd aan een voor ieder geval specifiek scenario. Zo omvat de keuze van een geschikt systeem voor de behandeling van selenium, technische en economische overwegingen, maar ook aspekten gerelateerd aan sociale acceptatie en politiek beleid. **Tabel 9.1** geeft een samenvatting van de belangrijkste resultaten van dit proefschrift, gebruik makend van verschillende microbiële groepen die zouden moeten worden overwogen bij het ontwerpen van een biologisch systeem voor de behandeling van seleniumvervuiling.

## 9.4.1 De te behandelen seleniumconcentraties



Het eerste wat in acht moet worden genomen bij de behandeling van een afvalstroom is de seleniumconcentratie. De behandeling van hooggeconcentreerde afvalstromen (tot 620 mg $L^{-1}$ in seleniumverwerkende industrie [64]), zou mogelijk kunnen plaatsvinden met behulp van fysisch-chemische methodes zoals adsorptie, precipitatie of filtratie (**Tabel 1.2**). Vooral de fysisch-chemische processen die niet gebaseerd zijn op de reductie van selenium-oxyanionen, resulteren echter in de vorming van een hooggeconcentreerde pekel. Deze pekel moet op een verantwoorde manier worden verwerkt, wat resulteert in hoge operationele kosten van deze systemen (**Tabel 1.2**) [106; 140]. Zeer geconcentreerde afvalstromen zouden biologisch kunnen worden behandeld met behulp van seleniumrespirerende organismen, aangezien deze hoge seleniumconcentraties tolereren en kunnen omzetten. Hoewel seleniumrespirerende organismen tolerant zijn ten opzichte van seleniumoxyanionen, zouden ze gevoelig kunnen zijn voor andere giftige stoffen die mogelijk aanwezig zijn in een afvalstroom, zoals sulfide (**Hoofdstuk 4**). Sulfide-toxiciteit zou door de beschikbare methodes voor sulfideverwijdering kunnen worden verhinderd [119]. Toxiciteit van seleniumoxyanionen voor verschillende microbiële groepen, waaronder methanogenen (**Hoofdstuk 7**) en sulfaatreducerende bacteriën (**Hoofdstuk 4**),

zal de toepassing van mengcultures beperken. Zelfs wanneer de concentratie van seleniumoxyanionen in bioreactoren wordt verlaagd tot concentraties waarbij geen remming plaatsvindt, is een homogene menging vereist om irreversibele toxiciteit te verhinderen. Deze homogene menging kan worden bereikt door gebruik te maken van efficiënte influentdistributiesystemen (bijvoorbeeld geperforeerde distributieplaten of membranen), of door menging met de effluent recyclestroom, voordat het influent naar de reactor wordt gevoerd (**Hoofdstuk 7**).

De behandeling van grote hoeveelheden seleniumhoudend afvalstromen met een hoog volume en een lage concentratie vraagt om goedkope, selectieve processen, zoals bijvoorbeeld biologische reductie. Emissie van selenium naar de atmosfeer, veroorzaakt door biologische vervluchtiging zoals bijvoorbeeld in laag geconcentreerd landbouw drainagewater, zou in afgelegen gebieden aanvaardbaar kunnen zijn. De sterk geur [206] en potentiële chronische toxiciteit van gealkyleerde selenium soorten belemmert echter een ongecontroleerde emissie naar de atmosfeer in bevolkte gebieden. Daarnaast moet een blootstellingsrisico door acute toxiciteit [25] worden overwogen voor arbeiders, wanneer selenium in afgesloten bioreactoren wordt behandeld.

## 9.4.2 Gewenste streefwaarden



Dit proefschrift toont aan dat selenaat efficiënt bij korte hydraulische verblijftijden (6 uur) biologisch kan worden omgezet. Een substantiele hoeveelheid selenium kan echter in gealkyleerd- of colloïdaal selenium worden omgezet (**Hoofdstuk 5**). Wanneer er geen nabehandeling wordt toegepast, zullen beide fracties bijdragen aan een hogere seleniumconcentratie in het effluent, aangezien gealkyleerde seleniumsoorten in water oplosbaar zijn en het colloïdale selenium niet door eenvoudige technieken, zoals een externe bezinker, kan worden afgescheiden (**Hoofdstuk 5**).

Een nauwkeurige procesbeheersing kan alkylering van selenium vermijden (**Hoofdstuk 5**). De tijdsvertraging tussen een verstoring van het proces en alkylering (**Figuur 5.7**) zou de mogelijkheid kunnen bieden om hogere effluentconcentraties van selenium tegen te gaan door bijvoorbeeld extra buffertanks te plaatsen of verhoogde hydraulische verblijfstijden toe te passen. IJzertoevoeging kan de concentratie verlagen van zowel seleniumoxyanionen als organische selenium componenten [294], maar is nauwelijks toepasbaar voor directe behandeling van grote volumes selenium-houdend water (**Hoofdstuk 1, sectie 1.5.1.4**). IJzertoevoeging zou wel toegepast kunnen worden als nabehandeling, wanneer voldaan moet worden aan strenge lozingswaarden of wanneer de effluentconcentraties van organisch selenium hoog zijn.

Tabel 9.1 Opsomming van de belangrijkste resultaten van dit proefschrift, gebruikmakend van de verschillende microbiële groepen voor biologische seleniumbehandeling (de getallen tussen haakjes verwijzen naar hoofdstukken van dit proefschrift)

| | Methanogene UASB | | Sulfatereducerende UASB | | Nitraat reducerende UASB | | Geimmobiliseerde specialisten | |
|---|---|---|---|---|---|---|---|---|
| | + | - | + | - | + | - | + | - |
| Vloeistof- / gasfase speciatie | Lage $Se_{opl}$ (onverstoord) **(4)** | Hoge $Se_{opl}$ (verstoord): DM(D)Se DMSeS **(5)** | | Hoge $Se_{opl}$; onbekende Se species **(4)** | | | Lage $Se_{opl}$ **(8)** | |
| Biomassa vaste fase speciatie | Hoge Se in slib **(4),** Se (0) na lange duur **(6)** | Se (-II) en organisch Se **(3,6)** | Pure elementaire Se na lange duur **(3)** | Lage Se in slib **(4)** | | | | |
| Precipitaten | | nm-grootte **(5)** | | nm-grootte **(4)** | | nm-grootte **(8)** | µm grootte **(8)** | Se + S deeltjes **(8)** |
| Selectiviteit | Hoog **(4)** | | | Laag **(4)** | | | | |
| Limitatie | | $S^{2-}$ **(4)**, $SeO_3^{2-}$, $SeO_4^{2-}$ remming **(7)** | $S^{2-}$resistentie **(4)** | Verhouding $SO_4^{2-}$: $SeO_4^{2-}$ **(4)**; $SeO_4^{2-}$ remming | | | | Cementation mogelijk **(8)** |
| Kosten / Baten | Energie terugwinning via $CH_4$ **(4,5)** | | Metaalsulfide precipitatie | | $NO_3^-$ verwijdering **(8)** | Geen $SO_4^{2-}$ verwijdering **(8)** | Veelzijdig toepasbaar (arsenate,…), snelle start-up | |

De influentconcentratie in methanogene UASB reactoren van 790 µg Se $L^{-1}$ werd door middel van eenvoudige filtratie (0,45 µm) teruggebracht tot een minimale waarde van 73 µg Se $L^{-1}$ (**Hoofdstuk 4**) en tot 39 µg Se $L^{-1}$ bij gebruik van seleniumrespirerende specialisten (**Hoofdstuk 8**). De effluentconcentraties in methanogene systemen werd door middel van filtratie (0,2 µm), gevolgd door centrifugeren, verder verlaagd tot 28 µg Se $L^{-1}$ (**Hoofdstuk 5**). Effluentconcentraties bleven dus ver beneden de USEPA "Universal Treatment Standard" [242] voor afvalwater (820 µg Se $L^{-1}$). Merk op dat het criterium voor chronische toxiciteit, dat beschermt tegen onaanvaardbare gevolgen van lange termijn (ononderbroken) blootstelling, zou kunnen worden overschreden als gevolg van bio-accumulatie, ook al zijn de effluentconcentraties laag (**Figuur 1.8**).

De emissie van nano-seleniumdeeltjes die tijdens de biologische behandeling worden geproduceerd, zou moeten worden vermeden aangezien deze door directe assimilatie [131; 202; 285] of her-oxidatie [291] biobeschikbaar zou kunnen worden. In het verleden is dissolved air flotation toegepast om colloïdale seleniumdeeltjes te verwijderen [69; 185], maar de her-oxidatie van gereduceerde seleniumcomponenten naar selenaat zou kunnen plaatsvinden wanneer er gebruik wordt gemaakt van samengeperste lucht. Dissolved gas flotation [271] zou, gebruik makend van bijvoorbeeld biogas, als veelbelovende nabehandeling moeten worden onderzocht, aangezien hiermee colloïdale seleniumdeeltjes en gealkyleerde seleniumcomponenten gelijktijdig kunnen worden verwijderd. Wanneer zeer lage waarden van selenium vereist zijn, is een nabehandeling met omgekeerde osmose aan te raden [160].



## 9.4.3 Economische overwegingen

De economische haalbaarheid van seleniumbehandeling kan vastgesteld worden vanuit verschillende optieken: ten eerste kan de seleniumbehandeling worden toegepast om lozingsboetes te vermijden, waarbij de keus wordt gemaakt voor een systeem met een "minimale inspanning" [71]. Afhankelijk van de vastgestelde streefwaarden, zal door bedrijven een goedkoop, minder efficiënt systeem zoals ionenuitwisseling (**Tabel 1.2**) worden toegepast. Lagere streefwaarden kunnen door biologische behandeling worden bereikt (**Hoofdstukken 4, 5** en **8**).

Een deel van de investerings- en operationele kosten kan worden teruggewonnen wanneer seleniumverwijdering wordt gecombineerd met terugwinning in een "proces georiënteerde" aanpak [71]. Bij een proces bestaande uit een slib-bed reactor, een gefluidizeerde bed reactor, flocculatie en micro-filtratie, is het gelukt om selenium- en sulfaatrijk agrarisch drainage water te behandelen. Hierbij kon meer dan 90% van de operationele kosten worden

teruggewonnen door de productie van een bijproduct (natriumsulfaat) [214]. De terugwinning van zuiver elementair selenium zou de kosten verder kunnen drukken. In tegenstelling tot verscheidene andere studies [104; 115; 133; 167], wordt in dit proefschrift aangetoond dat elementair selenium niet het enige product van biologische selenaat reductie is (**Hoofdstukken 3** en **6**), en niet in zuivere vorm kan worden teruggewonnen. Het precipitaat zou echter kunnen worden opgewerkt, bijvoorbeeld in een pyrometallurgisch proces. Afhankelijk van de markt voor seleniumproducten, zouden de precipitaten van lage kwaliteit of de opgewerkte producten met behulp van een "marktgerichte" benadering kunnen worden verkocht aan externe klanten [71]. Zowel de markt voor biologisch gewonnen seleniumproducten als mechanismen voor kwaliteitsbeheersing van het gewonnen seleniumproduct, moet echter nog worden ontwikkeld.

Het gebruik van een electronendonor is vaak de belangrijkste factor voor de bedrijfskosten van biologische systemen [289], aangezien de meeste met selenium vervuilde stromen hieraan een tekort hebben (**Tabel 7.1**). De combinatie van COD-rijke afvalstromen, zoals molasse [289] of methanol [170] met selenium vervuild afvalwater, zou energieterugwinning via methaan mogelijk kunnen maken (**Hoofdstukken 4** en **5**). Hierbij zou wel rekening gehouden moeten worden met het feit dat tijdens seleniumverwijdering de methaanopbrengsten ernstig kunnen verminderen vanwege toxiciteit van selenaat en seleniet voor zowel acetotrofe als hydrogenotrofe methanogenen (**Hoofdstuk 7**). De in dit proefschrift beschreven laagst mogelijke organische belasting (OLR) waarbij selenaatreductie nog kon worden gehandhaafd, is 0.5 g COD $L^{-1}$ $dag^{-1}$ (**Hoofdstuk 5**, dag 103-122). Nog lagere belastingen zijn in de toekomst mogelijk haalbaar (vergelijk **sectie 9.5.2.3**).



# 9.5. Aanbevelingen voor toekomstig onderzoek

## 9.5.1 Seleniumspeciatie en selenium-zwavel interacties

De interactie tussen gealkyleerd selenium en zwavel, waaruit zich een mengsel van selenium-zwavel verbindingen vormt (bijv. dimethyl selenylsulfide, **Hoofdstuk 5**), beinvloedt de efficiëntie van de seleniumverwijdering met behulp van bioreactoren (**Figuur 5.6**). Dit vraagt om opheldering van de chemische alsook de microbiële achtergrond van zowel vorming als afbraak van dergelijke componenten. Voor de identificatie en de kwantificatie van deze stoffen lijkt de toepassing van technieken

gebaseerd op massaspectrometrie geschikt te zijn. De analyse van stabiele isotopen zou kunnen bijdragen aan het bepalen van de rol van biologische processen, analoog aan de analyse van de aanwezigheid van zwavelisotopen in de natuur [ bijv. [107]].

Hoewel de efficiëntie van biologische processen voor het verlagen van opgeloste seleniumconcentraties in verscheidene hoofdstukken werd bewezen (**Hoofdstuk 4, 5** en **8**), zou een vergelijking van de efficiëntie van detoxificatie in toekomstige studies moeten worden meegenomen, aangezien ecotoxicologische gevolgen niet direct gerelateerd zijn aan totale seleniumconcentraties [60], maar een functie zijn van concentratie en biologische beschikbaarheid. Langdurige mesocosm experimenten zijn echter duur en arbeidsintensief. Vaste-fase microextractie is onlangs toegepast om de biologische beschikbaarheid van hydrofobe verontreinigingen in te schatten [ bijv. [98; 274; 277]]. Deze toepassing zou met gealkyleerde seleniumcomponenten kunnen worden uitgebreid.

Onlangs is “Secondary Ion Massa Spectrometrie” (SIMS) gecombineerd met “Fluoresce In Situ Hybridisatie” (FISH) methodes, waardoor de fylogenetische microbiële samenstelling, alsmede de verdeling van isotopen op het niveau van intacte cellen kan worden vastgesteld [123]. Deze benadering zou ook kunnen worden gebruikt om selenaat reducerende micro-organismen te merken en seleniumprecipitatie ter plaatse te volgen.



De oxidatie van selenide die is waargenomen tijdens blootstelling van slib waarin selenium is opgehoopt aan de buitenlucht (**Hoofdstuk 6**), opent een onderzoeksgebied naar de natuurlijke selenium kringloop op aërobe/anaërobe grensvlakken (bijvoorbeeld sediment/water of mijn afvalwater/lucht). Nu een reeks van natuurlijke en synthetische stoffen, inclusief minder bestudeerde Se (-1) selenides, beschikbaar is (**Hoofdstuk 3**), zou de toepassing van op XAFS gebaseerde technieken vergroot kunnen worden om de samenstelling van gemengde selenium-zwavel precipitaten te kunnen bepalen (**Hoofdstuk 8**). Vooral het bijkomend gebruik van XAFS technieken voor zwavel [178; 179] en selenium is veelbelovend. Omdat bij deze techniek macro-stralen werden gebruikt, bemoeilijkte de bijdrage van het XANES spectrum van verschillende selenium mineralen de bepaling van het exacte mechanisme van minerale overgang. De ruimtelijke variatie in seleniumspeciatie kan echter hoog zijn. Een verhoogde resolutie zou daarom leiden tot een beter begrip van de oxidatieprocessen, en een beter begrip van de rol van de biofilm in selenium depositie (**Figuur 7.7A en B**). Daarom zouden µ- of nano XAFS studies [162; 218] moeten worden toegepast om seleniumspeciatie op verschillende plaatsen in biofilms te bestuderen. Het gebruik van Scanning Transmission X-ray Microscopie (SXTM) (**Figuur 9.1**) zou het overlappen van verschillende seleniumsoorten kunnen verhinderen, aangezien de monsters in dunne secties worden geprepareerd. Helaas is STXM nu alleen mogelijk bij de L-edge van selenium. De gevoeligheid van deze methode zou mogelijk voor problemen kunnen zorgen wanneer biologische monsters met een lage selenium

concentratie worden gebruikt [1]. Met tijdsafhankelijke µ-XAFS experimenten [200] bleek het mogelijk om oxidatiesnelheden van minerale overgang te kwantificeren. De aanwezigheid van intermediairen van selenium, die als organisch selenium zijn opgehoopt in het slib (**Hoofdstuk 3** en **6**), zou mogelijk kunnen worden afgeleid met gebruikmaking van $^{77}$Se gelabelde componenten in combinatie met Nuclear magnetic resonance (NMR) spectroscopie [96].

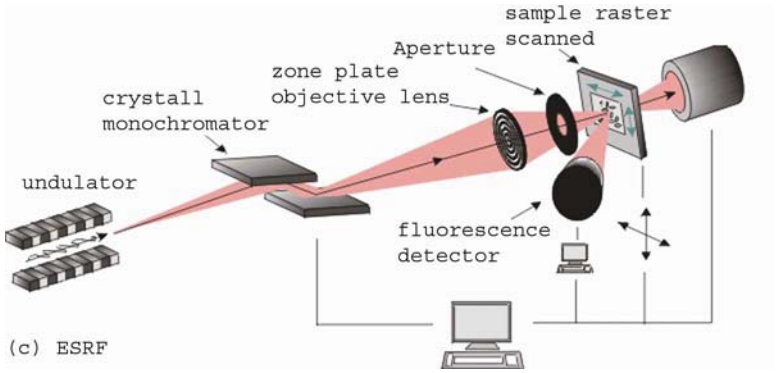


Figuur 9.1 Scanning X-ray transmissie microscopie opgezet bij beamline "ID21" (European Synchotron Radiation Facility, Grenoble, Frankrijk) [50].



## 9.5.2 Proces technologie

### 9.5.2.1 Inoculum

Anaëroob korrelslib is een veelzijdige slib dat verschillende groepen micro-organismen bevat, zoals bijvoorbeeld sulfaat- en nitraatreduceerders en methanogenen, maar ook gespecialiseerde seleniumrespirerende organismen (**Hoofdstukken 4, 5** en **8**). In de toekomst zou de toepassing hiervan kunnen worden vergroot voor de behandeling van andere oxyanionen, zoals chromaat, arsenaat, molybdaat en uranaat. In **Hoofdstuk 8** is aangetoond dat seleniumrespirerende organismen kunnen worden geïmmobiliseerd in niet-afbreekbare gels, waarbij de selenium reducerende activiteit gedurende een periode van tenminste 60 dagen behouden bijft. Het organisme dat werd gebioaugmenteerd (*Sulfurospirillum barnesii*) is veelzijdig in het gebruik van elektronenacceptoren (selenaat, arsenaat, telluraat, enz.) [8; 130], wat een breed toepassingsgebied voor bioremediatie mogelijk maakt.

## 9.5.2.2 Reactor ontwerp en bedrijf

Wanneer bacteriën geïmmobiliseerd zijn in kleine polyacryamide gel bolletjes, die een ideaal volume-oppervlakte verhouding hebben, kunnen deze in gepakte bedreactoren worden toegepast en de verdrijving door andere bacteriën verhinderen die in een eerdere studie werd waargenomen [20] (**Figuur 1.11A**). Wanneer met immobilisatieprocedures de selenaat reductie activiteit niet langdurig gehandhaafd kan worden, zouden seleniumrespireerders in membraanbioreactoren kunnen worden toegepast, aangezien hierin betere biomassa retentie plaatsvindt [250]. Echter, het gebruik van membranen wordt mogelijk beperkt door cakevorming [94] door colloïdaal elementair selenium of de vorming van metaalselenides.

## 9.5.2.3 De elektronendonor

Omdat de elektronendonor meestal de belangrijkste kosten vertegenwoordigd in bioremediatie systemen, bemoeilijkt competitie door methanogenese, nitraat- en sulfaatreductie de haalbaarheid van het proces. Co-immobilisatie van seleniumrespirerende organismen met stoffen die waterstof als elektronendonor vrijgeven [109] in slow-release capsules [91], zou gebruikt kunnen worden om de competitie te overwinnen door de nabijheid van elektronendonor en seleniumrespireerder. De snelheid van het vrijkomen van elektronendonor zou dan moeten worden aangepast aan de minimale vraag naar elektronendonor die nodig is voor de volledige reductie van seleniumoxyanionen naar elementair selenium. Zoals beschreven in **Hoofdstukken 4, 5** en **8**, werd selenaat gevoed met een snelheid van 40 µM L reactor$^{-1}$ d$^{-1}$, dus zijn er 40 × 6 µmol elektronen L $_{reactor}^{-1}$ d$^{-1}$ vereist voor de reductie van selenaat (+ VI) naar elementair selenium (0). Dit komt overeen met 20 µM lactaat L reactor$^{-1}$ d$^{-1}$. Dergelijk lage organische belastingen zijn echter alleen voldoende voor selenaatreductie onder ideale (geen concurrentie) omstandigheden. Er moeten dus verdere lab,- pilot- of full-scale experimenten worden gedaan om de minimale OLR te bepalen waarbij nog volledige seleniumverwijdering wordt bereikt. In hoog geconcentreerde stromen zou waterstof als efficiënte elektronendonor [26] kunnen worden gedoseerd (**Hoofdstuk 7**). Waterstof kan het best worden gedoseerd met behulp van een membraan [26] of bellenvrije dosering [52]. Tevens zou waterstof kunnen worden gebruikt in een gaslift reactor (wat reeds op volle schaal wordt toegepast voor microbiële sulfaatreductie [252]), al zullen de operationele kosten hoger zijn, bijvoorbeeld door kosten voor de levering van waterstof en vanwege veiligheidsmaatregelen.

## 9.5.4 Afscheiding van vaste deeltjes

Om seleniumdeeltjes met behulp van eenvoudige middelen van de waterstroom te scheiden, bijvoorbeeld door middel van bezinking, zijn grote, ongeladen deeltjes gewenst met een hoge dichtheid. In **Hoofdstukken 2, 3, 4** en **5**, wordt echter aangetoond dat de gevormde deeltjes amorf zijn, klein (< 0,5 µm), en niet gemakkelijk bezinken. **Figuur 9.2** toont SEM beelden van seleniumprecipitaten die door anaëroob korrelslib worden gevormd (10 mM selenaat). In vergelijking met het drogen bij kamertemperatuur (**Figuur 9.2A**), resulteert het drogen bij een verhoogde temperatuur (105°C, **Figuur 9.2B**) in de transformatie van amorfe bioprecipitaten naar grotere kristallen. Dit is waarschijnlijk toe te schrijven aan de overgang van het rode amorfe selenium naar trigonaal of hexagonaal elementair selenium [148]. Vooral de vorming van trigonaal polymorf selenium is voordelig, aangezien het een 13% hogere dichtheid heeft in vergelijking met amorf selenium [148] en het grote kristallen kan vormen (**Figuur 1.5**). Daarom zouden thermofiele condities (of nabehandeling) moeten worden onderzocht om de bezinkbaarheid van seleniumprecipitaten te verbeteren, aangezien deze polymorfe selenium transformaties bij 70°C of lager worden waargenomen [148]. Deze temperatuur zou toegepast kunnen worden bij extreem thermofiele sulfaatreductie [249]. Daarnaast zouden reactorconcepten met lage afschuifkrachten in toekomstige studies moeten worden onderzocht, om grotere deeltjes te krijgen (**sectie 9.2.2.1**). Toekomstig onderzoek zou zich ook op vraag moeten richten of de oppervlaktelading van de deeltjes door de gebruikte condities kan worden beïnvloed. Dit zou het terugwinnen van bioprecipitaten kunnen verbeteren, en zo de momenteel toegepaste techniek van coagulatie nabehandeling kunnen optimaliseren [20].



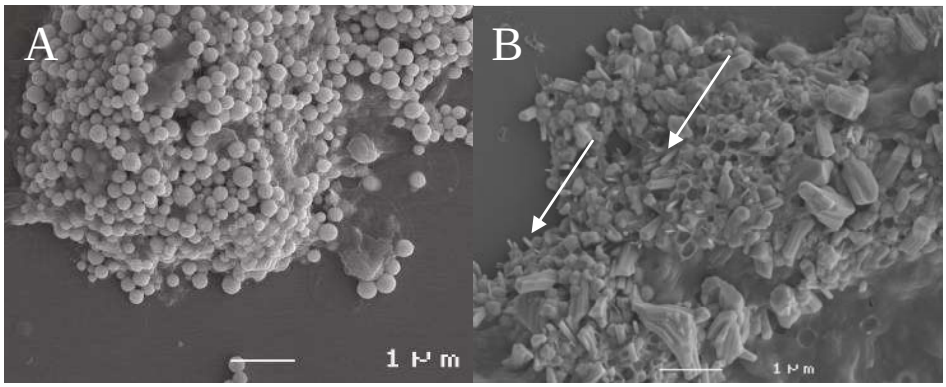


**Figuur 9.2** Elektronenmicroscopische beelden van seleniumprecipitaten, gevormd tijdens batch experimenten met anaëroob korrelslib dat 10 mM selenaat behandelt. Precipitaten zijn gedroogd bij 20°C (A) en 105°C (B). Pijlen markeren de minerale structuur die lijkt op die van trigonaal selenium (vergelijk [95]).

# References


[34] Dhillon, K.S., Dh
seleniferous so
Press. p 119-18
[35] Dhillon, K.S., D
bioavailability
Punjab, India.
643.
[36] Diels, L., Spaans,
Wouters, H., V
others. 2003. H
metal sorbing
235-241.
[37] Dowdle, P.R., Ore
selenium in s
Science & Tech
[38] Drake, E.N. 2006.
not an antioxida
[39] Dreher, G.G. 199
Powder River
19(3), 155.
[40] Dudzińska-Huczuk
baltic sea atmos
[41] Dungan, R., Franke
*Enterobacter*
Biogeochemistı
[42] Dungan, R.S., Fran
of Selenium an
Bioremediat. J.
[43] Dungan, R.S., Fra
elemental selen
Qual. 27(6), 130
[44] Eaton, A.K.K., Cle
Standard meth
American Publi
[45] EC. 2002. Europea
programmes un
official publicat

[1] Akabayov, B., Doonan, C.J., Pickering, I.J., George, G.N., Sagi, I. 2005. Using softer X-ray absorption spectroscopy to probe biological systems. J. Synchrotron. Radiat. 12(4), 392-401.

[2] Albayati, M.A., Raabe, O.G., Teague, S.V. 1992. Effect of inhaled dimethylselenide in the fischer 344 male-rat. J. Toxicol. Environ. Health 37(4), 549-557.

[3] Alderman, L.C., Bergin, J.J. 1986. Hydrogen selenide poisoning - an illustrative case with review of the literature. Arch. Environ. Health 41(6), 354-358.

[4] Amweg, E.L., Stuart, D.L., Weston, D.P. 2003. Comparative bioavailability of selenium to aquatic organisms after biological treatment of agricultural drainage water. Aquat. Toxicol. 63(1), 13-25.

[5] Astratinei, V., van Hullebusch, E.D., Lens, P.N.L. 2006. Bioconversion of selenate in methanogenic anaerobic granular sludge. J. Environ. Qual. 35(5), 1873-1883.



[6] Azaizeh, H., Salhani, N., Sebesvari, Z., Shardendu, S., Emons, H. 2006. Phytoremediation of selenium using subsurface-flow constructed wetland. Int. J. Phytorem. 8(3), 187-198.

[7] Azaroff, L.V., Kaplow, R., Kato, N. 1974. X-Ray Diffraction: McGraw-Hill. 652 p.

[8] Baesman, S.M., Bullen, T.D., Dewald, J., Zhang, D., Curran, S., Islam, F.S., Beveridge, T.J., Oremland, R.S. 2007. Formation of tellurium nanocrystals during anaerobic growth of bacteria that use Te oxyanions as respiratory electron acceptors. Appl. Environ. Microbiol. 73(7), 2135-2143.

[9] Banuelos, G.S., Lin, Z.-Q., Arroyo, I., Terry, N. 2005. Selenium volatilization in vegetated agricultural drainage sediment from the San Luis Drain, Central California. Chemosphere 60(9), 1203-1213.

[10] Barceloux, D.G. 1999. Selenium. Clin. Toxicol. 37(2), 145 - 172.

[11] Barthelmy, D. 2006. Mineralogy Database. Available online at http://www.webmineral.com/chem/Chem-Se.shtml.

[12] Bebien, M., Kirsch, J., Mejean, V., Vermeglio, A. 2002. Involvement of a putative molybdenum enzyme in the reduction of selenate by *Escherichia coli*. Microbiol. SGM 148, 3865-3872.

[13] Beytut, E., Karatas, F., Beytut, E. 2002. Lambs with white muscle disease and selenium content of soil and meadow hay in the region of Kars, Turkey. Vet. J. 163(2), 214-217.

[14] BMU. 2004. - Federal Ministry for the Environment, Nature Conservation and Nuclear Safety. Promulgation of the new version of the ordinance on requirements for the discharge of waste water into waters. Waste water ordinance, Federal law gazette BGBl. I p. 1108.



[15] Boon, N., De Gelder, L., Lievens, H., Siciliano, S.D., Top, E.M., Verstraete, W. 2002. Bioaugmenting bioreactors for the continuous removal of 3-Chloroaniline by a slow release approach. Environ. Sci. Technol. 36(21), 4698-4704.

[16] Bosco, M.L., Varrica, D., Dongarra, G. 2005. Case study: Inorganic pollutants associated with particulate matter from an area near a petrochemical plant. Environ. Res. 99(1), 18-30.

[17] Brinkman, M., Buntinx, F., Muls, E., Zeegers, M.P. 2006. Use of selenium in chemoprevention of bladder cancer. Lancet Oncol. 7(9), 766-774.

[18] Buchanan, B.B., Bucher, J.J., Carlson, D.E., Edelstein, N.M., Hudson, E.A., Kaltsoyannis, N., Leighton, T., Lukens, W., Shuh, D.K., Nitsche, H. and others. 1995. A XANES and EXAFS investigation of the speciation of selenite following bacterial metabolization. Inorg. Chem. 34(6), 1617-1619.

[19] Butterman, W.C., Brown, R.D. 2004. U.S. Geological Survey - Mineral commodity profiles selenium.

[20] Cantafio, A.W., Hagen, K.D., Lewis, G.E., Bledsoe, T.L., Nunan, K.M., Macy, J.M. 1996. Pilot-scale selenium bioremediation of San Joaquin drainage water with *Thauera selenatis*. Appl. Environ. Microbiol. 62(9), 3298-3303.

[21] Carvalho, K.M., McGettigan, M.J., Martin, D.F. 2001. GC/MS analysis of volatile organic selenium species produced during phytoremediation. J. Environ. Sci. Health, Part A 36(7), 1403-1409.



[22] Castaldi, F.J., Behrens, G.P., Hargrove, O.W. 2001. Removal of selenium from FGD scrubber purge water. Conference Proceedings - Water Environment Federation Annual Conference and Exposition, Atlanta, Geogia, USA.

[23] Chasteen, T.G. 1993. Confusion between dimethyl selenenyl sulfide and dimethyl selenone released by bacteria. Appl. Organomet. Chem. 7(5), 335-342.

[24] Chasteen, T.G., Bentley, R. 2003. Biomethylation of selenium and tellurium: microorganisms and plants. Chem. Rev. 103(1), 1-25.

[25] Cherdwongchareonsuk, D., Aguas, A.P., Henrique, R., Upatham, S., Pereira, A.S. 2003. Toxic effects of selenium inhalation: acute damage of the respiratory system of mice. Hum. Exp. Toxicol. 22(10), 551-557.

[26] Chung, J., Nerenberg, R., Rittmann, B.E. 2006. Bioreduction of selenate using a hydrogen-based membrane biofilm reactor. Environ. Sci. Technol. 40(5), 1664-1671.

[27] Coleman, L., Bragg, L.J., Finkelman, R.B. 1993. Distribution and mode of occurrence of selenium in US coals. Environ. Geochem. Health 15(4), 215-227.

[28] Coleman, R.G., Delevaux, M.H. 1957. Occurrence of selenium in sulfides from some sedimentary rocks of the western United States. Econ. Geol. 52(5), 499-527.

[29] Combs, G.F., Garbisu, C., Yee, B.C., Yee, A., Carlson, D.E., Smith, N.R., Magyarosy, A.C., Leighton, T., Buchanan, B.B. 1996. Bioavailability of selenium accumulated by selenite-reducing bacteria. Biol. Trace Elem. Res. 52(3), 209-225.

[30] Cruz, F., Ferry, J.G. 2006. Interaction of iron-sulfur flavoprotein with oxygen and hydrogen peroxide. Biochim. Biophys. Acta 1760(6), 858-864.

[31] Cutter, G.A., Bruland, K.W. 1984. The marine biogeochemistry of selenium: a re-evaluation. Limnol. Oceanogr. 29(6), 1179-1192.



[32] Daniels, J.L., Das, G.P. 2006. Leaching behavior of lime-fly ash mixtures. Environ Eng Sci 23(1), 42-52.

[33] de Bok, F.A.M., van Leerdam, R.C., Lomans, B.P., Smidt, H., Lens, P.N.L., Janssen, A.J.H., Stams, A.J.M. 2006. Degradation of methanethiol by methylotrophic methanogenic archaea in a lab-scale upflow anaerobic sludge blanket reactor. Appl. Environ. Microbiol. 72(12), 7540-7547.

[34] Dhillon, K.S., Dhillon, S.K. 2003. Distribution and management of seleniferous soils. Advances in Agronomy. Academic Press. p 119-184.

[35] Dhillon, K.S., Dhillon, S.K., Pareek, N. 2005. Distribution and bioavailability of selenium fractions in some seleniferous soils of Punjab, India. Archives of Agronomy and Soil Science 51(6), 633 - 643.

[36] Diels, L., Spaans, P.H., Van Roy, S., Hooyberghs, L., Ryngaert, A., Wouters, H., Walter, E., Winters, J., Macaskie, L., Finlay, J. and others. 2003. Heavy metals removal by sand filters inoculated with metal sorbing and precipitating bacteria. Hydrometallurgy 71(1-2), 235-241.

[37] Dowdle, P.R., Oremland, R.S. 1998. Microbial oxidation of elemental selenium in soil slurries and bacterial cultures. Environ. Sci. Technol. 32(23), 3749-3755.

[38] Drake, E.N. 2006. Cancer chemoprevention: Selenium as a prooxidant, not an antioxidant. Medical Hypotheses 67(2), 318-322.



[39] Dreher, G.G. 1992. Selenium mobilization in a surface coal mine, Powder River Basin, Wyoming, U.S.A. Environ. Geol. Water Sci. 19(3), 155.

[40] Dudzińska-Huczuk, B., Bolałek, J. 2007. Particulate selenium in the baltic sea atmosphere. Water. Air. Soil Pollut. 179, 29-41.

[41] Dungan, R., Frankenberger, W. 2001. Biotransformations of selenium by *Enterobacter cloacae* SLD1a-1: formation of dimethylselenide. Biogeochemistry 55(1), 73-86.

[42] Dungan, R.S., Frankenberger Jr, W.T. 1999. Microbial transformations of selenium and the bioremediation of seleniferous environments. Bioremediat. J. 3(3), 171-188.

[43] Dungan, R.S., Frankenberger Jr., W.T. 1998. Reduction of selenite to elemental selenium by *Enterobacter cloacae* SLD1a-1. J. Environ. Qual. 27(6), 1301-1306.

[44] Eaton, A.K.K., Clesceri, L.S., Greenberg, A.E., Franson, M.A.H. 1995. Standard methods for the examination of water and wastewater. American Public Health Association, Washington, USA.

[45] EC. 2002. European Commission - DG Environment. Assessment of the programmes under article 7 of the directive 76/464/EEC. Office for official publications of the european communities, Luxembourg.

[46] El Fantroussi, S., Agathos, S.N. 2005. Is bioaugmentation a feasible strategy for pollutant removal and site remediation? Curr. Opin. Microbiol. 8(3), 268-275.

[47] El Fantroussi, S., Ntibahezwa, E., Thomas, S., Naveau, H., Agathos, S.N. 1998. Effect of specific inhibitors on the anaerobic reductive dechlorination of 2,4,6-trichlorophenol by a stable methanogenic consortium. Anaerobe 4(4), 197-203.

[48] Espańa, J.S., Pamo, E.L., Pastor, E.S., Andrés, J.R., RubÍ, J.A.M. 2006. The Impact of acid mine drainage on the water quality of the odiel river (Huelva, Spain): evolution of precipitate mineralogy and aqueous geochemistry along the Concepción-Tintillo segment. Water. Air. Soil Pollut. 173(1-4), 121-149.

[49] Esposito, G., Veeken, A., Weijma, J., Lens, P.N.L. 2006. Use of biogenic sulfide for ZnS precipitation. Sep. Purif. Technol. 51(1), 31-39.

[50] ESRF. 2008. SXM at ID21. Description available at http://www.esrf.eu/UsersAndScience/Experiments/Imaging/ID21/Sxm/sxmend.

[51] Farges, F., Brown, G.E., Petit, P.-E., Munoz, M. 2001. Transition elements in water-bearing silicate glasses/melts. part I. a high-resolution and anharmonic analysis of Ni coordination environments in crystals, glasses, and melts. Geochim. Cosmochim. Acta 65(10), 1665-1678.

[52] Fedorovich, V., Greben, M., Kalyuzhnyi, S., Lens, P., Hulshoff Pol, L. 2000. Use of hydrophobic membranes to supply hydrogen to sulphate reducing bioreactors. Biodegradation 11(5), 295-303.

[53] Fermoso, F.G., Collins, G., Bartacek, J., O'Flaherty, V., Lens, P.N.L. 2007. Acidification of methanol-fed anaerobic granular sludge bioreactors by cobalt deprivation: Induction and microbial community dynamics. Biotechnol. Bioeng. 99(1), 49 - 58.

[54] Finke, N.N., Vandieken, V., Jørgensen, B.B. 2007. Acetate, lactate, propionate, and isobutyrate as electron donors for iron and sulfate reduction in arctic marine sediments, Svalbard. FEMS Microbiol. Ecol. 59(1), 10.



[55] Finley, J.W. 2006. Bioavailability of selenium from foods. Nutr. Rev. 64(3), 146-151.

[56] Fisher, W.W., Flores, F.A., Henderson, J.A. 1992. Comparison of chalcocite dissolution in the oxygenated, aqueous sulfate and chloride systems. Miner. Eng. 5(7), 817-834.

[57] Fisk, A.T., de Wit, C.A., Wayland, M., Kuzyk, Z.Z., Burgess, N., Letcher, R., Braune, B., Norstrom, R., Blum, S.P., Sandau, C. and others. 2005. An assessment of the toxicological significance of anthropogenic contaminants in Canadian arctic wildlife. Sci. Total Environ. 351-352, 57-93.

[58] Flohe, L., Günzler, W.A., Schock, H.H. 1973. Glutathione peroxidase: a selenoenzyme. FEBS Lett. 32(1), 132-134.

[59] Fordyce, F.F. 2007. Selenium geochemistry and health. Ambio 36(1), 94-97.

[60] Frankenberger, W.T., Amrhein, C., Fan, T.W.M., Flaschi, D., Glater, J., Kartinen, E., Kovac, K., Lee, E., Ohlendorf, H.M., Owens, L. and others. 2004. Advanced treatment technologies in the remediation of seleniferous drainage waters and sediments. Irr. Drain. Syst. 18(1), 19-42.

[61] Frankenberger, W.T., Arshad, M. 2001. Bioremediation of selenium-contaminated sediments and water. Biofactors 14(1-4), 241-254.

[62] Frankenberger, W.T., Karlson, U. 1989. Environmental factors affecting microbial production of dimethylselenide in a selenium contaminated sediment. Soil Sci. Soc. Am. J. 53(5), 1435-1442.

[63] Friel, H., Lederman, H. 2006. A nutritional supplement formula for influenza A (H5N1) infection in humans. Medical Hypotheses 67(3), 578-587.

[64] Fujita, M., Ike, M., Kashiwa, M., Hashimoto, R., Soda, S. 2002. Laboratory-scale continuous reactor for soluble selenium removal using selenate-reducing bacterium, *Bacillus sp* SF-1. Biotechnol. Bioeng. 80(7), 755-761.

[65] Fujita, M., Ike, M., Nishimoto, S., Takahashi, K., Kashiwa, M. 1997. Isolation and characterization of a novel selenate-reducing bacterium, *Bacillus sp. SF-1*. J. Ferment. Bioeng. 83(6), 517-522.

[66] Gao, S., Tanji, K.K., Lin, Z.Q., Terry, N., Peters, D.W. 2003. Selenium removal and mass balance in a constructed flow-through wetland system. J. Environ. Qual. 32(4), 1557-1570.

[67] Gao, S., Tanji, K.K., Peters, D.W., Lin, Z., Terry, N. 2003. Selenium removal from irrigation drainage water flowing through constructed wetland cells with special attention to accumulation in sediments. Water. Air. Soil Pollut. 144(1-4), 263-284.

[68] Gonzalez-Gil, G.G., Lens, P.N.L., Van Aelst, A.C., Van As, H., Versprille, A.I., Lettinga, G. 2001. Cluster structure of anaerobic aggregates of an expanded granular sludge bed reactor. Appl. Environ. Microbiol. 67(8), 3683.

[69] Green, F.B., Lundquist, T.J., Quinn, N.W.T., Zarate, M.A., Zubieta, I.X., Oswald, W.J. 2003. Selenium and nitrate removal from agricultural drainage using the AIWPS (R) technology. Water Sci. Technol. 48(2), 299-305.

[70] Guo, X.M., Sturgeon, R.E., Mester, Z., Gardener, G.K. 2003. Photochemical alkylation of inorganic selenium in the presence of low molecular weight organic acids. Environmental Science & Technology 37(24), 5645-5650.

[71] Hagelaar, G.J.L.F., Van der Vorst, J.G.A.J., Marcelis, W.J. 2004. Organising life-cycles in supply chains: Linking environmental performance to managerial designs. Greener Manag. Int.(45), 27-42.



[72] Hamilton, S.J. 2002. Rationale for a tissue-based selenium criterion for aquatic life. Aquat. Toxicol. 57(1-2), 85-100.

[73] Hamilton, S.J. 2004. Review of selenium toxicity in the aquatic food chain. Sci. Total Environ. 326(1-3), 1-31.

[74] Hammel, C., Kyriakopoulos, A., Rösick, U., Behne, D. 1997. Identification of selenocysteine and selenomethionine in protein hydrolysates by high-performance liquid chromatography of their o-phthaldialdehyde derivatives. Analyst 122, 1359–1363.

[75] Hanson, B., Garifullina, G.F., Lindblom, S.D., Wangeline, A., Ackley, A., Kramer, K., Norton, A.P., Lawrence, C.B., Pilon-Smits, E.A.H. 2003. Selenium accumulation protects *Brassica juncea* from invertebrate herbivory and fungal infection. New Phytol 159, 461-469.

[76] Hartman, T.J., Taylor, P.R., Alfthan, G., Fagerstrom, R., Virtamo, J., Mark, S.D., Virtanen, M., Barrett, M.J., Albanes, D. 2002. Toenail selenium concentration and lung cancer in male smokers (Finland). Cancer Causes Control 13(10), 923-928.

[77] Harzdorf, C., Janser, G., Rinne, D., Rogge, M. 1998. Application of microwave digestion to trace organoelement determination in water samples. Anal. Chim. Acta 374(2-3), 209-214.

[78] Hatfield, D.L. 2001. Selenium: Its Molecular Biology and Role in Human Health.

[79] Haug, A., Graham, R.D., Christophersen, O.A., Lyons, G.H. 2007. How to use the world's scarce selenium resources efficiently to increase the selenium concentration in food. Microb. Ecol. Health Dis. 19(4), 209-228.



[80] Haygarth, P.M. 1994. Global importance and global cycling of selenium. In *Selenium in the Environment*, W. T. Frankenberger, Sally Benson (ed.). Marcel Dekker, New York, USA., 1-28.

[81] Henderson, A.D., Demond, A.H. 2007. Long-term performance of zero-valent iron permeable reactive barriers: a critical review. Environ. Eng. Sci. 24(4), 401-423.

[82] Herbel, M.J., Blum, J.S., Oremland, R.S., Borglin, S.E. 2003. Reduction of elemental selenium to selenide: experiments with anoxic sediments and bacteria that respire Se-oxyanions. Geomicrobiol. J. 20(6), 587-602.

[83] Hillwalker, W.E., Jepson, P.C., Anderson, K.A. 2006. Selenium accumulation patterns in lotic and lentic aquatic systems. Sci. Total Environ. 366(1), 367-379.

[84] Hockin, S., Gadd, G.M. 2006. Removal of selenate from sulfate-containing media by sulfate-reducing bacterial biofilms. Environ. Microbiol. 8(5), 816-826.

[85] Hockin, S.L., Gadd, G.M. 2003. Linked redox precipitation of sulfur and selenium under anaerobic conditions by sulfate-reducing bacterial biofilms. Appl. Environ. Microbiol. 69(12), 7063-7072.

[86] Huber, R., Sacher, M., Vollmann, A., Huber, H., Rose, D. 2000. Respiration of arsenate and selenate by hyperthermophilic archaea. Syst. Appl. Microbiol. 23(3), 305.

[87] Hullebusch, E.D.v., Gieteling, J., Zhang, M., Zandvoort, M.H., Daele, W.V., Defrancq, J., Lens, P.N.L. 2006. Cobalt sorption onto anaerobic granular sludge: Isotherm and spatial localization analysis. J. Biotechnol. 121(2), 227-240.



[88] Hulshoff Pol, L.W., De Castro Lopes, S.I., Lettinga, G., Lens, P.N.L. 2004. Anaerobic sludge granulation. Water Res. 38(6), 1376-1389.

[89] Hunsaker, D.M., Spiller, H.A., Williams, D. 2005. Acute selenium poisoning: Suicide by ingestion. J Forensic Sci 50(4), 942-946.

[90] Hunter, W.J., Kuykendall, L.D. 2004. Determination of dimethylselenide and dimethyldiselenide by gas chromatography-photoionization detection. J. Chromatogr. A 1038(1-2), 295-297.

[91] Hyuk Im, S., Jeong, U., Xia, Y. 2005. Polymer hollow particles with controllable holes in their surfaces. Nat. Mater. 4(9), 671-675.

[92] Jalilehvand, F. 2006. Sulfur: not a silent element any more. Chem. Soc. Rev. 35(1256-1268).

[93] Jan, Y.-L., Wang, T.-H., Li, M.-H., Tsai, S.-C., Wei, Y.-Y., Teng, S.-P. 2008. Adsorption of Se species on crushed granite: A direct linkage with its internal iron-related minerals. Applied radiation and isotopes 66(1), 14-23.

[94] Jeison, D., van Lier, J.B. 2006. Cake layer formation in anaerobic submerged membrane bioreactors (AnSMBR) for wastewater treatment. J. Membr. Sci. 284(1-2), 227-236.

[95] Jiang, Z.-Y., Xie, Z.-X., Xie, S.-Y., Zhang, X.-H., Huang, R.-B., Zheng, L.-S. 2003. High purity trigonal selenium nanorods growth via laser ablation under controlled temperature. Chem. Phys. Lett. 368(3-4), 425-429.

[96] Johansson, L., Gafvelin, G., Arner, E.S.J. 2005. Selenocysteine in proteins- properties and biotechnological use. Biochim. Biophys. Acta 1726(1), 1-13.



[97] Jones, J.B., Dilworth, G.L., Stadtman, T.C. 1979. Occurrence of selenocysteine in the selenium-dependent formate dehydrogenase of Methanococcus vannielii. Archives of Biochemistry and Biophysics 195(2), 255-260.

[98] Jonker, M.T.O., vanderHeijden, S.A., Kreitinger, J.P., Hawthorne, S.B. 2007. Predicting PAH bioaccumulation and toxicity in earthworms exposed to manufactured gas plant soils with solid-phase microextraction. Environ. Sci. Technol. 41(21), 7472-7478.

[99] Jonnalagadda, S.B., Rao, P.V.V.P. 1993. Toxicity, bioavailability and metal speciation. Comp. Biochem. Physiol. C Comp. Pharmacol. Toxicol. 106(3), 585-595.

[100] Kabir, M.Z., Emelianova, E.V., Arkhipov, V.I., Yunus, M., Kasap, S.O., Adriaenssens, G. 2006. The effects of large signals on charge collection in radiation detectors: Application to amorphous selenium detectors. J. Appl. Phys. 99(12).

[101] Karlson, U., Frankenberger Jr, W.T. 1988. Determination of gaseous selenium-$^{75}$ evolved from soil. Soil Sci. Soc. Am. J. 52(3), 678-681.

[102] Karlson, U., Frankenberger, W.T. 1993. Biological alkylation of selenium and tellurium. Metal Ions in Biological Systems 29, 185-227.

[103] Kashiwa, M., Nishimoto, S., Takahashi, K., Ike, M., Fujita, M. 2000. Factors affecting soluble selenium removal by a selenate-reducing bacterium Bacillus sp. SF-1. J. Biosci. Bioeng. 89(6), 528-533.

[104] Kenward, P.A., Fowle, D.A., Yee, N. 2006. Microbial selenate sorption and reduction in nutrient limited systems. Environ. Sci. Technol. 40(12), 3782-3786.



[105] Kessi, J., Hanselmann, K.W. 2004. Similarities between the abiotic reduction of selenite with glutathione and the dissimilatory reaction mediated by *Rhodospirillum rubrum* and *Escherichia coli*. J. Biol. Chem. 279(49), 50662-50669.

[106] Kharaka, Y.K., Ambats, G., Presser, T.S., Davis, R.A. 1996. Removal of selenium from contaminated agricultural drainage water by nanofiltration membranes. Appl. Geochem. 11(6), 797-802.

[107] Knoller, K., Fauville, A., Mayer, B., Strauch, G., Friese, K., Veizer, J. 2004. Sulfur cycling in an acid mining lake and its vicinity in Lusatia, Germany. Chem. Geol. 204(3-4), 303-323.

[108] Knotek-Smith, H.M., Crawford, D.L., Moller, G., Henson, R.A. 2006. Microbial studies of a selenium-contaminated mine site and potential for on-site remediation. J. Ind. Microbiol. Biotechnol. 33(11), 897-913.

[109] Koenigsberg, S., Willett, A., Sutherland, M. 2006. Controlled release electron donors: hydrogen release compound (HRC) - an overview of a decade of case studies. Bioremediat. J. 10(1-2), 45-57.

[110] Kryukov, G.V.G.V. 2004. The prokaryotic selenoproteome. EMBO Rep 5(5), 538-543.

[111] Kulp, T.R., Pratt, L.M. 2004. Speciation and weathering of selenium in upper cretaceous chalk and shale from South Dakota and Wyoming, USA. Geochim. Cosmochim. Acta 68(18), 3687-3701.

[112] Kunli, L., Lirong, X., Jian'an, T., Douhu, W., Lianhua, X. 2004. Selenium source in the selenosis area of the Daba region, South Qinling Mountain, China. Environmental Geology 45, 426-432.



[113] Lasorsa, B., Casas, A. 1996. A comparison of sample handling and analytical methods for determination of acid volatile sulfides in sediment. Mar. Chem. 52(3-4), 211-220.

[114] Lawson, S., Macy, J.M. 1995. Bioremediation of selenite in oil refinery wastewater. Appl. Microbiol. Biotechnol. 43(4), 762-765.

[115] Lee, J.-H., Han, J., Choi, H., Hur, H.-G. 2007. Effects of temperature and dissolved oxygen on Se(IV) removal and Se(0) precipitation by *Shewanella sp. HN-41*. Chemosphere 68(10), 1898-1905.

[116] Leenen, E.J.T.M., Dos Santos, V.A.P., Grolle, K.C.F., Tramper, J., Wijffels, R.H. 1996. Characteristics of and selection criteria for support materials for cell immobilization in wastewater treatment. Water Res. 30, 2985-2996.

[117] Lemly, A. 2007. A procedure for NEPA assessment of selenium hazards associated with mining. Environ. Monit. Assess. 125(1), 361-375.

[118] Lemly, A.D. 2004. Aquatic selenium pollution is a global environmental safety issue. Ecotoxicol. Environ. Saf. 59(1), 44-56.

[119] Lens, P., Vallero, M., Esposito, G., Zandvoort, M. 2002. Perspectives of sulfate reducing bioreactors in environmental biotechnology. Rev. Environ. Sci. Biotechnol. 1(4), 311-325.

[120] Lens, P., Vergeldt, F., Lettinga, G., Van As, H. 1999. 1H NMR characterisation of the diffusional properties of methanogenic granular sludge. Water Sci. Technol. 39(7), 187-194.

[121] Letavayova, L., Vlckova, V., Brozmanova, J. 2006. Selenium: From cancer prevention to DNA damage. Toxicology 227(1-2), 1-14.



[122] Lettinga, G., Hulshoff Pol, L.W. 1991. USAB-process design for various types of wastewaters. Water Sci. Technol. 24(8), 87-107.

[123] Li, T., Wu, T.D., Maze?as, L., Toffin, L., Guerquin-Kern, J.L., Leblon, G., Bouchez, T. 2008. Simultaneous analysis of microbial identity and function using NanoSIMS. Environ. Microbiol. 10(3), 580-588.

[124] Li, Y., Zimmerman, W.T., Gorman, M.K., Reiser, R.W., Fogiel, A.J., Haney, P.E. 1999. Aerobic soil metabolism of metsulfuron-methyl. Pestic. Sci. 55(4), 434-445.

[125] Lloyd, J.R. 2003. Microbial reduction of metals and radionuclides. FEMS Microbiol. Rev. 27(2-3), 411-425.

[126] Losi, M.E., Frankenberger Jr., W.T. 1998. Microbial oxidation and solubilization of precipitated elemental selenium in soil. J. Environ. Qual. 27(4), 836-843.

[127] Lovley, D.R. 1995. Bioremediation of organic and metal contaminants with dissimilatory metal reduction. J. Ind. Microbiol. 14(2), 85-93.

[128] Lovley, D.R., Fraga, J.L., Coates, J.D., Blunt-Harris, E.L. 1999. Humics as an electron donor for anaerobic respiration. Environ. Microbiol. 1(1), 89-98.

[129] Lovley, D.R., Phillips, E.J.P., Lonergan, D.J. 1989. Hydrogen and formate oxidation coupled to dissimilatory reduction of iron or manganese by *Alteromonas putrefaciens*. Appl. Environ. Microbiol. 55(3), 700-706.

[130] Luijten, M.L.G.C., Weelink, S.A.B., Godschalk, B., Langenhoff, A.A.M., van Eekert, M.H.A., Schraa, G., Stams, A.J.M. 2004. Anaerobic reduction and oxidation of quinone moieties and the reduction of oxidized metals by halorespiring and related organisms. FEMS Microbiol. Ecol. 49(1), 145-150.

[131] Luoma, S.N., Johns, C., Fisher, N.S., Steinberg, N.A., Oremland, R.S., Reinfelder, J.R. 1992. Determination of selenium bioavailability to a benthic bivalve from particulate and solute pathways. Environ. Sci. Technol. 26(3), 485-491.

[132] Lyons, G., Stangoulis, J., Graham, R. 2003. High-selenium wheat: biofortification for better health. Nutr Res Rev 16(1), 45-60.

[133] Ma, J., Kobayashi, D.Y., Yee, N. 2007. Chemical kinetic and molecular genetic study of selenium oxyanion reduction by *Enterobacter cloacae SLD1a-1*. Environ. Sci. Technol. 41(22), 7795-7801.

[134] Macy, J.M., Lawson, S. 1993. Cell yield ($Y_{(M)}$) of *Thauera selenatis* grown anaerobically with acetate plus selenate or nitrate. Arch. Microbiol. 160(4), 295-298.

[135] Mahmoud, N., Zeeman, G., Gijzen, H., Lettinga, G. 2003. Solids removal in upflow anaerobic reactors, a review. Bioresour. Technol. 90(1), 1-9.

[136] Maidak, B.L., Olsen, G.J., Larsen, N., Overbeek, R., McCaughey, M.J., Woese, C.R. 1996. The Ribosomal Database Project (RDP). Nucl. Acids Res. 24(1), 82-85.

[137] Manceau, A., Gallup, D.L. 1997. Removal of selenocyanate in water by precipitation: characterization of copper-selenium precipitate by X-ray diffraction, infrared, and X-ray absorption spectroscopy. Environ. Sci. Technol. 31(4), 968-976.

[138] Marcason, W. 2008. What is the latest research on the connection between selenium and diabetes. J. Am. Diet. Assoc. 108(1), 188-146.



[139] Marinas, B.J., Selleck, R.E. 1987. Desalination of agricultural drainage return water. Part II: Analysis of the performance of a 13,000 GDP RO unit. Desalination 61(3), 263-274.

[140] Marinas, B.J., Selleck, R.E. 1992. Reverse osmosis treatment of multicomponent electrolyte solutions. J. Membr. Sci. 72(3), 211-229.

[141] Martens, D.A., Suarez, D.L. 1997. Selenium Speciation of soil/sediment determined with sequential extractions and hydride generation atomic absorption spectrophotometry. Environ. Sci. Technol. 31(1), 133 -139.

[142] Martens, D.A., Suarez, D.L. 1999. Transformations of volatile methylated selenium in soil. Soil Biol. Biochem. 31(10), 1355-1361.

[143] Masscheleyn, P.H., Patrick Jr., W.H. 1993. Biogeochemical processes affecting selenium cycling in wetlands. Environ. Toxicol. Chem. 12(12), 2235-2243.

[144] Matlock, M.M., Howerton, B.S., Atwood, D.A. 2002. Chemical precipitation of heavy metals from acid mine drainage. Water Res. 39(19), 4757-4764.

[145] Matusiewicz, H., Krawczyk, M. 2006. On-line hyphenation of hydride generation with in situ trapping flame atomic absorption spectrometry for arsenic and selenium determination. Anal. Sci. 22(2), 249-253.

[146] Meija, J., Montes-Bayon, M., Le Duc, D.L., Terry, N., Caruso, J.A. 2002. Simultaneous monitoring of volatile selenium and sulfur species from se accumulating plants (wild type and genetically modified) by GC/MS and GC/ICPMS using solid-phase microextraction for sample introduction. Anal. Chem. 74(22), 5837-5844.



[147] Michalke, K., Wickenheiser, E.B., Mehring, M., Hirner, A.V., Hensel, R. 2000. Production of volatile derivatives of metal(loid)s by microflora involved in anaerobic digestion of sewage sludge. Appl. Environ. Microbiol. 66(7), 2791-2796.

[148] Minaev, V.S., Timoshenkov, S.P., Kalugin, V.V. 2005. Structural and phase transformations in condensed selenium. J. Optoelectron. Adv. M. 7(4), 1717.

[149] Mohan, S.V., Kisa, T., Ohkuma, T., Kanaly, R.A., Shimizu, Y. 2006. Bioremediation technologies for treatment of PAH-contaminated soil and strategies to enhance process efficiency. Reviews in environmental science and bio-technology 5(4), 347-374.

[150] Morita, M., Uemoto, H., Watanabe, A. 2007. Reduction of selenium oxyanions in wastewater using two bacterial strains. Eng. Life Sci. 7(3), 235-240.

[151] Morrison, S.J., Metzler, D.R., Dwyer, B.P. 2002. Removal of As, Mn, Mo, Se, U, V and Zn from groundwater by zero-valent iron in a passive treatment cell: reaction progress modeling. J Contam Hydrol 56(1-2), 99-116.

[152] Müller, S., Heider, J., Böck, A. 1997. The path of unspecific incorporation of selenium in *Escherichia coli*. Arch. Microbiol. 168(5), 421-427.

[153] Muyzer, G., De Waal, E.C., Uitterlinden, A.G. 1993. Profiling of complex microbial populations by denaturing gradient gel electrophoresis analysis of polymerase chain reaction-amplified genes coding for 16S rRNA. Appl. Environ. Microbiol. 59(3), 695-700.

[154] Naveau, A., Monteil-Rivera, F., Guillon, E., Dumonceau, J. 2007. Interactions of aqueous selenium (-II) and (IV) with metallic sulfide surfaces. Environ. Sci. Technol. 41(15), 5376-5382.



[155] Nelson, D.C., Casey, W.H., Sison, J.D., Mack, E.E., Ahmad, A., Pollack, J.S. 1996. Selenium uptake by sulfur-accumulating bacteria. Geochim. Cosmochim. Acta 60(18), 3531-3539.

[156] Nerenberg, R., Rittmann, B.E. 2004. Hydrogen-based, hollow-fiber membrane biofilm reactor for reduction of perchlorate and other oxidized contamitants. Water Sci. Technol. 49(11-12), 223-230.

[157] Neufeld, J.D., Wagner, M., Murrell, J.C. 2007. Who eats what, where and when? Isotope-labelling experiments are coming of age. ISME J. 1(2), 103-110.

[158] Niess, U.M., Klein, A. 2004. Dimethylselenide demethylation is an adaptive response to selenium deprivation in the archaeon *Methanococcus voltae*. J. Bacteriol. 186(11), 3640-3648.

[159] NIOSH. 2005. - National Institute for Occupational Safety and Health. Extremely hazardous substances (EHS) chemical profiles. Available online at http://yosemite.epa.gov/oswer/ceppoehs.nsf/EHS_Profile?openform.

[160] Nishimura, T., Hashimoto, H., Nakayama, M. 2007. Removal of selenium(VI) from aqueous solution with polyamine-type weakly basic ion exchange resin. Sep. Sci. Technol. 42(14), 3155-3167.

[161] NSMP. 2007. Identification and assessment of selenium and nitrogen treatment technologies and best management practices. Available at http://www.ocnsmp.com/library.asp

[162] Oger, P.M., Daniel, I., Cournoyer, B., Simionovici, A. 2004. In situ micro X-ray absorption near edge structure study of microbiologically reduced selenite ($SeO_3^{2-}$). Spectrochim. Acta. Part B: At. Spectrosc. 59(10-11), 1681-1686.

[163] Ohlendorf, H.M. 2002. The birds of Kesterson Reservoir: a historical perspective. Aquat. Toxicol. 57(1-2), 1-10.



[164] Olivas, R.M., Donard, O.F.X., Camara, C., Quevauviller, P. 1994. Analytical techniques applied to the speciation of selenium in environmental matrices. Anal. Chim. Acta 286(3), 357-370.

[165] Omil, F., Lens, P., Hulshoff Pol, L., Lettinga, G. 1996. Effect of upward velocity and sulphide concentration on volatile fatty acid degradation in a sulphidogenic granular sludge reactor. Process Biochem. 31(7), 699-710.

[166] Oremland, R.S., Blum, J.S., Bindi, A.B., Dowdle, P.R., Herbel, M., Stolz, J.F. 1999. Simultaneous reduction of nitrate and selenate by cell suspensions of selenium-respiring bacteria. Appl. Environ. Microbiol. 65(10), 4385-4392.

[167] Oremland, R.S., Herbel, M.J., Blum, J.S., Langley, S., Beveridge, T.J., Ajayan, P.M., Sutto, T., Ellis, A.V., Curran, S. 2004. Structural and spectral features of selenium nanospheres produced by Se respiring bacteria. Appl. Environ. Microbiol. 70(1), 52-60.

[168] Oremland, R.S., Zehr, J.P. 1986. Formation of methane and carbon dioxide from dimethylselenide in anoxic sediments and by a methanogenic bacterium. Appl. Environ. Microbiol. 52(5), 1031-1036.

[169] Otero-Rey, J.R., Mato-Fernandez, M.J., Moreda-Pineiro, J., Alonso-Rodriguez, E., Muniategui-Lorenzo, S., Lopez-Mahia, P., Prada-Rodriguez, D. 2005. Influence of several experimental parameters on As and Se leaching from coal fly ash samples. Anal. Chim. Acta 531(2), 299-305.

[170] Owens, L.P. 1997. Bioreactors in removing selenium from agricultural drainage water. In: Frankenberger, W.T., Engberg, R.A. (Eds.) Environmental chemistry of selenium. CRC, New York; USA. pp. 501-514.



[171] Panter, K.E., Hartley, W.J., James, L.F., Mayland, H.F., Stegelmeier, B.L., Kechele, P.O. 1996. Comparative toxicity of selenium from seleno-DL-methionine, sodium selenate, and *Astragalus bisulcatus* in pigs. Toxicol. Sci. 32(2), 217-223.

[172] Papp, L.V.L.V. 2007. From selenium to selenoproteins: Synthesis, identity, and their role in human health. Antioxid. Redox Signaling 9(7), 775-806.

[173] Parodi, G., Farges, F., Gros, M., Guiraud, M., Miska, S. 2008. A Gandolfi chamber adapted to a curved multichannel detector for identifying mineral species. American Mineralogist (submitted).

[174] Peltier, E., Dahl, A.L., Gaillard, J.F. 2005. Metal speciation in anoxic sediments: when sulfides can be construed as oxides. Environ. Sci. Technol. 39(1), 311-316.

[175] Pickering, I.J., Brown, G.E., Tokunaga, T.K. 1995. Quantitative speciation of selenium in soils using X-ray-absorption spectroscopy. Environ. Sci. Technol. 29(9), 2456-2459.

[176] Pitts, L., Fisher, A., Worsfold, P., Hill, S.J. 1995. Selenium speciation using high-performance liquid chromatography-hydride generation atomic fluorescence with on-line microwave reduction. J. Anal. At. Spectrom. 10(8), 519-520.

[177] Postgate, J. 1949. Competitive inhibition of sulfate reduction by selenate. Nature 164, 670–671.

[178] Prange, A., Arzberger, I., Engemann, C., Modrow, H., Schumann, O., Trüper, H.G., Steudel, R., Dahl, C., Hormes, J. 1999. In situ analysis of sulfur in the sulfur globules of phototrophic sulfur bacteria by X-ray absorption near edge spectroscopy. Biochim. Biophys. Acta 1428(2-3), 446-454.

[179] Prange, A., Chauvistre, R., Modrow, H., Hormes, J., Trüper, H.G., Dahl, C. 2002. Quantitative speciation of sulfur in bacterial sulfur globules: X-ray absorption spectroscopy reveals at least three different species of sulfur. Microbiology 148(1), 267-276.

[180] Presser, T. 1994. The Kesterson effect. Environ Manag 18(3), 437-454.

[181] Presser, T.S. 1994. Geologic origin and pathways of selenium from the California coast ranges to the west-central San Joaquin Valley. Selenium in the Environment, Frankenberger, W.T. (Editor ), Marcel Dekker, New York, 139-155.

[182] Presser, T.S., Luoma, S.N. 2007. Forecasting selenium discharges to the San Francisco Bay-delta estuary: Ecological effects of a proposed San Luis Drain extension- Available at http://pubs.usgs.gov/pp/p1646/pdf/pp1646.pdf.

[183] Prince, R.C., Gailer, J., Gunson, D.E., Turner, R.J., George, G.N., Pickering, I.J. 2007. Strong poison revisited. Journal of Inorganic Biochemistry 101(11-12), 1891-1893.

[184] Profumo, A., Spini, G., Cucca, L., Mannucci, B. 2001. Sequential extraction procedure for speciation of inorganic selenium in emissions and working areas. Talanta 55(1), 155-161.

[185] Quinn, N.W.T., Lundquist, T.J., Green, F.B., Zárate, M.A., Oswald, W.J., Leighton, T. 1996. Algal-bacterial treatment facility removes selenium from drainage water. Calif. Agric. 54(6), 50-56.

[186] Rickard, D., Morse, J.W. 2005. Acid volatile sulfide (AVS). Mar. Chem. 97(3-4), 141-197.

[187] Roest, K., Heilig, H.G.H.J., Smidt, H., de Vos, W.M., Stams, A.J.M., Akkermans, A.D.L. 2005. Community analysis of a full-scale anaerobic bioreactor treating paper mill wastewater. Syst. Appl. Microbiol. 28(2), 175-185.



[188] Rojas, I., Murillo, M., Carrion, N., Chirinos, J. 2003. Investigation of the direct hydride generation nebulizer for the determination of arsenic, antimony and selenium in inductively coupled plasma optical emission spectrometry. Anal. Bioanal. Chem. 376(1), 110-117.

[189] Rotruck, J.T., Pope, A.L., Ganther, H.E., Swanson, A.B., Hafeman, D.G., Hoekstra, W.G. 1973. Selenium: biochemical role as a component of glutathione peroxidase. Science 179(4073), 588-590.

[190] Rowe, C.L., Hopkins, W.A., Congdon, J.D. 2002. Ecotoxicological implications of aquatic disposal of coal combustion residues in the United States: a review. Environ. Monit. Assess. 80(3), 207-276.

[191] Ryser, A.L., Strawn, D.G., Marcus, M.A., Fakra, S., Johnson-Maynard, J.L., Moller, G. 2006. Microscopically focused synchrotron X-ray investigation of selenium speciation in soils developing on reclaimed mine lands. Environ. Sci. Technol. 40(2), 462-467.

[192] Ryser, A.L., Strawn, D.G., Marcus, M.A., Johnson-Maynard, J.L., Gunter, M.E., Möller, G. 2005. Micro-spectroscopic investigation of selenium-bearing minerals from the Western US phosphate resource area. Geochem. Trans. 6(1), 1-11.

[193] Sabaty, M., Avazeri, C., Pignol, D., Vermeglio, A. 2001. Characterization of the reduction of selenate and tellurite by nitrate reductases. Appl. Environ. Microbiol. 67(3-12), 5122-5126.

[194] Saikia, N.N. 2006. Behavior of B, Cr, Se, As, Pb, Cd, and Mo present in waste leachates generated from combustion residues during the formation of ettringite. Environ. Toxicol. Chem. 25(7), 1710.

[195] Sampaio, R.M.M., Timmers, R.A., Xu, Y., Keesman, K.J., Lens, P.N.L. 2007. Selective precipitation of Cu from Zn in a pS controlled continuously stirred tank reactor. Int. J.Environ. Waste Manage. (accepted for publication).



[196] Santana, R.R., McDowell, L.R., Macchiavelli, R., Vázquez, A., Wilkinson, N.S. 2006. Selenium fertilization of star grass pastures in central Puerto Rico. Commun Soil Sci Plant Anal 37(5-6), 673-678.

[197] Santegoeds, C.M., Damgaard, L.R., Hesselink, G., Zopfi, J., Lens, P., Muyzer, G., de Beer, D. 1999. Distribution of sulfate-reducing and methanogenic bacteria in anaerobic aggregates determined by microsensor and molecular analyses. Appl. Environ. Microbiol. 65(10), 4618-4629.

[198] Sappington, K.G. 2002. Development of aquatic life criteria for selenium: a regulatory perspective on critical issues and research needs. Aquat. Toxicol. 57(1-2), 101-113.

[199] Sarathchandra, S.U., Watkinson, J.H. 1981. Oxidation of elemental selenium to selenite by Bacillus megaterium. Science 211(4482), 600-601.

[200] Sarret, G., Avoscan, L., Carriere, M., Collins, R., Geoffroy, N., Carrot, F., Coves, J., Gouget, B. 2005. Chemical forms of selenium in the metal-resistant bacterium *Ralstonia metallidurans CH34* exposed to selenite and selenate. Appl. Environ. Microbiol. 71(5), 2331-2337.

[201] Scheinost, A.C., Charlet, L. 2008. Selenite reduction by mackinawite, magnetite and siderite: XAS characterization of nanosized redox products. Environ. Sci. Technol.

[202] Schlekat, C.E., Dowdle, P.R., Lee, B.G., Luoma, S.N., Oremland, R.S. 2000. Bioavailability of particle-associated Se to the bivalve *Potamocorbula amurensis*. Environ. Sci. Technol. 34(21), 4504-4510.



[203] Schloske, L., Waldner, H., Marx, F. 2002. Optimisation of sample pre-treatment in the HG-AAS selenium analysis. Anal. Bioanal. Chem. 372(5-6), 700-704.

[204] Schrauzer, G.N. 2000. Selenomethionine: a review of its nutritional significance, metabolism and toxicity. J. Nutr. 130(7), 1653-1656.

[205] Schröder, I.I. 1997. Purification and characterization of the selenate reductase from *Thauera selenatis*. J. Biol. Chem. 272(38), 23765-23768.

[206] Schulz, S.S., Dickschat, J.S. 2007. Bacterial volatiles: the smell of small organisms. Nat. Prod. Rep. 24(4), 814-842.

[207] Seby, F., Potin-Gautier, M., Giffaut, E., Borge, G., Donard, O.F.X. 2001. A critical review of thermodynamic data for selenium species at 25°C. Chem. Geol. 171(3-4), 173-194.

[208] See, K.A., P.S., L., Dillon, J., Ginsberg, R. 2006. Accidental death from acute selenium poisoning. Med J Aust 185(7), 388-389.

[209] Shuh, D.K., Kaltsoyannis, N., Bucher, J.J., Edelstein, N.M., Clark, S.B., Nitsche, H., Almahamid, I., Torretto, P., Lukens, W., Roberts, K. and others. Environmental applications of XANES: Speciation of Tc in cement after chemical treatment and Se after bacterial uptake. Proceedings of the 1994 MRS Spring Meeting; 1994; San Francisco, CA, USA. Materials Research Society. p 323-328.

[210] Simmons, J., Ziemkiewicz, P., Black, C. 2002. Use of steel slag leach beds for the treatment of acid mine drainage. Mine Water Environ. 21(2), 91-99.

[211] Singh, R.P., Kumar, S., Ojha, C.S.P. 1999. Nutrient requirement for UASB process: a review. Biochem. Eng. J. 3(1), 35-54.



[212] Sonstegard, J.J. 2006. Bioreactors: An approach for removing biological selenium from FGD wastewater. Ultrapure water 23(1), 49-52.

[213] Sousa, D.Z., Pereira, M.A., Stams, A.J.M., Alves, M.M., Smidt, H. 2007. Microbial communities involved in anaerobic degradation of unsaturated or saturated long-chain fatty acids. Appl. Environ. Microbiol. 73(4), 1054-1064.

[214] Squires, R.C., Groves, G.R., Johnston, W.R. 1989. Economics of selenium removal from drainage water. J. Irrig. Drain. Eng. 115(1), 48-57.

[215] Stams, A.J.M., Grolle, K.C.F., Frijters, C.T.M., Van Lier, J.B. 1992. Enrichment of thermophilic propionate-oxidizing bacteria in syntrophy with *Methanobacterium thermoautotrophicum* or *Methanobacterium thermoformicicum*. Appl. Environ. Microbiol. 58(1), 346-352.

[216] Stolz, J.E., Basu, P., Santini, J.M., Oremland, R.S. 2006. Arsenic and selenium in microbial metabolism. Annu. Rev. Microbiol. 60, 107-130.

[217] Stolz, J.F., Ellis, D., Blum, J.S., Ahmann, D., Lovley, D., Oremland, R. 1999. *Sulfurospirillum barnesii sp. nov.* and *Sulfurospirillum arsenophilum sp. nov.*, new members of the *Sulfurospirillum* clade of the ε proteobacteria. Int. J. Syst. Bacteriol. 49(3), 1177-1180.

[218] Strawn, D., Doner, H., Zavarin, M., McHugo, S. 2002. Microscale investigation into the geochemistry of arsenic, selenium, and iron in soil developed in pyritic shale materials. Geoderma 108(3-4), 237-257.



[219] Sundberg-Jones, S.E., Hassan, S.M. 2007. Macrophyte sorption and bioconcentration of elements in a pilot constructed wetland for flue gas desulfurization wastewater treatment. Water. Air. Soil Pollut. 183(1-4), 187-200.

[220] Sundberg, S.E., Hassan, S.M., Rodgers, J.J.H. 2006. Enrichment of elements in detritus from a constructed wetland and consequent toxicity to *Hyalella azteca*. Ecotoxicol. Environ. Saf. 64(3), 264-272.

[221] Swearingen, J., Jerry W., Frankel, D.P., Fuentes, D.E., Saavedra, C.P., Vasquez, C.C., Chasteen, T.G. 2006. Identification of biogenic dimethyl selenodisulfide in the headspace gases above genetically modified *Escherichia coli*. Anal. Biochem. 348(1), 115-122.

[222] Taavitsainen, J., Lange, H., Laitinen, R.S. 1998. An ab initio MO study of selenium sulfide heterocycles $Se_nS_{8-n}$. J. Mol. Struct. 453(1-3), 197-208.

[223] Taggart, M.A., Figuerola, J., Green, A.J., Mateo, R., Deacon, C., Osborn, D., Meharg, A.A. 2006. After the Aznalcollar mine spill: arsenic, zinc, selenium, lead and copper levels in the livers and bones of five waterfowl species. Environ. Res. 100(3), 349-361.

[224] Tan, J., Zhu, W., Wang, W., Li, R., Hou, S., Wang, D., Yang, L. 2002. Selenium in soil and endemic diseases in China. Sci. Total Environ. 284(1-3), 227-235.

[225] Tapiero, H., Townsend, D.M., Tew, K.D. 2003. The antioxidant role of selenium and seleno-compounds. Biomed Pharmacother 57(3-4), 134-144.

[226] Tchobanoglous, G. 2002. Wastewater engineering: treatment and reuse. Mc Graw Hill, New york, USA.

[227] Templeton, A.S., Trainor, T.P., Spormann, A.M., Brown, J., Gordon E. 2003. Selenium speciation and partitioning within *Burkholderia cepacia* biofilms formed on [alpha]-$Al_2O_3$ surfaces. Geochim. Cosmochim. Acta 67(19), 3547-3557.



[228] Thauer, R.K., Jungermann, K., Decker, K. 1977. Energy conservation in chemotrophic anaerobic bacteria. Microbiol. Mol. Biol. Rev. 41(1), 100-180.

[229] Thomson, C.D. 2004. Assessment of requirements for selenium and adequacy of selenium status: A review. Eur. J. Clin. Nutr. 58(3), 391-402.

[230] Tirez, K., Brusten, W., Van Roy, S., De Brucker, N., Diels, L. 2000. Characterization of inorganic selenium species by ion chromatography with ICP-MS detection in microbial-treated industrial waste water. J. Anal. At. Spectrom. 15(9), 1087-1092.

[231] Tokunaga, T.K., Lipton, D.S., Benson, S.M., Yee, A.W., Oldfather, J.M., Duckart, E.C., Johannis, P.W., Halvorsen, K.E. 1991. Soil selenium fractionation, depth profiles and time trends in a vegetated site at Kesterson Reservoir. Water. Air. Soil Pollut. 57-58, 31-41.

[232] Tomei, F.A., Barton, L.L., Lemanski, C.L., Zocco, T.G., Fink, N.H., Sillerud, L.O. 1995. Transformation of selenate and selenite to elemental selenium by *Desulfovibrio desulfuricans*. J. Ind. Microbiol. 14(3-4), 329-336.

[233] Torma, A.E., Habashi, F. 1972. Oxidation of copper (II) selenide by Thiobacillus ferrooxidans. Can. J. Microbiol. 18(11), 1780-1.

[234] Tucker, M.D., Barton, L.L., Thomson, B.M. 1998. Reduction of Cr, Mo, Se and U by *Desulfovibrio desulfuricans* immobilized in polyacrylamide gels. J. Ind. Microbiol. Biotechnol. 20(1), 13-19.

[235] Tucker, M.D., Barton, L.L., Thomson, B.M. 1998. Removal of U and Mo from water by immobilized Desulfovibrio desulfuricans in column reactors. Biotechnol. Bioeng. 60(1), 88-96.



[236] Turner, R.J., Weiner, J.H., Taylor, D.E. 1998. Selenium metabolism in *Escherichia coli*. Biometals 11(3), 223-227.

[237] Twidwell, L., McCloskey, J., Miranda, P., Gale, M. 2000. Potential technologies for removing selenium from process and mine wastewater. . In: Young, C. (Eds.) Minor Elements 2000: Processing and Environmental Aspects of As, Sb, Se, Te, and Bi. Society for Mining Metallurgy & Exploration, pp. 53-66.

[238] Uden, P.C. 2002. Modern trends in the speciation of selenium by hyphenated techniques. Anal. Bioanal. Chem. 373(6), 422-431.

[239] Uden, P.C., Boakye, H.T., Kahakachchi, C., Tyson, J.F. 2004. Selective detection and identification of Se containing compounds - review and recent developments. J. Chromatogr. A 1050(1), 85-93.

[240] USEPA. 2001. Final report selenium treatment / removal alternatives demonstration project - Available at http://www.epa.gov/ORD/NRMRL/std/mtb/mwt/a3/mwtp191.pdf.

[241] USEPA. 2002. National Recommended Water Quality Criteria. Available at http://www.epa.gov/waterscience/criteria/wqcriteria.html.

[242] USEPA. 2005. Environmental Protection Agency - Protection of Environment (CFR Title 40) - Chapter I, Volume 26, § 268.48.

[243] USEPA. 2008. Draft Selenium Aquatic Life Criterion: Fact Sheet. Available at http://www.epa.gov/waterscience/criteria/selenium/.

[244] USGS. 2007. Historical Statistics for Mineral and Material Commodities in the United States. Available at http://minerals.usgs.gov/ds/2005/140/#selenium.



[245] USGS. 2007. Mineral Commodity Summaries - Selenium 2007. Available at http://minerals.usgs.gov/minerals/pubs/commodity/selenium/.

[246] USGS. 2007. Minerals Yearbook Selenium and Tellurium (2005,2006). Available at http://minerals.usgs.gov/ds/2005/140/#selenium.

[247] USGS. 2008. Distribution and occurence of selenium in the USA. Available at http://tin.er.usgs.gov/geochem/doc/averages/se/usa.html.

[248] USHHS. 2003. United States Department for Health and Human Services. Toxicological profile for selenium. . Available at http://0-www.atsdr.cdc.gov.pugwash.lib.warwick.ac.uk/toxprofiles/tp92.html.

[249] Vallero, M.V.G., Camarero, E., Lettinga, G., Lens, P.N.L. 2004. Thermophilic (55-65°C) and extreme thermophilic (70-80°C) sulfate reduction in methanol and formate-fed UASB reactors. Biotechnol Prog 20(5), 1382-1392.

[250] Vallero, M.V.G., Lettinga, G., Lens, P.N.L. 2005. High rate sulfate reduction in a submerged anaerobic membrane bioreactor (SAMBaR) at high salinity. J. Membr. Sci. 253(1-2), 217-232.

[251] Van der Veen, A., Fermoso, F.G., Lens, P.N.L. 2007. Bonding from analysis of metals and sulfur fractionation in methanol-grown anaerobic granular sludge. Eng. Life Sci. 7(5), 480-489.

[252] van Houten, B.H.G.W., Roest, K., Tzeneva, V.A., Dijkman, H., Smidt, H., Stams, A.J.M. 2006. Occurrence of methanogenesis during start-up of a full-scale synthesis gas-fed reactor treating sulfate and metal-rich wastewater. Water Res. 40(3), 553-560.



[253] Van Huysen, T., Terry, N., Pilon-Smits, E.A. 2004. Exploring the selenium phytoremediation potential of transgenic Indian mustard overexpressing ATP sulfurylase or cystathionine-gamma-synthase. Int. J. Phytorem. 6(2), 111-118.

[254] van Langerak, E.P.A., Ramaekers, H., Wiechers, J., Veeken, A.H.M., Hamelers, H.V.M., Lettinga, G. 2000. Impact of location of $CaCO_3$ precipitation on the development of intact anaerobic sludge. Water Res. 34(2), 437-446.

[255] Van Roy, S., Vanbroekhoven, K., Dejonghe, W., Diels, L. 2006. Immobilization of heavy metals in the saturated zone by sorption and in situ bioprecipitation processes. Hydrometallurgy 83(1-4), 195-203.

[256] Viamajala, S., Bereded-Samuel, Y., Apel, W., Petersen, J. 2006. Selenite reduction by a denitrifying culture: batch- and packed-bed reactor studies. Appl. Microbiol. Biotechnol. 71(6), 953-962.

[257] Vorholt, J.A., Vaupel, M., Thauer, R.K. 1997. A selenium-dependent and a selenium-independent formylmethanofuran dehydrogenase and their transcriptional regulation in the hyperthermophilic *Methanopyrus kandleri*. Mol. Microbiol. 23(5), 1033-1042.

[258] Walsh, J.J., Burch, G.E. 1963. White muscle diseases. Am. Heart J. 66(1), 139-140.

[259] Wang, M.C., Chen, H.M. 2003. Forms and distribution of selenium at different depths and among particle size fractions of three Taiwan soils. Chemosphere 52(3), 585-593.

[260] Watts, C.A., Ridley, H., Condie, K.L., Leaver, J.T., Richardson, D.J., Butler, C.S. 2003. Selenate reduction by Enterobacter cloacae SLD1a-1 is catalysed by a molybdenum-dependent membrane-bound enzyme that is distinct from the membrane-bound nitrate reductase. FEMS Microbiol. Lett. 228(2), 273-279.



[261] Watts, C.A., Ridley, H., Dridge, E.J., Leaver, J.T., Reilly, A.J., Richardson, D.J., Butler, C.S. 2005. Microbial reduction of selenate and nitrate: Common themes and variations. Biochem. Soc. Trans. 33(1), 173-175.

[262] Weijma, J., Stams, A.J.M., Pol, L.W.H., Lettinga, G. 2000. Thermophilic sulfate reduction and methanogenesis with methanol in a high rate anaerobic reactor. Biotechnol. Bioeng. 67(3), 354-363.

[263] Wen, H., Carignan, J. 2007. Reviews on atmospheric selenium: Emissions, speciation and fate. Atmos. Environ. 41(34), 7151-7165.

[264] Whitman, W., Bowen, T., Boone, D. 2006. The Methanogenic Bacteria. The Prokaryotes. p 165-207.

[265] WHO. World Health Organization (1996) - Trace Elements in Human Nutrition and Health.

[266] Wiberg, E., Wiberg, N., Holleman, A.F. 2001. Inorganic Chemistry - Elsevier.

[267] Winterer, M. 1997. XAFS - A data analysis program for materials science. Journal De Physique. IV : JP 7(2), C2.243-C2.244.

[268] Witzke, T. 2008. Available at http://tw.strahlen.org/fotoatlas1/selenium_foto.html.

[269] Wright, M.T., Parker, D.R., Amrhein, C. 2003. Critical evaluation of the ability of sequential extraction procedures to quantify discrete forms of selenium in sediments and soils. Environ. Sci. Technol. 37(20), 4709-4716.



[270] Wu, L. 2004. Review of 15 years of research on ecotoxicology and remediation of land contaminated by agricultural drainage sediment rich in selenium. Ecotoxicol. Environ. Saf. 57(3), 257-269.

[271] Yalcin, T., Byers, A. 2006. Dissolved gas floatation in mineral processing. Miner. Process. Extr. Metall. Rev. 27, 87-97.

[272] Yan, R., Gauthier, D., Flamant, G., Wang, Y. 2004. Behavior of selenium in the combustion of coal or coke spiked with Se. Combust. Flame 138(1-2), 20-29.

[273] Yang, K.X., Husain, L. 2006. Ultratrace determination of selenium by hydride generation-inductively coupled plasma mass spectrometry operated under nonrobust plasma conditions. Spectrosc. Lett. 39(2), 187-201.

[274] Yang, W.C., Hunter, W., Spurlock, F., Gan, J. 2007. Bioavailability of permethrin and cyfluthrin in surface waters with low levels of dissolved organic matter. J. Environ. Qual. 36(6), 1678-1685.

[275] Yee, N., Ma, J., Dalia, A., Boonfueng, T., Kobayashi, D.Y. 2007. Se(VI) Reduction and the precipitation of Se(0) by the facultative bacterium Enterobacter cloacae SLD1a-1 are regulated by FNR. Appl. Environ. Microbiol. 73(6), 1914-1920.

[276] Yoon, T.H., Johnson, S.B., Benzerara, K., Doyle, C.S., Tyliszczak, T., Shuh, D.K., Brown, G.E. 2004. In situ characterization of aluminum-containing mineral-microorganism aqueous suspensions using scanning transmission X-ray microscopy. Langmuir 20(24), 10361-10366.

[277] You, J., Landrum, P.F., Trimble, T.A., Lydy, M.J. 2007. Availability of polychlorinated biphenyls in field-contaminated sediment. Environ. Toxicol. Chem. 26(9), 1940-1948.



[278] Yu, R., Coffman, J.P., Van Fleet Stalder, V., Chasteen, T.G. 1997. Toxicity of oxyanions of selenium and of a proposed bioremediation intermediate, dimethyl selenone. Environ. Toxicol. Chem. 16(2), 140-145.

[279] Yudovich, Y.E., Ketris, M.P. 2006. Selenium in coal: A review. Int. J. Coal Geol. 67(1-2), 112-126.

[280] Zandvoort, M.H., Hullebusch, E.D.v., Fermoso, F.G., Lens, P.N.L. 2006. Trace metals in anaerobic granular sludge reactors: bioavailability and dosing Strategies. Eng. Life Sci. 6(3), 293-301.

[281] Zandvoort, M.H., van Hullebusch, E.D., Gieteling, J., Lens, P.N.L. 2006. Granular sludge in full-scale anaerobic bioreactors: Trace element content and deficiencies. Enzyme Microb. Technol. 39(2), 337-346.

[282] Zandvoort, M.M. 2002. Effect of nickel deprivation on methanol degradation in a methanogenic granular sludge bioreactor. J. Ind. Microbiol. Biotechnol. 29(5), 268.

[283] Zehr, J.P., Oremland, R.S. 1987. Reduction of selenate to selenide by sulfate-respiring bacteria: Experiments with cell suspensions and estuarine sediments. Appl. Environ. Microbiol. 53(6), 1365-1369.

[284] Zeng, H., Combs Jr., G.F. 2008. Selenium as an anticancer nutrient: roles in cell proliferation and tumor cell invasion. J. Nutr. Biochem. 19(1), 1-7.

[285] Zhang, J., Wang, H., Yan, X., Zhang, L. 2005. Comparison of short-term toxicity between nano-Se and selenite in mice. Life Sci. 76(10), 1099-1109.



[286] Zhang, Y., Amrhein, C., Frankenberger Jr., W.T. 2005. Effect of arsenate and molybdate on removal of selenate from an aqueous solution by zero-valent iron. Sci. Total Environ. 350(1-3), 1-11.

[287] Zhang, Y., Frankenberger, J.W.T. 2007. Supplementing Bacillus sp. RS1 with Dechloromonas sp. HZ for enhancing selenate reduction in agricultural drainage water. Sci. Total Environ. 372(2-3), 397-405.

[288] Zhang, Y., Moore, J.N. 1996. Selenium fractionation and speciation in a wetland system. Environ. Sci. Technol. 30(8), 2613-2619.

[289] Zhang, Y., Okeke, B.C., Frankenberger Jr, W.T. 2008. Bacterial reduction of selenate to elemental selenium utilizing molasses as a carbon source. Bioresour. Technol. 99(5), 1267-1273.

[290] Zhang, Y., Wang, J., Amrhein, C., Frankenberger Jr., W.T. 2005. Removal of selenate from water by zerovalent iron. J. Environ. Qual. 34(2), 487-495.

[291] Zhang, Y., Zahir, Z.A., Frankenberger, W.T., Jr. 2004. Fate of colloidal-particulate elemental selenium in aquatic systems. J. Environ. Qual. 33(2), 559-564.

[292] Zhang, Y.Q., Frankenberger, W.T. 2000. Formation of dimethylselenonium compounds in soil. Environ. Sci. Technol. 34(5), 776-783.

[293] Zhang, Y.Q., Frankenberger, W.T. 2003. Removal of selenate in simulated agricultural drainage water by a rice straw bioreactor channel system. J. Environ. Qual. 32(5), 1650-1657.

[294] Zhang, Y.Q., Frankenberger, W.T. 2006. Removal of selenate in river and drainage waters by Citrobacter braakii enhanced with zero-valent iron. J. Agric. Food Chem. 54(1), 152-156.

[295] Zieve, R., Peterson, P.J. 1981. Factors influencing the volatilization of selenium from soil. Sci. Total Environ. 19(3), 277-284.

# Acknowledgements

During the four years of my PhD, I have filled numerous pages with reports and publications; however this section is outstanding for two reasons: firstly, it is characterized by the highest “time spent” to “word written” ratio. Secondly, the section certainly misses its aim, the acknowledgement of all persons that have contributed to this thesis. The fact that I mention only some explicitly does not imply any valuation; it is simply due to my habit to finish writing close to approaching dead-lines.

Firstly, I would like to thank the European Union for financing my PhD. I feel deeply thankful that I was granted the opportunity to participate in a Marie Curie Action, involving research groups from all over Europe. My sincere thanks go to Piet Lens, my daily supervisor and promotor, for his dedication, enthusiasm and humor during the numerous discussions. Thank you for all the hours that you have invested in my training and “double-thank-you” for all of them that were outside regular working hours. Furthermore, I would like to thank Cees Buisman, my other promoter, for the open discussions and his truly inspiring vision. I would also like to give credit to the members of my PhD committee that have accepted all this additional work load of evaluating this thesis.

I thank especially Eric van Hullebusch and François Farges for introducing me into the world of solid phase analysis. Although it may seem strange, I can truly say that the long shifts in the synchrotron experimental hatches of SLS and ESRF, not realizing the time of the day in the outside world, gave me the largest “boost” I have experienced so far in my scientific career. I am grateful to Adriaan van Aaelst that I was allowed to touch the controls of the SEM at last. I thank furthermore Andreas Schäffer, Philippe Corvini and Gregor Hommes for giving me training on molecular fingerprinting. I thank Martijn Smit for introducing me to the GC-MS. Although we never met in person, I would like to acknowledge Anne Marie Enright for her great piece of work in sequencing my biofilm samples. I thank Peter Luimes (and Industriewater Eerbeek) for providing the anaerobic sludges and for the open discussions we had. During the four years of my PhD, I greatly enjoyed supervising 4 BSc and 2 MSc students. Arne Gmerek, Niklas Janzen, Alexander Kölm, Patrick Binder, Chris Roubos and Dai Yue have contributed to a great extent to this work and I whish them all the best for their future careers, hoping that at least some of them follow me into science.

I would like to thank the colleagues of Environmental Technology for providing a pleasant and inspiring working atmosphere, opening my eyes for all these challenging topics that are out there. Fernando, I would like to thank for all the evenings (and beers) in Droevendaal,

enjoying a nice movie in the only cinema, where you do not need to shut up during the presentation. Jan and Jana have nothing less than saved our lives for many, many times, when introducing Lar and me to climbing. Apart from that, they have been great cooks and guests on our mutual lunch-to-dinner meetings. Thank you Geert for your intent of showing me how to sail and all the other good times we spent. I appreciated very much the coffee-circle of room 707b (Cees K., Sara, Jan, Fernando F., Ale, Pim, Fernando A, Ruben, Ruud and sometimes many more), providing me with proper coffee and laughs during lunch break. Although I lived in the Netherlands for 4 years, I would not have been able to write the summary in Dutch, thus I would like to thank Pim and Roel very much for taking this burden. I would like to thank Cees K. and Jean for their always cheerful "Guten Morgen" and Ardy for the discussions about music. I appreciated very much the company of my "roomie" Alex and elaborating on the Dutch mentality with Tania. I thank David for lending me non-scientific literature. I would also like to thank the secretary team Liesbeth, Anita and Gusta, for all their patience in explaining me the fax, the time registration and the still mysterious "Optare" system.

Lar, I cannot thank you enough for following me first to the Netherlands and now to Switzerland, leaving your family, your friends and your job behind. You are the greatest point of rest in my life. Without you, I would not have had the endurance to finish this thesis. Ich möchte mich auch bei meinen Eltern bedanken. Ihr habt mich in einzigartiger Weise unterstützt und zu meinem Beruf ermutigt, auch wenn es eine hohe Arbeitslosigkeit unter Biologen gibt und das Familien-Architekturbüro direkt gegenüber ist. Ihr habt mich regelmäßig zu Zeiten hohen Stresses daran erinnert, daß es wichtigere Dinge im Leben gibt als die Arbeit und uns immer spüren lassen, dass es etwas Besonderes ist, wenn wir in die Eifel kommen. Rainer, auch wenn wir sehr verschiedene Ansichten zu fast allen Dingen des Lebens haben, so möchte ich Dir doch sagen, dass ich sehr stolz auf Dich bin in dem was Du machst und dass ich Deine Zielstrebigkeit bewundere. Ich möchte mich dafür bedanken, dass Du mich daran erinnerst, dass reine Naturwissenschaft nicht der Schlüssel zu allen Wahrheiten ist. Me gustaría agradecer a mi "otra" familia que me hace sentir como en casa incluso lejos de Eifel, *mais carallo, de vez en cando non teño nin idea do que andan falando!* Eine dritte Heimat (neben Hasselbach und Alicante) war uns immer der Blücherplatz in Aachen. Ich möchte Claudia und Günter sowie allen, die die Abende dort (und anderswo) so lustig gestaltet haben (Uli, Michael, Mario, Hardy, Dominik A., Sven und Nina) von ganzem Herzen danken.

# About the author

Markus Lenz was born on the 12th of March 1979 in Prüm (Eifel), Germany. Between 1998 and 2004, he studied Biology ("Diplom") at the Technical University of Aachen (RWTH) with his major subject in Environmental Analysis and minor subjects in Biotechnology, Plant Physiology and Economics.

His thesis dealt with the environmental fate of cyanides and heavy metals in sediment and was conducted within a German Research Foundation (DFG) financed project at the chair of Environmental Biology and Chemodynamics (Biology V) hold by Prof. Schäffer.

In July 2004 he started his PhD research described in this thesis at the Sub-department of Environmental Technology at Wageningen University.

After his PhD graduation, he will work as a post-doc at the University of Applied Sciences Northwestern Switzerland (Muttenz) at the Chair for Ecopreneurship of Prof. Corvini.



## New work address:

University of Applied Sciences Northwestern Switzerland

Life Sciences School

Institute for Ecopreneurship

Gründenstrasse 40

CH-4132 Muttenz

Markus.Lenz@fhnw.ch

www.fhnw.ch/lifesciences

# List of publications and presentations

## Selected oral presentations

Lenz, M., Ebel, M., Schäffer, A., (2004). Aspects of environmental fate of cyanides. Oral Presentation, 2nd Joint annual meeting SETAC-GLB & GDCh-FG, 6.-8. October, Aachen, Germany.

Lenz, M., Lens, P. N. L., (2005). Change of selenium speciation in anaerobic granular sludge caused by bioconversion. Oral presentation.10th Workshop on Progress in Analytical Methodologies in Trace Metal Speciation. 6.- 9. April, Luxembourg

Lenz, M., Gmerek, A., Lens, P. N. L. (2005). Bioremediation of selenium contaminated waters via dissimilatory metal reduction and its optimization possibilities. Oral presentation. National Young Researchers Conference, 27.-28. October, Aachen, Germany.

Lenz, M., Gmerek, A., Lens, P.N.L. (2005). Optimization of bioremediation processes for selenium contaminated wastewaters using anaerobic granular sludge. Oral presentation. SETAC North America 26th Annual Meeting, 13.-17. November, Baltimore, USA.

Lenz, M., Manconi, I., Roubos, C., Gmerek, A., Lens, P.N.L., (2006). Enhanced biotreatment of selenium via specialized bacterial groups. Oral Presentation. Interfaces against pollution, 4.-7. June, Granada, Spain.



Lenz, M., Roubos, C., Lens, P.N.L., (2006). Role of sulphate reducing bacteria in the biological treatment of selenium containing wastestreams. Oral Presentation. 34th International Symposium on Environmental Analytical Chemistry (ISEAC 34), 4.-8. June, Hamburg, Germany.

Lenz, M., Dai, Y., Lens, P. N. L. (2006). Continuous treatment of selenium containing wastestreams using bioaugmented bioreactor systems. Oral Presentation. 7th European Meeting on Environmental Chemistry (EMEC7), 6.-9. December, Brno, Czech Republic.

Lenz, M., Smit, M., Farges, F., Van Hullebusch, E.D., Lens, P. N. L. (2007). Selenium speciation analysis in anaerobic bioremediation. Oral presentation. Euroanalysis 2007, 9.-14. September, Antwerp, Belgium.

Lenz, M., Smit, M., Farges, F., Van Hullebusch, E.D., Lens, P. N. L. (2007). Bioremediation of Selenium containing waters: Importance of selenium speciation analysis. Oral presentation. TraceSpec 2007, 4.-7. September, Münster, Germany.

Lenz, M., van Aelst, A., Lens, P.N.L. (2008). Biological selenium removal and selenium nanoparticle production. Oral presentation. 12th NBC Crossing borders in biotechnology conference. 13.-14. March, Ede, The Netherlands.

## Publications

Höllrigl-Rosta, A., Vinken, R., Lenz, M., Schäffer, A. (2003): Sorption and dialysis experiments to assess the binding of phenolic xenobiotics to dissolved organic matter in soil. Environmental Toxicology and Chemistry 22, 746–752.

Lenz, M., Gmerek, A., Lens, P. N. L. (2006). Selenium speciation in anaerobic granular sludge. International Journal of Environmental Analytical Chemistry, 86 (9/10), 615-627.

Van Hullebusch, E., Farges, F., Lenz, M., Lens, P., G. E. Brown, Jr. (2007). Selenium Speciation in Biofilms from Granular Sludge Bed Reactors Used for Wastewater Treatment. AIP Conference Proceedings 882, 229 – 231.

Lenz, M., Van Hullebusch, E., Hommes, G., Corvini, P. F. X., Lens, P. N. L. (2008). Selenate removal in methanogenic and sulfate-reducing upflow anaerobic sludge bed reactors. Water Research. 42 (8/9), 2184-2194.

Lenz, M., Smit, M., Binder, P., van Aelst, A.C., Lens, P. N. L. (2008). Biological alkylation and colloid formation of selenium in methanogenic UASB reactors. Journal of Environmental Quality (in press).



Lenz, M., Janzen, N., Lens, P. N. L. (2008). Inhibition of hydrogenotrophic and acetoclastic methanogenesis by selenium oxyanions. (submitted).

Lenz, M., van Hullebusch, E.D., Farges, F., Nikitenko, S., Borca, C.N., Grolimund, D., Lens, Piet N. L. (2008). Selenium speciation in anaerobic biofilms assessed by X-ray absorption spectroscopy and sequential extraction procedures. (submitted).

Lenz, M., Lens, P. N. L. (2008). The essential toxin: the changing perception of selenium in environmental sciences. (submitted).

Lenz, M., Enright, A.M., O'Flaherty, V., van Aelst, A. C., Lens, P. N. L. (2008). Bioaugmentation of UASB reactors with immobilized *Sulfurospirillum barnesii* for simultaneous selenate and nitrate removal. (in preparation).

Netherlands Research School for the
Socio-Economic and Natural Sciences of the Environment

# CERTIFICATE

The Netherlands Research School for the
Socio-Economic and Natural Sciences of the Environment
(SENSE), declares that

## Markus Lenz

Born on: 21 March 1979 at: Prüm, Germany



has successfully fulfilled all requirements of the
Educational Programme of SENSE.

Place: Wageningen Date: 27 May 2008

| the Chairman of the SENSE board | the SENSE Director of Education |
|---|---|
| Prof. dr. R. Leemans | Dr. C. Kroeze |

This work was supported by the European Union within the Marie Curie Excellence TEAM Grant “Novel biogeological engineering processes for heavy metal removal and recovery” (MEXT-CT-2003-509567).

The work was further supported by the Netherlands Organization for Scientific Research (Nederlandse Organisatie voor Wetenschappelijk Onderzoek, NWO) and European Economic Community, financing the trips to ESRF and SLS.



Cover picture: Scanning electron microscopic picture of biologically produced selenium nanoparticles